ISBN: 978-604-76-1628-2

ORGANIZERS

UNIVERSITY OF TRANSPORT & COMMUNICATIONS (UTC)

FENG CHIA UNIVERSITY (FCU)

SPONSOR

HO CHI MINH CITY DEPARTMENT OF SCIENCE & TECHNOLOGY

CONFERENCE PROCEEDINGS

International Conference

BUILDING SMART CITIES IN VIETNAM

VISION & SOLUTIONS

HO CHI MINH CITY - VIETNAM
5TH SEPTEMBER 2018

NHÀ XUẤT BẢN GIAO THÔNG VẬN TẢI

ORGANIZER

Organizational Units

- University of Transport and Communications
- Feng Chia University

Sponsor

- Ho Chi Minh City Department of Science and Technology

Steering Committee

1. Assoc.Prof. Nguyen Ngoc Long
2. Assoc.Prof. Nguyen Van Hung
3. Assoc.Prof. Nguyen Duy Viet
4. Dr. Vo Truong Son
5. Assoc.Prof. Bui Ngoc Toan
6. Vu Tien Sy

Organizer

1. Assoc.Prof. Nguyen Van Hung
2. Dr. Vo Truong Son
3. Dr. Ngo Chau Phuong
4. Dr. Nguyen Van Binh
5. Assoc.Prof. Bui Ngoc Toan
6. Vu Tien Sy
7. Nguyen Van Hai
8. Assoc.Prof. Nguyen Canh Minh
9. Assoc.Prof. Nguyen Thanh Hai
10. Dr. Nguyen Quoc Tuan
11. Dr. Tran Xuan Truong
12. Assoc.Prof. Le Van Bach
13. Tran Quang Hai Bang

Program Committee

1. Assoc.Prof. Nguyen Thanh Hai
2. Dr. Nguyen Van Binh
3. Prof. Le Hung Lan
4. Assoc.Prof. Dao Manh Hung
5. Assoc.Prof. Ho Lan Huong
6. Dr. Trinh Quang Khai
7. Dr. Nguyen Quoc Tuan

Secretariat

1. Dr. Nguyen Van Binh
2. Nguyen Van Hai
3. Dr. Tran Xuan Truong
4. Nguyen Thi Mai Nhung
5. Nguyen Thi My Hanh

Table of Contents

INTRODUCTION

The rapid pace of urbanization in a single country has led to many other relating problems such as exhaustion of resources, environmental pollution; climate change; the infrastructure overload of transportation, hospitals, schools,…; flooding due to heavy rains and tides; the shortage of lands, energy, water, space;... In such circumstances, the need for effective management and use of natural resources has become increasingly urgent. This is urging the authorities of each country including Vietnam to seek and develop advanced management models. Building smart city is seen as a strategic solution to deal with problems arising from population growth and rapid urbanization. At the same time, it will be the driving force for improving the business environment as well as bringing economic development opportunities to each urban.

This issue has been addressed by many countries. Nowadays, the worldwide market for smart city solutions is extremely vibrant, with hundreds of different providers, including providers of common platform solutions or specific solutions in each field such as energy, water resources, e-government, transportation,…

In implementation of Directive 16/CT-TTg dated 04 May 2017 of Prime Minister of the Socialist Republic of Vietnam on strengthening capacity to approach the Industrial Revolution 4.0, with the approval of the Ministry of Education and Training, the University of Transport and Communications in collaboration with Feng Chia University hold the International Conference, named **"Building Smart Cities in Vietnam: Vision and Solutions"**.

The conference is an important forum for national and international scientists, managers, academics, experts to discuss and exchange new and extraordinary thoughts, scientific arguments, valuable practical experiences of developed countries. The contributions are essential for the researching and building of smart city models, including intelligent transportation systems in Vietnam.

We would like to express our gratitude to the scientists, the keynote speakers who contribute the articles published and reported at the conference. We also would like to express our sincere thanks to the organizations in the country and abroad for the support given to us to organize this meaningful conference.

Conference Organization Committee

VIBRATION MEASUREMENT SYSTEM BASED ON IOT

NGO THANH BINH, NGUYEN CANH MINH
NGUYEN ANH NHAT, NGUYEN ANH TRONG QUY
University of Transport and Communications, Hanoi, Vietnam
Corresponding author's email: ngobinh74@utc.edu.vn

Abstract: *The monitoring system is crucial for public infrastructures to manage condition and maintain. Vibration and movement measurement systems based on Internet of Things (IoT) for transport infrastructure are being more and more relied on research and development. However, choosing low cost and reliable INS sensor with a suitable data processing method to have good accuracy, coverage, and performance often is a challenging problem. In this article, we design and create measurement modules using 9-DOF MEMS INS sensor for capturing data, processing and transmitting them by XBee wireless platforms to capture vibration and movement from the supervised objects. The station will plot the data in the real-time chart on the website monitoring. We have processed the calibration to remove the error data of IMU sensor due to the impact of internal and external factors, drifting data and offsets. And some experiments have been performed for the purpose of employing a wireless sensor network for transport infrastructures in smart cities.*

Keywords: *IMU Calibration, MEM INS, Vibration measurement, IoT, wireless sensor.*

I. INTRODUCTION

Vibration and movement measurement equipment operating based on Industry 4.0's technology is getting more and more attention and applied in many fields, especially in transport infrastructure in smart cities. A variety of applications of these systems used INS (Initial Navigation System) based on MEMS (Micro Electro Mechanical Systems), worked on the Internet environment and built into wireless sensor networks [7]. This equipment will measure, handle and send data to the data center, and then upload them to the web server. In another way, they can also be directly upload to sites located at measurement points or single cluster depending on network's configuration. Users are granted access on each cluster or the whole network at the data center depended on their account.

Currently, in Vietnam, there are some oscillation measure devices on construction sites using MEMS INS. They are standard devices by foreign brands, using multi-channel single-axis measurements, which are calibrated using documents provided by each brand. Most of these devices can only provide single-axis data, then transfer these data to a computer to calculate roll, pitch, yaw angles. Normally, these angle values calculated from single-axis MEMS IMU (Inertial Measurement Unit) have been added cumulative errors over time. This creates cumulative errors

when measuring oscillation, displacement calculations and rotation of objects. It's the reason why most of these devices have large errors over time and must be re-calibrated frequently during usage. MEMS INS's accuracy is one of the main elements which decides modern monitoring devices' accuracy. These devices are connected via internet, creating a sensor network for managing and monitoring system on IoT (Internet of Things) foundation. It's applied in security systems or managing infrastructures, natural disaster warnings beforehand to reduce casualties. Thus, the challenge for these applications using low-cost MEMS INS sensors is to solve the data error, including IMU calibration, cumulative errors and drifting data, to improve accuracy of vibration monitoring and management sensor network based on IoT.

II. VIBRATION MEASUREMENT BASED ON IOT SYSTEM

The vibration in transport infrastructure is the movement or oscillation of component or frame. Therefore, in vibration monitor, accelerometers are used to determine the type vibration such as transverse, rotation and lateral. However, by using only acceleration it can't calculate exactly orientations and angular velocity of the object. We propose to use an economy MEMS INS 9-DOF (Degree Of Freedom) sensor for each measurement unit. The sensors are low cost IMU 9- DOF Razor stick and GY-85. Both of them are packed sensors of an ITG-3200 (MEMS triple-axis gyro), ADXL345 (triple-axis accelerometer), and HMC5883L (triple-axis magnetometer) to give nine degrees of freedom for inertial measurement.

2.1. IMU Data Processing

In navigation, there are several coordinate systems (or frames) including: the ECI {i} Earth Centered Inertial frame, in which the IMU measures linear acceleration and angular velocity with respect to this frame; the ECEF {e} Earth - Centered Earth - Fixed frame which coincides with the inertial frame, but it rotates with the Earth; the NED {n} North-East-Down frame or navigation frame, defined relative to the Earth's reference ellipsoid (WGS 84); and the Body frame {b}, also is fixed frame of IMU, which is located in the center of IMU and move along with it.

The X axis of body frame is usually pointed toward, along the side of the object, the Z axis points down and the Y axis is cross produce of X axis and Z axis (right-handed rule). The orientation of IMU is described by three rotations, in which whose order is important. The angular rotations are called the Euler angles. They are defined as rotate the body around each axis with respect to {n} frame, which is aligned to {b} frame. The rotation along X axis is called roll (ϕ), the rotation along Y axis is called pitch (θ), and the rotation along Z axis is called yaw (ψ).

The rotation matrix R consist of cosines of angles between the axes of two different coordinate system, which is known as Rotation matrix (R) described by ϕ, θ, ψ [2]:

$$R = [R_x \quad R_y \quad R_z] \qquad \text{(eq. 1)}$$

Where: $R_x = \begin{bmatrix} \cos\theta\cos\psi \\ \cos\theta\sin\psi \\ -\sin\theta \end{bmatrix}$; $R_y = \begin{bmatrix} \sin\phi\sin\theta\cos\psi - \cos\phi\sin\psi \\ \sin\phi\sin\theta\sin\psi + \cos\phi\cos\psi \\ \sin\phi\cos\theta \end{bmatrix}$

$$R_z = \begin{bmatrix} \cos\phi \sin\theta \cos\psi + \cos\phi \sin\psi \\ \cos\phi \sin\theta \sin\psi - \sin\phi \cos\psi \\ \cos\phi \cos\theta \end{bmatrix} \quad \text{(eq. 2)}$$

The rotation (Q) of {b} frame's vector with respect to the e-frame (Ground) is made through by multiply of Direction Cosine Matrix (DCM) with body vector (B):

$$Q_G = R.Q_B \quad \text{(eq. 3)}$$

DCM matrix contain all the information to describe the orientation of the object with respect to the ground. To improve the quality of MEMS INS, different with using quaternion solution [4], we solved INS additional error problem by DCM self-correction based on [5] with a development of using two flexible PIs. As described in previous step [1], by using 9-dof INS based on [6], we have enough parameters to process successfully DCM algorithm to solve accumulation errors. In detail, firstly, we calculated yaw angle from internal magnetometer built-in inside INS based on vector recalculation instead of heading angle from GPS signal [5], or from an external compass [4]. After that, we calculated correction and renormalization values, and pushed them to feedback controller to recalculate DCM. Corrected Euler angles were calculated from updated DCM. The variation of offset caused by supply voltage and temperature is usually rather slow, so that DCM can continually remove the offset and maintain lock. Drift around all three axes could be completely eliminated with DCM even the bus didn't move continuously. Thus, our DCM self-correction method had solved the accumulated errors in INS systems and could help MEMS INS 9-dof systems operate independently.

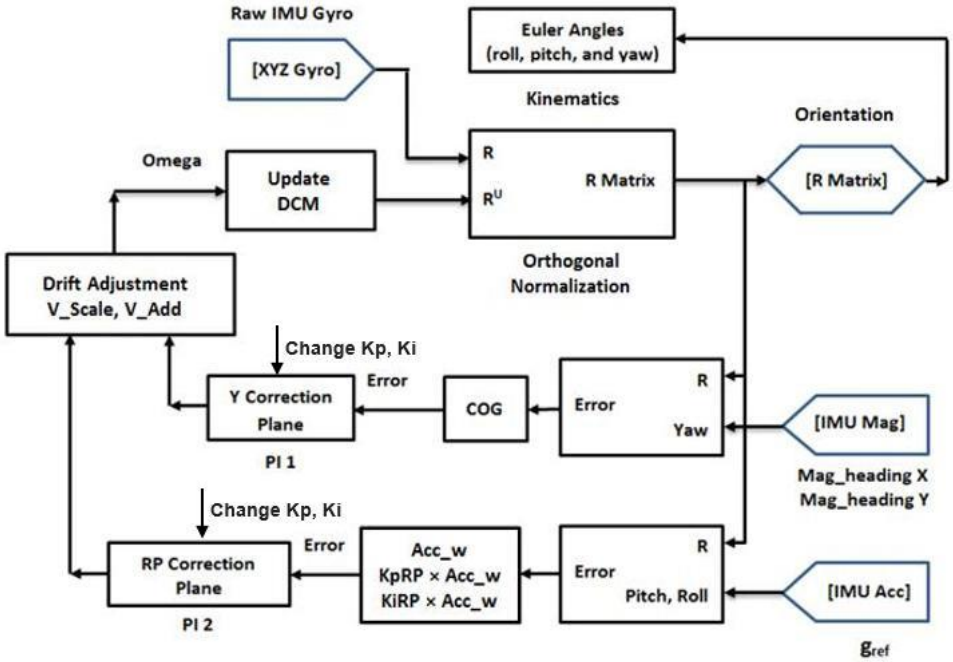

Figure 2. *The DCM algorithm using 9-DOF IMU sensors*

2.2. Calibration

Before operating MEMS INS, users must follow the brands' multi-axis calibration process to calibrate the sensors. These IMU sensors are integrated to create a multi-axis MEMS INS. A multi-

axis MEMS INS has different threshold, even if it's created from similar IMU sensors. Users must calibrate the MEMS INS by themselves to get correct thresholds of each INS before using it. If there are no calibration devices, users must calibrate manually or use the default maximum/minimum values. This normally creates incorrect measurements on the device.

Sensor calibration is a method of improving performance by removing error such as bias, offset and noise in sensor output data. Depended on the time usage the internal biases will increase, which affect to output data and the orientation angle output, for example bias is 0.1deg/s. If it not corrected sensor output data will drift even the sensor does not move, which is called zero drift. After calibrated it gives over-all accuracy in real-time measurement. Based on [6], the calibration process is performed on our DIY 3-DOF calibration mechine own designed, as shown in figure 3 below:

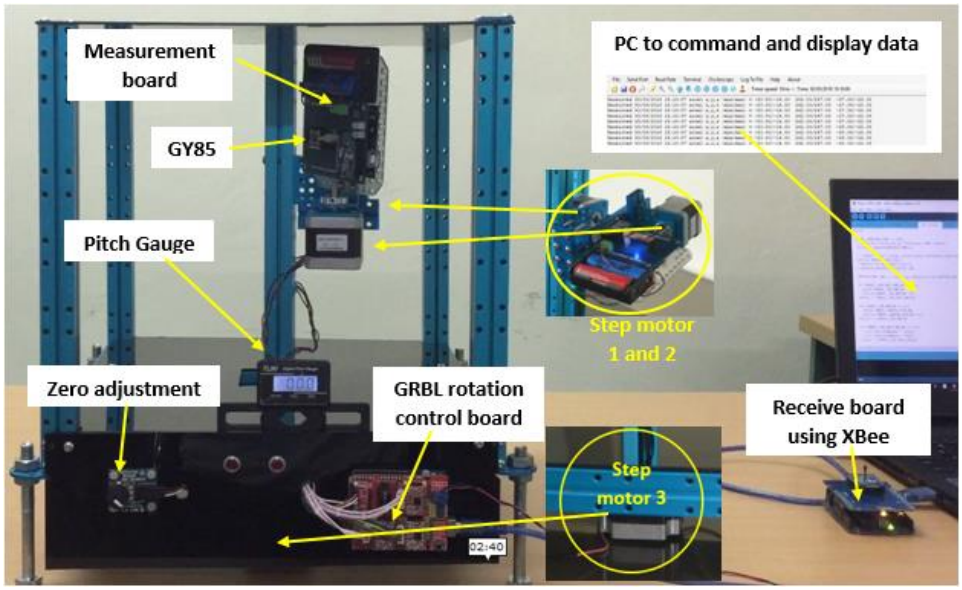

Figure 3. *Our 3dof calibration platform*

Raw accelerometer sensor data is collected by rotating straight down along each axis of sensor to measure the gravity apply on each axis. Then we determine raw magnetometer data by rotating as same as accelerometer calibrate rotation. Finally, place sensor flat on desk so it can calculate average from its tri-axes.

2.2.1. Hard iron and Soft iron distortions in calibration

A magnetometer is used to measure the strength and direction of the local magnetic field, which is a combination of both local earth's magnetic field and another magnetic field around it [3]. Distortions of the earth's magnetic field are results of external magnetic field. There are two main distortions: Hard iron and Soft iron distortions. Errors of hard-iron and soft-iron distortions are dependent upon the distortion material rotating or moving along with the sensor. For example, in case of measuring vibration of cable-stay bridge, these measurement units held MEMS INS sensor inside will be mounted on cables of the bridge, which has many distorted magnetic fields around mounted sensor area.

Hard-iron distortion is created by an object produces magnetic field. For example, in this experiment, a speaker will produce a hard-iron distortion which cause a static (permanent) bias in the magnetometer output data. Hard iron distortions can be identified by an offset that shifts the center of the circle away as shown below on the left of figure 4.

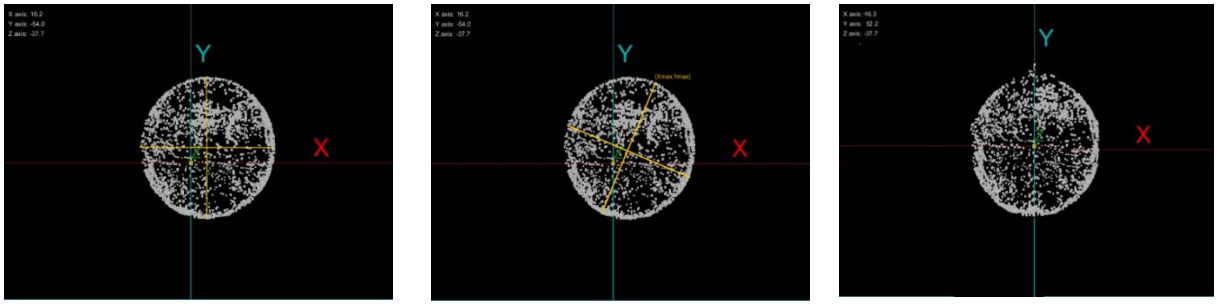

Figure 4. *Hard iron and soft iron distortion and after calibration*

Compensating for hard iron distortions can be accomplished by defining the X and Y axes offsets, which is the average of maximum and minimum values of each axes by using calibration machine described in figure 3 above. These distances are calculated to compensate from original position to distorted position, as below:

$$B_x = \frac{X_{max}+X_{min}}{2} \quad B_y = \frac{Y_{max}+Y_{min}}{2} \quad B_z = \frac{Z_{max}+Z_{min}}{2} \qquad \text{(Eq. 4)}$$

Where: B_x, B_y, B_z - Axes Offset; $X_{max}, Y_{max}, Z_{max}$ - Axes maximum value; $X_{min}, Y_{min}, Z_{min}$ - Axes minimum value.

Soft-iron distortions are considered deflections or alterations in the existing magnetic field such as metal material (nickel, iron, …). These distortions will stretch or distort the magnetic field depending upon which direction of the field relatives to the sensor. Soft iron distortion will warp the magnetic field into an elliptical shape. Soft iron distortion not only stretch or distort the magnetic field, it also makes rotated ellipse which is represented for the distorted magnetic field as shown on the center of figure 4. The rotate matrix is used to align ellipse to horizon, by finding the max value of data points, with the coordinate (x_{max}, y_{max}) value, the angle is calculated following equation (5) and equation (6). Once angle δ has been founded, apply axes vector value to the rotation matrix, is given below:

$$r = \sqrt{x^2 + y^2} \qquad \text{(eq. 5)}$$

$$\delta = \sin x^{-1}\left(\frac{y}{r}\right) \qquad \text{(eq. 6)}$$

Eliminating Hard and Soft iron distortions, we apply the bias to the vector of raw magnetometer data, then multiply with the transformation matrix to create an equation, as shown below:

$$\begin{bmatrix} X_c \\ Y_C \\ Z_C \end{bmatrix} = \begin{bmatrix} M_{11} & M_{12} & M_{13} \\ M_{21} & M_{22} & M_{23} \\ M_{31} & M_{32} & M_{33} \end{bmatrix} * \left(\begin{bmatrix} X_{nc} \\ Y_{nc} \\ Z_{nc} \end{bmatrix} - \begin{bmatrix} B_x \\ B_y \\ B_z \end{bmatrix} \right) \qquad \text{(Eq. 7)}$$

In this case, the XY-plane is being consider because the rotation matrix is limited to rotation within a single plane (XY, YZ, XZ) in our processing data method, as shown in equation (8).

$$\begin{bmatrix} X_C \\ Y_C \\ Z_C \end{bmatrix} = \begin{bmatrix} M_{11} & M_{12} & 0 \\ M_{21} & M_{22} & 0 \\ 0 & 0 & 1 \end{bmatrix} * \left(\begin{bmatrix} X_{nc} \\ Y_{nc} \\ 0 \end{bmatrix} - \begin{bmatrix} B_x \\ B_y \\ 0 \end{bmatrix} \right) \quad \text{(Eq. 8)}$$

After calibration and data fusion to have result as shown in the right of figure 4, magnetometer data will be used as a compass, represented by yaw angle. When rotating sensor around Z axis, heading X axis to the North, the angle will be 0^0 and stable as shown on figure 5b on the right of figure 5. Comparing to figure 5a on the left of figure 5, in which hard and soft iron are not calibrated, we can see that yaw data are changed continuously and become not stable caused of significant angle drift.

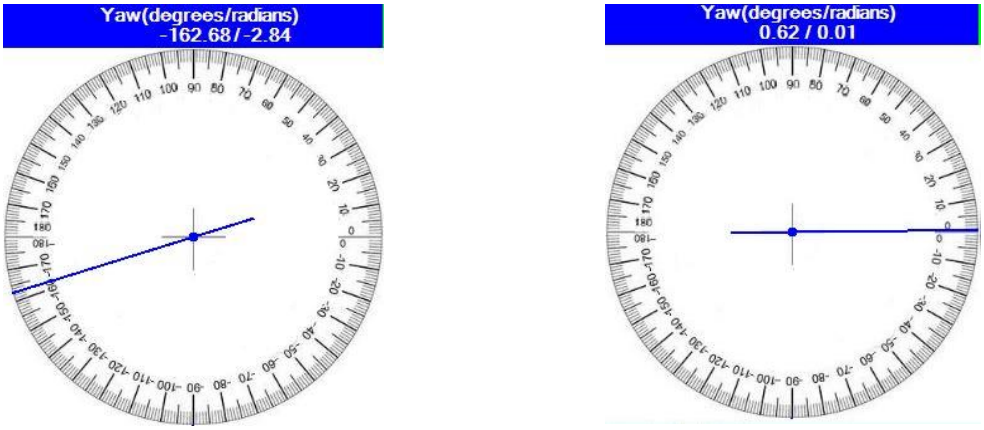

***Figure 5.1**. Yaw before and after calibrated*

2.2.2. Data Before and After Calibration

The main purpose of this part is process MEMS INS data in static mode to apply in movement measuring of object in next part. IMU is placed on flat surface and the X axis points to the North, Y axis points to the East and the Z axis points down, during measure Roll-Pitch-Yaw (RPY) data. RPY data before using DCM and calibration have very poor performance as shown on figure 6. In his case, the signals of roll, pitch and yaw were drifting rapidly. The data are not stable, increase and decrease continuously over time. At the interval of two minutes, deviation of roll is 50^0, pitch is 30^0 and yaw varies up to 120^0, as shown on the left of figure 6. This achievement led to big accumulating errors when calculating the rotation matrix element, thereby it causes major discrepancies in position of object.

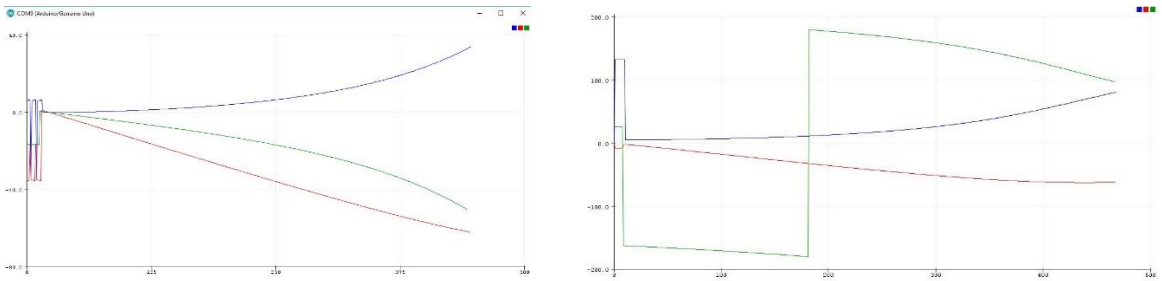

***Figure 6.** Accumulation error and flipping axes of RPY when not using DCM and calibration*

One more important problem happened is flipping axes phenomenon. This situation occurs when DCM algorithm and calibration aren't used. From that, roll, pitch and yaw angles have been

added accumulating error to be over $+180^0$ or -180^0, as shown on the right of figure 6, in which yaw data have been added accumulating error to be over -180^0 and become $+180^0$ in green line. That means if this MEMS INS is installed to control a drone, in this situation, without command but this drone will be flip one circle because of accumulating error.

After using DCM, we have better RPY without accumulation error as shown on the left of figure 7. The values of roll, pitch and yaw in static mode are not varied for long working time, but still have a little bit shifting data. The best results archived after calibration. With the same position, we got better data of RPY as shown on the right of figure 7, in which all of YPR data are zero and stable. During more than two minutes and longer, the roll (Green), pitch (Red) and yaw (Blue) data still are given out at nearly the same results. The maximum in data base logged on station changing values below 0.04^0 for roll, 0.06^0 for pitch, and 0.06^0 for yaw.

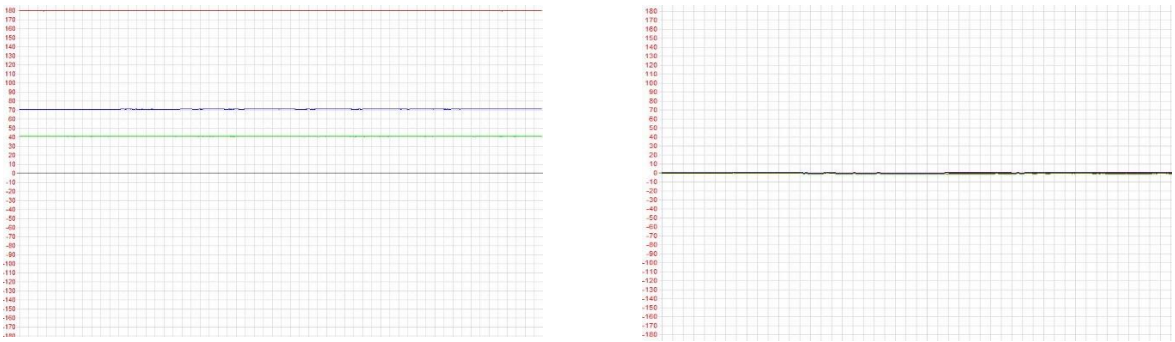

Figure 7. *RPY after using DCM and calibration*

These values are not being cumulative over time and automatically corrected. The measured values indicate that the data oscillate around equilibrium and stability during the working time of the MEMS INS. In second experiment, vibration unit is place on 110cc bike engine type. Figure 8 shows the vibration of engine run quite stable after started by roll data which can be used to monitor frequency of engine in automated vehicle as maximum of 14^0 when starting, and 2^0 when running normally. Note that with low speed internet, these data can not be pushed on internet to draw charts on time.

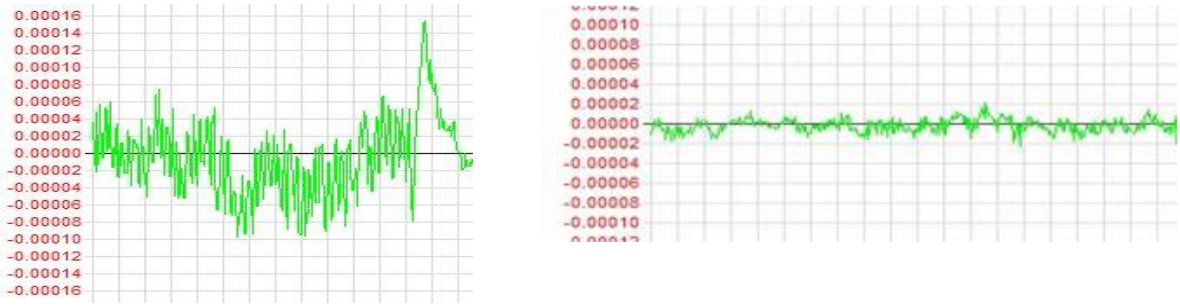

Figure 8. *Engine's vibration after starting and running normally*

2.3. Sensor Monitoring System

The fabricated board based on Arduino includes a XBee module and separate connectors for each MEMS INS SparkFun 9-DOF Sensor Stick or GY85 [8]. The structure of IoT system that forms this sensor's network includes Base Station (a), Sensor Nodes (b), and Master Arduino (c),

described below:

a) Base Station (Webserver): A server/personal computer will act as a webserver and store the data sent by the Arduino with the CC3000 shield installed. The Base Station receives the data then stores it in the MySQL database using a JSON script. We can also send simple command codes to the Arduino in case we include a command-sending function.

b) Sensor Nodes (Arduino with MEMS INS and a XBee module): Process and calculate Roll, Pitch, Yaw value in real time using values from the MEMS INS, and print out the results to Software Serial, sending the data over pre-configured XBee network. Data will be recorded including: accelerometer, gyroscope, magnetometer, Roll, Pitch, Yaw. These data will be sent to the master Arduino every 20 milliseconds.

c) Master Arduino (Arduino with CC3000 shield): The Arduino is set up to poll the Base station at a set interval. The Arduino sends a URI to the webserver that hosts the Base station. The URI includes a "id", which is a step counter for each polling session and the MEMS INS data. Due to the lack of buffer and interrupts in Arduino's Software Serial library, a minimum interval of 800 is suitable. There are three data handlers. The Master Arduino is currently using only one handler to conserve SRAM.

Data processing is described in figure 9, which can be divided into five different components, including Sensor Unit (a), XBee (b), Base Station (c), Data Base (d), and Data Visualization (e), as shown below:

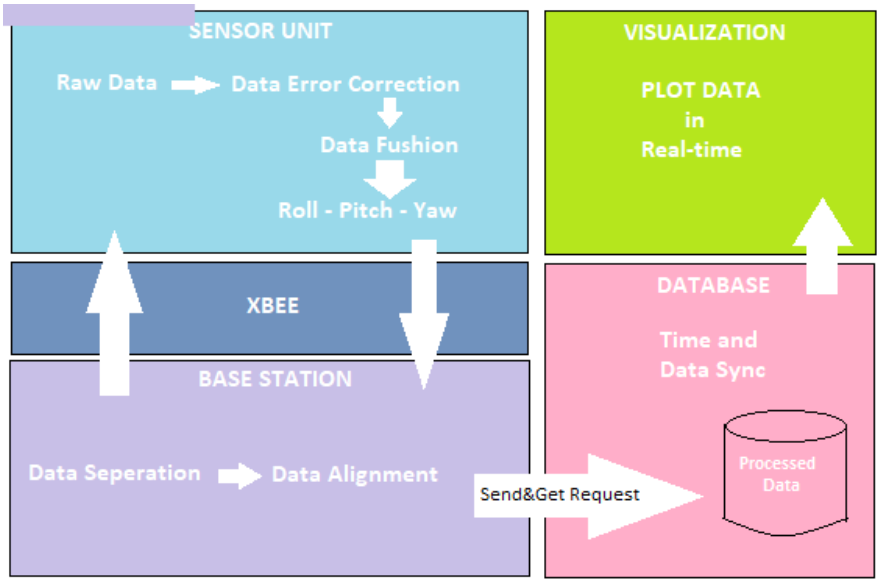

Figure 9. *Data processing model*

Firstly, raw data will be processed using algorithm in data fusion to remove error in output data. Then data is delivered to base station via Xbee module. Wireless platform is built following Star topology, where sensor node is router and base station is coordinator. When base station has confirmed received right data format, it starts separate needed data while CC3000 establishes connection to data base.

To perform this experiment, we firstly build a hotspot with free account. This is not fast

enough to have a real time vibration measurement. We use PHP as the primary server-side language with the Laravel framework and MySQL as the primary database management tool. CC3000 wifi shield establishes a connection to an address of a pre-set webserver and sends the GET requested enclosing a URI that sends the data needed to be sent, and then the webserver stores that data in SQL. In testing of a slow vibration and movement object, where data is synced, we have charts and data in the database after time synchronized measurement with time server as shown below:

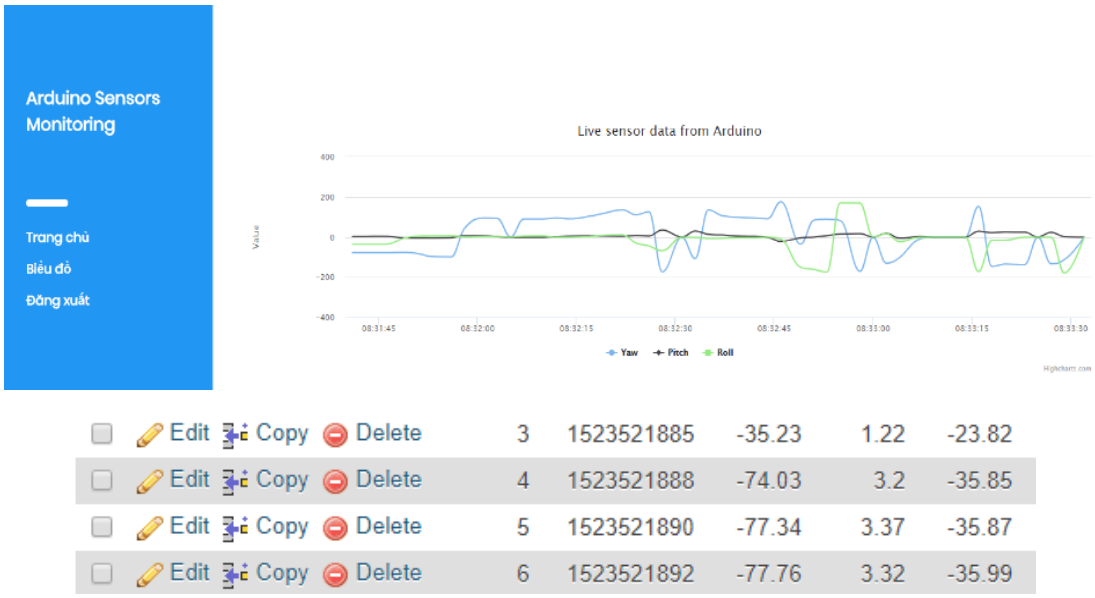

Edit Copy Delete	3	1523521885	-35.23	1.22	-23.82
Edit Copy Delete	4	1523521888	-74.03	3.2	-35.85
Edit Copy Delete	5	1523521890	-77.34	3.37	-35.87
Edit Copy Delete	6	1523521892	-77.76	3.32	-35.99

Figure 10. *Website interface and Data base*

On our experiment website, user will be provided an account to get access to their database and monitor data. However, our website is currently still in alpha testing, and the responsive between webserver and base station is limited.

III. CONCLUSION

Based IoT, sensor monitoring system has shown the visibility of slow vibration, both of angular angles and movement. From there information we can see the condition, how good of performance of monitored object. Using economy MEM INS 9-DOF IMU, we developed calibration and data processing methods to show the effectiveness in measuring states. Further, this system can be developed by integrated GPS module to create an advanced positioning and management system, worked as AHRS system applying in many fields such as transportations, military, aerospace, maritime, earthquake monitoring, and vibration measurement at factories.

In fact, with low speed internet and not very fast equipment, this system is slow and not very suitable for on-line vibration measurement. That's why we just have tests with vibration objects at local station without pushing data to internet, and slow movement objects when pushing data on internet is required. This problem will be solved easily in case of using high speed internet and faster equipment. However, with this system, we can also use this Base station in a lot of applications, such as equip the Sensor nodes with suitable sensors to monitor temperature,

humidity, sound, light levels, or adding command parameters to make a two-way system if a user want to operate systems such as fans or watering system in a smart garden. Scripts can be incorporated to the PHP files to process all kinds of information gathered from the internet.

In transport and communication field, by using faster internet and equipment, these systems are presented as measurement equipment controlling and warning movement of bridges, abutments, and stay cables oscillation. These systems measure oscillation, shaking and twisting data. Based on these data, they can give out warnings about the bridge's safety. These kinds of measurement devices can be used on small bridges as well. They can also be used on automated railway oscillation and speed monitor, making sure trains run safely and preventing incidents.

In Vietnam, high-speed and elevated railways are developing day by day. These systems are getting special interest. Researching to design these devices is a great direction for transport infrastructure. This is a forestalling technology for the elevated rail system. MEMS INS devices are also integrated with GPS installed on its black boxes for special road vehicles. These devices can not only help in managing accurately speed and trajectory, but also manage the vehicles' movement status such as shakes, acceleration, rotation angle and navigation to rate the driver's behavior and driving style.

References

[1]. *Ngo Thanh Binh, Nguyen Canh Minh, Le Minh Tuan* (2017). INS Data Processing and Application in Drone Balance Control. Science Journal of Transportation-No.8, pp. 69-77.

[2]. *D. Vujicic, R. Pavlovic, Z. Cvetkovic, S. Randic and D. Jagodic* (2017), Telescope Pointing Based on Inertial Measurement Unit. Serb. Astron. J. No.194, pp. 101 – 107.

[3]. *Vishwatheja S., Venkataratnam P., Siva Yellampalli* (2016). The soft iron and hard iron calibration method using extended Kalman filter for attitude and heading reference system. International Research Journal of Engineering and Technology (IRJET), pp. 179 – 182.

[4]. *N. H. Q. Phuong, H.-J. Kang, Y.-S. Suh, and Y.-S. Ro* (2009). A DCM based orientation estimation algorithm with an inertial measurement unit and a magnetic compass. Journal of Universal Computer Science, Vol. 15, No. 4, pp. 859–876.

[5]. *William Premerlani, Paul Bizard and Sergiu Baluta*. DCM tutorial - An introduction to orientation kinematics. Starlino Electronics, USA 2009. Available online: http://www.starlino.com/dcm_tutorial.html. (Retrieved on 14th July 2018).

[6]. *Peter Bartz*. Ahrs firmware for the sparkfun 9dof razor imu and sparkfun 9dof sensor stick. Available online: https://github.com/Razor-AHRS/razor-9dof-ahrs (Retrieved on 14th July 2018).

[7]. National Intelligence Council. Disruptive Technologies - Six Technologies with Potential Impacts on US Interests Out to 2025. (2008). Available online: http://www.fas.org/irp/nic/disruptive.pdf (Retrieved on 14th July 2018).

[8]. *Robert Faludi* (2010). Building Wireless Sensor Networks. O'Reilly books, pp. 40 – 56.

TOWARDS AUTOMATIC PARKING SYSTEMS FOR VEHICLES

VU VAN TAN[1], OLIVIER SENAME[2], PHAM TAT THANG[1], DAO MANH HUNG[1]
[1]*University of Transport and Communications, Hanoi, Vietnam*
[2]*Univ. Grenoble Alpes, CNRS, GIPSA-lab, Control Systems Dpt, Grenoble, France*
Corresponding author's email: vvtan@utc.edu.vn

Abstract: *Automatic parking is an autonomous vehicle-maneuvering system that moves a vehicle from a traffic lane into a parking space to perform parallel, perpendicular, or angular parking. Nowadays, this system is being used extensively in some modern vehicles. This paper deals with the construction of the vehicle trajectory in a parallel parking situation, when there are two vehicles already parked in front of and behind the desired parking position. By using the side, front and rear sensors around the vehicle, the automatic parking system can change the combination between the steering, braking systems and the vehicle speed. The initial results are visually simulated by the Matlab/Simulink software.*

Keywords: *Automatic parking system, Path planning, Trajectory planning, Vehicle dynamics, Automotive control*

I. INTRODUCTION

Over time the population in major cities has been increasing steadily, and therefore also the number of vehicles, especially cars, has increased significantly compared with the previous century. There are over 1.3 billion vehicles in use over the world, which is expected to increase even more in the coming years. However, the area of parking spaces is very limited, which makes it difficult to park vehicles. Because of that, the study of the automatic parking system is of great interest to well-known vehicle manufacturers and brands in the world and has been applied in practice in some luxury cars such as Ford, BMW, Audi, etc.

The automatic parking system aims to enhance the comfort and safety of driving in constrained environments where much attention and experience is required to correctly steer the vehicle [1]. Although some research has been carried out on the development of parking assistance systems, however the fully automatic algorithm has not been investigated yet [2]. The general parking algorithm consists of 3 steps [3], [4]:

First step: Building a local map from the parking space, based on the information of the empty slot which can be obtained from sensor data or vision systems. So in this step, the parking space dimensions can be detected by navigating the vehicle forward or backward.

Second step: Reaching a ready-to-reverse position while plotting the orientation parallel to the parking space.

Third step: Planning the motion that brings the vehicle from its initial posture to its goal parking position. This motion planning problem has been widely investigated and is still not solved in a satisfactory way.

In this paper, the authors initially investigate the case of vehicles in parallel parking, assuming that the sensors are perfect, and the vehicle velocity is adjusted to the steering angle. We focus mainly on building the ideal vehicle trajectory for parallel parking and this is simulated in the Matlab environment.

II. AUTOMATIC PARKING SYSTEM ON VEHICLES

There are four basic types of parking that we need to consider is: (1) forward garage parking, (2) backward garage parking, (3) forward parallel parking, (4) backward parallel parking option [3], is described in figure 1. In addition to the above cases, we also need to mention the case of the angular parking.

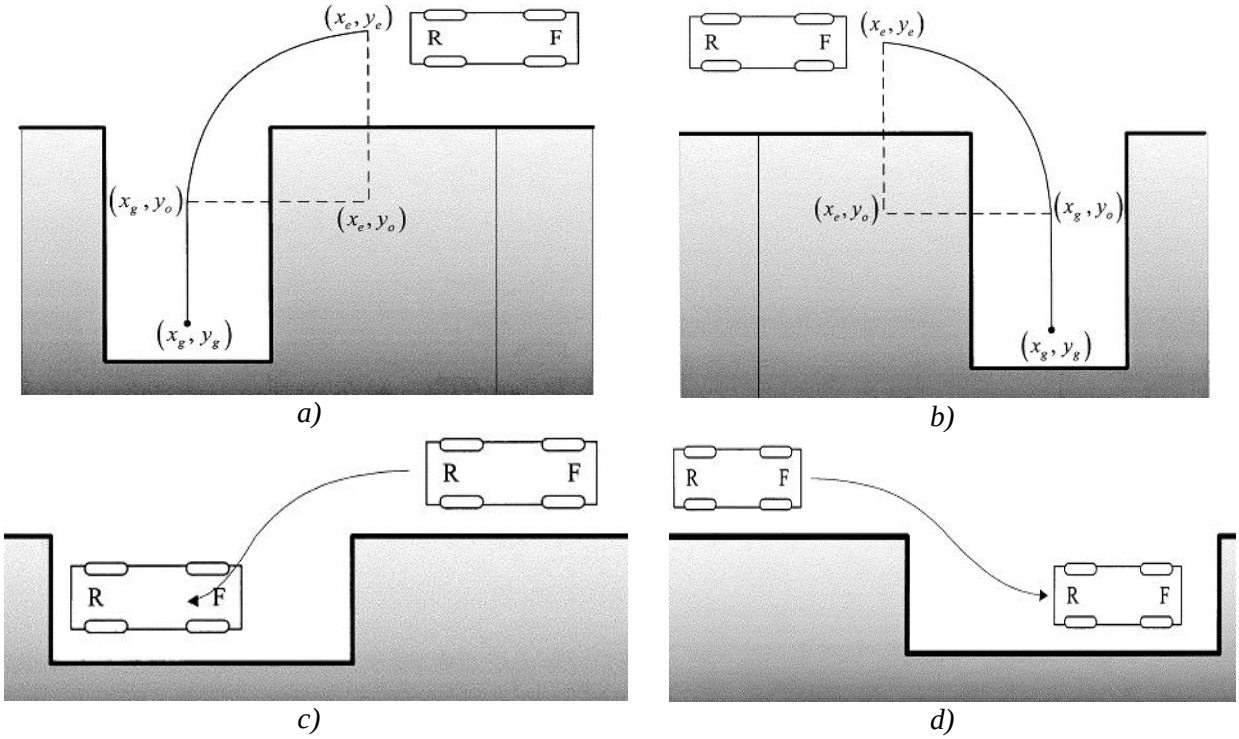

Figure 1. *Reference trajectories for (a) forward garage parking, (b) backward garage parking, (c) forward parallel parking and (d) backward parallel parking*

The automatic parking system works based on the sensor information of the free space size (empty slot), the relative position of the vehicle to the parking position and other vehicles already parked. The two sensors employed in this system are the distance sensor and rotary encoders. The ultrasonic distance sensors are active type sensors. This sensor determines the perpendicular distance of an object or a body from the point of their placement, from the time of movement [1]. These sensors are placed on the outer body above the wheels symmetrically on either side, as shown in figure 2.

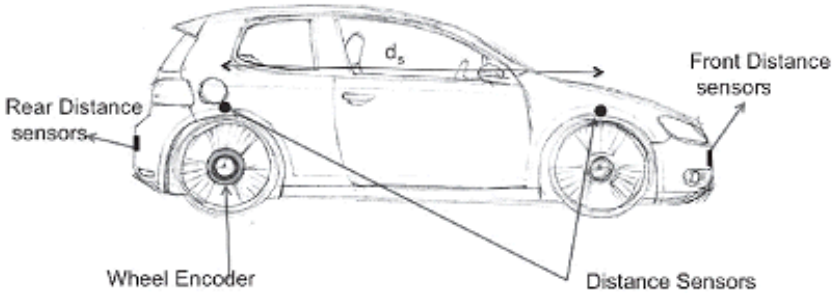

Figure 2. *Placement of sensors on a car*

An intuitive way of describing the movement of vehicles for parking progress is shown in Figure 3. Nowadays, modern generations of vehicles have applied this system in a relatively efficient way, especially in the Northern European automobile market. Most of them use the fuzzy control method to park the car [5-8]. In the rest of this paper, we focus on the forward parallel parking case.

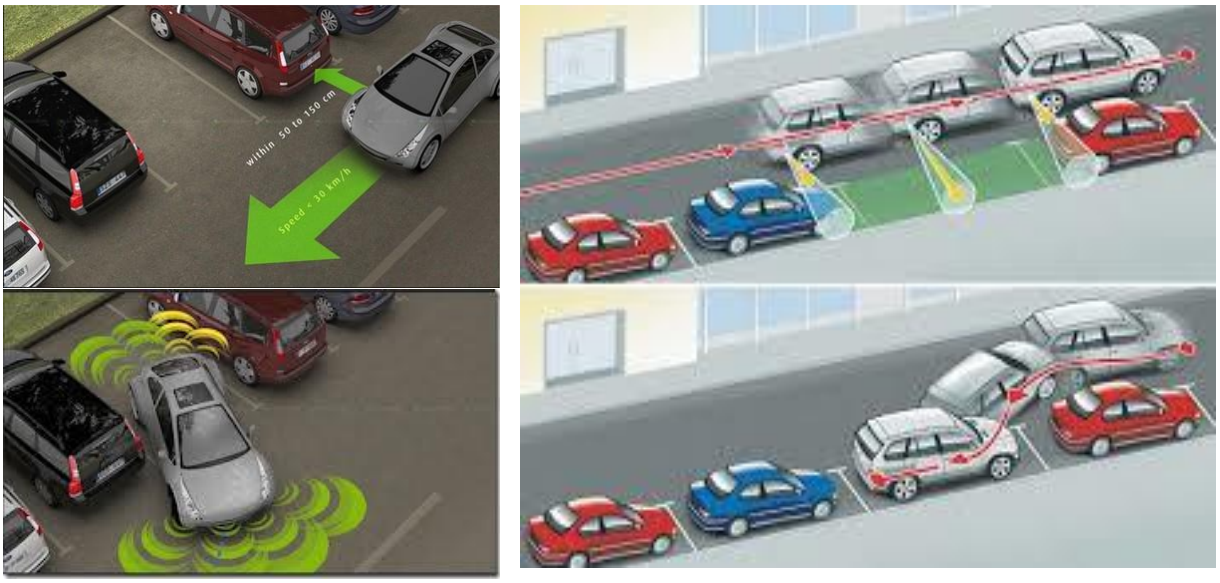

Figure 3. *Describing the vehicle movement for parking progress*

III. PATH PLANNING AND KINEMATIC EQUATIONS FOR THE FORWARD PARALLEL PARKING

The path planning involves simple geometrical equations in the automatic parking system. The path that the vehicle travels before maneuvering into the parallel parking space, perfectly aligned, has three main differentiable phases to consider. The first phase is the straight forward line and the other two phases are the arcs of circles. The whole parking trajectory is calculated only from the knowledge of the distance between the parking vehicle and the vehicle already parked which is obtained from the distance sensors [1]. All other parameters required from path planning are either constant or are derived from the above-mentioned distance parameter using equations explained further in this section.

3.1. Parking path geometry for the forward parallel parking

The vehicle trajectory in the forward parallel parking is described in figure 4. The three main

phases are described as follows:

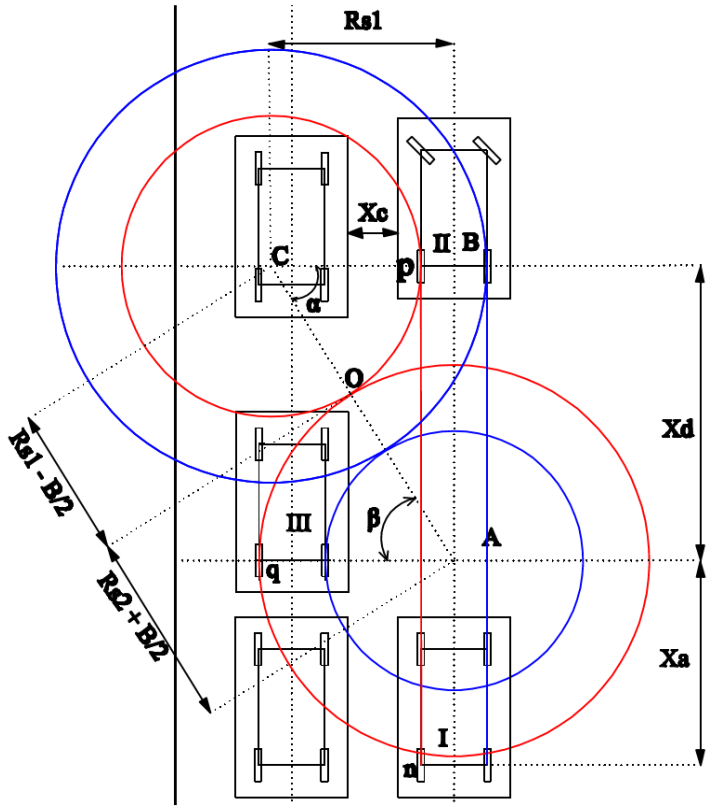

Figure 4. *Path planning and parking trajectory of the forward parallel parking*

+ **Phase I - The vehicle is in straight forward motion:** In this phase, the vehicle is tasked with finding the parking position (determining the parking position and the relative position of the vehicle to the parking space as well as the vehicle already parked). At the end of this phase, the vehicle moves to position B, then switches into the reverse number of the gearbox, turn the steering wheel to the left with the angle of 45^0.

The distance that vehicle travels in phase I is determined as follows [9]:

$$X = X_a + X_d \tag{1}$$

Where:
$$X_d = \sqrt{\left(R_{s1} + R_{s2}\right)^2 - R_{s1}^2} \tag{2}$$

+ **Phase II -** The vehicle turns into the left, with the turning point C and the steering angle is kept constant at 45^0. At the end of phase II, the left rear wheel stays at the point O.

The rotation angle of the rear axle is defined as follows:

$$\alpha = \beta = \tan^{-1}\left(\frac{X_d}{R_{s1}}\right) \tag{3}$$

The left rear wheel moves in a circular arc Op: $$Op = \frac{\alpha}{360} 2\pi \left(R_{s1} - \frac{B}{2}\right) \tag{4}$$

Where B is the distance between the points of contact of the rear wheels.

+ Phase III - The vehicle turns into the right, with the turning point A and the steering angle is change to -45^0 compared to the phase II. By the end of phase III, the vehicle is parallel to the parking space (pavement).

The left rear wheel moves in a circular arc Oq:

$$Oq = \frac{\beta}{360} 2\pi \left(R_{s2} + \frac{B}{2} \right) \quad (5)$$

In addition to the three main phases above, this system will add another phase to move the vehicle into the center of the parking space. We can call that Phase IV.

3.2. Simulation results for the forward parallel parking

Based on the parking path geometry as explained in the previous section, in this section we use the Matlab software to accurately describe the process of moving a vehicle into the parking space for the forward parallel parking manoeuvre. We have two vehicles already parked, denoted in red and blue. Figure 5 shows the four phases of the forward parallel parking manoeuvre.

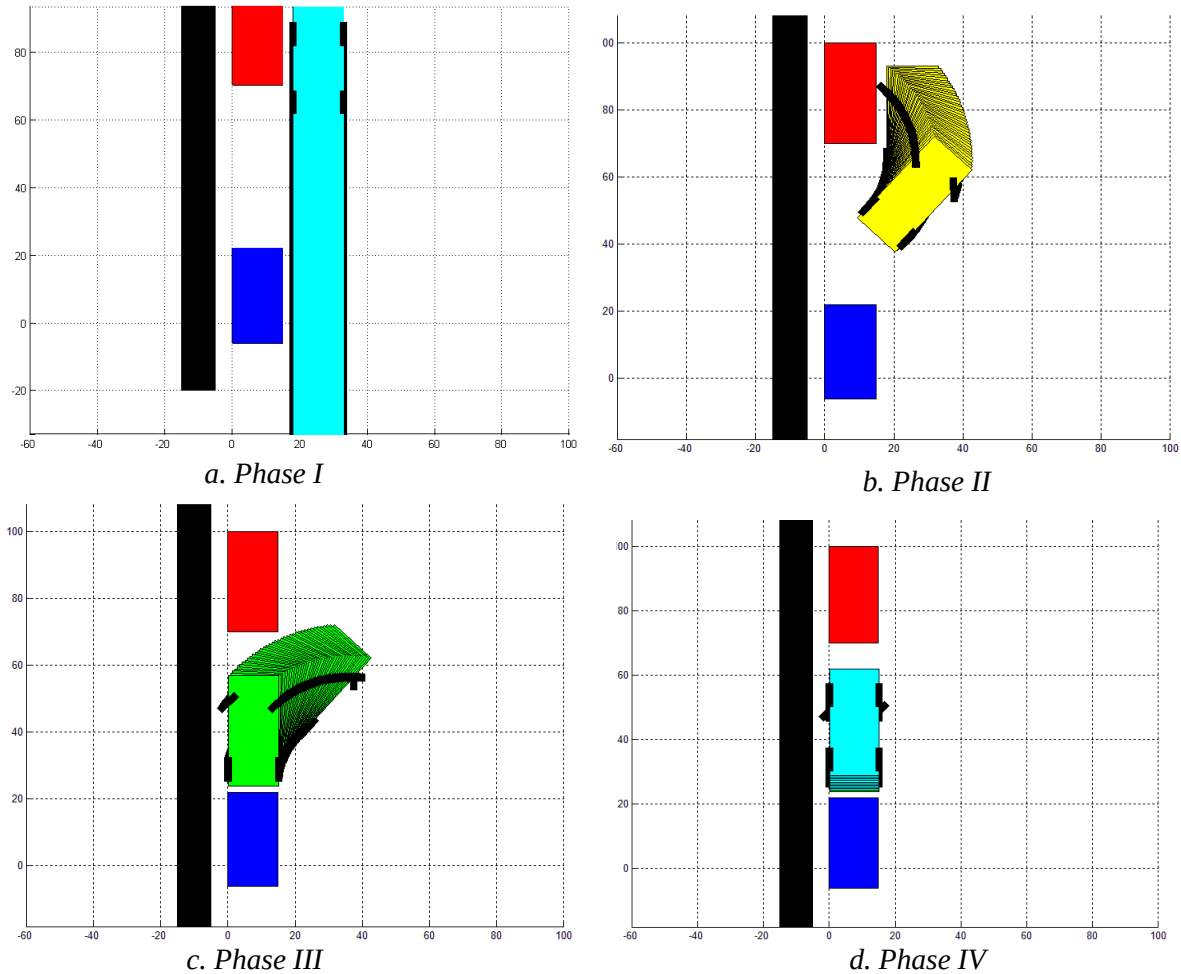

a. Phase I *b. Phase II*

c. Phase III *d. Phase IV*

Figure 5. *Vehicle trajectory in the forward parallel parking*

III. CONCLUSION

The automatic parking system is being studied and applied to some modern vehicles. In this paper, the authors initially approached this system and determining the vehicle trajectory and successfully simulating the principle of this system in the case of the forward parallel parking is the basis for perfecting the necessary manoeuvres in every parking situation.

In the future, we will apply advanced control methods to simulate the vehicle model taking into account the steering system. The purpose is to move the controlled vehicle to being closest to the ideal trajectory that is proposed in this paper.

Acknowledgements

The authors acknowledge the support of the French Embassy in Vietnam for the project "**Intelligent and autonomous vehicles for improving transport and road safety in Vietnam**".

References

[1]. *Ankit Gupta and Rohan Divekar*, "Autonomous parallel parking methodology for Ackerman configured vehicles", International conference on control, communication and power engineering, 2010.

[2]. *Emese Szadeczky-Kardoss and Balint Kiss and Istvan Wahl*, "Design of a Semi-Autonomous Parking Assist System", In European Control Conference, 2009.

[3]. *Shih-Jie Chang and Tzuu-Hseng S. Li*, "Autonomous Fuzzy parking control of a car-like mobile robot", IEEE Transactions on systems - man - cybernetics, Volume 33(4), 2003.

[4]. *Oliver Bühler and Joachim Wegener*, "Automatic Testing of an Autonomous Parking System using Evolutionary Computation", SAE International, 2004.

[5]. *Tarik Ozkul and Mohammed Mukbil and Suheyl Al-dafri*, "A Fuzzy Logic Based Hierarchical Driver Aid for Parallel Parking", 7th International conference on Artificial Intelligence, Knowledge Engineering and Databases, 2008.

[6]. *Sh. Azadi and Z. Taherkhani*, "Autonomous parallel parking of a car based on parking space detection and fuzzy controller", International journal of automotive engineering, Volume 2(1), 2012.

[7]. *Chen-Kui Lee and Chun-Liang Lin*, "Autonomous Vehicle Parking Using Artificial Intelligent Approach", 4th International Conference on Autonomous Robots and Agents, 2009.

[8]. Admed Hechri and Anis Ladgham and Faycal Hamdaoui and Abdellatif Mtibaa, "Design of fuzzy logic controller for autonomous parking of mobile robot", International journal of sciences and techniques of automatic control and computer engineering, Volume 5(2), 2011.

[9]. *Sungwoo CHOI and Clément Boussard and Brigitte d'Andréa-Novel*, "Easy Path Planning and Robust Control for Automatic Parallel Parking", Proceedings of the 18th World Congress - The International Federation of Automatic Control Milano (Italy) August 28 - September 2, 2011.

WIRELESS MONITORING OF VEHICLE ON ROAD USING A FLEXIBLE ORGANIC PRESSURE PASSIVE SENSOR AND A TABLET

DAO THANH TOAN[1,2]
[1]Faculty of Electrical-Electronic Engineering, [2]Vietnam-Japan Research and Development Center
University of Transport and Communications, Hanoi, Vietnam
Corresponding author's email: daotoan@utc.edu.vn

Abstract: *Monitoring of vehicle on the road can lead to establish an intelligent transportation system for smooth transportation and reduced road accidents. The embedded sensor on the road is one of the key technologies of the non-intrusive monitoring. This paper presents the flexible sensor for the vehicle sensing and demonstrated the wireless system for monitoring vehicle on the road. A 100mm-thick polyurethane film was sandwiched by top/bottom electrodes to complete the flexible pressure sensor fabrication. A clear response against a pressure load of 0.7 N/mm2 was observed, which is same pressure as that at car-tire area contacted with road. The field test was carried out by embedding the sensor on the road and crossing the sensor by a car. And the signal displaying on the tablet indicates that the sensing system can be well used for wireless monitoring of the vehicle on the road.*

Keywords: *Flexible organic pressure sensor, wireless DAQ, non-intrusive monitoring*

I. INTRODUCTION

Traffic monitoring is one of the essential technologies in the traffic engineering to ensure smooth transportation and to reduce road accidents, where non-intrusive and intrusive sensors are often employed for the monitoring [1]. As for the monitoring by non-intrusive sensor, vehicle sensing by means of pressure sensors embedded in the road has been one of the research targets. In particular, the application of printed flexible pressure sensors fabricated from organic/polymer materials would be promising thanks to its advantages of mechanical-flexibility and low-cost of fabrication. On the other hands, recent study on the flexible pressure sensor has been mainly focusing on the research field of human healthcare [2] and structural health monitoring (SHM) [3, 4]. The application of the sensors in the research field of SHM suggests us that the flexible sensors are compatible to be embedded in the construction including building and road. However, to our best knowledge, so far, there is no report on application of flexible pressure sensor in the research field of the traffic engineering.

In this paper, a fabricated flexible organic pressure sensor connected with a wireless data acquisition (DAQ) system is presented. And a tablet computer-based application (App) is also developed for the monitoring. The real-time vehicle sensing has successfully achieved by the sensor the with the wireless DAQ system embedded on the road and the tablet computer.

II. EXPERIMENTAL PROCEDURE

Figure 1 shows the device structure and photo of the flexible sensor. A 100-μm-thick organic film of polyurethane was employed as a sensing layer, which was sandwiched between two electrodes of Aluminum foil, following by laminating at 80 ^{o}C for twice. The sensor size is 70×70 mm^2. For protection, the sensor was also covered with a plastic film by lamination method at 80 ^{o}C. Finally, a copper wire was attached to electrode to form the connecting lead of the sensor. To examine the influence of the sensing thickness, the devices with different film thicknesses of polyurethane (200, 300, and 500m) were also fabricated. The characterization of the sensors was performed using a universal compression testing machine (UH 500-kN, SHIMADZU) and a capacitance meter (YF-150, Tenmars Electronics) at room temperature. The dynamic range of the sensor was tuned to be varied from 0 to c.a. 1.0 N/mm^2, which is same pressure as that at car-tire area contacted with road.

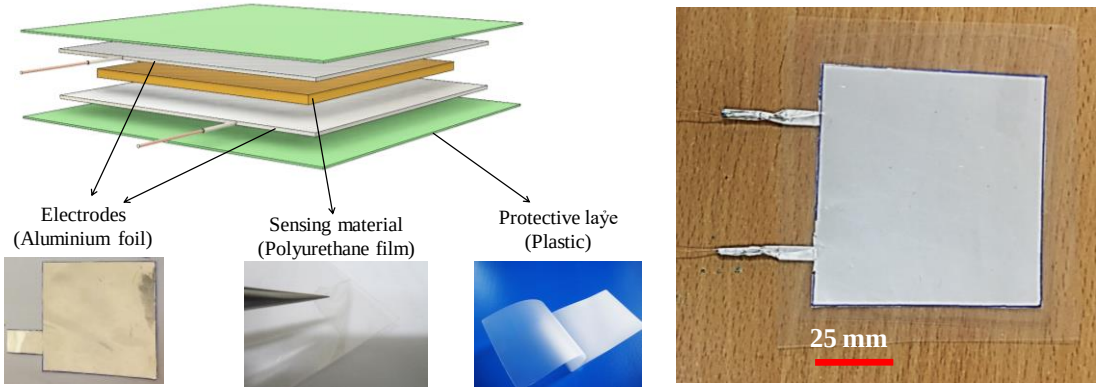

Figure 1. *Device structure and photo of flexible pressure sensor*

III. RESULT AND DISCUSSION

Figure 2 shows the capacitance-pressure characteristics of the sensors. The steep increment of capacitance was observed at low-pressure region and the increment tended to saturate with increasing applied pressure (P). These characteristics are typical among the capacitive sensors [5,6]. It should be noted that the pressure range at around 0.7 N/mm^2 is same as the pressure that at car-tire area contacted with road. And thus, we confirmed that the sensors are durable for the pressure and available for the vehicle sensing. In order to be quantitative the influence of sensing thickness, the effective capacitance change was estimated with the equation:

$$\frac{\Delta C}{C_0} = \frac{C_{max} - C_0}{C_0} \quad (1)$$

Where C_{max} is the capacitance at P = 0.7 N/mm^2, and C_0 is the capacitance at P = 0. We found that the $\Delta C/C_0$ significantly decreased from 1.070 to 0.274, 0.172 and 0.116 when the polyurethane thickness increased from 100 to, 200, 300 and 500 μm, respectively. This is could be due to the fact that the reduction in the distance between the top and bottom electrodes in a thin

device is more considerable.

The sensitivity (S) was calculated using the equation:

$$S = \frac{\delta(\Delta C / C_0)}{\delta P} \quad (2)$$

The S at three pressure ranges and different film thicknesses is shown in table 1.

The thinner device exhibits a higher S, which results from its factor of $\Delta C/C_0$ is higher. The S values at range of 0.2-0.6 N/mm^2 for each device are 1.18×10^{-4}, 5.57×10^{-5}, 5.07×10^{-5}, and 8.35×10^{-5}, respectively. Overall, the 100μm-based sensor exhibits the best performance in terms of the $\Delta C/C_0$ and S. Significantly, the S obtained from the 100 μm based-sensor up to 8×10^{-2} kPa^{-1} at 0.003 N/mm^2, which can be comparable to that in previous pressure sensor systems [7, 8].

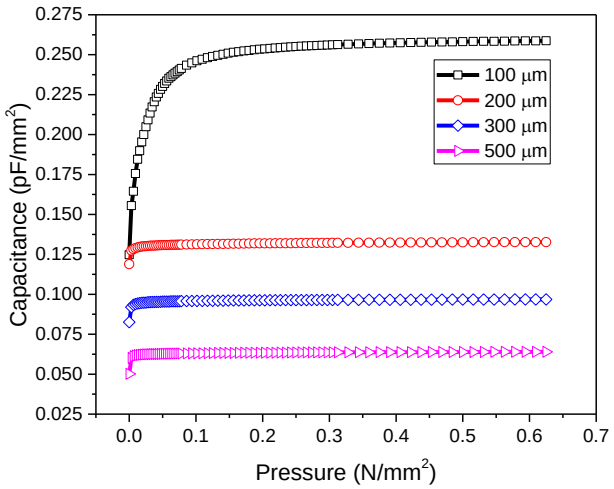

Figure 2. *Capacitance-pressure characteristics of 100μm-based sensors. Inset shows capacitance-pressure characteristics of 200, 300, and 500μm-based sensors*

Table 1. *Sensitivity at different pressure ranges or film thicknesses*

Pressure range (N/mm^2)	Sensitivity (kPa^{-1})			
	t = 100 μm	t = 200 μm	t = 300 μm	t = 500 μm
0-0.03	2.42×10^{-2}	3.40×10^{-3}	5.33×10^{-3}	8.77×10^{-3}
0.03-0.2	2.98×10^{-3}	1.64×10^{-4}	1.89×10^{-4}	2.30×10^{-4}
0.2-0.6	1.18×10^{-4}	5.57×10^{-5}	5.07×10^{-5}	8.35×10^{-5}

In order to confirm the reproducibility of the change in capacitance values under constant P, the repeatable properties of the sensor in response to constant P of 0.7 N/mm^2 were checked with the 100 μm based-sensor (fig. 3). The capacitance at P = 0.7 N/mm^2 showed good reproducibility. In contrast, capacitance at P = 0 N/mm^2 was not returned to the initial value when the pressure was released. This would be due to the deformation of the polyurethane film. However, from the second cycle, the repeatable characteristics were well observed as shown in fig. 3.

For the purpose of the field test using the flexible pressure sensor, a completed electronic system using the sensor, a wireless DAQ was designed with a circuit diagram presented in Fig. 4, where a NE555 based-oscillator is utilized to convert the sensing capacitance to a pulse train. The capacitance is computed from the frequency value of the pulse train with a microcontroller of ATmega328P and sent to a tablet PC via a wireless Bluetooth module of HC-05. A tablet App

written with Android Studio allows to real-time display the sensed signal and to export the data in an Excel format for further analyses.

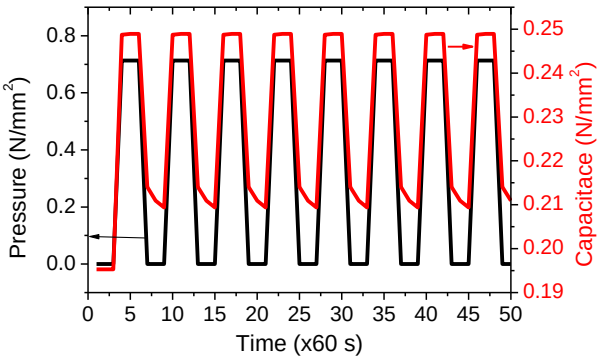

Figure 3. *Endurance cycle test of 100 μm-based sensor in response to constant P of 0.7 N/mm^2*

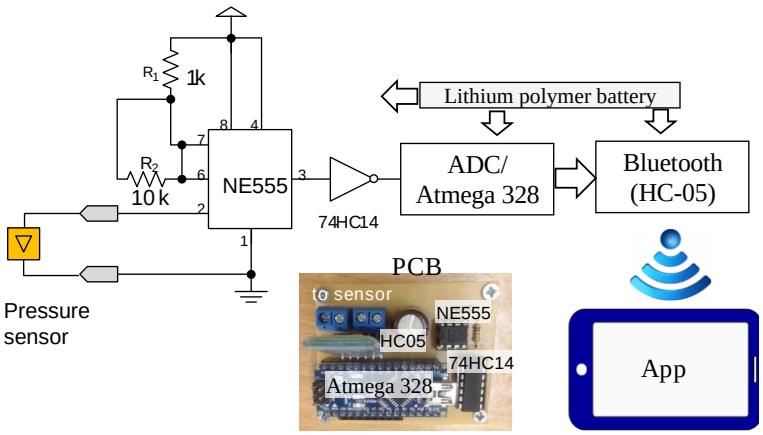

Figure 4. *Diagram of wireless DAQ. Inset shows printed circuit board (PCB). Size of PCB is 65×45 mm^2*

Figure 5 shows a field test of the vehicle sensing using the system, where the sensor was embedded between the paper hardcover and mounted on the road line. The sensor is easily mounted on the road due to its advantage of flexibility.

The typical sensed signals displaying on tablet are shown in fig. 6. The signal level is low in the normal state (fig. 6a). And rapidly increase of the signal level was successfully observed on the screen of tablet when the vehicle was crossed on the sensor (fig. 6b). When the vehicle moves off the sensor, the signal returned to the initial as shown in fig. 6c.

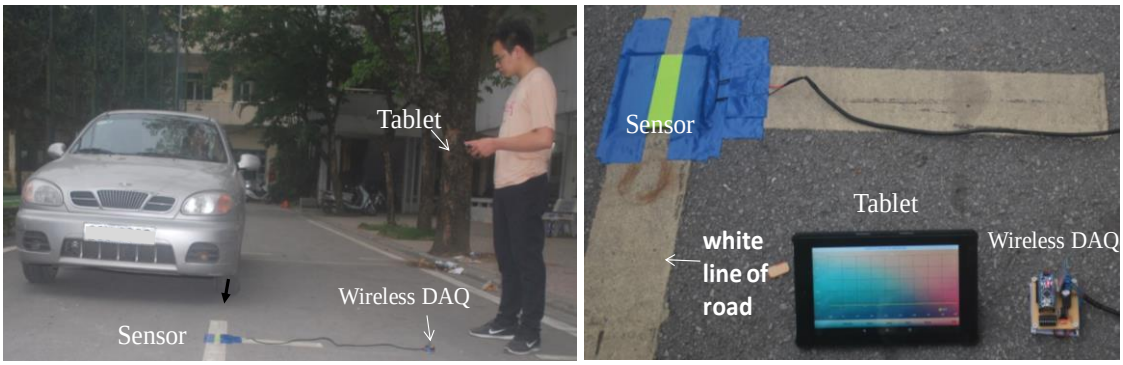

Figure 5. *(left) Experimental overview of vehicle sensing using the system and (right) close-up view of sensor mounted on road*

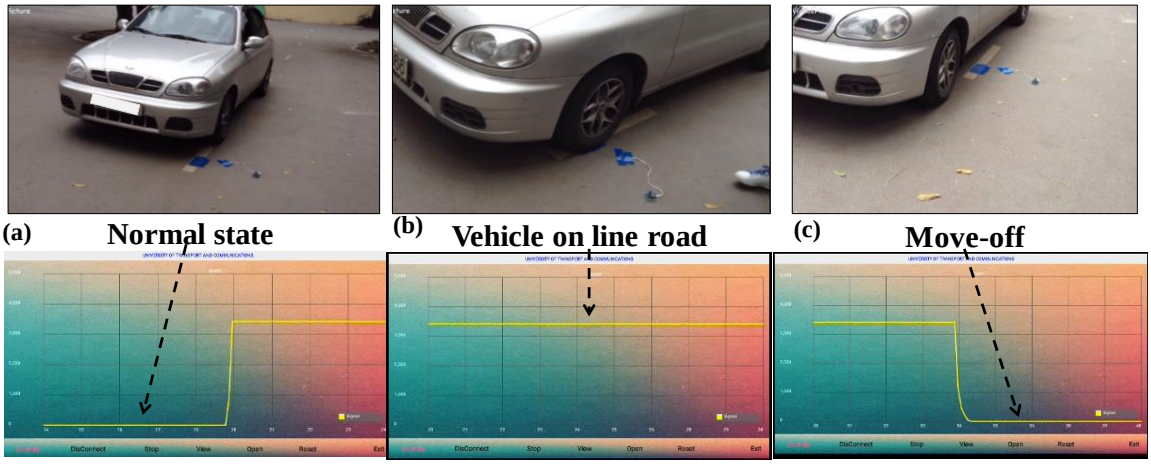

Figure 6. *Change in signal by App on tablet at (a) normal-state, (b) vehicle on line of road, and (c) move-off*

IV. CONCLUSION

In conclusion, the flexible sensor for the vehicle sensing together with the wireless system for monitoring vehicle on the road have been demonstrated. Owing to its mechanical-flexibility and large-size ability, the sensor is easy to be embedded on the road line. The App on tablet computer can help to observe the detection of car on the sensor. The experimental achievements suggest that the sensing system including flexible pressure sensor, wireless DAQ and App would be promising system in the research field of the traffic engineering as the next-generation low-cost technology for monitoring the vehicle state on the road.

Acknowledgements

This work was funded by Vietnam National Foundation for Science and Technology Development (NAFOSTED) under grant number "103.02-2017.34".

References

[1] *J. Guerrero-Ibanez, S. Zeadally, and J. Contreras-Castillo*, "Sensor technologies for intelligent transportation systems", Sensors 18 (2018) 1212.
[2] *T. Sekine et al*., "Fully printed wearable vital sensor for human pulse rate monitoring using ferroelectric polymer", Sci. Rep. 8 (2018) 4442.
[3] *A. Seppanen, M. Hallaji, and M. Pour-Ghaz*, "A functionally layered sensing skin for detection of corrosive elements and cracking", Struct. Health Monit. 16, (2017) 215.
[4] *S. Laflamme, F. Ubertini, H. Saleem, A. D. Alessandro, A. Downey, H. Ceylan, and A. L. Materazzi*, "Dynamic characterization of a soft elastomeric capacitor for structural health monitoring", J. Struct. Eng. 141 (2015) 04014186.
[5] *S.-H. Shin et al*., "Integrated arrays of air-dielectric graphene transistors as transparent active-matrix pressure sensors for wide pressure ranges", Nat. Commun. 8 (2017) 14950.
[6] *Dao Thanh Toan*, "Soft pressure sensor using polymer material for strurural health monitoring", UTC Journal of Transportation Science and Technology, 2017 (Tạp chí KH GTVT, in Vietnamese).
[7] *W. Choi et al.*, "Enhanced sensitivity of piezoelectric pressure sensor with microstructured polydimethylsiloxane layer", Appl. Phys. Lett. 104 (2014) 123701.
[8] *S. Baek et al.*, "Flexible piezocapacitive sensors based on wrinkled microstructures: toward low-cost fabrication of pressure sensors over large areas", RSC Adv. 7 (2017) 39420.

OPTIMIZATION OF A COMPLEX URBAN INTERSECTION USING OPEN-SOURCE SIMULATION SOFTWARE AND MINIMIZING QUEUE LENGTHS METHODS

DO VAN MANH[1], LIANG-TAY LIN[1], PEI LIU[2]
[1]College of Construction and Development, [2]Office of International Affairs
Feng Chia University, Taichung, Taiwan
Corresponding author's email: manhdv@utc.edu.vn

Abstract: *This study aim to determine the best resolution to simulate the complex urban intersection by open- source software specifically SUMO software and also suggest these algorithms to minimize the count of idling automobiles at the intersection referring to queue lengths. Traffic congestion has become a serious problem in many countries, specifically in urban transportation. The main problem occurs at the intersections. One of the solutions that can be proposed to reduce is to implement traffic signal control strategy at the intersection [1]. There are mix variety of strategies to control traffic at the intersection but the optimal solution is traffic simulation by using software and algorithms to find the performance index that has a big impact on traffic jam in peak period. The benefits of open source are tremendous and have gained huge popularity in the field of IT and traffic simulation in recent years. This is mainly because the advantages of open-source software is that it's free to use and its greatest advantage. As it is developed by a non-profit community and SUMO software is an example. SUMO is an open source traffic simulation package including net import and demand modelling components. SUMO helps to investigate several research topics e.g. route choice and traffic light algorithm or simulating vehicular communication [2]. Besides this point, this paper also showed the methodology to find the optimal algorithm based on the information of incoming traffic and the current signal timing plan which can be used to predict queue lengths and the number of queuing vehicles for every second or other time interval assigned according to the needs of a traffic control centre to input into SUMO for optimization of the complex urban intersection purpose.*

Keywords: *Insert up to five keywords here, Times New Roman font, 11-point size, left-justified.*

I. INTRODUCTION

Open source software (OSS) is crowd-sourced. As a result it has benefits cost, flexibility, freedom, security, and accountability that are unsurpassed by proprietary software solutions. OSS also has long-term viability and is always on the cutting-edge of technology. It's created and supported by a worldwide community of organizations and individual developers, many of

whom also live by open source values like collaboration and volunteerism. In Intelligent Transport System (ITS) specifically for the coordination at intersection Sumo software is a brilliant idea to control, manage and find the optimal solution for reducing traffic congestion purpose at the complex intersection.

The German Aerospace Centre (DLR) started the development of the open source traffic simulation package SUMO back in 2001. SUMO is a microscopic traffic simulation which means that each vehicle is modeled explicitly. Independently configurable models are used to define different aspects of each vehicle's driving dynamics. Multiple car-following models which describe longitudinal movements are implemented and there are also multiple lane-changing models for defining lateral movements [4]. Since then SUMO has evolved into full featured suite of traffic modelling utilities including a road network capable to read different source formats, demand generation and routing utilities from various input sources (origin destination matrices, traffic counts, etc.), a high performance simulation usable for single junctions as well as whole cities including a "remote control" interface (TraCI) to adapt the simulation online [2].

Moreover, TraCI tool is the short term for "Traffic Control Interface" giving access to a running road traffic simulation, it allows to retrieve values of simulated objects and to manipulate their behavior "on-line". Conventionally, traffic simulations are helping in the design and development of both, strategic actions as well as road infrastructure changes. Consequently, established commercial traffic simulations have incorporated pedestrian and/or bicycle dynamics in recent years [5]. The most traffic simulation important is optimal signal timing for simulation of real-life networks transportation, specifically for the complex intersection. Traffic signals at intersections exist to keep traffic safe, both for automotive and pedestrian traffic. Intersections pose the greatest safety risk to traffic, as this is where traffic meets that travels in cross directions. The duration of traffic signals must be manipulated in order to optimize the safe flow of traffic through the intersection. Moreover, optimizing traffic signals to reduce the number of idling vehicles can also benefit the reduction in fuel consumption and emissions as well. Typically, Webster's method is widely applied to determine the optimal cycle length based on delays. However, at high saturation flows, the cycle length could be overestimated [2]. Although, in most cases, delay and queue length approaches are more common to determine the optimal signal plan based on the geometric and current video detector (VD) data at the intersection.

This paper describes the current implementation of the intersection control model used in SUMO and TraCI tool to control and coordinate signal timing at the intersection. Section 1 will be illustrated the optimal solution for complex intersection simulation by using sumo software, the core methodologies also indicated. Besides, the rest of this document is structured as following: In section 2 to describe the implementation for real complex intersection in Taichung city, Taiwan. In section 3 this study will present our conclusions and also highlight the future work.

II. THE OPTIMAL SOLUTION FOR COMPLEX INTERSECTION SIMULATION BY USING SUMO SOFTWARE

2.1. Requirements for running a Sumo Simulation at the Intersection

There are basically two different pieces of information necessary in order to start a SUMO simulation:

• A Network Topology

• A Traffic Pattern Demand

A Network Topology comprises a network of roads, railways, pedestrian ways, aquatic routes or other means of moving cars, buses, trams, trucks, trains, boats or people. A Traffic Pattern Demand comprises the cars, buses, trams, trucks, trains, boats or people moving around, in a given pattern along the network. These two requirements can be unified in terms of a configuration, which needs to be defined in order to run a simulation. A configuration can be defined in SUMO in an XML configuration file "cross.netccfg file" (see Fig.1).

Almost every file used in SUMO package is encoded in XML file including road network descriptions, route and/or demand descriptions, infrastructure descriptions, etc.). A SUMO network file (*.net.xml) describes the traffic-related part of a map, the roads and intersections where the simulated vehicles run along or across. At a coarse scale, a SUMO network is a directed graph. Nodes, usually named junctions in SUMO-context, represent intersections, and edges roads or streets.

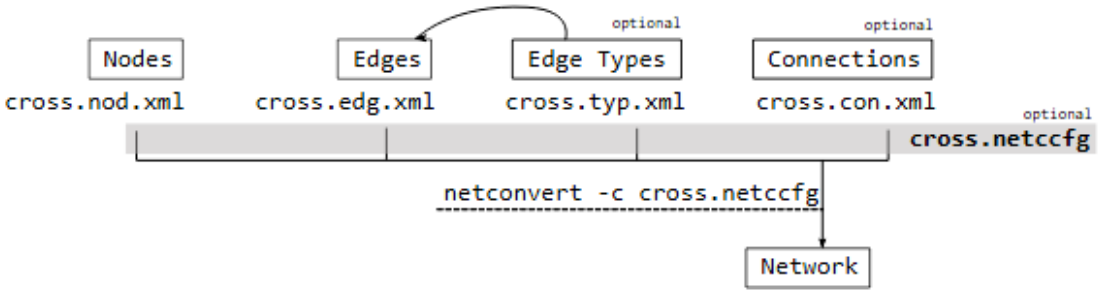

Figure 1. *The process of generating a network*

Typically, there are four main solution to create the network topology file including creating abstract topologies, constructing topologies by hand, using a graphic tool to create a topology and importing a topology from other formats.

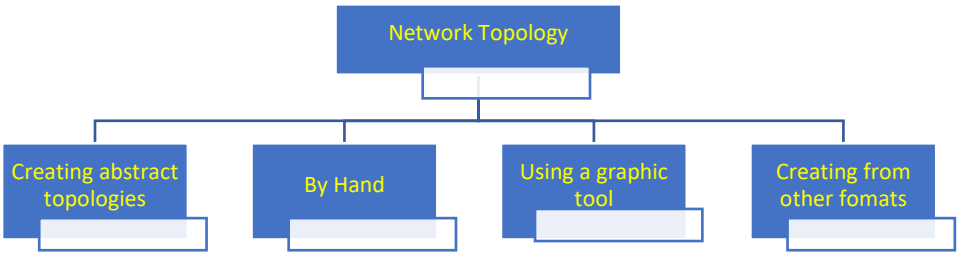

Figure 2. *Creating the network topology*

The effective solution to generate network simulation for road or intersection depend on the project purpose and current issue need to deal with but there are mix variety of benefits from creating the network by hand and create from other formats. Specifically, creating by hand could make more network detail and solve the problem statement by algorithm, methodologies and coding the solution by programming.

The network topology file contains lots of generated information such as structures within an intersection and right-of-way logic including node files ("*.nod.xml"), edge files ("*.edg.xml"), type files ("*.type.xml"), connection files ("*.con.xml") and traffic lights logic files ("*.tll.xml") which are important for the consistency of the simulation. These are generated automatically by NETCONVERT sub-software. Each of the generation algorithms has a set of options, which allow adjusting the network's properties [7]. Figure 4 shows examples of the generated networks.

Figure 3. *Examples of abstract road networks as built using "netgenerate"; from left to right: grid ("manhattan", spider, and random network)*

Besides, creating from other formats can make more advances like the use of OpenStreetMap (OSM) data in traffic simulation environments that is very common nowadays. No other traffic network data sources offer such high-quality data in urban areas for free without difficult licensing restrictions. Nevertheless, there are still some areas in OpenStreetMap, which could be improved to make traffic simulations out of OpenStreetMap data even better [6]. Traffic Lights in OpenStreetMap are usually modeled using only one node per intersection, regardless of the number of actual traffic lights, number of lanes at that intersection or intersection geometry (see Figs.4). Today, there exists no concept in OpenStreetMap, which can be used to represent detailed traffic light information [6]. There are proposed features that try to model more advanced signals information at intersections with focus on optimized information for navigation systems, but these cannot be used to include signal information nor are they optimized for simulation purposes. There are proposed features that try to model more advanced signals information at intersections with focus on optimized information for navigation systems, but these cannot be used to include signal information nor are they optimized for simulation purposes. In order to solve the limit of OSM data, the collecting different material or metric from incoming traffic and the current signal timing is necessary.

Figure 4. *Intersection Geometry from left to right: Complex traffic light controlled intersection, satellite view of complex intersection and SUMO traffic simulation with junction connections shown.*

Traffic Pattern Demand need to define after having generated a network. Finished network generation but no cars would be driving around. One still needs some kind of description about the vehicles and how they flow in the network topology. This is called the traffic demand. In order to understand the traffic demand, the following terminology is necessary [8]. A trip is a vehicle (or people) movement from one place to another defined by the starting edge (street), the destination edge, and the departure time. A route is an expanded trip, which is a route definition contains not only the first and the last edge, but all edges the vehicle will pass through, from its origin up to its final destination. SUMO and SUMO-GUI need routes as input for vehicle movements. This means that a route for each vehicle, since the vehicle enters into a street (which can happen anywhere in the topology) until its final destination (which again, can be anywhere in the topology), passing through all middle streets, need to be provided in order or the simulation to run. There are several tools to generate routes for SUMO. By now, SUMO contains four applications for generating routes.

2.2. TraCI interact with the simulation

After building the network topology, with a map containing roads and pathways for the simulation intersection and generating a traffic with different modalities of available information from traffic pattern demand. The control in this simulation will assume fixed programs for the traffic lights controlling the junctions. The behaviour of these traffic lights can be defined automatically by SUMO but all the lights will run with fixed controllers. SUMO allows external programs to interact with the simulation, being able to grab information from each involved object in the simulation (vehicles, people, traffic lights, inductive loops, etc.). The interaction with external programs is made available using TraCI, the "Traffic Control Interface".

Giving access to a running road traffic simulation, it allows external programs to retrieve many parameters and variables from simulated objects and to control their behaviour "on-line" in a SUMO instance. TraCI uses a TCP based client/server architecture to provide access to SUMO. Moreover, SUMO acts as a server that is started with a few additional command-line options.

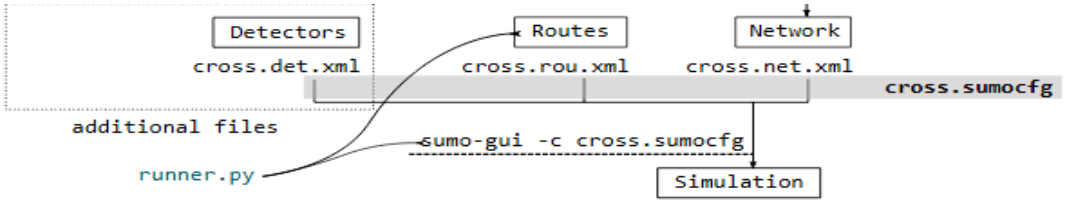

Figure 5. *The process and structure of TraCI illustration*

In order to pass through the complex intersection without stop of vehicles, besides the network topology in network file ("*.net.xml") and the traffic pattern demand in routes file ("*.rou.xml") typically the simulation for intersection by TraCI need information from detector file to detect the vehicle coming and extended information from traffic coordination. The model traffic simulation at the intersection will be associated with Python programming or Java scripts ("runner.py") to control and find some better solution for the coordination of intersection (see Fig.5).

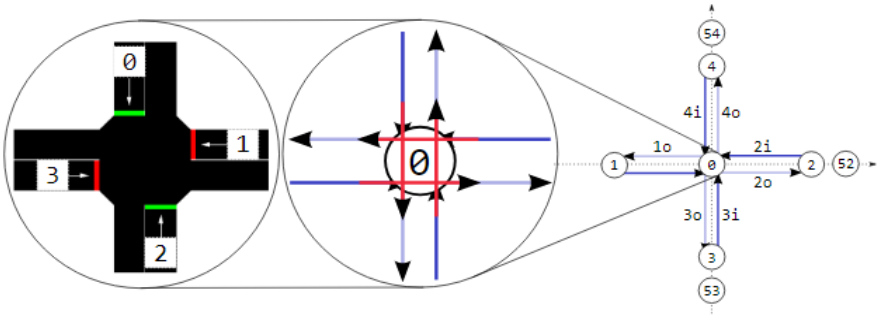

Figure 6. *Controlling traffic light and induction loop*

Each SUMO model is built on a network of roads, junctions, traffic lights, and other infrastructure items such as induction loop detectors. Compared to the vehicles and their movements, these are the static elements of the model. For TraCI, it is good practice to separate these definitions from the Python scripts to control the traffic light and induction loop (see Fig. 6).

2.3. Algorithms for minimizing queue lengths at the complex intersection

2.3.1 Minimizing total queue length of four direction at the Intersection

This algorithm indicated to the queue length of vehicles that is the considered parameter to measure traffic congestion. The queue length of vehicles in direction 1 and direction 3 after one cycle is shown in equation 1. The queue length of vehicles in direction 0 and direction 2 after one cycle is shown in equation 2 [1] (see Fig.6).

$$Q = Q_0 + (\lambda - \mu).t_g + \lambda.t_r \quad (1)$$

$$Q = Q_0 + \lambda.t_g + (\lambda - \mu).t_r \quad (2)$$

Where:

Q is a queue length of vehicles after one cycle; Q0 is a queue length of vehicles at the beginning of cycle; λ is the number of vehicles entering each direction intersection per second; μ is the number of vehicles going out of each direction intersection per second; tg is green time is the length of time of the green phase for direction 1 and direction 3, and also the length of time of the red phase for direction 0 and direction 2. Red time (tr) is the length of time of the red phase for direction 1 and direction 3, and also the length of time of the green phase for direction

0 and direction 2. The cycle time is tn. In the calculation, the length of time of the yellow phase is included in the green phase.

The optimization of queue length of vehicles at road intersection. The optimization was solved by using the parabolic interpolation method to reduce the congestion that occurs at the road intersection. Results showed that the calculation with a cycle time in min Q total calculation.

$$\min \sum_{i=1}^{4} Q_i \tag{3}$$

2.3.2 The Linear model for complex phase's duration

Punyaanek Srisurin suggested that the goal of minimizing the number of automobiles idling at the intersection, considering the typical arrival rates of vehicles, and existing effective green durations for vehicles to turn left or making through movement should follow the objective function (4) [3].

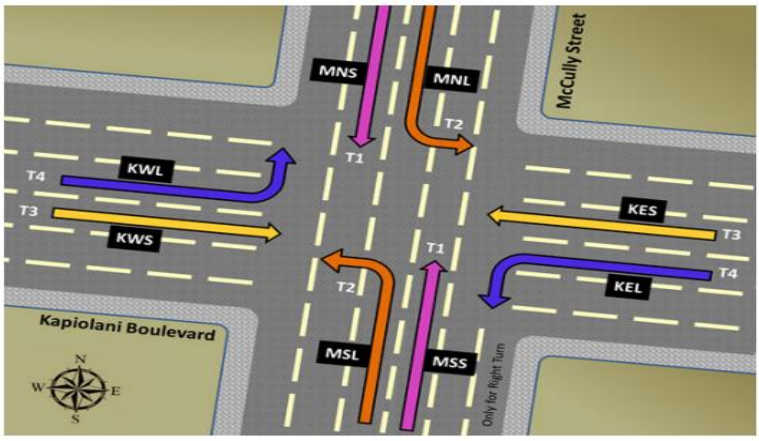

Figure 7. *Complex phase's duration*

Min [KWL (T1 + T2 + T3) + KWS (T1 + T2 + T4) + MNS (T2 + T3 + T4) + MNL (T1 + T3 + T4) + KES (T1 + T2 + T4) + KEL (T1 + T2 + T3) + MSL (T1 + T4 + T3) + MSS (T2 + T3 + T4)]. (4)

Where:

KWL, KWS, MNS, MNL, KES, KEL, MSL, MSS are the number of vehicles which are turning from other directions and T1, T2, T3, T4 are the time duration for each phases at the intersection.

2.3.3 Webster's method

The Webster's optimal cycle length formula, as shown in equation 19 that is the use of optimal cycle length results from such mainstream delay-based approaches as the Highway Capacity Manual (HCM) [9].

$$\text{Copt} = \frac{1.5L+5}{1-\sum\left(\frac{v}{s}\right)ci} \tag{5}$$

Where:

Copt = Optimum cycle length (s); L = Sum of the lost time from all phases (s); (v/s) ci = Flow ratio, which is the design flow rate of critical lane group divided by saturation flow rate.

Typically, this is some solutions for decrease the queue length or event cycle length in the coordination at intersections. The effective way should follow the reality of the intersection including geometry, network topology, and traffic pattern demand. On the other hand, the optimal traffic signal timing projects should use another method for reference purpose and the best outcome. Normally, the complex intersections have complicated phase duration or link. Hence, in this study, the simulation at the complex intersection to find out performance index for decreasing queue length should use the linear model for complex phase duration (II.3.2) and associated with Webster's method.

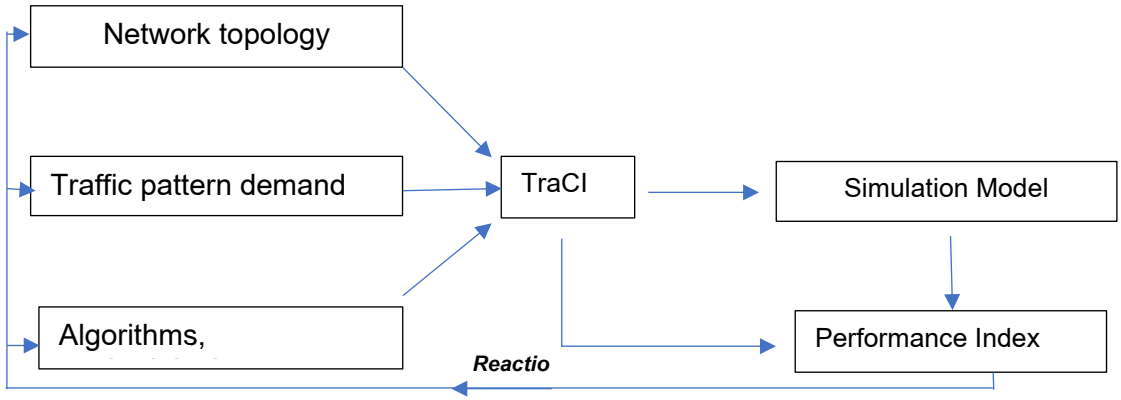

Figure 8. *Optimization of simulation for the complex urban intersection*

Briefly highlight that the optimal solution to simulate the complex intersection for coordination intersection purpose should follow these step: creating the network topology by OSM file, generating the traffic pattern demand follow the incoming traffic and the current signal timing plan data at the intersection and using TraCI to interact with the simulation model associated with the Sumo software that has the higher customization than other commercial software or proprietary software to find the performance index. The performance indexes like queue length, cycle length, green time interval...are very important in coordination at the intersection and need a lot of studies to find algorithms and methodologies. Moreover, the encoding of these algorithms and methodologies by Python programming and Java scripts will impact again the network, traffic demand or event traffic signal timing at the complex intersection for optimal transportation purpose (see Fig.8).

III. IMPLEMENTATION OF TAIWAN BOULEVARD- HUICHUNG ROAD INTERSECTION SIMULATION

This experiment considers a real intersection in Taichung city, Taiwan, which is shown in Figure 9. The complex intersection consists of a main road (Taichung Boulevard) in east/west

direction and a minor road (Taichung road) in north/south direction. Taichung Boulevard includes twelve lanes on both sides of the intersection. Moreover through movements, for both sides, are allowed on the four rightmost lanes. For each side, the left turn from Taichung Boulevard to Huichung road is allowed on the edge lane, while the other lanes on the left are allowed for vehicles from the other directions to occupy.

Figure 9. *Taiwan boulevard- Huichung road intersection*

Comparably, Huichung road consists of seven lanes on the northbound and southbound. The intersection is fixed-time controlled with four phases signal sequence and a cycle length of 180s. The first phase corresponds to a green time of 88s for the main road. The second phase corresponds to a green time of 23s for the minor road. Two-phase rest of cycle length are 34s and 13s, respectively. The detail of timing signal will present in table 1.

Table 1. *Duration's phase at Taiwan blv-Huichung Rd*

Station : Taiwan Blv- Huichung Rd	Phase	Duration's phase			
		Green	Amber	all red	cycle
Huichung Rd 4 / 3 1 / Taiwan Blvd Taiwan Blvd / 2 / Huichung Rd	3 1	88	4	2	180
	3 1 2	23	3	2	
	4 2	34	3	2	
	4 2	13	3	3	

The analysis focuses on the interaction of TraCI to main traffic streams. The resulting connections on the intersection will be shown in the Figure 10. The links show the connections from the lane with incoming traffic flow to an outgoing lane. Moreover, this model generated a controlled intersection and defined a traffic light on the intersection followed the duration's phase data.

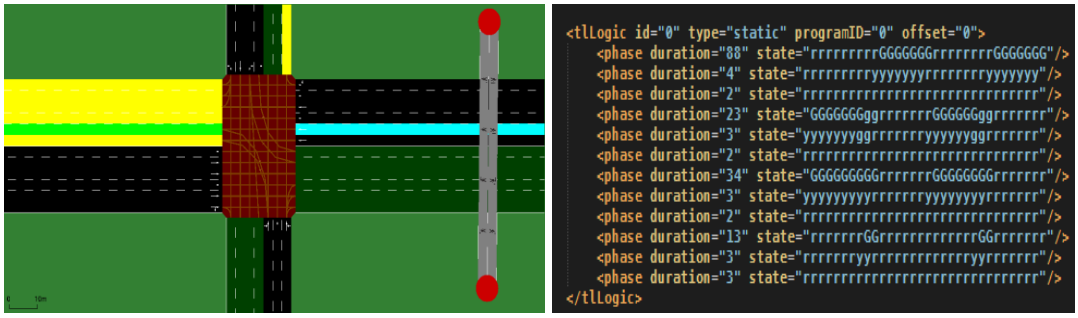

Figure 10. *Links and duration's phase model*

This study has defined a traffic light with four main phases (green and red signals) and 3 transition phases (yellow signals) as well as the connections. On the other hand, the signals that referred to the lanes and states of phases will be defined in Table 2.

Table 2. *Signal state definitions*

Character	Description
r	Red light' for a signal - vehicles must stop
y	Amber (yellow) light for a signal - vehicles will start to decelerate if far away from the junction, otherwise they pass
g	Green light for a signal, no priority - vehicles may pass the junction if no vehicle uses a higher priories foe stream, otherwise they decelerate for letting it pass
G	Green light for a signal, priority - vehicles may pass the junction
u	Red and yellow light for a signal, may be used to indicate upcoming green phase but vehicles may not drive yet
o	Off - blinking signal is switched off, blinking light indicates vehicles have to yield
O	Off - no signal signal is switched off, vehicles have the right of way

The simulation result is shown in the Figured 11. Basically, this result followed information of incoming traffic including the types and number of vehicles passed through the intersection after calculating Passenger Car Unit (PCU), and the current signal timing plan which is duration's phase at the intersection.

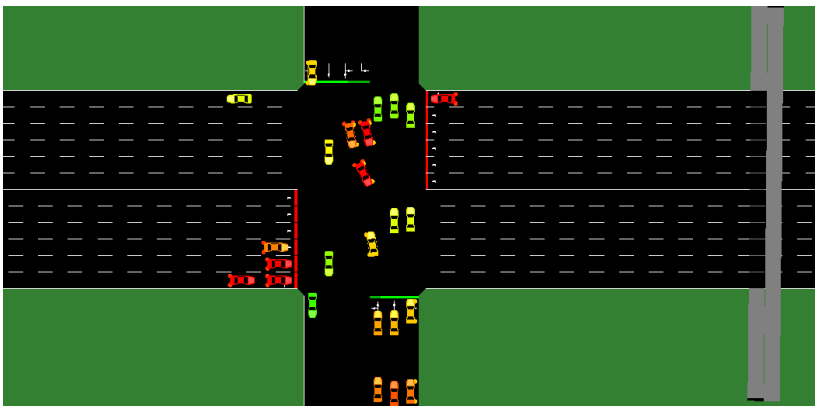

Figure 11. *The simulation of Taiwan boulevard- Huichung road intersection*

III. CONCLUSION

This study presented a coarse overview of the microscopic traffic simulation including tools and methodologies to reach the optimal signal timing at the complex intersection. The advantages of Sumo software which is the open-source traffic simulation software associated with TraCI tool, OpenStreetMap file (osm file), and Python programming also indicated. Moreover, some algorithms and methodologies referred to minimize queue length at the complex intersection will be the future work to deal with optimization coordination purpose of the complex intersection. Besides, the implementation for real complex intersection in Taichung city (Taiwan Boulevard- Huichung Road intersection) by adding relations with information of phases, generating network topology by osm file, upgrading traffic pattern demand from real data is the first step to generate the simulation model for the complex intersection. The performance indexes will be present in the future study to reactive the network, traffic demand and traffic signal timing at the intersection for optimization purpose.

References

[1]. *Mutiara Maulida*, "Queue Length Optimization of Vehicles at Road Intersection Using Parabolic Interpolation Method", International Conference on Automation, Cognitive Science, Optics, Micro Electro-Mechanical System, and Information Technology (ICACOMIT), Bandung, Indonesia, October 29–30, 2015.

[2]. *Michael Behrisch*, "SUMO Simulation of Urban MObility", the Third International Conference on Advances in System Simulation Berlin, Germany, 2011.

[3]. *Punyaanek Srisurin*, "Optimal Signal Plan for Minimizing Queue Lengths at a Congested Intersection", International Journal of Traffic and Transportation Engineering 2017, 6(3): 53-63, 2017.

[4]. *Jakob Erdmann*, "SUMO's Road Intersection Model", Springer-Verlag Berlin Heidelberg Germany, 2011.

[5]. *Jakob Erdmann and Daniel Krajzewicz*, "Modelling Pedestrian Dynamics in SUMO", international paper in ResearchGate Germany, 2015.

[6]. *David Rieck*, "Advanced Traffic Light Information in OpenStreetMap for Traffic Simulations", Springer International Publishing Switzerland, 2015.

[7]. *Daniel Krajzewicz*, "Recent Development and Applications of SUMO – Simulation of Urban MObility", International Journal on Advances in Systems and Measurements, vol 5 no 3 & 4, 2012.

[8]. *Ricardo R. Gudwin*, "Urban Traffic Simulation with SUMO", published by DCA-FEEC-UNICAMP, 2016.

[9]. Highway Capacity Manual, Transportation Research Board of the National Academies, Washington D.C., 2010.

ENERGY EFFICIENCY AND CARBON EMISSIONS OF DIFFERENT FORMS OF DISTRIBUTION IN VIETNAM AND A COMPARISON WITH FRANCE (CASE STUDY OF YOGURT)

LAM QUOC DAT
Department of Urban and Road Transport, Faculty of Transport and Economics,
University of Transport and Communication, Hanoi, Vietnam.
Corresponding author's email: lamquocdatutc@utc.edu.vn

Abstract: *Anthropoid greenhouse gas (GHG) emissions, by concentrating in the atmosphere, result in climate change. Increasing GHG concentrations, including GHG emissions from transportation activities in general and freight transport in particular, contribute to global warming. Transport is responsible for an increasing share of these emissions, mainly road transport and, in transport, the share of goods (about one-third) is growing. Currently, a large and growing share of freight transport is organized by a few large retailers who seek to control goods flows further and further upstream in the chain, to organize them for their benefit.*

The main objective of this study is to contribute to a better knowledge of energy efficiency and carbon emissions (CO2) in the supply chain. It analyses the energy and carbon efficiency of different forms of distribution implemented by the main distributors in Vietnam and compares them with corresponding supply chains in France. The differences between types of distribution, include the type of retail outlet: small downtown shops that can belong to the producer, a distribution chain or be independent shop and the other, supermarket and hypermarket of large distributors. This article answer the following questions: What are the most efficient types of retail outlets and logistics organizations for energy and GHG emissions in Hanoi, Vietnam?

Keywords: *GHG emissions; energy efficiency; distribution; supply chain*.

I. INTRODUCTION

Increasing anthropogenic greenhouse gas (GHG) emissions play an undeniable role in accelerating climate change (IPCC 2013); the increase in greenhouse gas concentrations in the atmosphere gives rise to fears of unprecedented climate changes for the future. Transport is responsible for an increasing share of these emissions, mainly road transport and, in transport, the share of goods (about one-third) is growing. Currently, a large and growing share of freight transport is organized by a few large retailers who seek to control logistical flows further and further upstream and organize them for their benefit.

Our research focuses on the quantification of energy and GHG emissions related to freight transport activities, particularly in the supply chain. The issue of climate change and global warming are the effects of the increase of GHGs in the transport activity in general and the

transport of goods in particular, mainly road transport. At the beginning of research in France on the energy consumption and carbon emission for yogurt and blue jean Rizet C., Keita B., (2005); fruit and vegetable Rizet. C et al (2008) or the other research about GHG emissions of supply chains from different retail systems in Europe Rizet C., et al (2010). To achieve these objectives, this article attempts to quantify and analyse energy consumption and GHG emissions on two products: yogurt from the raw material to the consumer's home. So, we first did a face-to-face survey of companies (producers, carriers, distributors) and a consumer web survey in Hanoi with help from Dean of Transport and Economics and Department of Urban and Road Transport at University of Transport and Communication (UTC) in Hanoi; the survey was conducted during 2013 and 2014 in Hanoi from this work, we have also been able to compare energy consumption and GHG emissions per kilo of product studied, from each of the stages of supply chain (road transport, platforms, retail outlets, consumer's trip etc.). On the other hand, different chains according to their organization. These chains are compared between types of retail outlets (hypermarket, supermarket, small shops of different types) and for a type of retail outlet, between France and Vietnam.

Visits and observations on logistic sites and field surveys with multiple stakeholders helped to understand the functioning of logistics chains and to quantify the energy used and the emissions of each chain, to describe the supply chain from the material supplier first upstream to the home of the downstream consumer. Through these surveys, we have collected data necessary for calculations and analyses. The results obtained were compared to previous work conducted on the same products in France by Rizet C., Keita B., (2005). This allows us to compare the energy consumption and carbon emissions of different types of retail outlets on the case of yogurt between Vietnam and France. Finally, these analyses aim to analyse and quantify energy consumption and GHG emissions in the different forms of distribution of supply chain in Vietnam answer the question: the most efficient types of retail outlets and logistics organizations.

II. MAIN CONTENTS

2.1. Methodology

The main greenhouse gas (GHG) emitted by supply chains is carbon dioxide (CO2) emitted by the combustion of hydro-carbons. The new emission factors used in France (ADEME, 2017) also accounts for other GHG, which have been converted in CO2 equivalent (CO2e). The amount of CO2e emitted at each stage of the chain is calculated as the product of the amount of energy used, multiplied by an emission factor specific to each type of energy. The emission factors used are shown in Table 1 below and come from the 'CO2 information guide for transport services (ADEME, 2017) for diesel, gasoline, bunker fuel oil and electricity in France and the' Ministry Natural Resources and Environment Vietnam, 2010 'for electricity in Vietnam. The amount of energy consumed in transport is itself calculated, at each stage of the chain, as the

product of the distance (distance under load and possibly empty distance) multiplied by a unit consumption (litters per hundred km for journeys road). Energy consumption and GHG emissions by step are then related to the corresponding quantity of product; they are finally summed up on the different stages of the supply chain. Surveys at companies, carriers and shippers were conducted face-to-face, in Vietnam and France, with the transport managers of these companies; the questions covered journeys, type of vehicle, total weight of the load and empty journey before and after the laden journeys.

a. Quantification of energy consumed and emissions from road transport:

Three forms of energy have been encountered in the studied chains:

- Diesel, an almost exclusive fuel for road transport, and gasoline used mainly for consumer journeys

- Electricity used in production plants, logistics platforms and retail outlets;

- Natural gas is used in yogurt factories.

In order to quantify the quantity of energy, these different energies have been converted in grammes of oil equivalent (goe), with the conversions factors shown in the second column of table 1. When the energy consumed and the emissions are related to the quantities produced or transported, the indicators used are the goe / kg and gCO2e / kg of product: Goe (gramme of oil equivalent) / kg product = ((loaded distance + empty distance in km) x unit consumption (liters / 100km for road trips)) x Conversion factor in kgoe / unit / (Purchase weight of load in kg); (goe/kg)

gCO2e / kg product = the amount of energy used (in goe / kg) x Emission factor for each type of energy (in gCO2e / unit).

Table 1 summarizes the coefficients used to convert these different forms of energy into a common unit, the gram of oil equivalent (goe) as well as the GHG emission coefficients of these energies in grams of CO2e (kgCO2e) per unit of energy. When the energy consumed and the emissions are related to the quantities produced or transported, the indicators used are the goe / kg and gCO2e / kg of yogurt. To be able to aggregate and compare the emissions of energies from different sources, in particular hydrocarbons and electricity, we use the emission coefficients 'from well to wheel' or 'combustion + upstream'.

Surveys of operators (producers and transporters and distributors) in both countries describe the logistic chains that yoghurt actually used in both countries and quantify the emissions at each stage, from the farm where the milk is product, to the store that sells the yoghurt. In addition, an online survey of consumers has quantified GHG emissions from the last stages of the supply chain: the displacement of the consumer who will buy the yogurt, depending in particular on the type of retail outlet where he goes shopping, in Hanoi or in the Paris region.

Table 1. *Energy equivalence and emission factors by energy type*

Type of energy	Conversion factor (kgoe / unit)	Coefficient of emission (kg CO2e / unit)		
		From the well to the reservoir	From tank to wheel	From the well to the wheel
1 liter of diesel (road transport)	0,83	0,68	3,17	3,85
1 liter of gas (road transport)	0,791	0,66	2,51	3,16
1 kWh of electricity				
consumed in France 1	0,086	0,048	0,000	0,048
consumed in Vietnam 2		0,413	0,000	0,413
Natural Gas 1 MWh PCI	0,77	0,7	2,81	3,51
Bunker Fuel oil (maritime transport)	0,99	0,68	3,17	3,85

Source: *1 'Guide information GHG for transport services (ADEME, 2017) for diesel, gasoline and electricity in France; 2 Ministry of Natural Resources and Environment of Vietnam, 2010 for Electricity in Vietnam.*

In France electricity is produced mainly from nuclear power while in Vietnam, fossil energy is still predominant. In fact, fossil fuels for electricity production in Vietnam ac-count for about 65-70% according to the Energy Report of the Vietnam Electricity Group by 2015.

b. Quantification of energy consumption of electricity

Logistic platforms and retail outlets consume electricity. This electricity consumption was estimated with the managers of these platforms and supply chain retail outlets studied. The energy consumed in the area occupied by the product under study was estimated with the help of the outlet managers, then divided by the quantity of products passing through this area (part of the retail outlet or platform). The values per m2 (energy consumption, quantity of products, emissions) allow a consistency check, as well as the average energy efficiency (all products) per site.

For the product P (yogurt or blue jeans):

Goe / kg of P = the electricity consumption of the area (KWh / year) divided by the quantity of P products sold (kg / year) x Electricity conversion factor (goe / kWh)

gCO2e = the electricity consumption of the product P (kWh / kg of P) x emission factor of the electricity (in gCO2e / kWh)

c. Quantification of energy consumption and consumer journey emissions

The energy consumption and the emission of the consumer's journey, for each mode, were estimated as follows for the journey between the retail outlet and the home (the journey to the retail outlet is not taken into account):

Goe / kg of consumer journey = [Car consumption per trip (liter / 100km) x Average distance travelled (km) x (% car + motorcycle) / 100) x Diesel conversion factor] /Total weight of purchase (kg)

GHG emission = ∑ (Energy consumption of the consumer trip) x [emission factor]

2.2. Energy and GHG (CO2 emissions) in the supply chain of yogurt in Vietnam and the comparison with France

Vietnam is experiencing an explosion in demand for dairy products that domestic production does not cover. To reduce imports, the government has decided to launch a vast national dairy plan (2010-2020) aimed at rapidly increasing milk production. The goal is to meet 80% of the demand for Vietnamese consumption in 2020. Currently, Vinamilk is a large dairy and dairy company in Vietnam. Yogurt is made in Vietnam by the company Vinamilk, from Vietnamese raw materials. It is a food product whose lifespan is short (about a month) as in France. Currently, there are 2 factories Vinamilk manufacturing: a factory in Bac Ninh in the north of Vietnam (a province 30 km from Hanoi) and one in Binh Duong in south of Vietnam (a province 25km from Saigon). In this research, we chose the yogurt supply chain in the North. There are more than 10 provinces that produce milk in North Vietnam, Son La, Tuyen Quang, Ha Tay, Ha Nam etc. ; at the Center of Vietnam in Nghe An, Ha Tinh, Thanh Hoa province and from the Central Mountain (Tay Nguyen) at the west of Vietnam to Cu Chi, Lam Dong, Binh Duong etc. These provinces supply milk to the Vinamilk factories located in industrial parks in the north and the south of Vietnam. At the Center of Vietnam, another company also produces yogurt: TH Truemilk Company. Dairy products in Vietnam are made mainly by: Vinamilk (90%), TH Truemilk (7%) and other companies. There are also a few imports from Japan, Australia, Germany, France, and the United Kingdom.

In this research, we are interested in yogurts consumed in Hanoi; they are produced by the Vinamilk factory in Bac Ninh, which is supplied with milk by the northern and central regions of Vietnam. Three farms provide most of the milk for the dairy products of this plant:

- the dairy farm in Moc Chau commune, Son La province, in the western part of northern Vietnam with a 300 km drive to the Bac Ninh factory;

- the dairy farm of Tuyen Quang, in the north-east of the northern region, with a journey of 180 km;

- the dairy farm in Nghia Dan Commune, Nghe An Province, at the North of Central Vietnam with a journey of 350 km.

The morphology of these chains is almost identical between the different types of distribution studied and we distinguish 7 stages for all the studied yogurt chains:

- Step 1- The collection of milk and other supplies of materials and products that make up the composition of yogurt.

- Step 2 - The yogurt production plant. In Vietnam, the factory studied is located in the province of Bac Ninh about thirty kilometers from Hanoi while in the French case the factory is located in the Lyon region to nearly 500 km from Paris.

- Step 3 - Transport from the factory to the platform just before the shop.

- Step 4 - The logistic platforms of the producer or distributor in Vietnam, the producer and the distributor in France.

- Step 5 - Transport from the last platform to the retail outlet.

- Step 6 - The retail outlet: hypermarkets, supermarkets and three types of shops (small factory or independent shops in Vietnam, neighborhood minimarket in France).

- Step 7 - The consumer's journey between the retail outlet and his home.

The Vietnamese yogurt plant uses 136.5 million liters of milk a year, for an annual production of 91,000 net tons of yogurt. The quantity of milk collected on the 3 state farms is 124 million liters; an additional 12.5 million liters of milk is purchased on the Vietnam market.

In France, the farms supplying the milk plant are located within a radius of 100 km around the plant. The vehicles used for milk collection are isothermal (non-refrigerated): trucks with trailers and semi-trailers. The reference plant uses 149 million liters of milk a year, while the quantity of milk thus collected represents only 124 million liters, resulting in a deficit of 25 million liters. This deficit is filled by the purchase of a supplement of milk on the national market. The main supply points for this supplement are, on average weighted by tonnages, 354 km from the plant. As these vehicles are very specialized, they always return empty. In addition to milk, the plant also obtains packaging and other ingredients necessary for the production of yoghurt (containers, fruits, lids, streamers, cleaning products, sugar, etc.). These products come from different regions of France and abroad (Germany, Poland, Spain). All these inputs are delivered by road, with adapted vehicles and represent nearly 2,500 deliveries per year for an estimated consumption of 276,000 liters of diesel. On the other hand, the production of yogurt also produces a residue, the serum, which is sent to another site located about 250 km from the yogurt factory, at the rate of 6 tanks of 22 tons on average per week. The energy consumption of this transport, which we count here with that of the supplies, is estimated at 51000 liters of diesel per year.

The energy consumption of logistics platforms is also low, especially the factory platforms; those of distributors (hyper and supermarkets), seem a little less effective. As a whole, these different chains corresponding to the types of stores are distinguished mainly by the last mile of

the consumer and it is the independent shops that seem the most effective, both on the last mile and overall.

Here we make three types of comparisons:

- The comparison of energy between types of distributions in Vietnam.

- Comparison of CO2 emissions between types of distributions in Vietnam.

- The comparison between energy and CO2 emissions of the hypermarket supply chain between France and Vietnam.

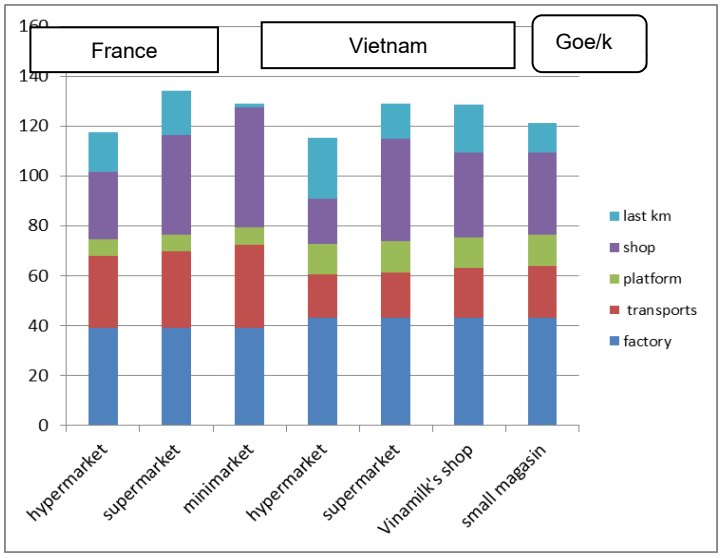

Figure 1. *Energy of different yogurt chains studied in Vietnam and France (gram of oil equivalent –goe/kg)*

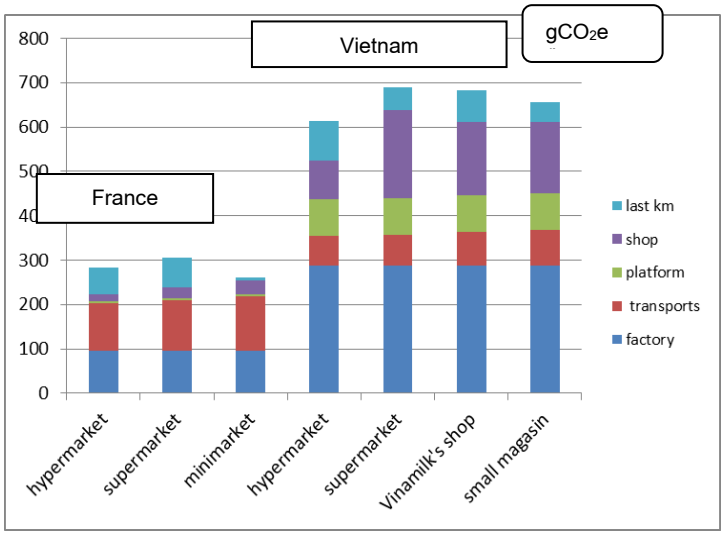

Figure 2. *gCO2e emissions of different yogurt chains studied in Vietnam and France (gCO2e/kg)*

Figure 1 does not indicate a significant difference in efficiency between the two countries. Energy consumption for the supply of yogurt plants is significantly higher in Vietnam (13.3 goe / kg yogurt) than it is in France (8.4 goe / kg yogurt). This is due both to far greater distances in Vietnam for milk collection, which is the main source of energy consumption for this stage and

for smaller vehicles and smaller loads for each of the three distinguished supply types, mainly related to mountainous terrain and road network. In Vietnam, the products made in the factory studied are, in addition to bottled milk, natural yogurt and fruit yogurts. In this research, we focus on the yogurt that comes in the form of 80 gram jars in packs of four, in boxes of 48 packets of 4 yogurts. To leave the factory, these packets are palletized by automated electric robots. The electricity consumption of this factory is 45,500 MWh/year and the factory does not use any other form of energy. In France, the factory studied produces almost exclusively yogurt and consumes mainly two types of energy: gas to heat (pasteurization, serum concentration and sterilization) and electricity to operate the engines and for cooling.

In Vietnam, from the factory, yogurt goes either to a distributor platform, to supply supermarkets and factory shops, or to the producer's platform for independent shops, while in France yogurt systematically goes through the two platforms: first to the producer platform, who groups together the production of his various factories for a region, then to the retailer platform which gathers the productions of different suppliers and prepares the orders for the retail outlets. In Vietnam, from distributors' platforms, hypermarkets, supermarkets and factory shops are delivered by refrigerated trucks with a 7.5 tonnes payload and from the factory platform, independent shops are delivered by refrigerated trucks with a 15 to 17 tonnes payload. This third stage of the logistics chains is organized by the factory itself for independent shops and by a transport and logistics provider (Inland Container Depot located in Tien Son, province of Bac Ninh, about 30 km from Hanoi) for the supermarket chains to hyper and supermarkets and the shops of the factory.

In France, the platforms of the distributors are delivered by refrigerated semi-trailers of 14,5 tons of payload. From this platform, yogurt is transported to retail outlets in the Ile de France region. The average distance of this stage is 658 km.

On the other hand, it shows slight differences in efficiency between the different forms of distribution analyzed. The different logistic chains lead to differences in energy consumption per kilogram of yogurt of 20% maximum with, in both countries, a slight advantage for the hypermarkets that seem to have the best energy efficiency among the different forms of distribution analyzed.

On the other hand, when this energy is transformed into GHG emissions, all the French chains emit much less than those of Vietnam and this is explained mainly by the difference between the emission coefficients of the electricity of the two countries.

The main difference lies in the use of platforms: in Vietnam, yogurt goes through a single logistics platform after its manufacture, while in France, it goes systematically through two platforms: a platform a form of producer allowing the grouping of products manufactured in different regions and a distributor platform for the preparation of their deliveries to the retail outlets. The two French platforms together consume less energy per kilo than the only Vietnamese platform, which seems to be linked to the over-sizing of Vietnamese platforms.

For a given type of retails, energy consumption is fairly close between France and Vietnam but the distribution of this energy between the stages of the chain is different: The energy spent on transport is greater in France, despite the relief and smaller trucks in Vietnam, due to longer distances. The carbon efficiency of the platforms is better in France whereas that of the retail

outlets seems better in Vietnam. Finally, the consumer journey is less differentiated between retail outlets in Vietnam than in France: in Vietnam, in the cases studied, a significant proportion of these trips are made by motorized transport whatever the type of retail outlet.

III. CONCLUSION

In this case study of yogurt product, in both countries, truck transport (or transport generally considered as 'goods', that is to say without counting the consumer's journey) is far from the most important element in the total energy consumption of the logistics chains studied: this transport by truck represents about 25% in the total energy of the French chain and only about 15% in the total energy of the Vietnamese chain. Energy consumption per kilogram of yogurt of different forms of distribution is higher in France than in Vietnam, because of the total transport distance is 3 times higher in France than in Vietnam. On the other hand, the carbon intensity of the yogurt supply chain is less important in France than in Vietnam because of the emission factor of electricity, which is 10 times lower (0.053 gCO2e / kWh) in France than in France that is in Vietnam (0.576 gCO2e / kWh), which allows the French chains emit less GHG (2.5 times less) than its Vietnamese counterpart.

An improvement in the carbon efficiency of logistics chains is possible in Vietnam, especially on the consumer's trip, by optimizing the location of retail outlets to reduce the distance of the last km and reducing the share of individual motorized transport (mainly motorcycles) in purchasing trips.

For the future, this article opens new research perspectives on energy efficiency and carbon emissions in the freight transport in general and the supply chain in particular. These perspectives are really needed in the research field and the use of other indicators to calculate and analyze the energy efficiency and carbon intensity. Research methods on energy quantification and carbon emissions in the different forms of distribution will be considered from a sustainable development perspective in Vietnam. Moreover, it could be applied to other products for other international comparisons that this article mentioned in the limitation of these research.

References

[1]. ADEME (2017), Methodology guide - GHG information on transport services? 239p.
[2]. IPCC (2013), scientific evidence of the Intergovernmental Panel on Climate Change, 222 p.
[3]. Emission factor of Viet Nam national grid- Clean Development Mechanism (CDP) project developers, Number 151 / KTTVBDKH, Ministry of Natural Resources and Environment of Vietnam, 2010
[4]. *Rizet C., Cornélis E., Browne M., and Léonardi J.* (2010) GHG emissions of supply chains from different retail systems in Europe, International Conference on City Logistics, Procedia Social and Behavioral Sciences, Elsevier .
[5]. *Rizet C, Browne M., Léonardi J., Allen J., Piotrowska M., Cornélis E., Descamps J.*, (2008) Chaînes logistiques et consommation d'énergie : cas des meubles et des fruits et légumes. Rapport de recherche INRETS. 2008, 167p. <hal-00544563>
[6]. *Rizet C., Keita B.*, (2005) Chaînes logistiques et consommation d'énergie: cas du yaourt et du jean. Rapport de recherche INRETS. 2005, 92p. <hal-00546042>

SMART MATERIALS FOR SUSTAINABLE ENVIRONMENT - APPLICATIONS FOR SMART CITIES IN VIETNAM

TRINH XUAN BAU, NGUYEN THI THU THUY
Faculty of Civil Engineering, University of Transport and Communications
Campus in Ho Chi Minh City, Vietnam
Corresponding author's email: bau@utc2.edu.vn

Abstract: *The research, development, and application of environment-friendly smart materials is one of the most interesting aspects in building smart cities. Utilising these materials in smart cities will result in a sustainable environment, low energy consumption and great benefits for the whole society.*

Thus, this article aims to present important applications of several typical smart materials such as Shape Memory Alloys, Piezoelectric, Magnetostrictive, and Optical Fibers to modern structures in developing building infrastructures in smart and environmentally sustainable cities. Based on this, it is proposed that these materials can be used to build a smart city in Vietnam.

Keywords: *Smart Material, Smart City, Sustainable Environment, Smart Building Materials*

I. INTRODUCTION

A smart city can be interpreted as a developed urban area that creates sustainable economic development and high quality of life by excelling key areas such as economy, mobility, environment, people, living, and government [1]. Smart cities address intelligent and sustainable environments, intelligent communication spaces, smart materials and smart devices [2]. The smart city uses technology, data and intelligent design to enhance the city's live ability, workability and sustainability [3].

A smart system or material is the one which has built-in or intrinsic sensor(s), actuator(s) and control mechanism(s) whereby it is capable of sensing a stimulus, responding to it in a predetermined manner and extent, in a short/appropriate time, and reverting to its original state as soon as the stimulus is removed [4]. Smart materials are useful in creating a sustainable environment which is an eco-friendly system and leads to less energy consumption which is beneficial to our society [2]. In addition, smart materials are those materials that can respond to any change in electricity, magnetic waves or heat [5].

Various materials and methods that have been used have a great impact on environment and on economy. Therefore, the ability to make numerous environment- friendly and economical choices without affecting material efficiency, structural integrity, longevity, cost and industrial probity is extremely important [6]. Intelligent and environment-friendly materials are one of the key factors and a lasting solution to the infrastructure of a smart city. These materials

can change their properties in response to changes in the surrounding environment, and are also capable of changing from one form of energy to another.

The advantages of using environment-friendly smart materials include high strength, high durability, high resistance to corrosion and chemicals, resistance to damages from natural causes, user friendly and allow automatic operation and control, [6]. At the same time, it does not affect material efficiency, ensure structural integrity, longevity, cost and industrial probity [7].

The applications of intelligent materials such as Shape Memory Alloys, Piezoelectric, Magnetostrictive and Optical Fibers in intelligent structures, for examples, Smart Concrete, Smart Bricks, Smart Windows Shades, Smart Roofings, Smart Ceilings and Green Materials will be presented in this article.

II. SMART MATERIALS FOR SUSTAINABLE ENVIRONMENT

Smart materials are the ones that can detect and react immediately to any environmental changes (such as electricity, magnetic waves or heat) [7], and can preserve the state of the materials used [8]. Smart materials are not only intelligent in terms of chemical composition but also intelligent in their adjustment to structural changes [2].

Smart materials with molecular structure will have changes and be controlled through physical interactions. They have one or more characteristics such as temperature, humidity, pH, or electric field, and the magnetic field that can change flexibly [9].

The two major types of energy conversion mechanisms, sensors and actuators, are critical to the use of smart materials. The sensor detects and converts the changes into a signal, the mechanisms structure then interprets the signal and carries out an action. Sensors and mechanisms structure usually follow the principle of being made by certain materials and have moving elements [10]. Some smart materials can simultaneously perform the function of some materials and other elements, thereby reduce the number of components, wear and tear, and corruption (Figure 1).

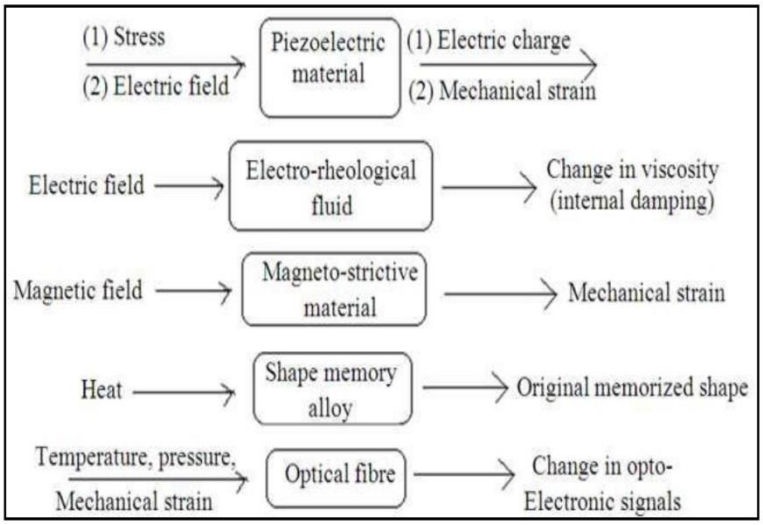

Figure 1. *Common smart materials and associated stimulus-response [10].*

From a practical point of view, the energy of the materials can be converted into heat, electricity, magnetic energy and vice versa. There are also other smart materials used in practice such as memory-form alloys, which mechanically impact the refractory, onto magnetic materials, and precision materials that their properties are controlled by creating a magnetic field and the material will swell under the chemical activation [10,11].

Environmental sustainability is one of the six characteristics of the smart city model. To ensure environmental sustainability, two of the five initiatives proposed in the smart city framework are environmental protection and building infrastructure with environment-friendly and intelligent purposes [12,13,14]. Environment-friendly materials are the basis for securing these two innovations in the smart city (Figure 2).

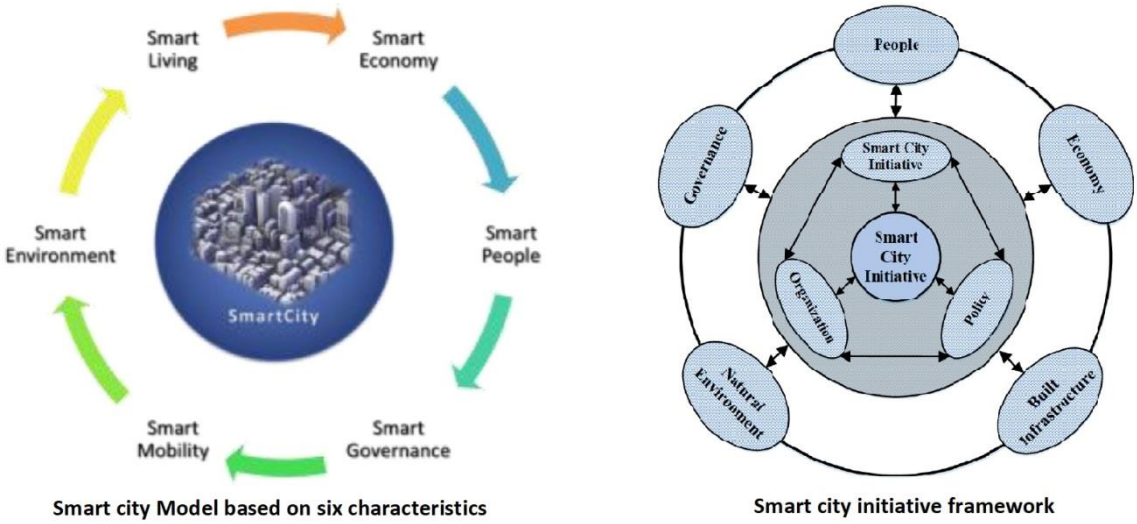

Figure 2. *Characteristics and initiative framework in Smart city [12,14]*

Building a smart city requires an integrated approach and interdisciplinary relation for sustainable development to achieve low carbon emissions, low rate of water usage, sustainability and eco-balance, recycled energy and energy saving [13,14]. To execute the above elements, the infrastructure must be designed to adapt to current and future impacts and climate change. Using the smart, sustainable, and environment-friendly materials is one of the primary factors applied in the model of smart and environment-friendly city.

III. CLASSIFICATIONS OF SMART MATERIALS AND THEIR USES

3.1. Shape Memory Alloys (SMAs)

Deformed materials that can be restored back to its original shape under heat action are called Shape Memory Alloys. The mechanism of shape memory effect is: When cooled, the center cubic side frame structure changes from austenite phase in high temperatures to martencit phase in low temperatures. Due to the stress caused by the cooling process, the phenomenon of martencit obtained from austenit phase is called twins – creating atomic structures with layers being arranged to form mirror symmetry.

Deformation destroys the phenomenon of twins – called the double decay. Double decay martensite phase has a quad chassis. When heated, the double decay martensite converts back to austenitic phase (Figure 3) [5].

The most popular SMAs are Cu-Al-Ni and Ni-Ti. Besides that, SMAs can be made from zinc, Copper, Gold, Iron...

The major application of SMAs includes accessories with rivet and pipe shapes, actions or temperature control in automatic control system, robot; dynamic motor, etc.

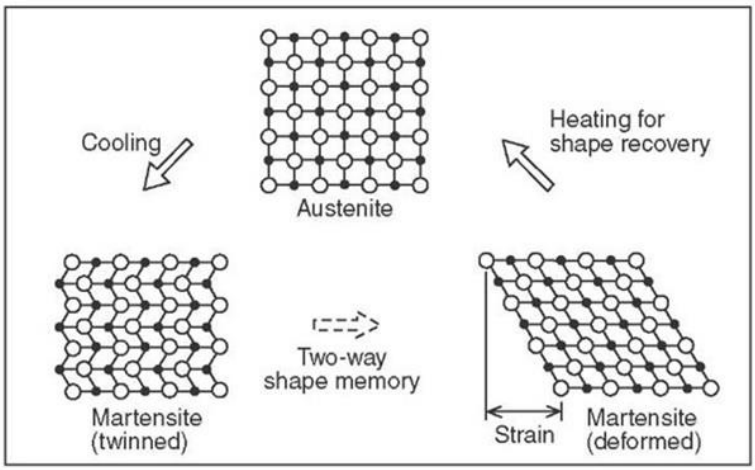

Figure 3. *Mechanism of Shape Memory Effect [5]*

3.2. Piezoelectric material

Piezoelectric material which has the chemical characteristic of ceramics, can change its shape when exposed to a magnetic field, and can create electrolysis on the specific surface when a mechanical force is applied on it [15].

It acts as a machine which can directly changes electric power to mechanical energy vice versa. If following the forward direction, meaning that a force is applied onto the physical item, it will generate power. On the other hand, if following a converse direction, it will generate converse piezoelectric. A physical item created by three PZT element including Lead, Zorconi, Titan will have a characteristic of the piezoelectric like quatz material.

Piezoelectric is applied widely as sensor, ultrasound machine, adjusting the small rotation angle of laser reflection mirror, noise destruction room, piezo motor, and other smart structure.

3.3. Magnetostrictive material

Magnetism is a special characteristic of iron materials, making changes of its shape and size during magnetic process (Figure 4). The magnetostrictive material can convert magnetic energy to mechanical power vice versa. It can be used for making actuators and sensor [2].

Iron, nickel and cobalt are the first three known magnetostrictive materials. Besides, the alloy Terfenol-D comprised of Terbium, Dysprosium and Fe is also known as a magnetostrictive

material and is considered as the most widely available material in many fields. PZT (lead, zorconium and titanium alloys) is a piezoceramic material that has low cost, light weight, high energy density, and is easy to implement.

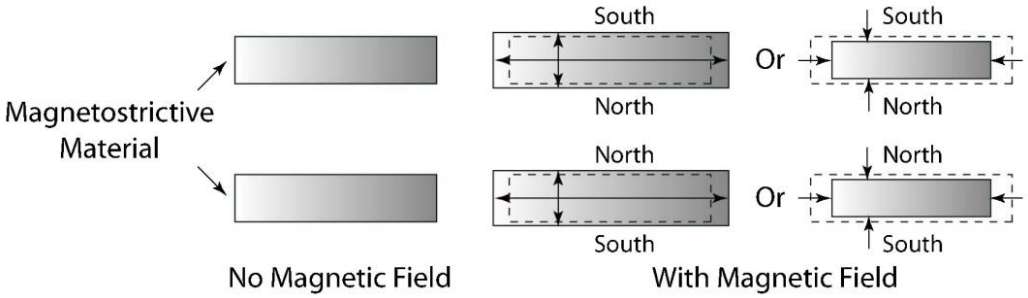

Figure 4. *Magnetostrictive material effect*

3.4. Optical Fiber

A transparent yarn is made of fiberglass or plastic with a diameter smaller than human hair (Figure 5). The basic principle is to use the characteristics of the fiber to provide the opto-electronic signal that represents the external parameters to be measured [2].

Fiber-optic material uses polarization, phase, intensity, or frequency to determine deformation, electromagnetic field, stress and measurement parameters. Some applications of optical fiber are optical fiber sensors, optical fiber lasers, power transmissions.

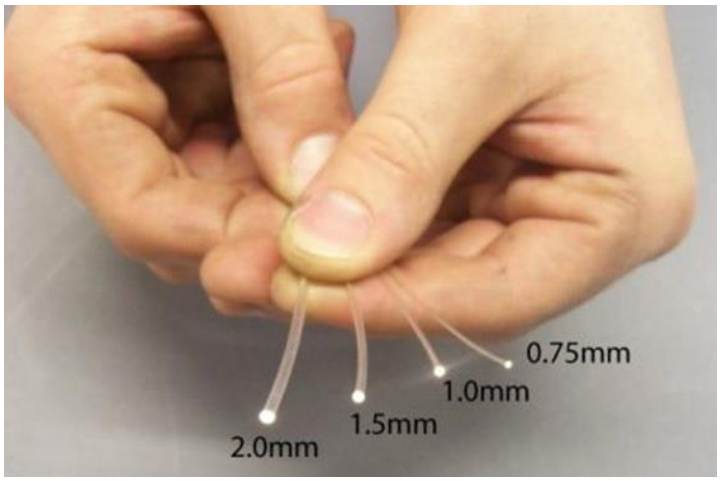

Figure 5. *Optical Fiber*

IV. SOME STUDIES ON SMART MATERIALS FOR SMART CITIES AND SUSTAINABLE ENVIRONMENT - PROPOSED APPLICATIONS IN VIETNAM

4.1. Smart Concrete

Adding about 0.2 to 0.5% weight of carbon fiber into concrete can change the resistance of the concrete mixture. This helps detect stresses and deformations in concrete. Structure fixed by Carbon-Fiber Reinforced Plastic (CFRP) construction contains a network of conductive carbon fibers creating a distributed sensor network that locates the electrode in the structure (Figure 6).

As a result, it can monitor and detect cracks in a timely manner for repair [6]. Smart concrete used in highway construction can also detect the location, weight and speed of the vehicles.

In Vietnam, such smart concrete products have been approached for research and development in addition to some self-healing concretes, ultra-high strength concrete (UHPC), or nano concrete, etc... are of interest.

Figure 6. *Self - healing Concrete as a Smart Concrete*

4.2. Smart Bricks

Smart bricks are piezoresistive clay bricks based on the principle of piezoelectricity. Sensorized bricks, signal processors and wireless communication links are used for detecting stress at dangerous locations or potential damage after earthquakes [1,6]. Smart bricks are made of nanocomposit materials which are produced by mixing Titania with clay.

This brick has significantly improved mechanical properties such as noise reduction, electrical conductivity enhance, high aesthetics and is environment-friendly. The smart bricks are also classified as Zero Energy Building Materials (ZEB) with very low energy consumption and extremely low emissions (Figure 7).

In Vietnam, the smart bricks are still new materials and have not been developed yet. However, they will have high potential for future use in a Smart city.

Figure 7. *Zero Energy Building with Smart Bricks*

4.3. Smart Windows

Smart window technology acts as a "light valve" to monitor the amount of light going through the window. Smart shade adjustable window works on the principle of shape memory alloys [6]. This smart window automatically opens and closes without human adjustment when the room temperature and lighting conditions are changed (Figure 8).

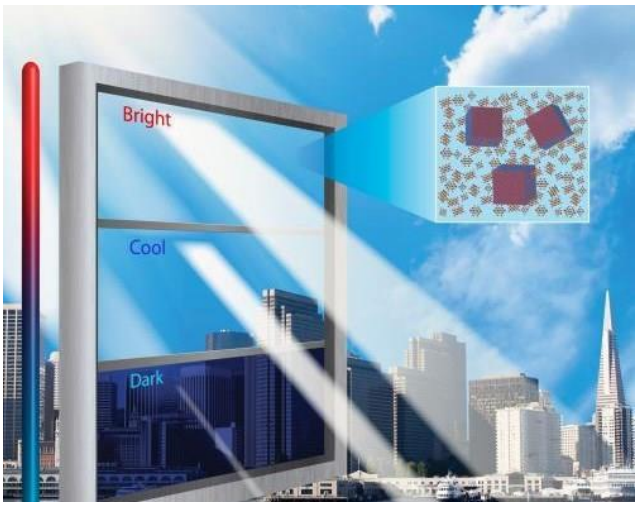

Figure 8. *Smart window*

It also adjusts the amount of CO2 and helps balance the air flow in the room with the outside environment. This helps to use energy efficiently, and at a reasonable cost. Computer equipment will remotely control the operation of this smart window and collect data on temperature and light in the room [1,11].

In Vietnam, the concept of smart window material is quite novel as Vietnam mostly receives technology from other developed countries. Therefore, the largest energy consumption is the air conditioning system in buildings in Vietnam, accounting for about 42%. The factors that cause energy losses in the building are the building cover, the design, the lighting system, the hot water supply, the elevator, etc.

4.4. Smart Roofing

The smart roof is mounted on the photo voltaic modules. Photovoltaic panels (PV Panel) are semiconductor elements that consists of a large number of light sensors on the surface. The light sensors are optical diodes which convert light energy into electrical energy.

This conversion is done by the photovoltaic effect. The operation of the solar cell is divided into three phases: (i) photon light absorbing electron-hole pairs; (ii) the electron-hole pair is then separated by different p-n junction types of semiconductors; (iii) The solar cell is then connected directly to the external circuit and generates an electric current (Figure 9) [16].

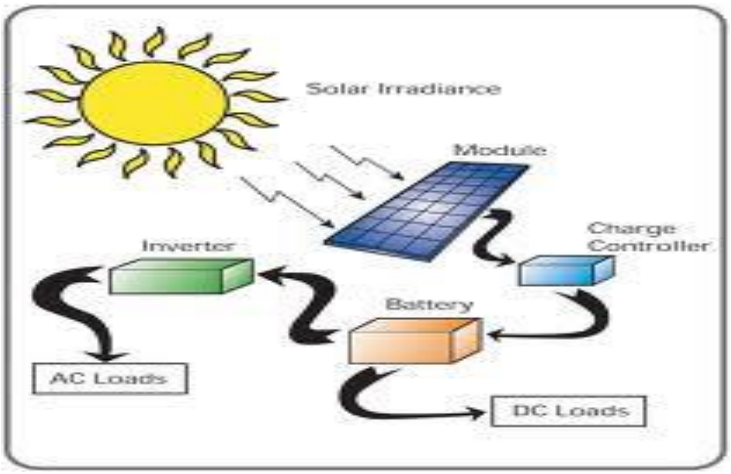

Figure 9. *PV panel Activity*

Today, solar panels are equipped with an automatic control unit that can rotate towards the direction of sunlight. This material is expensive to install initially but has low maintenance costs, so it is indeed a sustainable material for the environment.

In Vietnam, this material has not been developed much although solar energy is ubiquitous. At present, there are some foreign investors building photovoltaic power plants in Vietnam.

4.5. Nano Building Materials

Nanoparticles are materials that have the structure of particles, fibers, tubes, thin sheets, with a typical size of 1 ÷ 100 nm. The size of the nanomaterial is small enough to be comparable to the critical dimensions of some properties. Nanomaterials are located between the quantum properties of atoms and the mass properties of materials.

Nanomaterials are used in building smart homes with self-service, high-performance operating environments and low maintenance costs. It can describe the smart home with nanomaterials as follows: Metal roofs are coated with nanoparticles that automatically adjust the temperature to balance indoor air. Nano sensor equipped walls can automatically adjust the temperature when the weather changes. Kitchen surfaces made of titanium oxide can self-cleaning can prevent moldy bacteria. Bathroom tiles coated with nanoparticles can prevent buildup of deposits. The sunroof with light-sensitive glass absorbs much of the heat and reflects out. Structural parts are fitted with induction components to monitor bearing strength, deformation, subsidence, cracking, corrosion, etc.

Nanoparticles are commonly used in four layers: the decoration outermost layer, the power supply layer, the electronic chip layer to recognize changes of the external environment, and a layer to receive and transmit microwaves [17].

Today, nanomaterials can handle a great deal of energy, environment and health issues. In Vietnam this material was studied since 1997 but it is still yet popular in nowadays. Hence, we can use of the results from developed countries and optimize the product to suit Vietnam's

condition.

4.6. Photo- Catalytic materials to Clean the Environment

A photo-catalytic material is mixed in the concrete and whenever normal day light or solar energy falls on this concrete, the air is completely purified and with antiseptical actions, the pollutants are oxidized along with its special self-cleansing property [1].

Due to photo-catalytic properties a decomposition of organic dirt particles on the surface will take place and a simple clean with water can result in a clean surface for the entire life cycle of the structure (Figure10).

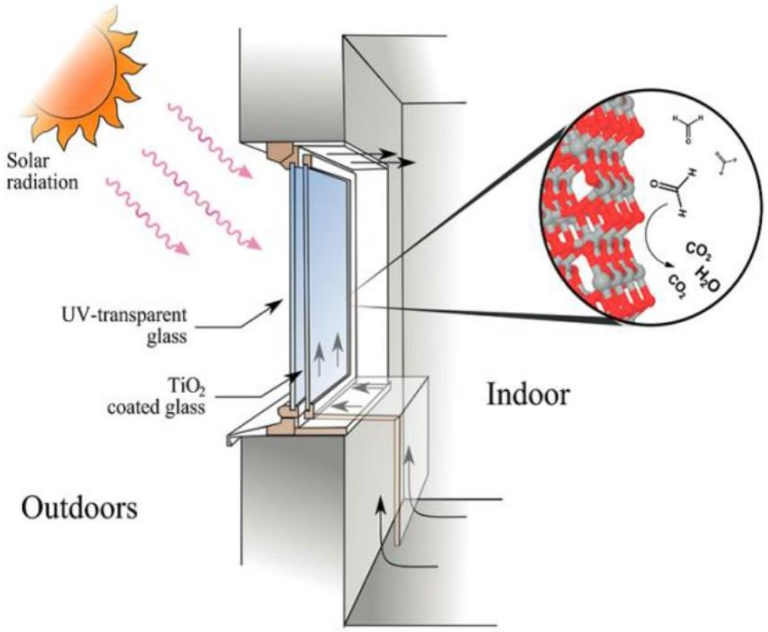

Figure 10. *Photo- catalytic materials to clean the environment*

4.7. Green Materials

Green materials are not considered smart materials for urban smart but are very environment-friendly. Some green building materials such as: (i) Insulating foam (XPS) made by PS plastic; (ii) Ecological roofing sheets are roofing made by cellulose organic fibers, waterproofing asphalt and acrylic by laminating technology; (iii) Green wall tiles are produced by pressing and steam pressure technology, wood is made by wood chips cut from branches; (iv) Green cement made by "flying ash" which is a waste disposed from thermal power plants that not only solves environmental problems caused by fly ash but also has many good features like Porland Cement; (v) Lightweight concrete with big core material as Karamzit granules which produces big sealed hollow but have high compressive strength. Lightweight concrete uses porous aluminum powder and then made into the autoclave with high temperature and pressure; (vi) Recyclable tiles are produced from broken bricks, debris generated in production, which help reuse waste and restrict the exploitation of clay raw materials, which pollute the resources.

These green materials are being developed and applied in Vietnam especially green cement

and lightweight concrete.

III. CONCLUSION

Environment-friendly materials play an important role in the building and sustainable development of smart cities.

Smart materials are developed in a sustainable way, such as energy and water savings. Using sustainable materials such as recycled, reused, originating one is good for human health and economic efficiency, etc.

Smart materials such as Shape Memory Alloys, Piezoelectric materials, Magnetostrictive materials, Optical Fibers work on the principle of converting energy forms back and forth according to specific needs. From there, we apply these principles to smart building materials to use exclusively for construction field of environment-friendly infrastructure of smart city.

References

[1]. *Vivek Mishra, Nidhi Gandhi, Parth Desani, Darshan Mehta*: Smarter Material for Smart Cities. Global Research and Development Journal for Engineering. March 2016, e-ISSN: 2455-5703.

[2]. *Swati Apurva, Satish Tailor, Neera Rastogi*: Smart Materials for Smart Cities and Sustainable Environment. Journal of Materials Science & Surface Engineering, Vol.5 (1), 2017 pp, 520-523.

[3]. Consult Australia and the Smart Cities Council Australia New Zealand: Smart Cities Guide for Built Environment Consultants. January 2018.

[4]. *Ahmad, I*: Smart Structures and I Materials. Proceedings of U.S. Army Research Office Workshop on Smart Materials, Structures and Mathematical Issues, edited by C. A. Rogers, September 15-16; Virginia Polytechnic Institute "& State University, Technomic Publishing Co. Inc, 1988, pp. 13-16.

[5]. *Otsuka K, Ren X*: Recent developments in the research of shape memory alloys. Intermetallics. 1999; 7:511–28.

[6]. *Swabarna Roy, Honey Mishra and B.G. Mohapatro*: Creating Sustainable Environment using Smart Materials in Smart Structures. Indian Journal of Science and Technology, Vol 9(30), August 2016.

[7]. *Mohamed S, Elattar S*: Smart structures and material technologies in architecture applications. Scientific Research and Essay. 2013 Aug; 8(31):1512–21.

[8]. *Hurlebaus S, Stocks T, Ozbulut OE*: Smart structures in engineering education. Journal of Professional Issues in Engineering Education and Practice. 2012 Jan; 138(1):86–94.

[9]. *Raju, P.R., Kumar, J.S., Prakash, M.L*: Bending analysis of smart material plates Using Higher Order Theory. International Journal of Science and Technology, 3(1), 2014.

REAL-TIME FLOOD FORECASTING WITH SUPPORT VECTOR MACHINE FOR YI-LAN RIVER, TAIWAN

NGUYEN DINH TY
Ph.D. Program for Civil Engineering, Water Resources Engineering, and Infrastructure Planning, Feng-Chia University, TaiChung, TaiWan.
Corresponding author's email: dinhtybkdn@gmail.com

Abstract: *As an extending area of application of hydrologic techniques, flood forecasting plays an important role in flood mitigation. In this paper, Support Vector Machine, a supervised learning approach, was adopted to build the real-time flood stage forecasting model. Rainfall and river stage were chosen as input variables. The time lags (delay time) between input variables were judged by using auto-correlation and cross-correlation methods. The optimal parameters were found by two-step grid search method. The proposed model accomplished 1 to 6-hour-ahead stage forecasts at Yi-Lan watershed, Taiwan. Forecasting results showed that the proposed model is effective in forecasting real-time flood stage in Yi-Lan River.*

Keywords: *flood forecasting, support vector machine, time lags, normalizing data.*

I. INTRODUCTION

Flood forecasting models have close correlation with flood warning system. It helps extend the lead time when issuing flood warnings, and produce extra information to improve decision making. This then provides the public and civil protection organizations with more time to prepare for flooding, ideally with less chance of false or missed alarms.

The main inputs which are required for a river forecasting model typically include river level, rain gage measurements, weather radar data, etc. It depends on which observation is available at the watershed. [1] discussed the advantages of using the flood stage over flood discharge in flood forecasting practices. [2] conducted the model making use of distributed rainfall information coming from several rain gauges in the mountain district and predicts the water level of the river at the section closing the mountain district.

Support vector machines (SVMs) are supervised learning models with associated learning algorithms that analyse data used for classification and regression analysis. SVMs perform structural risk minimization, theoretically minimizing the expected error of a learning machine. They are effective in high dimensional spaces. They use a subset of training points (support vectors) in the decision function so they are memory efficient. The application of SVMs has attracted attention in many fields and had a high success rate. There were lots of researches and publications which applied SVMs in hydrological modelling and predicting. Some are: [3] described an exploration in using SVM models in flood forecasting, with the focus on the

identification of a suitable model structure and its relevant parameters for rainfall runoff modelling. [4] proposed SVM to predict one-day-ahead stream flow of Bakhtiyari river in Iran using the local climate and rainfall data. [5] employed SVM to simulate runoff and sediment yield from watersheds, and the outputs of SVM were compared to those of artificial neural network (ANN). [6] performed SVMs prediction model for long-term discharge in Lancang river, and the results outperformed those of autoregressive and moving average model and ANN approach.

The objective of this study is to implement SVM to develop a robust and efficient flood stage forecasting model. The input data utilized herein are rainfall and river stage in Yi-Lan River in Taiwan where suffered from many typhoons every year. The time lags of input variables were determined by the concept of response time. The two-step grid search method and cross validation described by [7] were performed to find the optimal parameters. Model was calibrated by thirteen flood events from 2013 to 2017. Flood stages from one- to six-hour-ahead are forecasted and the robustness of the model is validated by some critical criteria.

II. MAIN CONTENTS

2.1. Support vector regression

Support vector regression (SVR) utilizes the structural risk minimization induction principle from statistical learning theory to minimize the expected risk based on limited data [8]. Suppose that there are l sets of data [(x1, y1), (x2, y2), …, (xl, yl)] used to develop the regression model, where xi are input variables and yi are corresponding output values (i = 1, …, l). The purpose in using SVR is to find the best regression function f(x, α) that can predict the output value y as precise as possible with an error tolerance ε. SVR function can be written as:

$$f(\mathrm{w},\mathrm{b}) = \mathrm{w}.\Phi(\mathrm{x}) + \mathrm{b} \tag{1}$$

where w is weight vector and b is bias. function Φ(x) maps the original input data onto some higher dimensional space, in which the data might be depicted linearity. [9] defines an ε-tube, which is correlated to ε-insensitive loss function as follow

$$L = \begin{cases} 0 & \text{if } \left|\mathrm{y_i} - (\mathrm{w}.\Phi(\mathrm{x_i}) + \mathrm{b})\right| < \varepsilon \\ \left|\mathrm{y_i} - (\mathrm{w}.\Phi(\mathrm{x_i}) + \mathrm{b})\right| & \text{otherwise} \end{cases} \tag{2}$$

SVR function becomes:

$$\begin{aligned} \min_{\mathrm{w},\mathrm{b},\xi_i,\xi_i^*} \quad & \frac{1}{2}\mathrm{w}^2 + C\sum_{i=1}^{l}(\xi_i + \xi_i^*) \\ \text{subject to} \quad & \mathrm{y_i} - (\mathrm{w}.\Phi(\mathrm{x_i}) + \mathrm{b}) \le \varepsilon + \xi_i \\ & (\mathrm{w}.\Phi(\mathrm{x_i}) + \mathrm{b}) - \mathrm{y_i} \le \varepsilon + \xi_i^* \\ & \xi_i,\ \xi_i^* \ge 0 \\ & \mathrm{i} = 1, 2, ..., l \end{aligned} \tag{3}$$

where ξ and ξ* are slack loss values. C is a positive parameter determining the trade-off between the empirical risk and the flatness of the function. Optimization problem in Eq.(3) is usually solved more easily in its dual form using Lagrange multipliers (α,α*) and the Kharush-Kuhn-Tucker (KKT) method (detailed in [10]) is applied. The approximating function can be expressed:

$$f(x_i) = \sum_{i,j=1}^{l} (-\alpha_i + \alpha_i^*) \left\langle x_i . x_j \right\rangle + b \tag{4}$$

where $\left\langle x_i . x_j \right\rangle$ is the inner product of xi and xj; Lagrange multipliers $0 \le \alpha i, \alpha j^* \le C$ and i, j =1,...,l. The input vectors that have nonzero Lagrange multipliers (–αi + αi*) are termed the support vectors.

The kernel function K(xi, xj) is applied to compute in the input space to overcome the problem of dimensionality. With kernel function, the inner products in feature space are directly yielded from the input points. Regarding to the work by other researchers ([11], [12], [13]), Radial Basis Function (RBF) kernel is utilized in this study (Eq. 5)

$$K(x_i, x_j) = \exp(-\gamma \left| x_i - x_j \right|^2) \tag{5}$$

where γ is kernel parameter. Eventually, the decision SVR function becomes

$$f(x_i) = \sum_{i=1}^{l} (-\alpha_k + \alpha_k^*) K\left(x_i . x_k \right) + b \tag{6}$$

k is number of support vector, xk is the support vector.

Using RBF in nonlinear SVR leads to tune three meta-parameters: the cost constant C, the insensitive tube radius ε, and kernel parameter γ.

2.2. Study area and data

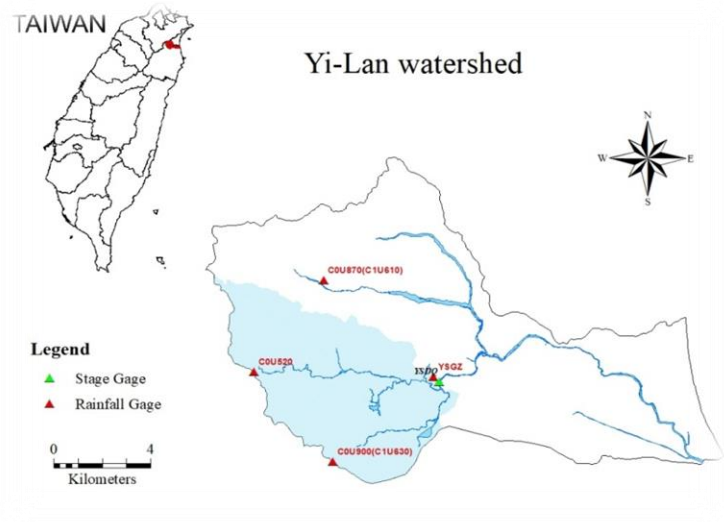

Figure 1. *Location of Yi-Lan river basin*

The Yi-Lan River Basin (Fig. 1) is in Yi-Lan county in north-eastern Taiwan. The main stream of the Yi-Lan River is approximately 17.25 km long and covers area of about 149.06 km^2. The main stream flows through a major city in the county, Yi-Lan city including. The major commercial activity along the river is agriculture. This basin contains the mountain and flat area, it also consists of the natural river systems and high potential inundation area. Our calculation is forecasting the lead time river stage at Yuan-Shan station, which covers the sub-basin of 45.72 km^2. Rainfall and river stage data of thirteen flood events from 2013 to 2017 was collected from four gages included. Rainfall data used in the model is average rainfall which calculated by Thiessen polygon method. The data are available on website of Taiwan Typhoon and Flood Forecasting Institute (http://wraew.ttfri.narl.org.tw/). This study doing on 13 flood events with 9 calibration events and others 4 events used for validation. Choosing events is based on principle that two third of events are calibration and one third of them are validation.

2.3. Model development

2.3.1. Normalising input data

In this study, we build a SVR model to predict the flood stages at Yuan-Shan station. The observed average rainfalls and river stages at Yuan-Shan station during flood events were chosen because the strong correlation between them and future stages. Thus, we have two variables: the average rainfall R and the river stage S at Yuan-Shan station. As defined by [14], Since the cross sections of the river definitely change after a flood, the absolute water stage may not provide appropriate information to distinguish floods. We chose the river stage increments, which are relative to the initial stage when the rainfall occurs, as stage variables in this study. Namely, each input stage was subtracted with the initial stage of the station, and the difference was employed as the stage variable.

One of the difficulties in the calculation is that the difference units of the input variables, as we have rainfalls and river stages herein. Also to avoid the domination of one input to others when the difference of them are seriously transparent, we normalized the data into the values from zero to one. [15] had shown that SVM model with normalized data is better than the unscaled one. Hence, the normalized rainfalls and river levels were utilized in this research. Finally, the output results would be rescaled to the initial units.

2.3.2. Determining lag of input variables

After data are normalized, the time lag should be determined. As experienced in [1], [16], the method to indicate time lag between rainfall and stage is calculating the coefficient of correlation with difference time lags n. For the rainfall and river stage at Yuan-Shan station, this value is chosen 3 hours.

The second type of variable in this study is the river stage. The previous flows are used as input variable cause highly relevant to the ahead stage, defined by the cross-correlation. [1] indicated that the forecasts are not much sensitive to the lags of the input variables, so the time

lag of input stage was set to 2 hours as the high correlation. The SVR model in this study constructed by 5 elements, output is expressed as below:

$$S(t+1) = f_{SVR}\left[S(t+1-m_s), R(t+1-m_R)\right] \quad (7)$$

where mS = 1,2; mR = 1,2,3; S is flood stage, R is rainfall data, t is time index, fSVR indicates the SVR model as defined as Eq. (6).

2.3.3. Determining Calibrating parameters

The non-linear SVR models are employed in this study with kernel function RBF as decided above. The target parameters set have to indicate is (C, ε, γ). C accounts for the penalty parameter, ε is error tolerance, and γ stands for kernel parameter.

The study collected 9 flood events with 592 rainfall and river stage data sets for calibrating. As [7], [1], two-step grid search method was used to derive SVR parameters. Minimum root mean square error (RMSE) of simulating calibration events are used to determine the optimal parameters. In this paper, we inherited the free software which are open to users LIBSVM developed by [17], revised by [1] to suit the application in this study. First step: coarse grid search is adopted to indicate the feasible 3-dimensional grid region of the optimal target parameters (C, ε, γ). Second step: finer grid search is constructed in feasible region to find the best set of (C, ε, γ). Fivefold cross validation was used in calibrating progress, and the optimal set (C, ε, γ) = (57.6; 0.0033; 0.27) is the mean value of five sets of cross-validation process. The value of RMSE = 0.046 m was indicated by simulating the calibration events. Graph of simulated stage are shown below (Fig. 2), it shows the seemingly identical between simulated data and original one, means we had a robust calibration method. Percentage of support vectors (SVs) is 64.7%, that is not too much distinct with the optimal percentage of SVs as experienced in [2], [18],[1],[14].

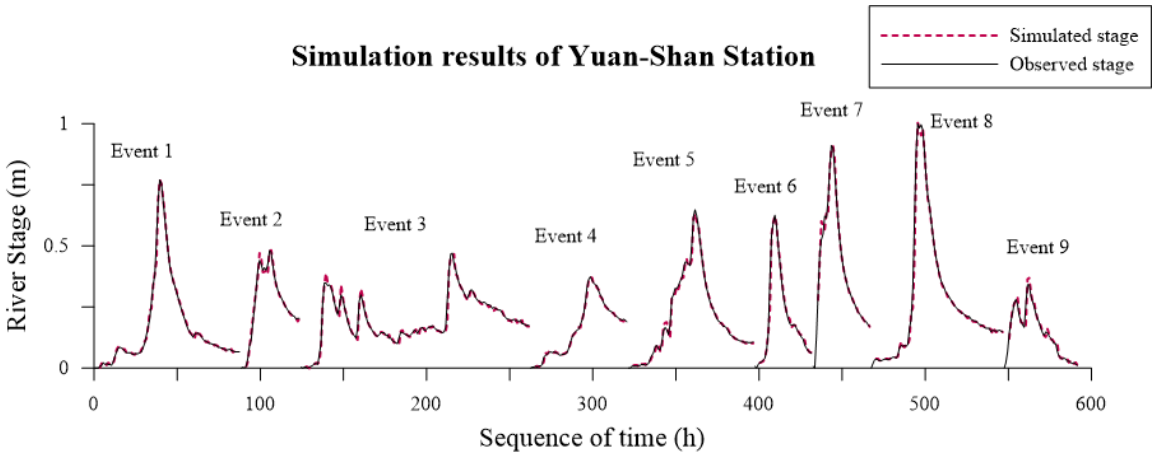

Figure 2. *Simulated results (calibration events 1 to 9).*

2.3.4. Forecasting future flood stages

Developing Eq. (7) we get equations for multiple hours ahead flood forecasting

$$S(t+i) = f_{SVR}\left[S(t+i-m_s), R(t+i-m_R)\right] \quad (8)$$

where the index i = 1 to 6 are multiple hours ahead; mS = 1,2; mR = 1,2,3; fSVR indicates the SVR model. With them, at the present time t, we can forecast the river stage at future time t + 1 to t+6. But one problem occurs that at the time from 2 hours to 6 hours, the value R(t+1) to R(t+5) does not exist, while values of S(t+1) to S(t+5) can be obtained by the previous forecasting model. To deal with this difficulty, a simple method called Naïve was applied. That is, the non-existent values were substituted by the previous observed ones, so that SVR models would have enough variables for construction.

2.4. Results and d assessment

One to six hours ahead flood stages can be generated by proposed SVR models. Fig. 3 describes the observed and forecasted river stages for 1 to 6 hours forward of event 11. The results then assessed by some following criteria, which are normally used in statistic evaluation.

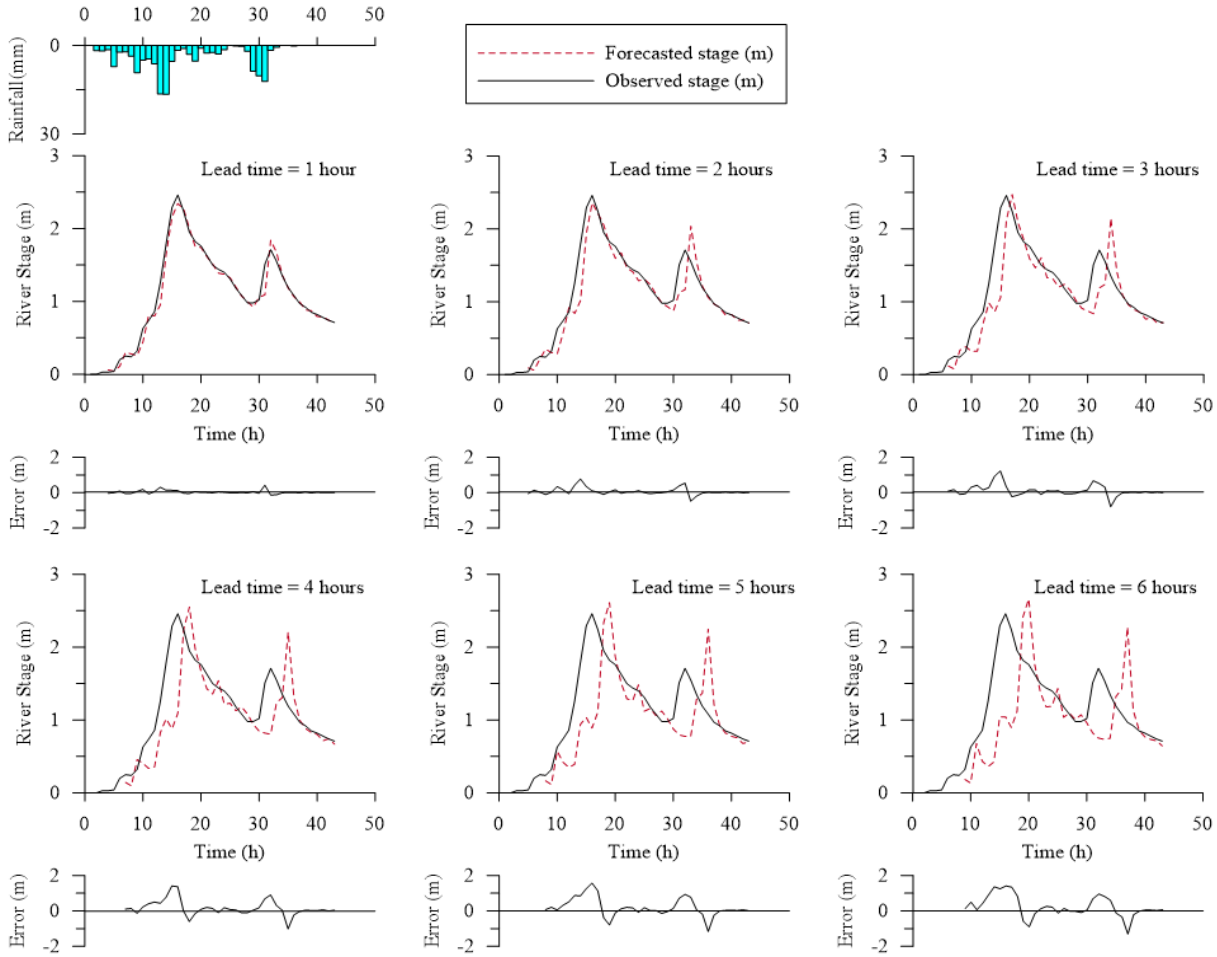

Figure 3. *Forecasting results (event 11)*

1. Coefficient of efficiency with respect to benchmark (CEbench) (Eq. (9)).

As published at [19], CEbench is suitable for forecasting models, the benchmark stage is predicted by using the Naïve model. High value of CEbench illustrates outperforming model to

the benchmark model. Where s_t is the observed stage; $\bar{s}$ is mean observed stage; $\hat{s}_t$ the forecasted stage; $\bar{\hat{s}}$ the mean forecasted value at time t, n accounts for number of stage data.

$$CE_{bench} = 1 - \frac{\sum_{t=1}^{n}(s_t - \hat{s}_t)^2}{\sum_{t=1}^{n}(s_t - s_t^{bench})^2} \quad (9)$$

2. Root mean square error (RMSE)

RMSE a frequently used measure of the differences between values predicted by a model and the values actually observed. The unit here is meter (m).

$$RMSE = \sqrt{\frac{\sum_{t=1}^{n}(s_t - \hat{s}_t)^2}{n}} \quad (10)$$

According to results Fig. 3, the observed and predicted data are seemingly alike for time step of 1 to 3 hours ahead with small value of RMSE (0.1m, 0.21m and 0.33m respectively). Meanwhile, 4 to 6 hours ahead results are acceptable (RMSE are 0.44m, 0.53m and 0.66m). As the value of CEbench all positive (in the range of [0.92;0.34]), that means the SVR models outperform the model of benchmark. From 2 to 6 hours ahead, even the input variables not only observed but also have replaced data, the results are still so good, suggesting the robust and effective SVR models.

III. CONCLUSION

The target in this paper is performing the robust and efficient river stage forecasting models which are necessary for flood warning during flood events. The SVR models were applied successfully in flood stages prediction at Yi-Lan watershed, northeast of Taiwan. The models used the input data of average rainfall of 4 rainfall stations and river stages at Yuan-Shan station. Data was collected from past 13 flood events. The important part in flood forecasting model is the lags of input variables are conducted based on concept of time of response. Then the inputs variables of calibrating process were identified. For the lack of future inputs variables, the simple model called Naïve was utilized. The flood stages of 1 to 6 hours forth were easily forecasted by SVR models, the results indicate the high performance of proposed models. However, this paper only showed the method (the software used) with data and variables that is needed for software, the selection of support vectors was not explained herein. The results of prediction for 4 to 6 hours ahead is not really perfect, maybe the area of watershed is small. These points should be improved in the future works.

References

[1]. *P.-S. Yu, S.-T. Chen, and I.-F. Chang*, "Support vector regression for real-time flood stage

forecasting," Journal of Hydrology, vol. 328, no. 3, pp. 704–716, Sep. 2006.

[2]. *Davide Mattera and S. H.*, "Support vector machines for dynamic reconstruction of a chaotic system. In S. H. Davide Mattera, Advances in kernel methods (pp. 211-241)." Cambridge, MA, USA: MIT Press Cambridge, MA, USA, 1999.

[3]. *M. Bray and D. Han*, "Identification of support vector machines for runoff modelling," Journal of Hydroinformatics, vol. 6, no. 4, pp. 265–280, Oct. 2004.

[4]. *M. Behzad, K. Asghari, M. Eazi, and M. Palhang*, "Generalization performance of support vector machines and neural networks in runoff modeling," Expert Systems with Applications, vol. 36, no. 4, pp. 7624–7629, May 2009.

[5]. *D. Misra, T. Oommen, A. Agarwal, S. K. Mishra, and A. M. Thompson*, "Application and analysis of support vector machine based simulation for runoff and sediment yield," Biosystems Engineering, vol. 103, no. 4, pp. 527–535, Aug. 2009.

[6]. *J.-Y. LIN, C.-T. CHENG, and K.-W. CHAU*, "Using support vector machines for long-term discharge prediction," Hydrological Sciences Journal, vol. 51, no. 4, pp. 599–612, Aug. 2006.

[7]. *Chih-Wei Hsu, Chih-Chung Chang, and Chih-Jen Lin*, "A Practical Guide to Support Vector Classification." Department of Computer Science National Taiwan University, 2010.

[8]. *V. Vapnik*, The Nature of Statistical Learning Theory, 2nd ed. New York: Springer-Verlag, 2000.

[9]. *C. Cortes and V. Vapnik*, "Support-vector networks," Mach Learn, vol. 20, no. 3, pp. 273–297, Sep. 1995.

[10]. *R. Fletcher*, Practical Methods of Optimization. John Wiley & Sons, 2013.

[11]. *G.-F. Lin, G.-R. Chen, P.-Y. Huang, and Y.-C. Chou*, "Support vector machine-based models for hourly reservoir inflow forecasting during typhoon-warning periods," Journal of Hydrology, vol. 372, pp. 17–29, Jun. 2009.

[12]. *D. Misra, T. Oommen, A. Agarwal, S. K. Mishra, and A. M. Thompson*, "Application and analysis of support vector machine based simulation for runoff and sediment yield," Biosystems Engineering, vol. 103, no. 4, pp. 527–535, Aug. 2009.

[13]. *D. Han, L. Chan, and N. Zhu*, "Flood forecasting using support vector machines," Journal of Hydroinformatics; London, vol. 9, no. 4, pp. 267–276, Oct. 2007.

[14]. *S.-T. Chen and P.-S. Yu*, "Real-time probabilistic forecasting of flood stages," Journal of Hydrology, vol. 340, no. 1, pp. 63–77, Jun. 2007.

[15]. *M. Bray and D. Han*, "Identification of support vector machines for runoff modelling," Journal of Hydroinformatics, vol. 6, no. 4, pp. 265–280, Oct. 2004.

[16]. *D. P. SOLOMATINE and K. N. DULAL*, "Model trees as an alternative to neural networks in rainfall - runoff modelling," Hydrological Sciences Journal, vol. 48, no. 3, pp. 399–411, Jun. 2003.

[17]. *C.-C. Chang and C.-J. Lin*, "LIBSVM: A library for support vector machines," ACM Transactions on Intelligent Systems and Technology, vol. 2, no. 3, pp. 1–27, Apr. 2011.

[18]. *V. Cherkassky and Y. Ma*, "Practical selection of SVM parameters and noise estimation for SVM regression," Neural Netw, vol. 17, no. 1, pp. 113–126, Jan. 2004.

[19]. *J. Seibert*, "On the need for benchmarks in hydrological modelling," Hydrological Processes, vol. 15, no. 6, pp. 1063–1064, Apr. 2001.

A NEW APPROACH FOR DETERMINING THE ROAD TRAFFIC ACCIDENT HOT SPOTS USING GIS-BASED TEMPORAL-SPATIAL STATISTICAL ANALYTIC TECHNIQUES A CASE STUDY IN HANOI CITY, VIETNAM

LE KHANH GIANG[1], PEI LIU[2], LIANG-TAY LIN[3]
[1]Doctoral Candidate, Ph.D program of Civil and Hydraulic Engineering, College of Construction and Development, [2]Professor, Chief of Office of International Affairs, [3]Professor, Department of Transportation and Logistics, Dean of College of Construction and Development, Feng Chia University, Taichung, Taiwan
Corresponding author's email: khanhgiang298@gmail.com

Abstract: *The article presents a new model to determine road traffic accident hot spots by applying GIS-based temporal and spatial statistical analytic techniques. Road traffic accident data in three years (2015-2017) in Hanoi, Vietnam used to analyse and test this approach. Firstly, road traffic accident (RTA) data was divided into four seasons in accordance with Hanoi's weather conditions, Vietnam and temporal intervals such as day time, night time, or the peak hour. Then, kernel density estimation (KDE) method was applied to analyse RTA hot spots according to seasons and temporal intervals. Finally, the results were presented by using the CoMap technique. The results of the paper show that the approach was effective and exact in identifying RTA hot spots in Hanoi, Vietnam, simultaneously these hot spots were ranked according to their level of dangerousness. These outcomes will not only enable traffic authorities to comprehend the causes behind each collision, but also to help them manage and deal with hazardous areas according to the prior order in case of limited budget and allocate traffic safety resources appropriately.*

Keywords: *Hot spots, road traffic accident (RTA), Geographic information system (GIS), kernel density estimation (KDE), temporal-spatial statistical analyses.*

I. INTRODUCTION

Road traffic accidents (RTA) are one of the important issues over the world. According to the reports of World Health Organization (WHO), there are more than 1.24 million deaths and about 50 million people injured as results of RTA every year in the world [1]. To decrease significantly the number of crashes, it is crucial to understand where and when traffic accidents happen frequently. The locations, where are identified by a high accident occurrence compared

with the other locations, are known as hot spots. The past studies showed that the occurrences of RTA are infrequently random in space and time. In fact, these locations identified by several key factors such as geometric design, traffic volume, or weather conditions, etc [2].

WHO reported that there were over a third of deaths owing to RTA in low and middle-income nations among vehicles, cyclists, and pedestrians [1]. Vietnam is a developing country; thus, RTA issue also is one of the most concerns of transportation authorities. The annual social expenditure of RTA in Hanoi, is the capital of Vietnam, in term of medical treatment, deaths, and property damage occupy 2.9% GDP (5-12 billion USD) [3].

In 2017, there were 20,000 traffic crashes, about 8,200 deaths and 17,000 injured on Vietnam's road networks [4]. Currently, non-spatial modelling has been used in Vietnam to identify RTA hot spots, namely: Accident Frequency Method (AFM) (classification by level of injury) over one year period [5]. This is the oldest and simplest method to identify dangerous locations. However, this method has many limitations such as lacking of visualizing, connecting between space and time, ranking of hot spot's priority, does not take into consideration traffic volume, which has a direct relationship with crash frequency. Therefore, the results have bias toward high-volume locations and suffers from the RTM bias [6]. Currently, there has not any study dealing with collision mapping in Vietnam.

Geographic Information System (GIS) is a very powerful tool for analyzing traffic safety. GIS can visualize the locations of accidents and store its attributes. Thus, it is easy to find the reasons behind each collision. Spatial data usage plays an important role on traffic safety analysis. GIS enables us to collect, store, manipulate, query, analyze, and visualize the spatial data [7].

Spatial analysis of RTA has been popularly applied to explore hot spots [8]. Kernel density estimation (KDE) is one of the most popular density-based methods and has been widely used for detecting dangerous road segments [9]. However, KDE method has a drawback is that it lacks an investigation of the statistical significance of the high-density locations [10].

In contrast to spatial analysis, temporal analysis of RTA is not significantly considered [11]. There were several past studies carried out temporal analysis of traffic collisions. However, their outcomes were mainly depicted by simple graphs or figures, which do not enable us to visualize crash clusters over time.

Currently, spatial-temporal analysis in identifying RTA hot spots is not almost considered. CoMap technique enables us to analyze temporal-spatial integration and introduced by Brunsdon (2001) [12]. The spatial pattern of fire incidents in Toronto varied over time was a typical example of applying CoMap method and performed by Asgary et al. (2010). The temporal-spatial interaction influence on single vehicle collisions was studied by Plug et al. (2011) [10]. Past studies indicated that the CoMap technique enables us to analyze temporal-spatial integration effectively.

Thus, in our study, spatial-temporal analysis will be carried out by applying GIS-based CoMap and KDE methods to determine RTA hot spots. The purpose of this paper was to explore the temporal-spatial patterns of RTA varying according to the seasons and the special time of the day. The remainders of the article are arranged as follows. Section two depicts main contents including study data, methods, and analysis results. Finally, conclusions are presented in section three.

II. MAIN CONTENTS

2.1. Study data

This study was carried out in Hanoi, Vietnam. Two different databases were used for this study. First, a road network map was provided in a shape file format, which includes specifications of roads such as road length, road width, road type, and speed limits. Second, a traffic accident database in three years (2015-2017) was provided by the Transport Police Department in Hanoi. There are 1,132 crashes were recorded on Hanoi's roads. The collision database was provided in an Excel file and contained significant accident parameters such as the date and time of a crash, crash location, accident types, age and sex of drivers, the number of the injured, etc.

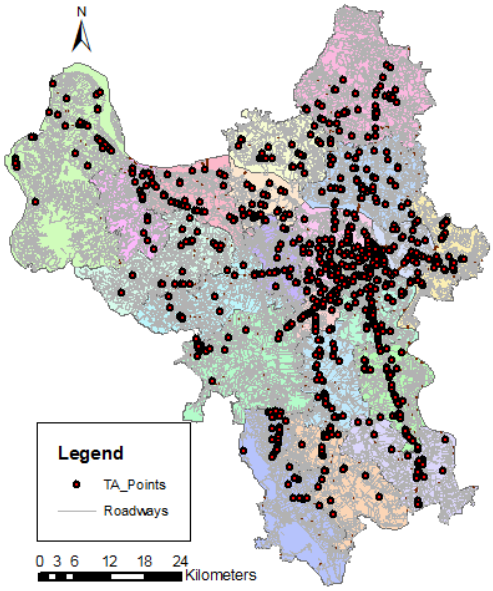

Figure 1. *Study area with distribution of all collisions in Hanoi (2015-2017)*

2.2. The process of building a GIS project

The steps of building a GIS project will be shown in the following map.

Figure 2. *Diagram of steps to build a GIS project*

2.3. Methods

2.3.1. Kernel density estimation method

KDE is one of the most effective methods to determine the spatial models of RTA. The density of events is calculated within a definite research radius in the study areas to create a smoothed surface. A kernel function is utilized to assign a weight to the area surrounding the events proportional to its distance to the point event. From there, the value is highest at the point event location centre and decrease smoothly to a value of zero at the radius of the research circle. At the end, a smoothed continuous density surface is generated by adding the individual kernels in the research area [8]. The intensity at a specific location is calculated by Eq. (1):

$$f(s)=\frac{1}{nh^2}\sum_{i=1}^{n} K\left(\frac{d_i}{h}\right) \quad (1)$$

where f(s) is the density estimate at the location s, n is the number of observations, h is the bandwidth or kernel size, K is the kernel function, and d_i is the distance between the location s and the location of the i^{th} observation.

2.3.2. CoMap technique

CoMap technique enables us to analyze temporal-spatial integration and introduced by Brunsdon (2001) [12]. CoMap method help to investigate the relationships between the location of RTA and their changing over time [12]. In this paper, the three-year (2015-2017) collision data in Hanoi, Vietnam is divided according to the seasons of the year in accordance with Hanoi's weather conditions. Next, KDE is used to calculate and analyze the density of each subset. Finally, the spatial distributions of RTA are demonstrated in different maps and show how traffic accident hot spots varied over time [10]. For our study purposes, the relationship between the spatial distribution of RTA and their changing according to the seasons and the different time of the day will be investigated.

The class boundaries should be overlapped each other suggested by some researchers [10]. In this study, the collisions were divided into four different seasons and have some days overlapped to avoid the temporal boundary problem as shown table 1.

Table 1. *Crashes classified into four sampling periods*

Season	**Winter**		**Spring**		**Summer**		**Fall**	
Duration	From	To	From	To	From	To	From	To
	Nov 01	Feb 30	Feb 01	Apr 30	Apr 20	Sep 10	Sep 01	Nov 10

2.4. Analysis Results

2.4.1. The distribution of season-related hot spots

In this part, a CoMap was generated to comprehend the temporal-spatial distribution of RTA. Figure 3 shows that the distribution of RTA hot spots in Hanoi varied among the seasons. According to statistic, the number of crashes is similar in summer and winter, namely 367 and 392 crashes respectively. More important thing is that, the distribution of RTA hot spots is quite similar in these both seasons, as shown in the panel 2 and 4 (Fig. 3). The amount of RTA in summer and winter is two times higher than the rest and RTA hot spots with higher intensity (in red) are concentrated mainly in the city centre where trade centers, schools, hospitals are located, and in particular along National Highway 1A section, that passes through Hanoi, especially in

Van Dien, Cho Tia, Thuong Tin station zones (encircled in black).

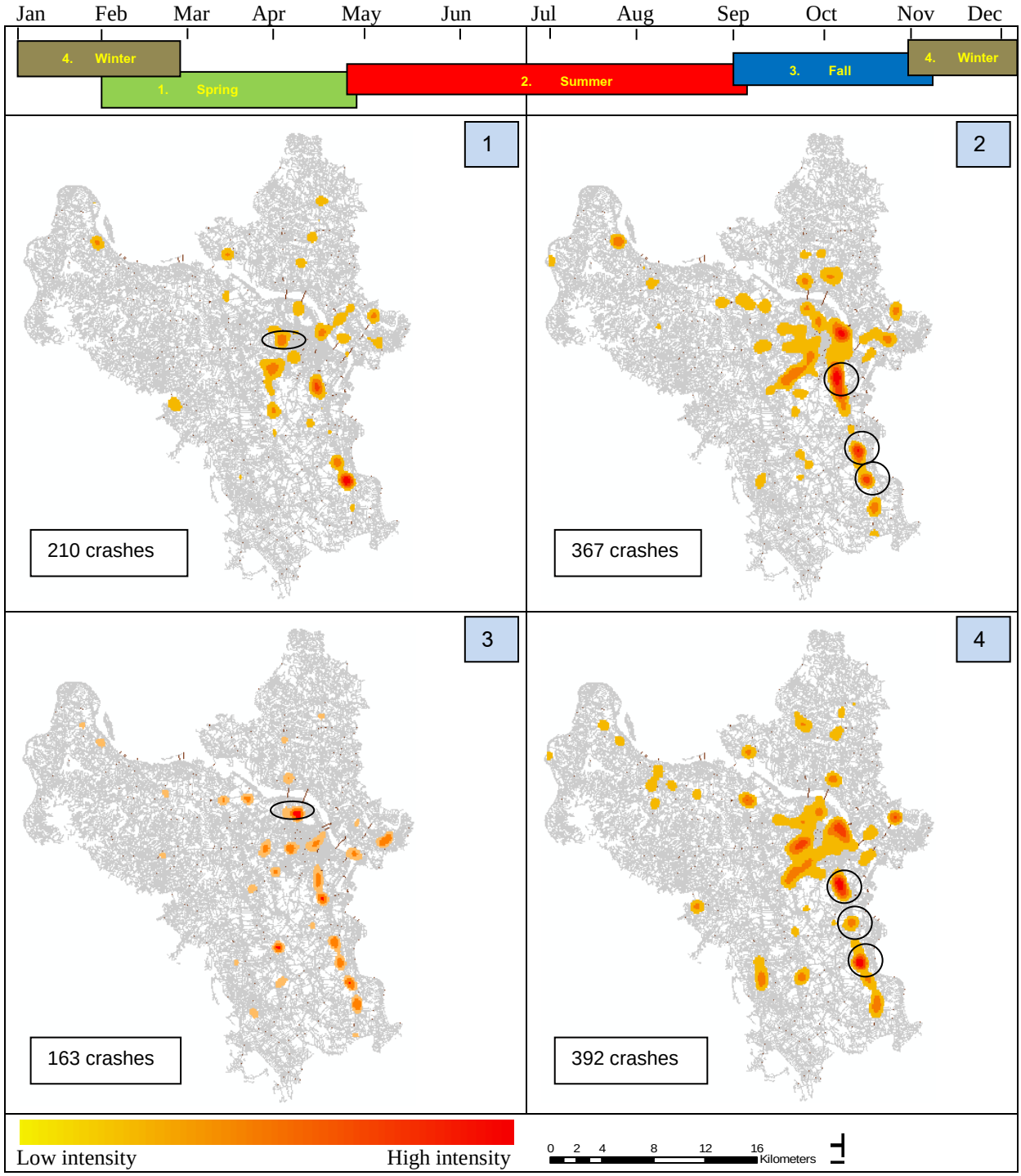

Figure 3. *CoMap for season-related RTA hot spots distribution in Hanoi*

RTA fluctuated in both space and time as shown in Fig. 3. There were several key factors affecting the level of changing. Namely, the weather conditions are really severe in summer and winter in Hanoi. The temperature can reach over 42 degree during summer and 6 degree during winter. In addition, there are several month-long rains in the summer (e.g., in June and July). These severe conditions make the number of crashes much higher than in fall and spring. In contrast to the harsh weather, fall in Hanoi is extremely pleasant, cool, no rain. It is probably thanks to this that the number of collisions is only 163 cases.

Besides, seasonal related RTA hot spots could be determined by CoMap. There were several seasonal related hot spots only occurred during a certain season. These hot spots surrounded by an eclipse. Namely, in fall, collisions often happened at Vo Chi Cong – Xuan La intersection, while its intensity was not high in other seasons. In spring, the collision intensity was high at Pham Hung – Duong Dinh Nghe intersection, while its density was not high in the others.

2.4.2. The distribution of temporal interval-related hot spots

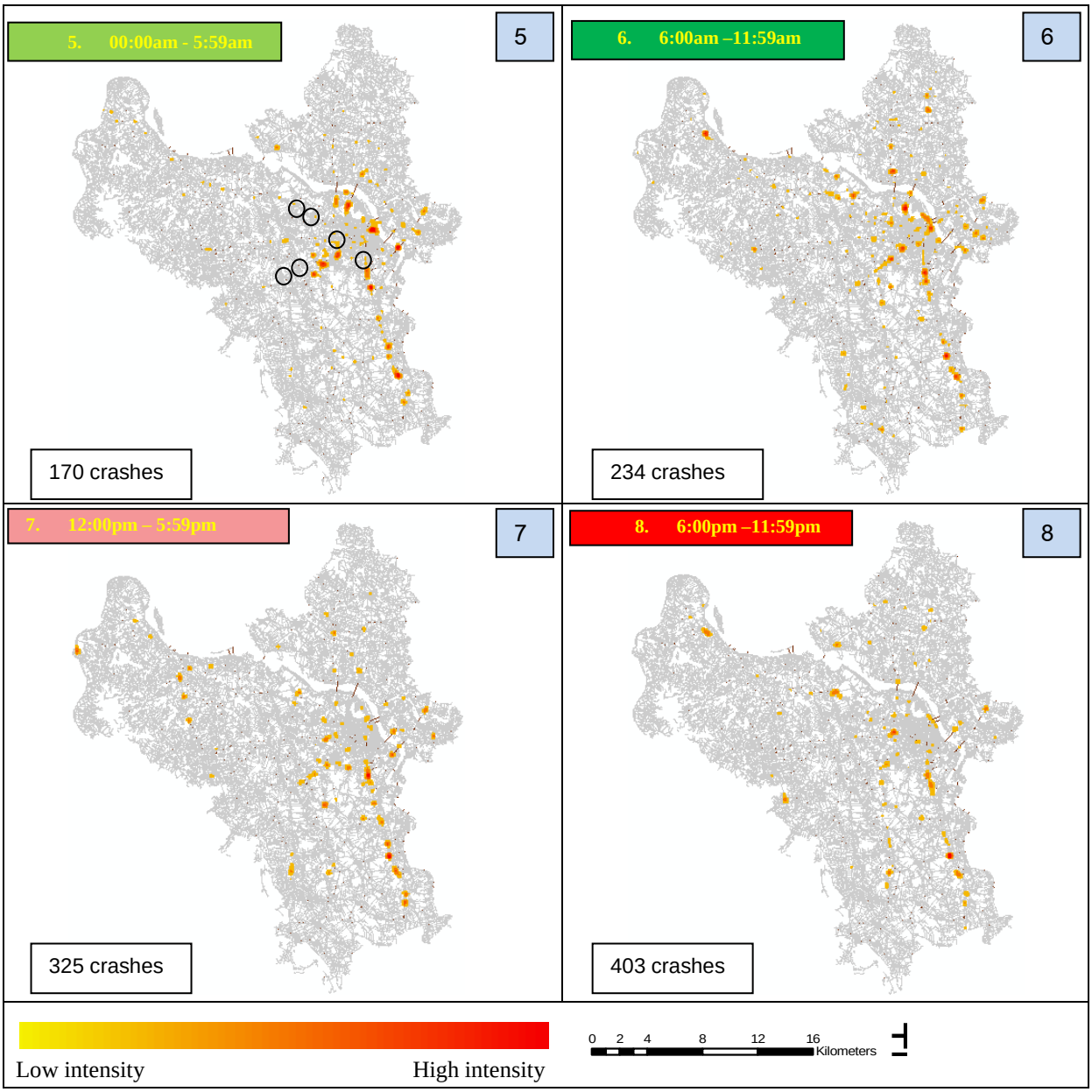

Figure 4. *CoMap for temporal interval-related RTA hot spots distribution in Hanoi*

Past studies have shown that traffic accidents varied over time of the day. Figure 4 demonstrates that the number of collisions occurring the most at night (6:00pm – 11:59pm) (see the panel 8), when people go back home after a hard-working day and everyone wants to go home quickly. Another possible cause is that at this time the vision is limited. Thus, those could be the main reasons for the high number of crashes.

In the early morning (00:00am - 5:59am), although there were not many traffic users, there were 170 crashes. As shown in the panel 5, the hot spots are mainly located in the southern part

of Thang Long bridge, Nhat Tan bridge, Chuong Duong bridge, Vinh Tuy bridge, and Nguyen Trai road (encircled in black). This explains that most traffic users at this time are workers from the suburb areas of Hanoi, and they frequently travel to the city center at this time. These points are also the RTA black spots as observed from the reality. This indicates that there are several RTA back spots that only occurred during specific time of the day as showed in the panel 5 (encircled in black). These spots with high intensity during (00:00am - 5:59am) period while its intensity was not high in other temporal intervals of the day.

III. CONCLUSION

The article has shown that the combined analysis of space and time in identifying RTA hot spots enables traffic authorities to capture the situation accurately and timely. In addition, black spots are ranked according to dangerous order. From there, the traffic authorities easily provide reasonable solutions to overcome these issues in case of limited budget and resources appropriately.

This new approach demonstrates strengths in traffic safety analysis, particularly in identifying RTA hot spots. The distribution of RTA hot spots varied over time according to the different seasons and specific temporal intervals of the day. Our study shows that traffic accidents occur frequently in summer and winter. In addition, night time is the dangerous time that traffic collisions happen frequently. This is also the first study about this issue in Vietnam, so the contribution of the article will help the traffic authorities easily solve this problem not only in Hanoi, but also can apply for other cities.

However, within the scope of the paper, there is a limitation is that does not take traffic volume in identifying RTA hot spots. Therefore, in the forthcoming studies, the authors will solve this issue. In addition, the authors will deploy this application online, which not only helps the traffic authorities, police patrol to update emergence information easily but also provide the citizen a black spot map in an updated, accurate, and visual way.

References

[1] *WHO,* "Global status report on road safety 2013. Supporting a decade of action", World Health Organization, Department of Violence and Injury Prevention and Disability, Geneva, 2013.
[2] *Chainey, S., Ratcliffe, J.,* "GIS and Crime Mapping", John Wiley & Sons, England, 2013.
[3] *Ha Mai,* "Việt nam mất khoảng 130 tỉ usd chi phí cho tai nạn giao thông trong 15 năm", https://thanhnien.vn/thoi-su/viet-nam-mat-khoang-130-ti-usd-chi-phi-cho-tai-nan-giao-thong-trong-15-nam-954438.html [access: 16:55, 07/06/2018].
[4] *Thu Giang,* "Ủy ban An toàn giao thông Quốc gia tổng kết công tác năm 2017", http://backantv.vn/tin-tuc-n17855/uy-ban-an-toan-giao-thong-quoc-gia-tong-ket-cong-tac-nam-2017.html [access: 10:09, 09/07/2018].
[5] *Thông tư 26/2012/TT-BGTVT,* "Quy định về việc xác định và xử lý vị trí nguy hiểm trên đường bộ đang khai thác", BGTVT, Vietnam, 2012.
[6] *Li, L.,* "A GIS-based Bayesian approach for analyzing spatial-temporal patterns of traffic crashes", Doctoral dissertation, Texas A&M University, 2006.
[7] *Lloyd, C. D., "*Spatial data analysis: an introduction for GIS users", Oxford University Press, 2010.
[8] *Anderson, T. K.,* "Kernel density estimation and K-means clustering to profile road accident hotspots", Accid Anal Prev, Elsevier, 2009.
[9] *Xie, Z., Yan, J.,* "Detecting traffic accident clusters with network kernel density estimation and local spatial statistics: an integrated approach", J. Transp. Geogr, Elsevier, 2013.
[10] *Plug, C., Xia, J.C. and Caulfield, C.,* "Spatial and temporal visualisation techniques for crash analysis", Accid Anal Prev, Elsevier, 2011.
[11] *El-Sadig, M., Norman, J.N., Lloyd, O.L., Romilly, P. and Bener, A.,* "Road traffic accidents in the United Arab Emirates: trends of morbidity and mortality during 1977–1998", Accid Anal Prev, Elsevier, 2002.
[12] *Brunsdon, C., Corcoran, J. and Higgs, G.,* "Visualising space and time in crime patterns: A comparison of methods", Computers, Environment and Urban Systems, 2007.

THE IOT APPLICATION SUPPORT MODEL TO MANAGE THE AIR ENVIRONMENTAL QUALITY OF THE SMART CITY IN VIETNAM

TRAN THIEN CHINH[1], NGUYEN CANH MINH[2]
[1]Reseach Institute of Posts and Telecommunications - Posts and Telecommunications Institute of Technology,
[2]Electric and Electronic Department - University of Transport and Communications, Hanoi, Vietnam
Corresponding author's email: trthchinh@gmail.com

***Abstract**: In recent years, Businesses and policymakers have paid a lot of attention to the Internet of Things (IoT). Numerous reports have shown (for example billions, even trillions of devices, have been linked), opening up opportunities for change in all economic activity. However, IoT still faces many obstacles such as: there are few initiatives beyond the pilot phase, the business model has not yet developed sufficiently to maintain the IoT infrastructure in long-term and the state management context has not met the requirements. So far, nations do not have a clear set of policy and institutional frameworks to facilities of IoT development, such as rules, regulations for on-site verification, data or security. In Vietnam, the ministries, branches, localities, as well as the business community and economic sectors in the society, have made great efforts in organizing the research, exploitation and application of smart city development in many different levels. Since 2015, Da Nang city has approved the project of building a smart city and implemented in the whole city. Nearly 30 localities have signed cooperation agreements with partners such as VNPT and Viettel to build smart city projects, many of which are Quang Ninh, Vinh Phuc, Bac Ninh and Ho Chi Minh City approved. The development of smart city is geared towards a qualitative change for the new urbanization process with the aims to apply modern science and technology, knowledge to change the way of urban management as well as bringing more effective and stable living environment for the people. Smart city quality not only must ensure the harmonious development, the overall aspects of the city but also meet the goal of growth, and towards the change of quality in all aspects. To meet the requirements of sustainable smart city development management, addressing environmental quality control issues in urban areas. The paper will propose the IoT application model to manage the air environment quality of smart cities in Vietnam. We have*

***Keywords:** the smart city, air environmental quality, IoT application model, Internet of things, data.*

I. INTRODUCTION

According to European Research Cluster on the Internet of Things (IERC), By 2020, we are going to see the development of corridor super-city and integrated, incorporated and branded

cities. With over 20% of the world's population expected to live in urban areas by the year 2025, urbanization will be a trend that will affect the lives and mobility of communities in the future. This will lead to the development of smart cities with eight smart features as: smart economy, smart buildings, smart mobility, smart energy, smart information and technology, smart planning, smart citizen, and smart governance. In particular, the authorities play an important role in deployment IoT.

According to the United Nations Economic and Social Commission 0, the International Telecommunication Union (ITU) report 2014 analyses more than 100 definitions related to smart city, and defines " A sustainable smart city is an innovative city that uses information and communication technology (ICT) and other means to improve the quality of people's lives, improve efficiency activities and provide services in the urban. to improve the business environment and to meet current and future needs in economic, social and environmental terms". From an informational perspective, smart city is a system of co-operative aspects. The integration of many systems based on openness and standardization are fundamental principles in smart city construction. From the urbanization point of view, the problems arising in urban areas are increasingly serious as the number of people coming to live in urban areas is increasing that require urban planning staffs need to solve these problems with intelligent science and technology when urbanization is excessive. From the perspective of industrial transformation, Vietnam is one of the countries that develop industries with high energy consumption, causing serious environmental pollution, industrial development is the spearhead of the economy. However, if we continue to develop our industry as before, the consequences are enormous, so the smart industry is the new path we need to address. At present, addressing urban issues is not just about solving a unique problem, for example, environmental pollution is not just about water pollution, domestic wastewater, but also many other issues like garbage, air, land ... Smart city cannot be merely a metropolitan ICT application, but its essence is the linkage, sharing and integration of information, urban development in depth, institutional and institutional reform. Thus, a smart city above all is a people-oriented urban area, dependent on an ICT infrastructure and continuous urban development, always taking into account environmental and economic sustainability, towards new urbanization. It is possible to identify smart city with the goal of applying ICT and IoT connecting sensors, high speed wireless networks, big data processing to improve the quality of life in urban areas, improving quality government service and security, reduced energy consumption, effective management of natural resources and environmental quality.

II. MAINCONTENTS

2.1. The reality of air pollution environment in Vietnam

According to PhD. Dang Van Loi and MSc. Nguyen Hoang Duc 0, air environmental pollution has negatively impacted on citizen health and caused considerable damage to industrial, agricultural, forestry and tourism industries. Air environmental pollution is tended to rising in large cities and industrial parks, so there must have drastic and effective management

solutions. The quality of the air environment in Vietnam is monitored and evaluated based on the annual environmental monitoring data of the national and local environmental monitoring systems. Monitoring data will be compared with National Technical Standards) on air environment to assess the level of pollution. According to statistics, calculations and evaluation reports for 2010 - 2012, the evolutions of air quality in some large cities of Vietnam (Hanoi, Ho Chi Minh City, Dong Nai, ...) tend to decline. The main concerns are dust and dine dust (Total Suspended Particle - TSP and Coarse Particulate Matter with a diameter 10 micrometers - PM_{10}), especially in areas under constructing and at intersections where having high traffic. In most of these areas, the airborne dust concentration and fine particles exceed the permitted standard. In some areas, which concentrated activities of industrial production also has exceeded level of particle. The main reason is that production facilities still use old technology, backward, have not invested and operate the waste gas treatment system has led to large industrial emissions to the environment. Over the years, Vietnam has implemented air quality management and control activities and achieved certain results. However, the fact are still many limitations, in particular: The responsibility for chairing and assigning the state management about air environmental quality is still fragmented and there is no clear focal point for management among the relevant ministries. While the policies and legislation on air pollution control are not yet specific and there are no plans for air quality management at central as well as local levels. In addition, the system of standards and regulations on the air environment is still lacking synchronous, the monitoring and checking of exhaust sources are limited, the lack of comprehensive and periodic monitoring programs for the areas rural areas and trade villages. Major air environmental pollutants are caused by the combustion gases of engine includes CO, NOx, SO_2, petrol vapour (CnHm, VOCs), PM_{10} .... Motorcycles account for a large share of CO, VOCs and TSP emissions, while motorcar account for a large share of SO_2 and NO_2 emissions 0.

According to the current state of national environment report 2016 0. In Vietnam, dust pollution in urban areas continues to maintain high levels also causing negative impacts on people's health. Data from the Ministry of Health also indicate that environmental pollution poses risks to the health of the citizen. Tens of thousands of people suffer from respiratory diseases caused by air environmental pollution in average every year. According to statistics, the number of people suffering from respiratory diseases accounts for 3% to 4% of the total population. In particular, the rate of people suffering from respiratory diseases in developed cities such as Ho Chi Minh City, Dong Nai, Ha Noi, Hai Phong, ... are often much higher than the less developed cities. In addition to the effects of pollutants in the air, noise pollution also has a negative impact on the health and well-being of live people. Noise directly affects human hearing. High noise levels frequently cause headaches, dizziness, unsettled mental states, fatigue, ... For people who live and work in environments where noise levels are high, deafness can be difficult to recover hearing. In big cities in Vietnam, noise is generated mainly from traffic and construction activities. Besides, at present, the pollution of canals, rivers and lakes in the inner city not only occurs in big cities but also in small and medium cities. Water pollution in rivers, lakes and canals in the inner city often causes stench, affecting the living conditions of people

living in neighbouring areas, causing loss of urban beauty and influence. to the water quality of the receiving sources (penetration into groundwater or receiving rivers, ...). Odour pollution from rivers, lakes and canals is a major problem in many urban areas, causing troubles for the local community. The smell of organic matter decomposes on canals, rivers and lakes spread into the air, seriously affecting the lives of people living in neighbouring areas. In addition, polluted river water, when flowing into other rivers or infiltration into underground water, also caused pollutes many areas. On the other hand, in urban areas, although reports show that the rate of residential solid waste collection is very high, however, the problem of waste pollution in the transmission station or stench, water leaks from vehicles, garbage vehicles are still causing significant impact on activities are still common in many residential areas.

2.2. Motivation activated IoT technology development

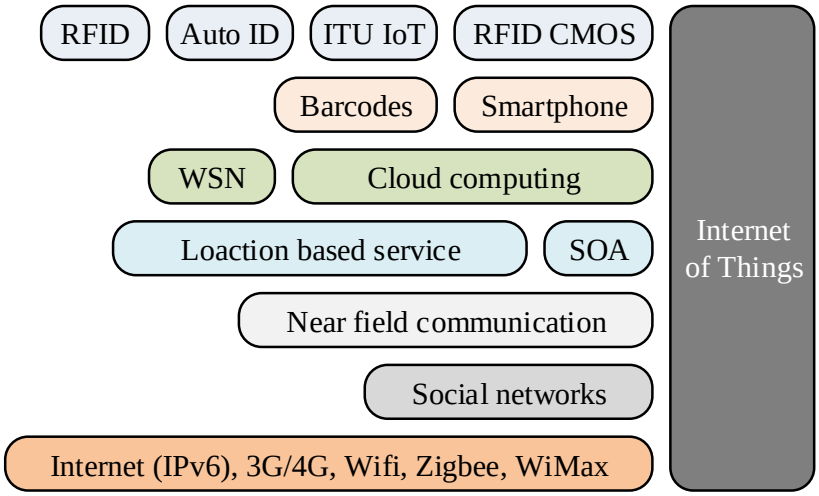

Figure 1. *Application technologies integrated with IoT*

IoT viewed as a global infrastructure include large amount of devices connected together to base on sensor, communication, network technologies and intelligent processing technologies. One of IoT platform technologies is radio frequency identification (RFID), which allowed microchips broadcast identified information to read header reader through radio communication. By used RFID read header can be automation identify, monitor and supervision for any objects fited with RFID card. One of other IoT platform technology is wireless sensor networks (WSN), essential use smart sensors have been connected in order to sensing and monitoring. WSN applications includes supervision for environments, health, industries and traffics, etc. Progress in RFID and WSN technologies important contribution to IoT developments, among them information and communication systems can be consideration embed hidden our around environment. These create giant amount of data can be stored, processed and performed in form easy compile, effect and continued. Cloud computing can provide for virtual infrastructure to count applications as above, integrated perform for monitor, storage devices and analyser tool, virtual platform and dispense to customers. The model based on the costs which cloud

computing supply will be permit to provide services from end to end for customers and users access to required applications at any place as Figure 1.

Intelligent connection to present networks and cloud computing use network resources are an indispensable part of IoT. With development of radio access technologies as Wi-Fi, 4G-LTE and 5G in the future, then the development towards information and communication networks at any place can be quite feasibility. However, in order to IoT become success then computing model required to more improved versus scenarios calculated traditional mobility use smart phones and portable devices to developed for link present objects and embed intelligent into medium. Besides, many technologies and other devices as bar code, social networks, location services, near-field communications, ZigBee, IPv6 used to present in order to make up wide area network support IoT.

2.3. IoT reference model

IoT reference model includes four layers with management and security capabilities applicated on the layers as declared in ITU-T Y.2060 (6/2012) 0. Proposal setup reference model of air environmental quality management system as Figure 2.

Reference model of air environmental quality management system have also four layers as well as management and security capabilities which are associated with these four layers. The four layers are as follows: i) IoT device layer includes physical sublayer with air environmental sensor devices and OSI data linkage sublayer with IoT gateways; ii) IoT network layer implementation two basic functions as network connection to IoT gateway and data link transportation of IoT devices; iii) IoT service support and IoT application support layer provide capabilities that IoT applications used; iv) IoT application layer contains all IoT applications interaction with IoT devices.

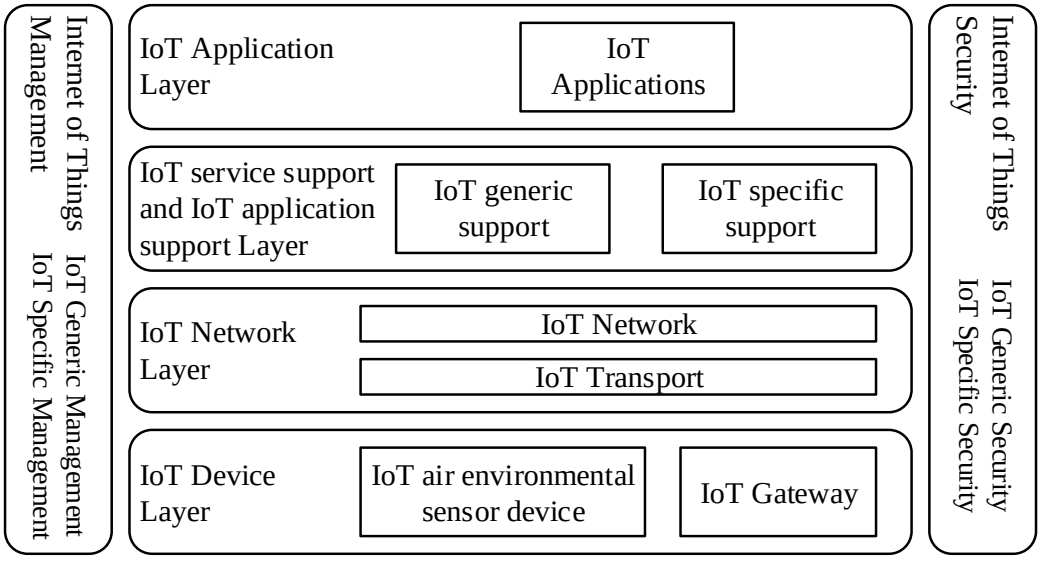

Figure 2. *IoT reference model for air quality management system*

Besides, there are two kinds of security capabilities: IoT generic security capabilities and IoT specific security capabilities. Generic security capabilities are independent of applications. They include: At the IoT application layer: authorization, authentication, application data confidentiality and integrity protection, privacy protection, security audit and anti-virus. At the IoT network layer: authorization, authentication, use data and signalling data confidentiality, and signalling integrity protection. At the IoT device layer: authentication, authorization, device integrity validation, access control, data confidentiality and integrity protection. Simultaneous, intelligent applications of model include: smart economy, smart buildings, smart mobility, smart energy, smart IT, smart planning, smart citizen, and smart governance.

2.4. IoT application support models

The IoT application support models refer to different sets of the IoT capabilities, including their relations, which can support IoT applications with some characteristic requirements, such as application adaptability, reliability and manageability 0.

The IoT application support models are used to guide the design, implementation and deployment of the IoT capabilities to fulfil application characteristic requirements, in order to establish a common service platform [ITU-T Y.4401] for support of IoT applications across different application domains. In particular, the purposes of the IoT application support models are as follows: the first one is to specify groups of IoT capabilities in order to facilitate the selection of IoT capabilities for the support of IoT applications with some characteristic requirements; the second one is to derive, based on the selected IoT capabilities, other IoT capabilities, as necessary in order to facilitate the design, implementation and deployment of the IoT capabilities for support of IoT applications with some characteristic requirements. There are 3 specific application support models as: the adaptable application support, the reliable application support and the configurable application support models.

2.4.1. The configurable application support model

The configurable application support model refers to the set of IoT capabilities, including their relations, to support the IoT applications with the characteristic requirement of configurability. The configurable application support model includes the IoT capabilities that can be configured by IoT applications, such as some service capabilities and communication capabilities that are related with the IoT applications. The configurable application support model consists of the functional view, implementation view and deployment view and related capabilities 0.

2.4.2. The reliable application support model

The reliable application support model refers to the set of IoT capabilities, including their relations, to support the IoT applications with the required degrees of reliability. The reliable application support model includes the IoT capabilities that can enhance the reliability of IoT applications, such as reliable data communication capability. The reliable application support

model consists of the functional view, implementation view and deployment view of descriptions on the reliable application support model and related capabilities 0.

2.4.3. The adaptable application support model

The adaptable application support model refers to the set of IoT capabilities, including their relations, to support the IoT applications with the characteristic requirement of adaptability. The adaptable application support model includes the IoT capabilities that are adaptable to different application contexts, such as content awareness capability and context awareness capability. The adaptable application support model consists of the functional view, implementation view and deployment view and related capabilities 0.

2.5. The proposal application support model for the smart city in Vietnam

Regarding the selection of the IoT applications support model depend on different application support requirements. If possible classification of IoT applications is based on the characteristics of things, characteristics of IoT users and other functional characteristics of IoT, then which may be too diverse to derive common application support models usable across different application domains. So this classification of IoT applications is not suitable as the basis to describe the IoT application support models. Another classification of IoT applications is based on the non-functional requirements of IoT applications as specified in [ITU-T Y.4100], such as reliability, availability, manageability and adaptability. Based on this classification, IoT applications can be classified into reliable applications, manageable applications, adaptable applications as above. Even if there are some differences among these non-functional requirements across different application domains, these differences consist in the absence of certain requirements in given application domain(s), or in the different strengths of certain requirements to be satisfied at the implementation and deployment level. So the application support models derived from this IoT application classification can be used across different application domains. This classification of IoT applications is suitable as the basis to describe the three IoT application support models specified as above and thus the proposal selection of the IoT applications support model to manage the air environmental quality (MAEQ) for smart city in Vietnam is based on the reliable MAEQ application support model (as shown 5.2 item above) consists of the functional view, implementation view and deployment view.

a) The functional view of the reliable MAEQ application support model consists of the reliable MAEQ management group, the reliable MAEQ data management group, the reliable MAEQ service provision group, the reliable MAEQ communication group, the reliable MAEQ connectivity group, the reliable MAEQ application support group and the interactions among these groups as illutrated in Figure 3. Each functional group contains related capabilities for support of the reliable MAEQ applications.

b) The implementation view of the reliable MAEQ application support model consists of the reliable MAEQ management and identity MAEQ management entity, the reliable MAEQ gateway entity, the reliable MAEQ end-user device entity, the reliable MAEQ transport control entity, the reliable transport control entity, the reliable service control entity, the reliable MAEQ

service control entity, the reliable MAEQ data management entity, the reliable MAEQ application support entity and the interactions among these entities as illustrated in Figure 4.

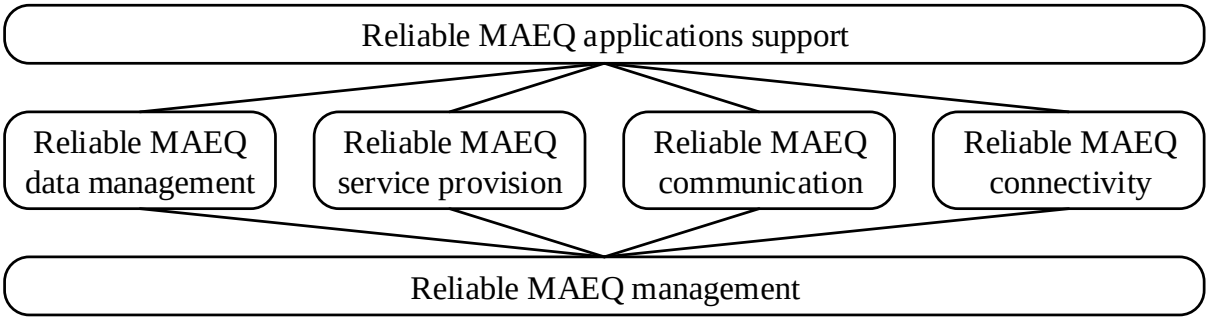

Figure 3. *The functional view of the reliable MAEQ application support model*

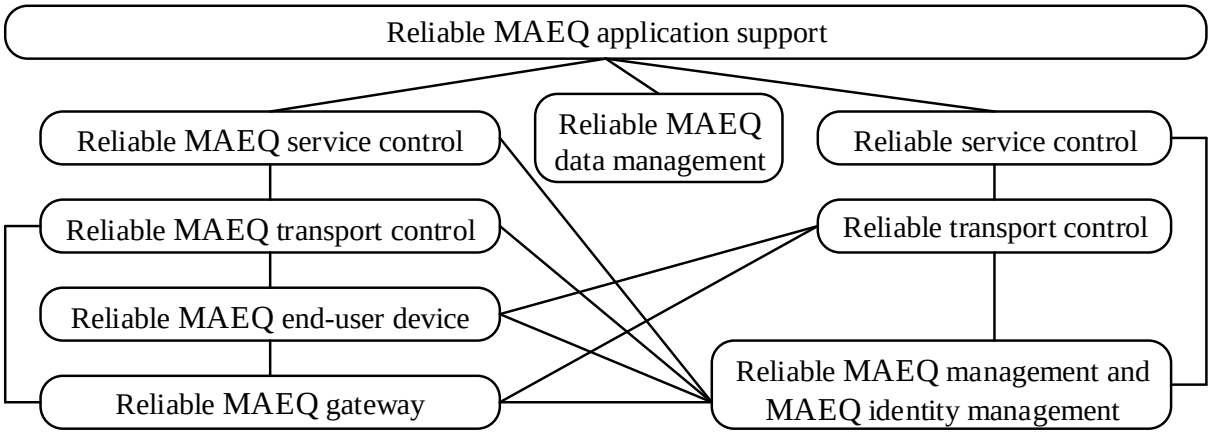

Figure 4. *The implemental view of the reliable MAEQ application support model*

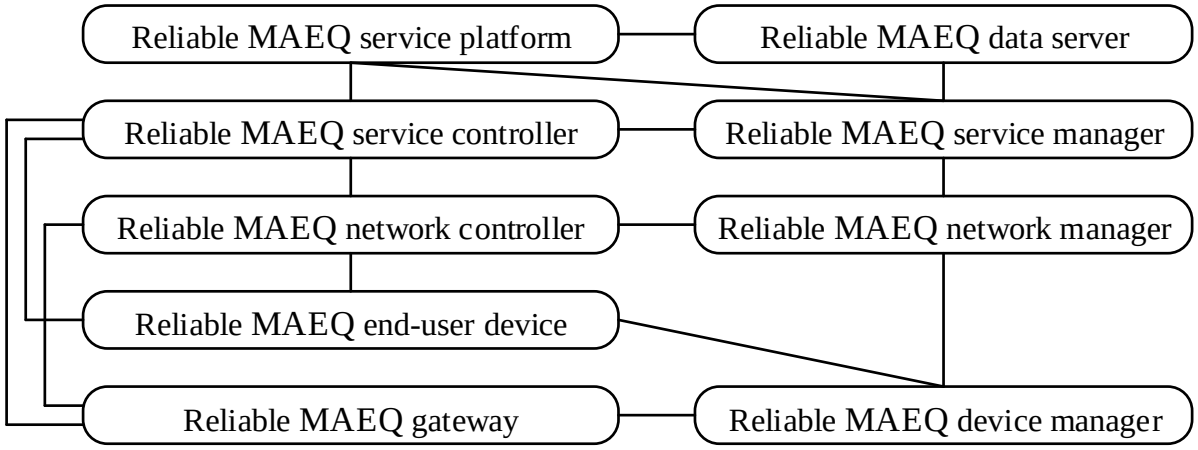

Figure 5. *The deployment view of the reliable MAEQ application support model*

c) The deployment view of the reliable MAEQ application support model consists of the reliable MAEQ device manager component, the reliable MAEQ gateway component, the reliable MAEQ end-user device component, the reliable MAEQ network manager component, the

reliable MAEQ network controller component, the reliable MAEQ service manager component, the reliable MAEQ service controller component, the reliable MAEQ data server component and the reliable MAEQ service platform component and the interactions among these components as Figure 5.

The capabilities of the reliable MAEQ application support model can be classified into the following functional groups: reliable MAEQ service provision capabilities, reliable MAEQ communication capabilities, reliable MAEQ application support capabilities, reliable MAEQ data management capabilities, reliable MAEQ management capabilities and reliable MAEQ connectivity capabilities.

III. CONCLUSION

Air environmental pollution and air retrograde was not only affects the ecological environment, climate change, but also directly affects the lives of the community, degrading the quality of life of people in urban areas. The proposed model to manage the air environmental quality for smart city in Vietnam will be take part in satisfy required sustainable development to ensure the balance between socio-economic development and environmental protection in toward of prevent pollution, restore and improve the environment in places and areas which have been degraded, step by step raising the quality of air environment in industrial parks and urban areas, contributing to sustainable socio-economic development, increment quality of life of the people.

References

[1] *Report of United Nations Secretary General,* Smart city and infrastructure, 26/02/2016.

[2] *PhD. Dang Van Loi and MSc Nguyen Hoang Duc,* Air quality management in Vietnam: Actual state and solutions, http://vea.gov.vn/vn/truyenthong/tapchimt/ cccs/Pages/.

[3] *Que Dinh Nguyen,* Dust is slient hazard, weekend people forum, http://www.nhandan.com.vn/.

[4] *Present condition report of national environment 2016,* Effect of environmental pollution of the urban areas, http://cem.gov.vn/Portals/0/quynh/2017/.

[5] *ITU-T, Standard Y.2060 (06/2012),* Overview of the Internet of things, 06/2012.

[6] *ITU-T, Standard Y.4552/Y.2078 (02/2016),* Application support models of the Internet of things, 02/2016.

BUSINESS ANALYTICS IN COLD-CHAIN LOGISTICS MANAGEMENT

LIANG-TAY LIN, PEI-JU WU
CHI-CHANG HUANG, CHAO-FU YEH, JAU-MING SU
Department of Transportation and Logistics, Feng Chia University, Taichung, Taiwan.
Corresponding author's email: ltlin@fcu.edu.tw

Abstract: *The quality of temperature-sensitive goods is closely related to cold-chain logistics. The aim of this study is to develop business analytics to manage cold-chain logistics. Specifically, the proposed cold-chain business analytics involve descriptive analytics, predictive analytics, and prescriptive analytics. Descriptive analytics investigate what happened when cold-chain logistics were implemented. Predictive analytics address what will happen in the execution of cold-chain logistics. Prescriptive analytics explore what should be done to achieve high-quality cold-chain logistics. They can be applied by logistics firms seeking high-quality cold-chain performance under varied temperature requirements. Furthermore, the proposed cold-chain business analytics provide academics and managers with a holistic view of strategies for making cold-chain logistics decisions.*

Keywords: *Cold-chain logistics, Logistics management, Business analytics, Temperature-sensitive goods*

I. INTRODUCTION

Damage to cold-chain goods can occur along the cold supply chain [1]–[3]. With the increasing focus on food safety and enforcement of the traceability of food products around the world [4], it is necessary to continuously check and control the temperature of cold-chain goods in logistics systems[5].

The quality of cold-chain goods is reliant on logistics stability [6]. In other words, cold-chain logistics play an important role in maintainingthe temperature along the cold supply chain within the required range for temperature-sensitive goods. Cold-chain goods, such as fresh foods and vaccines, are highly influenced by temperature and need to be shipped under rigorous temperature control [7], [8].

The purposes of this study were to tackle abnormal temperature issues in a temperature-controlled supply chain through business analytics of cold-chain logistics. The proposed cold-chain business analytics involve descriptive analytics, predictive analytics, and prescriptive analytics. They can be applied by logistics firms seeking high-quality cold-chain performance under varied temperature requirements.

The remainder of this paper is organized as follows. Section 2 conducts a literature review. Section 3 presentsdescriptive analytics. Section 4 includes predictive analytics. Section 5 describes prescriptive analytics. Finally, Section 6 is the conclusion.

II. LITERATURE REVIEW

Big data analytics can be applied to create marked changes in supply chain design and management [9]. Waller and Fawcett [10] also argued that exploiting big data using predictive analytics can enhance theoretical development of logistics and supply chain management. Hazen et al. [11] further discusseddata quality problems in big data analytics for supply chain management. Tachizawa et al. [12] stressed that the integration of big data and smart cities can enhance supply chain management.

In numerous studies, distinct analytical frameworks have been developed and applied to logistics and supply chain management. Zhong et al. [13] utilized a big data approach to retrieve logistics trajectory from RFID manufacturing data. Chae[14]established an analytical framework of Twitter analytics to explore supply chain tweets, as well as proposed supply chain practice and research based on SCM Twitter data. Zhao et al. [15] explored financial big data in the predictability of business failure of supply chain finance clients. Furthermore, Dutta and Bose [16] devised a framework for firms to execute a big data project and found salient factors for the implementation of a big data project based on a case study of a manufacturing company. Ilie-Zudor et al. [17] proposed a decision support platform of big data analytics to offer logistics solutions. Additionally, Wang et al. [18] developed a framework of supply chain analytics and proposed analytical approaches that make use of big data.

An approach for evaluating the performance of cold-chain logistcs is essential to improving the quality of cold supply chain. Thiel et al. [19] employed system dynamics to forecast the impacts of backlogs and superfluous inventory on sanitary risk in a poultry supply chain during a crisis. Srivastava et al. [20] utilized interpretive structural modeling (ISM) to identify supply chain risks in fresh food retail. Furthermore, Ruan and Shi [21] developed numerical simulations to monitor and appraise the freshness of in-transit fruits according to an IoT framework of e-commerce delivery. Badia-Melis et al. [22] used data estimation methods of artificial neural networks, kriging and capacitive heat transfer to forecast temperatures of fruit in refrigerated containers for improving food safety and reducing product losses. Additionally, Ma et al. [6] assessed logistics stability of table grapes under changeable temperature through contour diagram-based approach for cold-chain management.

Applications of information and communications technology can assist cold-chain stakeholders in managing cold supply chains. It is very important to enhance monitoring

technologies for cold-chain goods [22]. Ruiz-Garcia et al.[23] adopted ZigBee-based wireless sensor to monitor fruit in refrigerated cold-chain logistics.Abad et al.[24]developed an RFID smart tag to monitor the temperature and humidity of intercontinental fresh fish logistics. Moreover, Kuo and Chen [5] devised a multi-temperature joint distribution system to effectively manage perishable and temperature-sensitive goods. Kim et al. [25] proposed an intelligent risk management framework of ubiquitous cold-chain logistics for environmentally-sensitive items. Li and Chen [26] devised an eutectic solution for cold energy storage materials in food cold-chain logistics systems. In addition, Shih and Wang [27] proposed a food cold-chain system based on ISO 22,000 requirements and IoT framework.

III. DESCRIPTIVE ANALYTICS

In descriptive analytics, difference-in-differences analysis can be used to scrutinize the impact of each cold-chain technology on the performance of cold-chain logistics over time, for instance that of an on-board diagnostic system.A difference-in-differences analysis (Figure 1) represents a causal inference approach that resembles randomized experiments [28]–[30].

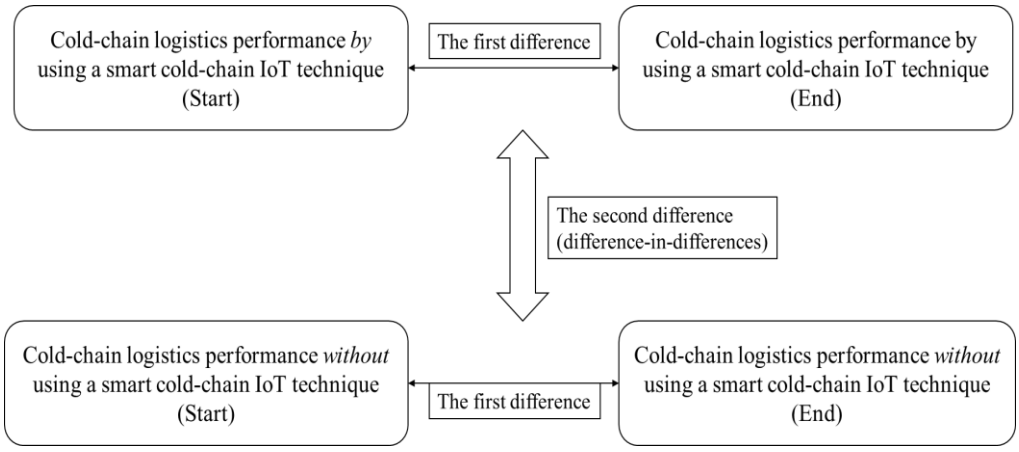

Figure 1. *Difference-in-differences Analysis of Cold-Chain Logistics*

IV. PREDICTIVE ANALYTICS

In predictive analytics, decision tree analysis[31] can be used to identify logistics behaviors withhigh-quality cold-chain performance, as shown in Figure 2. Herein, high-quality cold-chain performance in a logistics system represents a logistics firm that demonstrates positive growth in cold-chain performance over time.

V. PRESCRIPTIVE ANALYTICS

In prescriptive analytics, optimization models (Chen, Feng, Tsai, & Wu, 2013; Feng & Wu, 2009) can be utilized to seek optimal cold-chain logistics value. Figure 3 represents an optimization model of cold-chain logistics.

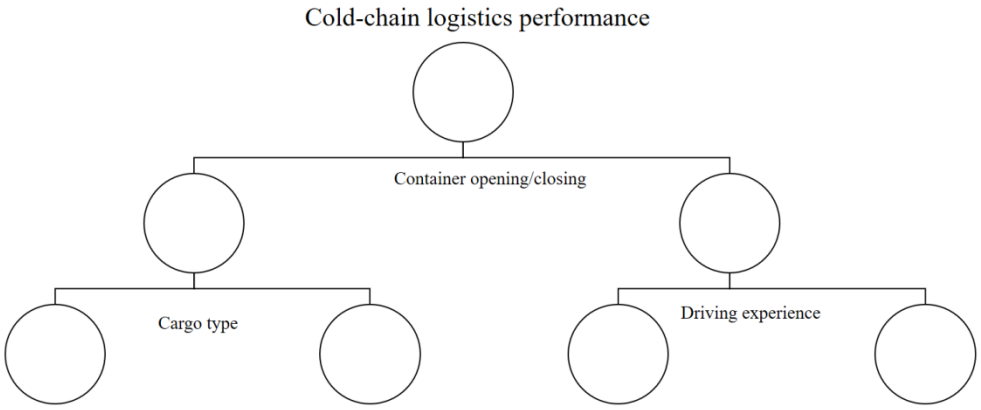

Figure 2. *A Decision Tree Model of Cold-Chain Logistics Performance*

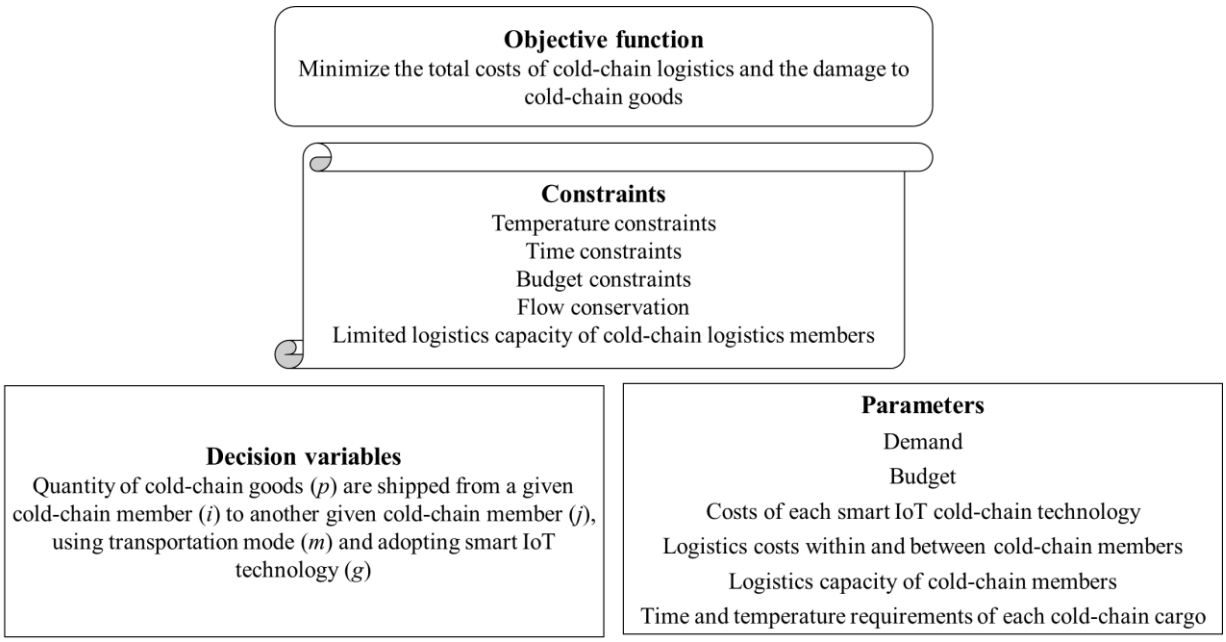

Figure 3. *Conceptual Model of Cold-Chain Logistics with Smart IoT Technologies*

III. CONCLUSION

Firms may lack knowledge on how to achieve high-quality cold-chain logistics. In this study, business analytics of cold-chain logistics were developed. Consequently, the results of this study provide academics and managers with a holistic view of strategies for making cold-chain logistics decisions.

The proposed business analytics includes descriptive analytics, predictive analytics, and prescriptive analytics. Descriptive analytics investigate what happened when cold-chain logistics were implemented. Difference-in-differences analysis can be applied to descriptive analytics. Predictive analytics address what will happen in the execution ofcold-chain logistics. Decision tree analysis with data mining technique can be utilized in predictive analytics. Prescriptive analytics explore what should be done to achieve high-quality cold-chain logistics. Optimization

models can be employed in prescriptive analytics.

The proposed model may stimulate future studies in the field of cold supply chain management, as well as help to address issues regarding the applications of business analytics to cold chains. Moreover, future studies should investigate smart IoT cold-chain logistics based on distributed computing platform.

References

[1] *R. Jedermann, L. Ruiz-Garcia, and W. Lang, "*Spatial temperature profiling by semi-passive RFID loggers for perishable food transportation," Comput. Electron. Agric., vol. 65, no. 2, pp. 145–154, Mar. 2009.

[2] *G. La Scalia, G. Aiello, A. Miceli, A. Nasca, A. Alfonzo, and L. Settanni,* "Effect of Vibration on the Quality of Strawberry Fruits Caused by Simulated Transport," J. Food Process Eng., vol. 39, no. 2, pp. 140–156, Apr. 2016.

[3] *W. Lang and R. Jedermann,* "What Can MEMS Do for Logistics of Food? Intelligent Container Technologies: A Review," Ieee Sens. J., vol. 16, no. 18, pp. 6810–6818, Sep. 2016.

[4] *C. Costa, F. Antonucci, F. Pallottino, J. Aguzzi, D. Sarria, and P. Menesatti,* "A Review on Agri-food Supply Chain Traceability by Means of RFID Technology," Food Bioprocess Technol., vol. 6, no. 2, pp. 353–366, Feb. 2013.

[5] *J.-C. Kuo and M.-C. Chen,* "Developing an advanced Multi-Temperature Joint Distribution System for the food cold chain," Food Control, vol. 21, no. 4, pp. 559–566, Apr. 2010.

[6] *C. Ma, X. Xiao, Z. Zhu, L. B. Vlad, and X. Zhang,* "Contour Diagram-Based Evaluation on Logistics Stability of Table Grapes under Variable Temperature," J. Food Process Eng., vol. 39, no. 4, pp. 391–399, Aug. 2016.

[7] *R. Montanari, "Cold chain tracking: a managerial perspective,"*Trends Food Sci. Technol., vol. 19, no. 8, pp. 425–431, 2008.

[8] *A. Vrdoljak et al.,* "Coated microneedle arrays for transcutaneous delivery of live virus vaccines," J. Controlled Release, vol. 159, no. 1, pp. 34–42, Apr. 2012.

[9] *M. A. Waller and S. E. Fawcett,* "Data Science, Predictive Analytics, and Big Data: A Revolution That Will Transform Supply Chain Design and Management," J. Bus. Logist., vol. 34, no. 2, pp. 77–84, Jun. 2013.

[10] *M. A. Waller and S. E. Fawcett,* "Click Here for a Data Scientist: Big Data, Predictive Analytics, and Theory Development in the Era of a Maker Movement Supply Chain," J. Bus. Logist., vol. 34, no. 4, pp. 249–252, Dec. 2013.

[11] *B. T. Hazen, C. A. Boone, J. D. Ezell, and L. A. Jones-Farmer,* "Data quality for data science, predictive analytics, and big data in supply chain management: An introduction to the problem and suggestions for research and applications," Int. J. Prod. Econ., vol. 154, pp. 72–80, Aug. 2014.

[12] *E. M. Tachizawa, M. J. Alvarez-Gil, and M. J. Montes-Sancho,* "How 'smart cities' will change supply chain management," Supply Chain Manag.- Int. J., vol. 20, no. 3, pp. 237–248, 2015.

[13] *R. Y. Zhong, G. Q. Huang, S. Lan, Q. Y. Dai, C. Xu, and T. Zhang,* "A big data approach for logistics trajectory discovery from RFID-enabled production data," Int. J. Prod. Econ., vol. 165, pp. 260–272, Jul. 2015.

[14] *B. Chae,* "Insights from hashtag #supplychain and Twitter Analytics: Considering Twitter and Twitter data for supply chain practice and research," Int. J. Prod. Econ., vol. 165, pp. 247–259, Jul. 2015.

[15] *X. Zhao, K. Yeung, Q. Huang, and X. Song,* "Improving the predictability of business failure of supply chain finance clients by using external big dataset," Ind. Manag. Data Syst., vol. 115, no. 9, pp. 1683–1703, 2015.

[16] *D. Dutta and I. Bose,* "Managing a Big Data project: The case of Ramco Cements Limited," Int. J. Prod. Econ., vol. 165, pp. 293–306, Jul. 2015.

[17] *E. Ilie-Zudor, A. Ekart, Z. Kemeny, C. Buckingham, P. Welch, and L. Monostori,* "Advanced predictive-analysis-based decision support for collaborative logistics networks," Supply Chain Manag.-Int. J., vol. 20, no. 4, pp. 369–388, 2015.

[18] *G. Wang, A. Gunasekaran, E. W. T. Ngai, and T. Papadopoulos,* "Big data analytics in logistics and supply chain management: Certain investigations for research and applications," Int. J. Prod. Econ., vol. 176, pp. 98–110, Jun. 2016.

[19] *D. Thiel, T. L. H. Vo, and V. Hovelaque,* "Forecasts impacts on sanitary risk during a crisis: a case study," Int. J. Logist. Manag., vol. 25, no. 2, pp. 358–378, 2014.

[20] *S. K. Srivastava, A. Chaudhuri, and R. K. Srivastava,* "Propagation of risks and their impact on performance in fresh food retail," Int. J. Logist. Manag., vol. 26, no. 3, pp. 568–602, 2015.

[21] *J. Ruan and Y. Shi,* "Monitoring and assessing fruit freshness in IOT-based e-commerce delivery using scenario analysis and interval number approaches," Inf. Sci., vol. 373, pp. 557–570, Dec. 2016.

[22] *R. Badia-Melis, U. Mc Carthy, and I. Uysal,* "Data estimation methods for predicting temperatures of fruit in refrigerated containers," Biosyst. Eng., vol. 151, pp. 261–272, Nov. 2016.

[23] *L. Ruiz-Garcia, P. Barreiro, and J. I. Robla,* "Performance of ZigBee-based wireless sensor nodes for real-time monitoring of fruit logistics," J. Food Eng., vol. 87, no. 3, pp. 405–415, Aug. 2008.

[24] *E. Abad et al.,* "RFID smart tag for traceability and cold chain monitoring of foods: Demonstration in an intercontinental fresh fish logistic chain," J. Food Eng., vol. 93, no. 4, pp. 394–399, Aug. 2009.

[25] *K. Kim, H. Kim, S.-K. Kim, and J.-Y. Jung,* "i-RM: An intelligent risk management framework for context-aware ubiquitous cold chain logistics," Expert Syst. Appl., vol. 46, pp. 463–473, Mar. 2016.

[26] *Y.-C. M. Li and Y.-H. A. Chen,* "Assessing the thermal performance of three cold energy storage materials with low eutectic temperature for food cold chain," Energy, vol. 115, pp. 238–256, Nov. 2016.

[27] *C.-W. Shih and C.-H. Wang,* "Integrating wireless sensor networks with statistical quality control to develop a cold chain system in food industries," Comput. Stand. Interfaces, vol. 45, pp. 62–78, Mar. 2016.

[28] *S. Chopra and P. J. Wu,* "Eco-activities and operating performance in the computer and electronics industry," Eur. J. Oper. Res., vol. 248, no. 3, pp. 971–981, Feb. 2016.

[29] *B. Black and W. Kim*, "The effect of board structure on firm value: A multiple identification strategies approach using Korean data," J. Financ. Econ., vol. 104, no. 1, pp. 203–226, Apr. 2012.

[30] *G. W. Imbens and J. M. Wooldridge,* "Recent Developments in the Econometrics of Program Evaluation," J. Econ. Lit., vol. 47, no. 1, pp. 5–86, Mar. 2009.

[31] *P.-J. Wu, M.-C. Chen, and C.-K. Tsau,* "The data-driven analytics for investigating cargo loss in logistics systems," Int. J. Phys. Distrib. Logist. Manag., vol. 47, no. 1, pp. 68–83, Jan. 2017.

WIRELESS FLOOD MONITORING SYSTEM NETWORK FOR TAICHUNG CITY

YEH CHAO HSIEN[1,4], LIN BING SHYAN[2,4], LIEN HUI PAN[1,4], JHONG YOU DA[2,4], LIANG SHI MING[3]

[1]Department of Water Resources Engineering and Conservation, [2]Construction and Disaster Prevention Research Center, [4]Feng-Chia University, Taichung, Taiwan

[3]Monitor Technology Division, Yang Pan Tec., Taichung, Taiwan

Corresponding author's email: chyeh@fcu.edu.tw

Abstract: *Due to climate change of high intensity rain fall and long durance of heavy rain fall amount, the growth of Taichung City modern development and pavement increase, brought large scale of massive flooding problem during 2006-2010. Therefore, flood control constructions for has been proposed in each regional cannel flooding area. But, since construction needs time to finish, disaster precaution facilities need to be setup during this unsafe period for residence nearby risk area. Feng-Chia University proposed a water level detect and rainfall monitor system correspond with image observation which helped the city government setup the national wide first dual wireless radio transmission mesh network in order to understand the relationship between rainfall intensity and amount which effect the runoff and setup an active flood pre-warning system for flood risk potential area.*

Keywords: *water level, rainfall monitor system, wireless radio transmission mesh network.*

I. INTRODUCTION

Since 2012, the Taichung City Government has established water level, image and rainfall observation and warning facilities in various district drainage, activity centers and district offices in the city as water monitoring. As of December 2017, setup 72 water level observation stations and 19 information relay stations for use as disaster prevention warnings. For considering the importance of these disaster prevention data, the city government put emphases on relying not only by wired network such as ADSL or GSN system, but also use free radio frequency to transmit small data amount. Therefore, by this kind of backup system, the observe warning data could be safely sent to government disaster management agency and also residents nearby.

II. MAIN CONTENTS

2.1. System setup

The hardware structure, through the establishment of the database and the monitoring point to assist in the management of the detection information of the observation equipment, the system alert and management information is synchronized through the APP program and shared with the Manager and the Water Resources Department. Overall architecture as below Figure 1.

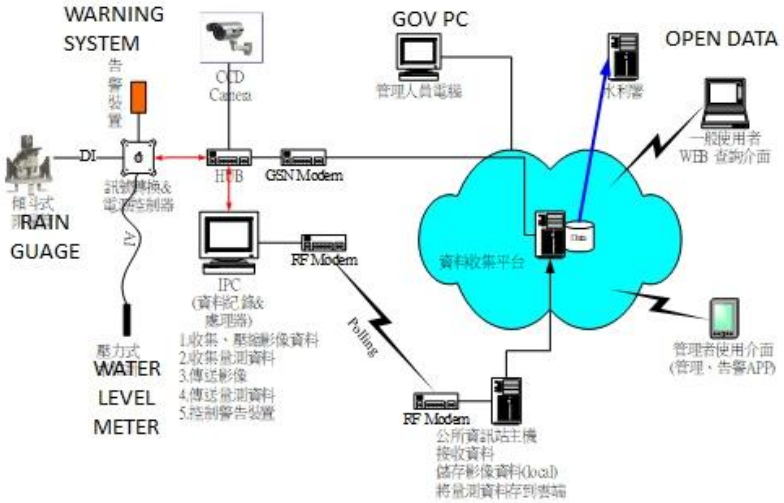

Figure 1. *System Map for Taichung Flood Monitoring System*

A. Monitor Unit

The monitor unit is composed of three different system, including detect device such as water level meter, rain gauge, CCD camera; Power device such as batteries, solar panel, pole electricity; And finally, protecting device, such as cage carrier, lighting rod and warning alert system, shown as Figure 2.

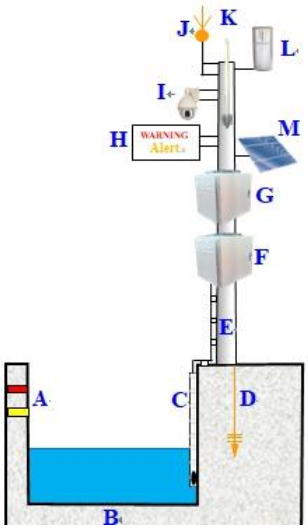

No	ITEM	Explanation
A	Water warning level	R-Class 1 Y-Class 2
B	Riverbed	
C	Pressure water meter	
D	Ground Line	
E	Monitor Pole	7.5m
F	Battery Cage	W=60cm H=65cm D=50cm
G	Equipment Cage	W=60cm H=65cm D=50cm
H	LED Plate	
I	CAMERA	30 m Night Vision
J	lightning rod	
K	antenna	Wireless radio transmit
L	Rain Gauge	1mm
M	Solar Plate	35W

Figure 2. *Monitoring site picture*

B. Transmit Unit

Transmit system is important for data collection. The unit includes wired network and also a wireless backup system when public network crushes. This include a VHF radio system band width of 128,000 bps which can send HD pictures and small data. The system help pull data from each individual monitor site show as Figure 3 every 1-10 minute depend on normal or disaster detect mode. Each wireless system can transmit more than 10-15km and data collect site shown in Figure ure 4 help collect more than 3-5 site nearby. If there is traffic jam in network, the system will depend on which wireless or wired transmit way.

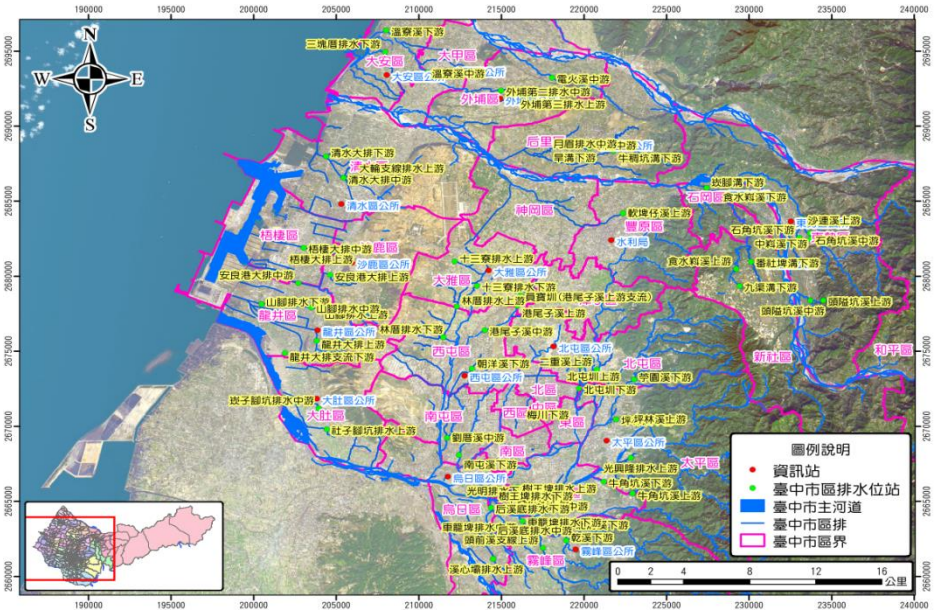

***Figure 3**. Monitor site*

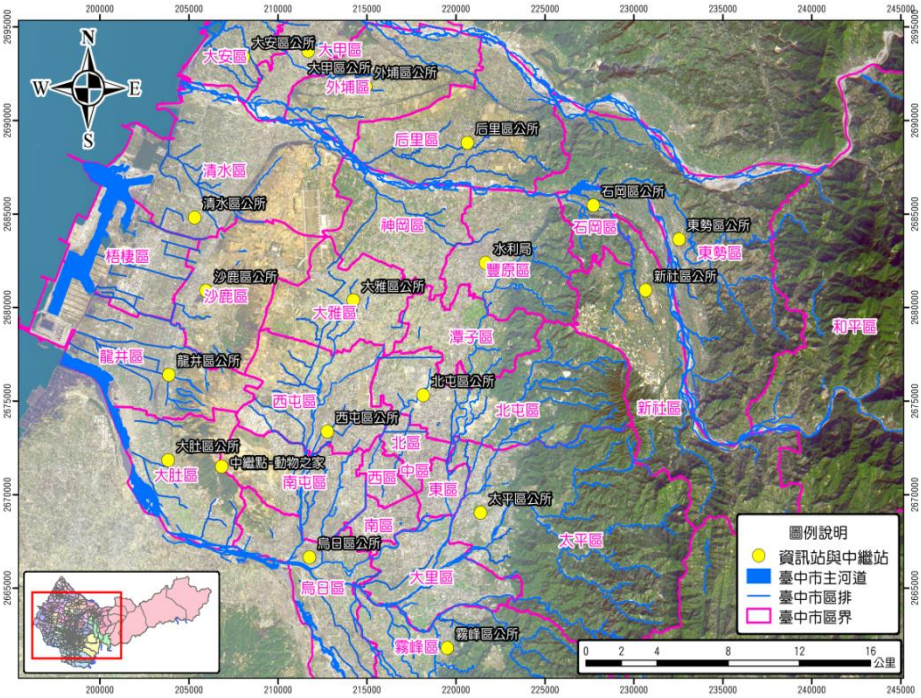

***Figure 4**. Data collect site*

C. Software and Display Unit

Figure 5. *Flood monitor report and APP display result*

The software of this entire monitor system includes detect data translate system, self-safety detect system (cage safety, temperature, battery life and electricity stability), wired and wireless transmit system detection, and finally the background display system which gives data monitor result and warning email and mms, also help the city government APP display the live data result and give daily report to analyze the region flooding potential shown in Figure 5.

2.2. Monitor Result

This system majorly provides water level changes and rainfall amount and setup relationship with different time sequence images. As below, different flood cases during 2014-2016 help evacuate residence and block dangerous roads shown in Figure 6. Self-produce monitor report is automatically sent to users to see the current rain amount and water level images, this system also helps predict the future water level raising or lowering speed and time which will help flooding management results show in Figure 7.

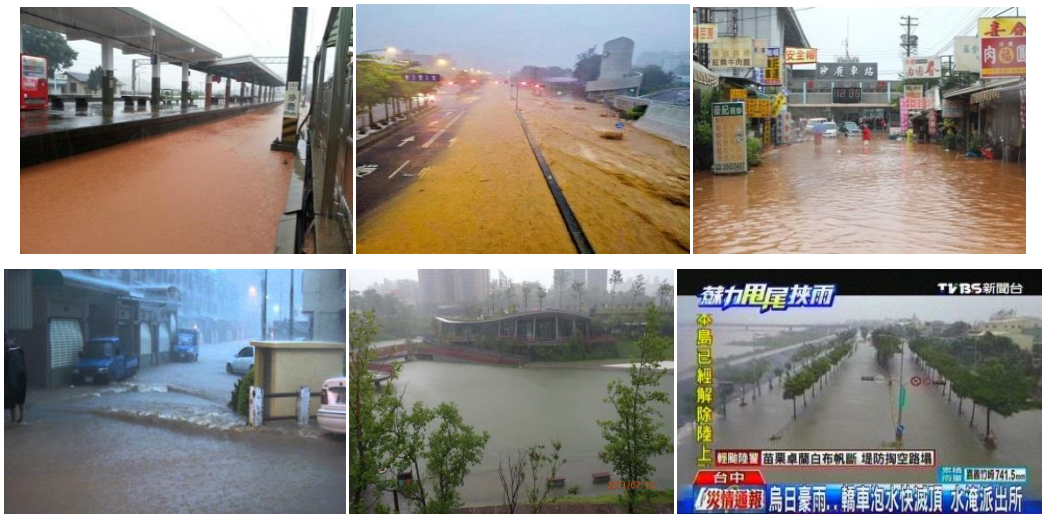

Figure 6. *Flood cases during 2014-2016*

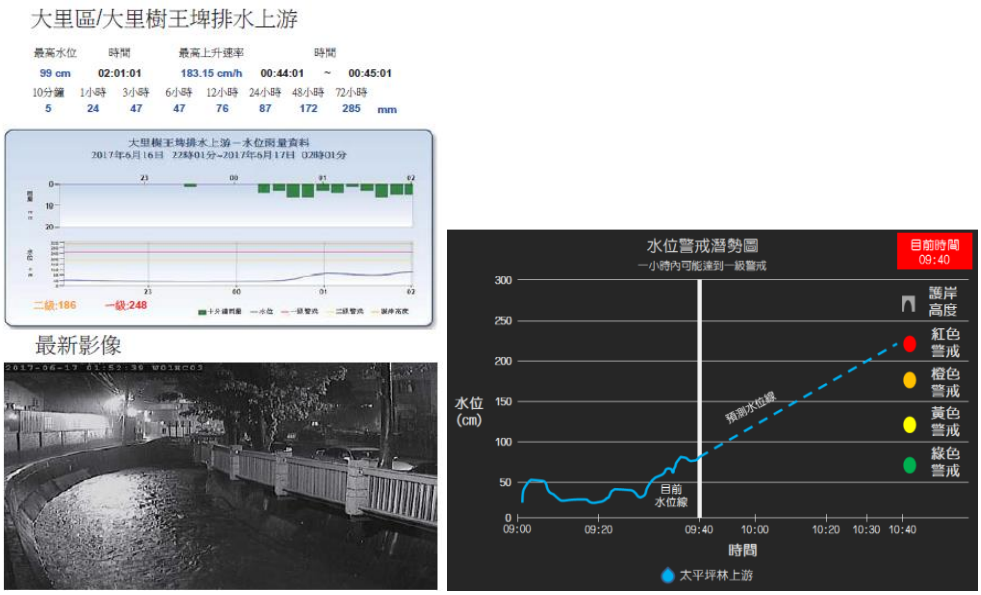

Figure 7. *Self-produce monitor and prediction report*

2.3. Extend Improvement

This year, due to past monitor result, many city flooding cases did not occur in river channels, but in lower sewage and chocking points. Therefore, based on exist monitoring sites, we will us small, low cost wireless detecting device to help detect low part ditches water level and use LORA system to send warning data to nearby site., shown as Figure 8.

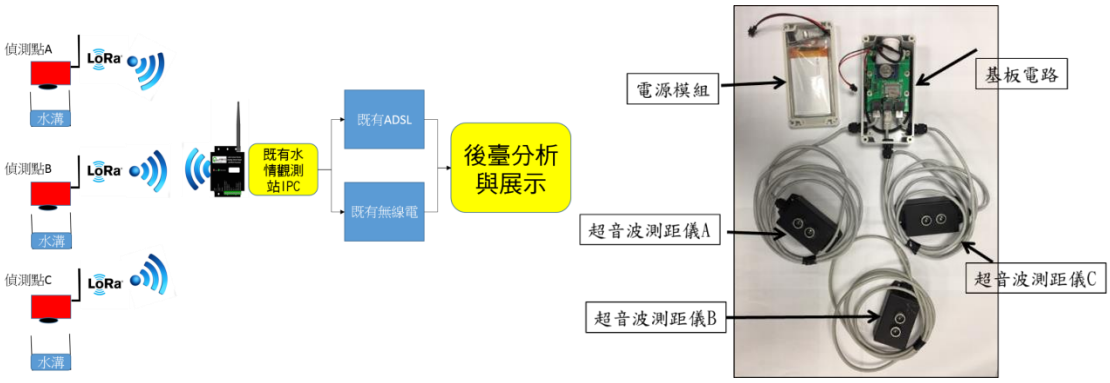

Figure 8. *Low cost LORA WATER level detect device*

III. CONCLUSION

This monitoring system has been working for 6 years and gave precaution warning has helped evacuate residents before many individual flooding cases. Therefore, in the future, if each site can send high quality live streaming images, this will help flood control management agency learn more about disaster prevention and give much accurate data before flooding occur.

References

[1] *Taichung City Government WATER RESOURCES BEREAU,* "2017 Taichung City Water Level Station Early Warning Facilities Maintenance and Function Enhancement Entrusted Professional Services", Taichung City Government, Taiwan, 2017

[2] *Taichung City Government WATER RESOURCES BEREAU,* "2016 Taichung City Water Level Station Early Warning Facilities Maintenance and Function Enhancement Entrusted Professional Services", Taichung City Government, Taiwan, 2016.

[3] *Taichung City Government WATER RESOURCES BEREAU,* "2015 Taichung City Water Level Station Early Warning Facilities Maintenance and Function Enhancement Entrusted Professional Services", Taichung City Government, Taiwan, 2015.

MULTIPLE VEHICLES TRACKING IN TRANSPORTATION SURVEILLANCE SYSTEMS

BUI NGOC DUNG[1,2]
[1]*University of Transport and Communications, Hanoi, Vietnam*
[2]*Thanh Tay University, Hanoi, Vietnam*
Corresponding author's email: dnbui@utc.edu.vn

Abstract: *Vehicles detection and tracking have become an important role to the traffic management system. Many vehicles tracking approaches have already proposed, however, these approaches were still lacking in distinguish vehicles from each other because of their similarity and complex transportation. In this paper, a method for tracking multiple vehicles in a surveillance camera is presented. The method is to detect vehicles using background subtraction based on Gaussian Mixture Model and to track vehicles using multiple Kalman filters. The method takes advantages of distinguish and tracking multiple vehicles individually. The experimental results demonstrate high accurately of the method.*

Keywords: *Multiple vehicles tracking, kalman filter, transportation surveillance*

I. INTRODUCTION

Identifying moving vehicles from camera is a fundamental task in transportation surveillance systems [1, 2]. The identifying vehicles is done by two steps, one is detection and analysis of vehicles, second is tracking these vehicles. The objective of vehicles detection and tracking is to identify target vehicles in consecutive time in the video. The output of these two algorithms will be send to the transport management center for further analysis such as vehicles speed detection, vehicles breaking traffic rule and traffic monitoring [3, 4]. Camera surveillance provide a flexible way of monitoring the transportation, especially monitor the complex transportation. These tasks are a part of intelligent transportation system (ITS) [5].

There are number of tracking approaches being used in surveillance systems where vehicle tracking is one of essential case. The most common method for object tracking is Kalman filter, which is recursive estimator of state of a dynamic system [6, 7]. To increase the accuracy, mean-shift was combined with Kalman filter to predict the search regions [8]. If the system does not fit into linear model, particle filter is an important method to track the object [9]. It combines gray and contour feature particles using fusion algorithm to balance the weights according to the present scene. Motion direction and assignment can be used to track the vehicles in their lanes and calculate the speed of the vehicles [10]. Image segmentation and pattern analysis techniques also applied in the system to detect and track the moving vehicles at day and night time [11] by recognize headlight and taillight of vehicles. Using cameras and the pattern recognition techniques, the traffic flow can be measured under various environments condition by detect vehicles [12].

The current techniques and algorithms in detection and tracking still cannot handle some challenge of transportation surveillance systems. If these technologies can be exploited well, it will be decreasing the number of accidents, decrease pollution, and also improve the efficient of

transport. However, the tracking algorithms cannot accurately control vehicles because the vehicles do not travel in order, effect of bad condition of weather, especially multiple vehicles run concurrently. This paper proposes a method of simultaneously tracking vehicles in video sequence using multiple Kalman filters. The method detects moving vehicles in each frame and associates these vehicles corresponding to the same in the next frame. The Kalman filter have used to predict the position and use this predicted position for association. Experimental results show the proposed algorithm is able to do efficient and robust multiple vehicles tracking.

The rest of this paper is organized as follow: Section 2 presents a framework of the vehicle detection and tracking. In this section, the proposed method for vehicles tracking using multiple Kalman filters is presented. Section 3 demonstrates the accuracy and robustness of the proposed method. Finally, Section 4 states the conclusions and future works.

II. MAIN CONTENTS

The goal of my research is to track multiple vehicles in complex transportation. In order to achieve this purpose, this paper propose to use multiple Kalman filters to track multiple vehicles. To do this, the number of vehicles have to detected in each frame using background subtraction algorithm. Then, multiple Kalman filters are created corresponding to the number of vehicles detected. The general framework of the method is given in figure 1.

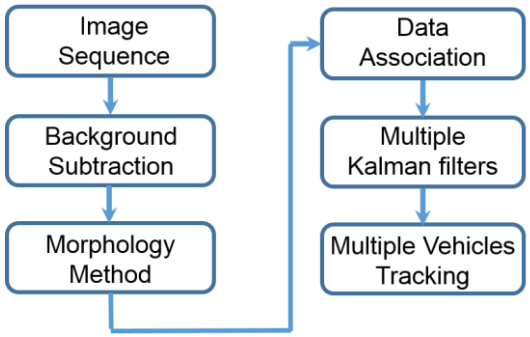

Figure 1. *The framework of the multiple tracking method*

2.1. Background subtraction

The popular method to detect the moving objects is background subtraction. In this method, input are frames that were captured using surveillance cameras, output are binary images which contains moving objects [13]. This technique try to detect moving fragment by subtract image point from current time to a background image which was created using average background images in a period of time called initial cycle. The general framework of background subtraction is given in Figure 2 [13]. To solve base model, a single Gaussian model or mixed Gaussian models are used. Statistical variables which were used to classify image points can be moving vehicles or background. Heikkila and Silven [14] used this combined method, in which each image point is presented using (x,y), in current image I_t is marked as highlight point if the below function is correct:

$$\left|I_t(x,y) - B_t(x,y)\right| > \tau$$

In which, τ is predefined threshold. B_t background image is updated using Infinite Impulse Respone (IIR) filter. The detailed updating process of background image B_t is: $B_{t+1} = \alpha I_t + (1-\alpha)B_t$

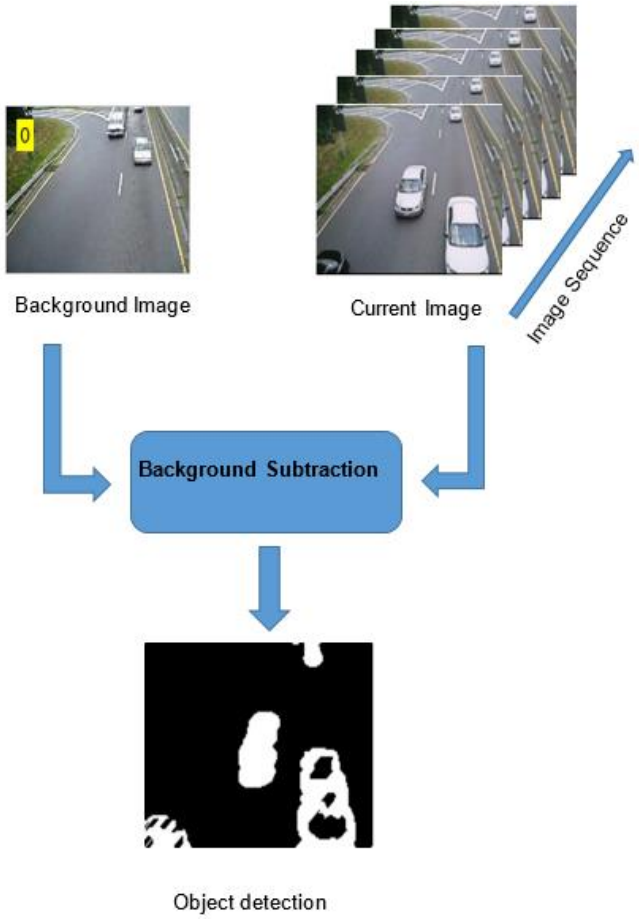

Figure 2. *Moving object detection based on background subtraction*

After subtracting background image, binary images of vehicle are created. We can use the centroid and regions of vehicles to track them.

2.2. Vehicles tracking

We use Kalman filter to predict each vehicle in current time. Normally, a Kalman filter is used to estimate the state of a linear system where the state is assumed to be distributed by a Gaussian. It is typically divided into two steps: prediction and correction. The prediction step is to estimate the state based on the state equation. Similarly, the correction step uses the current observations to update the vehicle's state. In this paper, to track multiple vehicle simultaneously, multiple Kalman filters as number of vehicles is used [13]. Each Kalman filter is represented as below:

$$x_k = Ax_{k-1} + w_k$$
$$z_k = Hx_k + v_k$$

Where $x = \left[p_x \; p_y \; v_x \; v_y \right]^T$, p_x, p_y are the center position of x-axis and y-axis, respectively. v_x, v_y are the velocity of x-axis and y-axis. Matrix A represents the transition matrix, matrix H is the measurement matrix, and T is the time interval between two adjacent fames. w_k and v_k are the Gaussian noises with the error covariances Q_k and R_k. The Kalman filter is process as follow:

Update the state: $x_{k|k-1} = Ax_{k-1|k-1}$

Predict the measurement: $z_{k|k-1} = Hx_{k|k-1}$

Update the state error covariance: $P_{k|k-1} = AP_{k-1|k-1}A^T + Q_k$

To track multiple vehicles in complex transportation, matching between vehicle and measurement should be performed correctly. In this paper, we employ the data association method, which split and merge the vehicles [13]. The overall tracking method is given in figure 3.

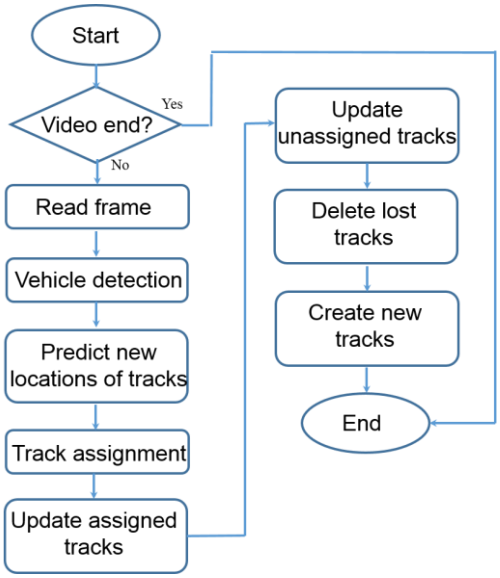

Figure 3. *The flow chart of vehicles tracking method*

2.3. Experimental Results

2.3.1. Vehicle detection

The first step of object tracking is object detection. The data used in this paper were collected from [14]. The vehicle was detected using background subtraction algorithm with Gaussian Mixture Model. Figure 4 (a) shows the motorbike in the image captured from camera. Figure 4 (b) shows the motorbike was detected as the block of white pixels while the background is black.

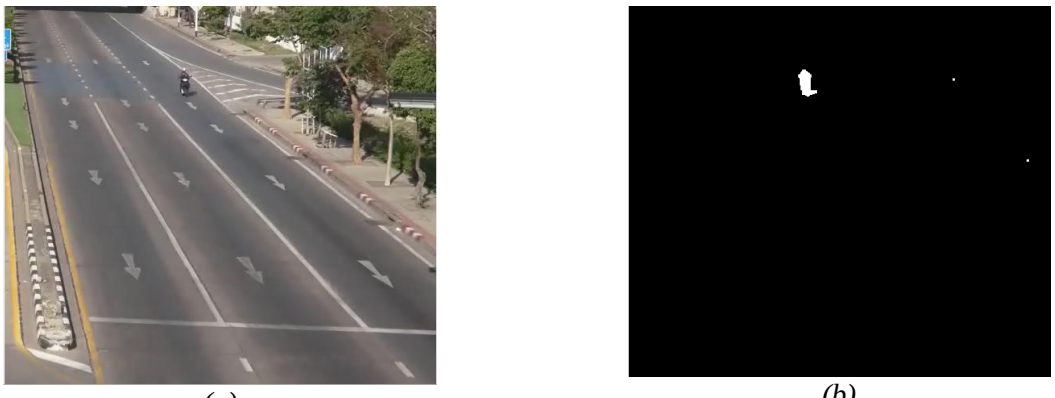

(a) *(b)*

Figure 4. *(a) sample image. (b) the motorbike detected*

The track was initialization with this object, the Kalman filter is used to estimate the vehicle in the next frame.

2.3.2. Vehicles tracking

Figure 5 shows the tracking results for the video of single motorbike was tracked using object

detection algorithm presented in the previous section. We use the number at the top of the motorbike for multiple vehicle tracking purpose. The Kalman filter implements two steps: prediction by estimate the state of the object and correction using measurement of object.

Figure 5. *Motorbike tracking*

Figure 6 shows the car was detected and tracking. With single object, the car detection and tracking are similarly the motorbike detection and tracking.

Figure 6. *Car tracking*

Figure 7 shows the results for the multiple vehicles tracking. When a car or motorbike come to the region of the camera, it will be assigned a new tracking object and initialize tracking window for this car. The tracking results of multiple vehicles show the tracking method is able to correctly track the new vehicle in transportation camera surveillance. For the case of several vehicles run near each other, we need data association method to distinguish each vehicle.

Figure 7. *Multiple vehicles tracking*

III. CONCLUSION

In this paper, we presented the tracking method for multiple vehicles based on Kalman filter. For each vehicle, the Kalman filter was established and use bounding box as feature. The Kalman filter estimates the state based on the state equation and corrects using the current observations to update the vehicle's state. Results of this paper show that this method can be applied in transport management center for traffic monitoring.

References

[1]. *B. E. Flinchbaugh and T. J.Olson*, "Autonomous video surveillance," Proceedings of the SPIE, vol. 2962, pp. 144–151, 1997.

[2]. *H. Moon, R. Chellapa, A. Rosenfeld*, "Performance analysis of a simple vehicle detection algorithm", Image and Vision Computing 20. 1–13, 2003.

[3]. *Wang C, Thorpe C, and Suppe A*.: 'Lidar-Based Detection and Tracking of Moving Objects from a Ground Vehicle at High Speeds'. Proceeding of the IEEE Intelligent Vehicles Symposium, 2003.

[4]. *C. Setchell and E. Dagless*, "Vision-based Road Traffic Monitoring Sensor", IEE Proc. Vision, Image Signal Processing, Vol. 148 (1), pp. 78-84, 2001.

[5]. *Baljit Singh Mokha and Satish Kumar*, "A Review of Computer Vision System for The Vehicle Identification and Classification from Online and Offline Videos, Signal & Image Processing: An International Journal (SIPIJ) Vol.6, No.5, October 2015.

[6]. *G. S. Manku, P. Jain, A. Aggarwal and L. Kumar*, "Object tracking using affine structure for point correspondence", IEEE conference of Computer Vision and Pattern Recognition, 704-709, 1997.

[7]. *L. Xin, W Kejun, W Wei, and L. Yang*, "A Multiple Object Tracking Method Using Kalman Filter", IEEE International Conference on Information and Automation, pp. 1862-1866,2010.

[8]. *D. Comaniciu and V. Ramesh*, "Mean shift and optimal predication for efficient object tracking", IEEE Int. Conf. Image Processing, vol. 3, pp. 70–73, Vancouver, Canada, 2000.

[9]. *Da-Peng Bai, Bing-Bing Lee*: Based-on Particle Filter For Vehicle Detection And Tracking In Digital Video: Proceedings of the Seventh International Conference on Machine Learning and Cybernetics, Kunming, 12-15 July 2008.

[10]. *H. S. Lai and H. C. Yung*, "Vehicle-Type Identification Through Automated Virtual Loop Assignment and Block-Based Direction-Biased Motion Estimation" ,IEEE Transactions on Intelligent Transportation System, Vol. 1, No. 2, June 2000.

[11]. *K. Dhanya, M. Manimekalai, B.Asmin and G. Vani*, "Tracking and Identification of Multiple Vehicles".

[12]. *Y. Iwasaki, M. Misumi, and T Nakamiya*, "Robust Vehicle Detection under Various Environments to Realize Road Traffic Flow Surveillance Using An Infrared Thermal Camera" The Scientific World Journal, Volume 2015, Article ID 947272, Hindawi Publishing Corporation.

[13]. *Jong-Min Jeong, Tae-Sung Yoon, and Jin-Bae Park*, Kalman Filter Based Multiple Objects Detection-Tracking Algorithm Robust to Occlusion, SICE Annual Conference, Japan, pp. 941-947, 2014.

[14]. *Shuo Zheng*, Tracking Multiple Objects In Surveillance Cameras, Technical Report, 2010.

LANDSLIDE POTENTIAL EVALUATION USING FRAGILITY CURVE MODEL

YI-MIN HUANG[1]*, TSU-CHIANG LEI[2], MENG-HSUN HSIEH[3], BING-JEAN LEE[4]
[1]Dept. of Civil Engineering, Feng Chia University, Taiwan, R.O.C*
[2]Dept. of Urban Planning and Spatial Information, Feng Chia University, Taiwan, R.O.C
[3]Construction and Disaster Prevention Research Center, Feng Chia University, Taiwan, R.O.C
[4]Dept. of Civil Engineering, Feng Chia University, Taiwan, R.O.C
Corresponding author's email: ninerh@mail.fcu.edu.tw

Abstract: *Landslide is a common natural disaster in the mountain areas of Taiwan. Because of the geological vulnerability and increasing severe weather conditions, the shallow landslides have occurred more often since the Chi-Chi Earthquake in 1999. In order to evaluate the potential of landslides given certain conditions, an empirical model of landslide fragility curves was proposed in this paper. The development of landslide fragility curves model included the collection and analysis of historical rainfall data, the satellite images (before and after typhoon events), and landslide areas. The model used two factors, rainfall index (hourly rainfall and accumulated rainfall) and landslide fragility, to assess the potential of landslide. The estimation of influence of rainfall and the fragility of shallow landslides were addressed in the paper. The critical hazard potential (Hc) and critical fragility potential (Fc) from the model were used in the proposed landslide warning procedure. A case study of Shenmu village in the Chen-Yu-Lan Watershed in Taiwan was addressed to demonstrate the application of landslide fragility curves and warning procedure by the events of Typhoon Morakot (Aug. 2009). The results of case study of Shenmu implied that the landslide fragility curve model was reasonable and practical for landslide disaster warning in terms of slope unit approach. Further case studies were necessary to enhance the fragility-based landslide warning model.*

Keywords: *landslide, fragility, landslide potential, warning model*

I. INTRODUCTION

Taiwan is ranked as the high risk of natural disasters in the world [1]. Most areas of Taiwan are hillsides, and the environment of steep topography and geological vulnerability make landslides more likely to occur in these areas during torrential rainfalls and typhoons. The increasing frequency and intensity of rainfalls in recent years has been the major cause of rainfall-induced shallow landslides, and the shallow landslide has become a serious concern to people in Taiwan.

The researches about the landslides usually used the landslide susceptibility analysis (LSA) to develop landslide evaluation model [2]. These LSA models basically use factors that are highly related to the occurrence of landslides, and the observed data is used to define the influence of

each factor. The common models developed for landslide hazard or landslide evaluation are usually deterministic analyses. Recently, a novel concept of applying probability to landslide evaluation had been proposed. The fragility curves, which is commonly used in the earthquake-induced structure failure analysis, had been adopted to represent the probability of landslide [3] [4].

In order to evaluate the potential of landslides given certain conditions, an empirical model of landslide fragility curves was proposed in this paper. The development of landslide fragility curves model included the collection and analysis of historical rainfall data and environmental conditions (e.g., the landslide areas and the land cover). The spatial statistics and geographic information systems (GIS) for data processing were performed on the slope-unit base. The proposed LFC model introduced the Landslide Fragility Surface (LFS) by considering the influence of both rainfall intensity and accumulation at the same time. The assessment of landslide potential was analyzed with the rainfall hazard potential in the landslide warning model in this study. The area of Chen-Yu-Lan Watershed was used to develop the LFC model, and the Shenmu area was selected for case study to illustrate the application of LFC model and landslide warning

II. STUDY AREA AND DATABASE

The Chen-Yu-Lan watershed is at the central part of Taiwan, as shown in fig. 1. The Chen-Yu-Lan River originates from the north peak of Yu Mountain and is one of the upper rivers of the Zhuoshui River system, which is the largest river system in Taiwan. Chen-Yu-Lan River has a length of 42.4 km with an average declination slope of 5 %, and its watershed area is about 45,000 hectares. This area was fragile after Chi-Chi Earthquake (occurred on September 21, 1999).

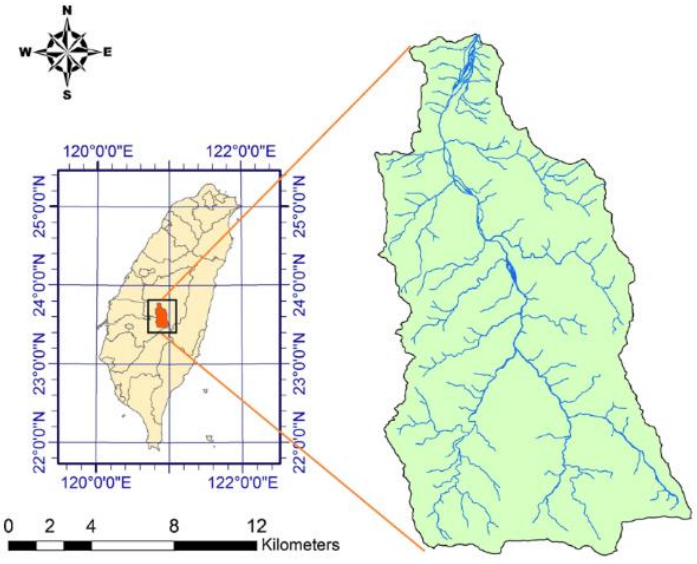

Figure 1. *Chen-Yu-Lan Watershed (after [2])*

The local environmental data was collected and GIS was used to process the data. The environmental database includes data of geology, geological layers, rock property, slope and slope aspects, and DEM, as shown in fig. 2. The areas of buildings, agricultural lands, and the river

reservations were not included in the analysis. The landslide increment was defined in fig. 3, and the increments of the study area (Fig. 4) were identified by using pre- and post-event satellite images of Typhoon Haitang in 2005, Tyhpoon Sinlaku in 2008 and Typhoon Morakot in 2009. These landslide increments were used for later Landslide Fragility Curves (LFC) model analysis. The vegetation status of the land surface in the area was also obtained by image processing from the satellite images. In addition to the hydrologic and geographic data, the rainfall data was collected to compute rainfall indices in the model.

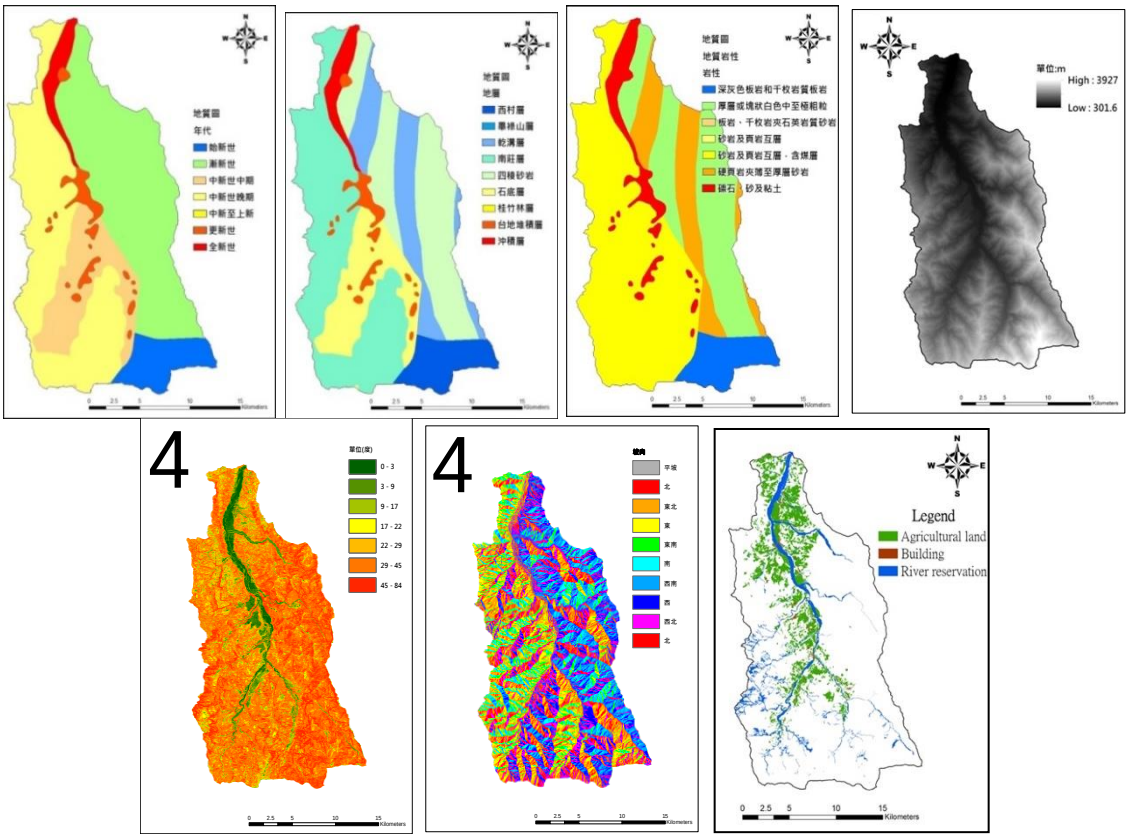

Figure 2. *The maps of environment database of Chen-Yu-Lan watershed: (from top left) geologic time, geologic layers, rock property, 5-m DEM, slope, slope aspect, and land cover.*

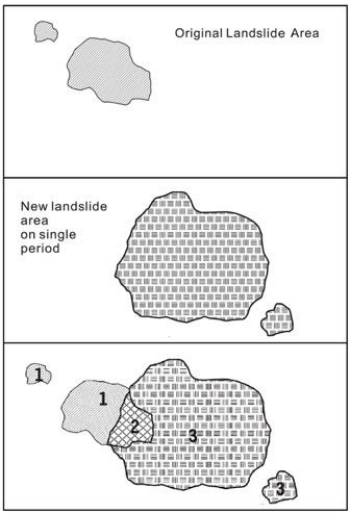

Figure 3. *Concept of mapping landslide area change: differences between two periods of SPOT image*

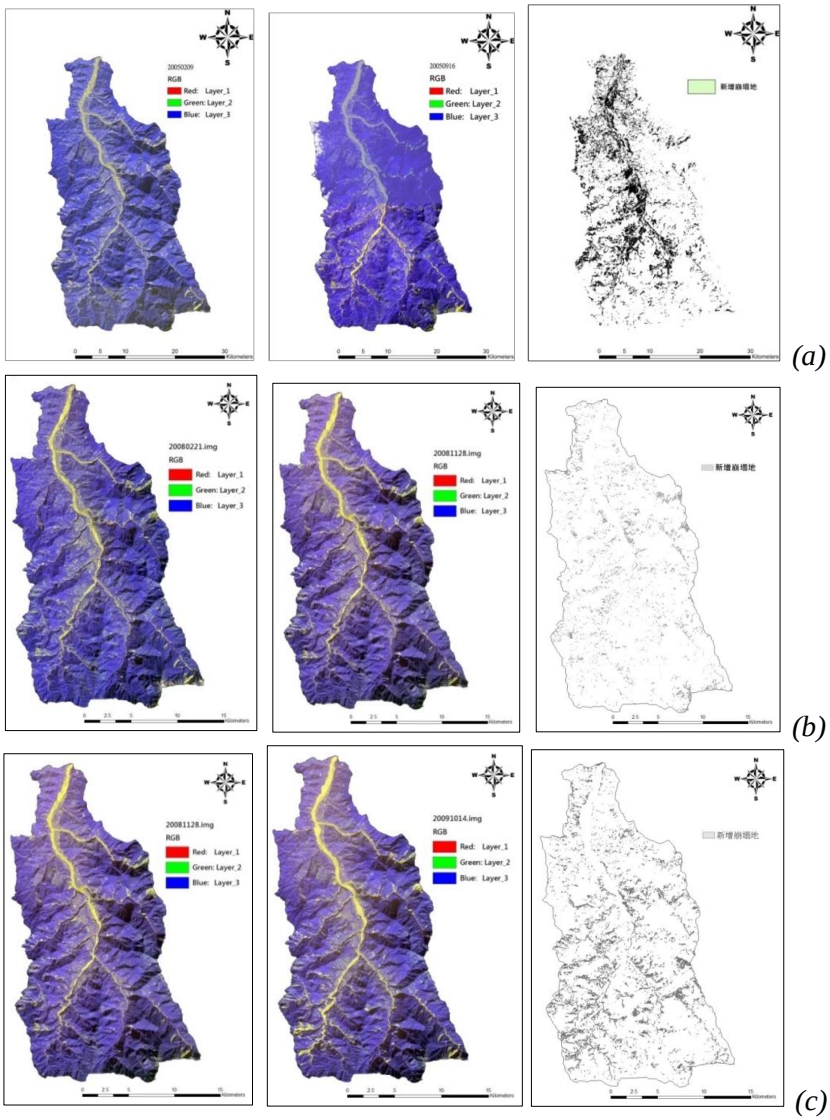

Figure 4. *Satellite images of pre- and post-events and the landslide increment areas in Chen-Yu-Lan watershed: (a) Typhoon Haitang (2005), (b) Typhoon Sinlaku (2008), and (c) Typhoon Morakot (2009)*

In order to construct the fragility curves of landslide, the study area was divided into pieces to construct slope units (fig. 5). The idea of using slope unit as the analysis basis was to properly and physically represent the local terrain features and conditions [3]. There are total of 5,872 slope units in Chen-Yu-Lan watershed.

(a) slope unit delineation *(b) slope units of Chen-Yu-Lan watershed*

Figure 5. *Slope unit in LFC model of Chen-Yu-Lan watershed*

III. LANDSLIDE MODELS

3.1. Landslide Fragility Curves Model

Based on the environmental database, the LFC model considers 2 triggering factors of max. hourly rainfall (I_{max}) and effective accumulated rainfall (R_{te}), and 8 environmental factors of geology (G), slope (S), distance to rivers (R), normalized difference vegetation index (N), and slope aspects (A) (fig. 6). Each environmental factor was further classified into levels to represent the difference. There were at most 48 classifications [3] [4]. Due to the sparse number of landslide cases, samples of certain classifications were combined together to improve the model optimization. Lognormal probability distribution was assumed to develop LFC model. The maximum likelihood estimation (MLE) was used in the computation to match the results for model optimization. Fig. 7 shows an example of fragility curves based on the classifications of rainfall intensity and slope level.

A 3D-like distribution was obtained in terms of Imax and R_{te}, as shown in Fig. 8. The landslide fragility surface was projected onto a 2D plane and a probability contour map was generated.

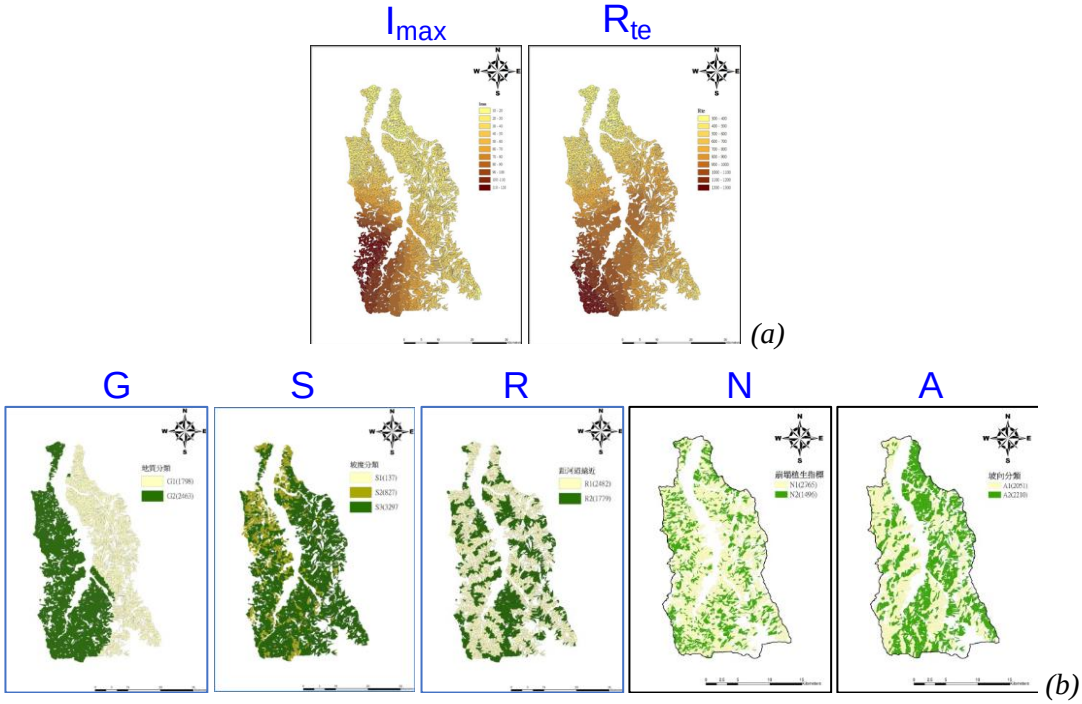

Figure 6. *The factors used for developing landslide fragility curve model. (a) triggering factors: rainfall intensity (I_{max}) and effective accumulated rainfall (R_{te}) (b) environmental factors: geology (G), slope (S), distance to river (R), vegetation NDVI (N), and slope aspect (A)*

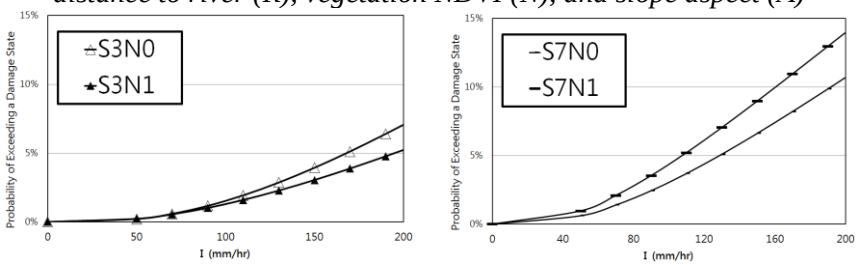

(a) Slope of Level 3 *(b) Slope of Level 7*

Figure 7. *Landslide fragility curves by I factors under different conditions of slope and vegetation indices*

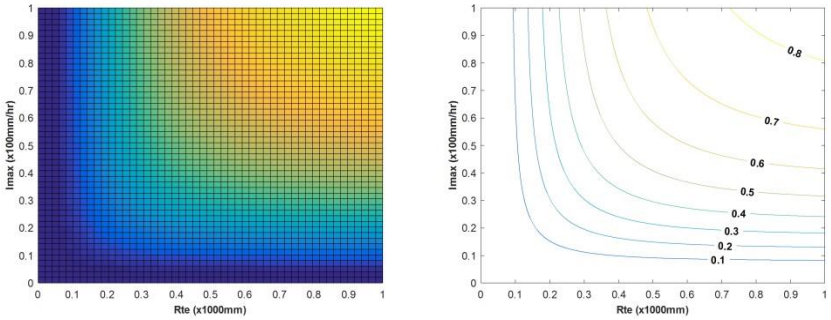

classification: G2S3A2R2N2

Figure 8. *Examples of the landslide fragility surface*

3.2. Landslide Warning Model

In addition to the LFC model, which was the vulnerability of landslide, the 10-year rainfall data was prepared to develop rainfall hazard. The rainfall indices of maximum hourly rainfall (I_{max}) and effective accumulated rainfall (R_{te}, see Equation (1)), as explained in fig. 9, were used for rainfall hazard estimation.

$$R_{te} = \sum_{i=0}^{7} \alpha^i R_i \text{ , where } \alpha = 0.7 \quad (1)$$

The lognormal standard probability distribution was assumed to construct the probability model of rainfall hazards. Joint Probability Mass Function (JPMF) and Joint Cumulative Distribution Function (JCDF) were used, in association with the rain patterns, to develop a 3D-like probability distribution of rainfall hazard (an example as in fig. 10). The probability distribution in fig. 10 was projected onto a 2D plane, and the correspondent distribution was expressed as a probability contour map.

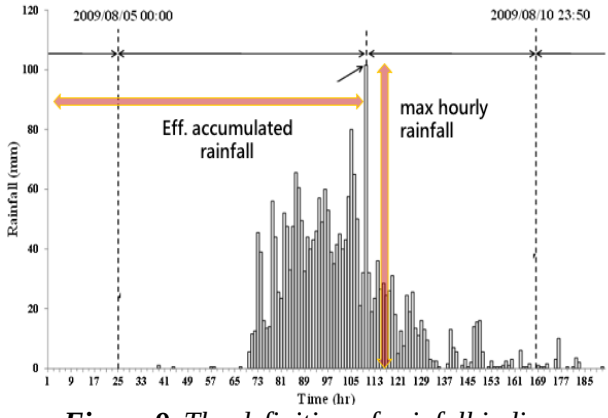

Figure 9. *The definition of rainfall indices*

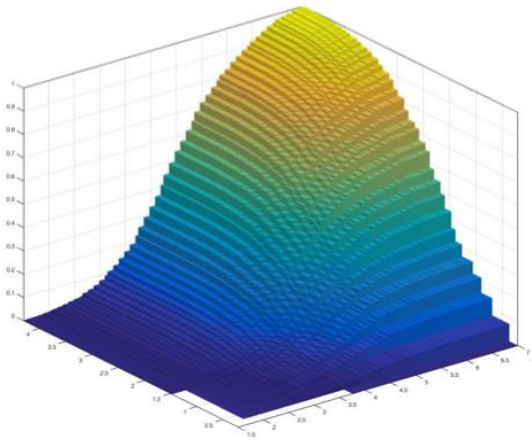

Figure 10. *The 3D probability distribution of rainfall hazard*

The potential of landslide was demonstrated by using the critical values of rainfall hazard and landslide fragility. The landslide warning was considered by the threshold values of hazard (H) and fragility (F). The critical values of landslide occurrence, H_c for rainfall hazard and F_c for landslide fragility, was determined from the landslide events. The warning status was illustrated

in fig. 11. It should be noted that there are two stages of unsafe status, Red I and Red II. Red I stage indicates that the situation has passed H_c and a rainfall hazard could occur. Red II stage implies the most serious condition that a landslide could occur, since it is over F_c. Both stages are determined with a probability when given a rainfall condition.

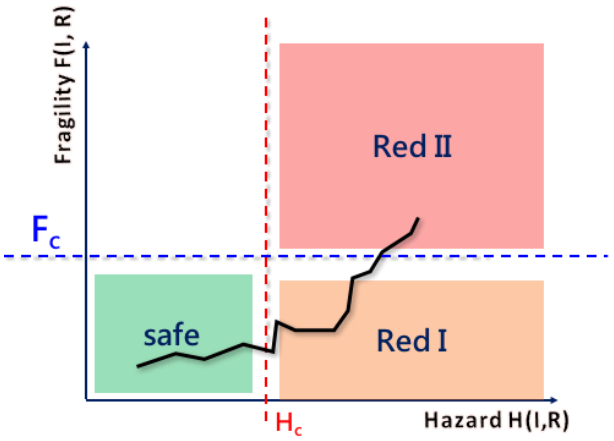

Figure 11. *The warning conditions based on landslide fragility (F_c) and rainfall hazard (H_c)*

IV. CASE STUDY AND RESULTS

The Shenmu area is a location where debris flows frequently occurred [5] [6]. The local village is adjacent to the confluence of three streams: Aiyuzi Stream (DF226), Huosa Stream (DF227) and Chushuei Stream (DF199). In Shenmu, the debris flows usually occurred at the Aiyuzi Stream due to its shorter length and large landslide area in its upstream [5]. Fig. 12 shows the terrain of three streams, and the slope units of Shenmu is in fig. 13.

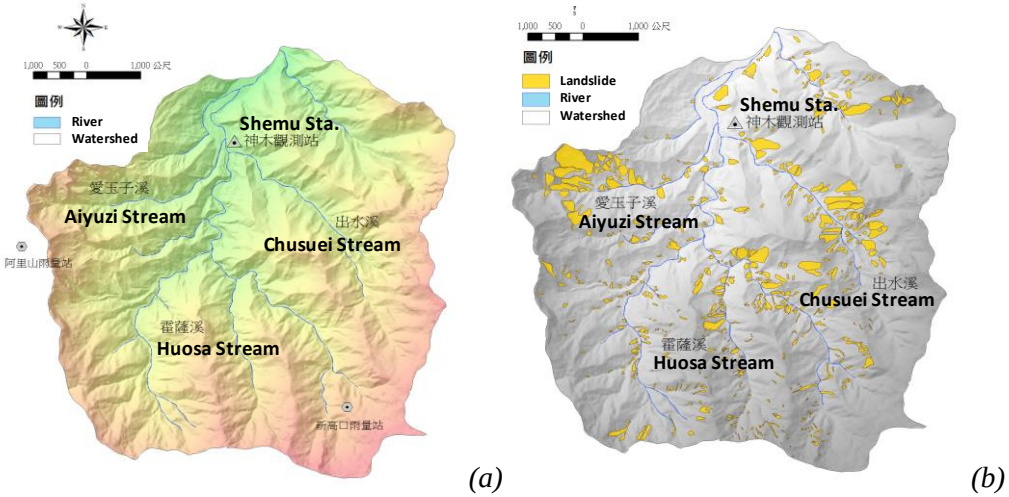

(a) *(b)*

Figure 12. *The terrain (a) and landslide areas (b) of Shenmu area*

Fig. 13 illustrates the rainfall hazard probability contour map of Shame area. This figure was later applied to determine Shemu's critical probability (H_c) of rainfall hazard when given hazard histories. The landslide fragility curves of Shemu was obtained as in fig. 14. Cases of landslides and debris flows in Shemu were collected issued by Soil and Water Conservation Bureau of Taiwan. As shown in fig. 15, total of 7 cases were used to determine the critical values of H_c (=0.91) and F_c (=0.23) of Shemu.

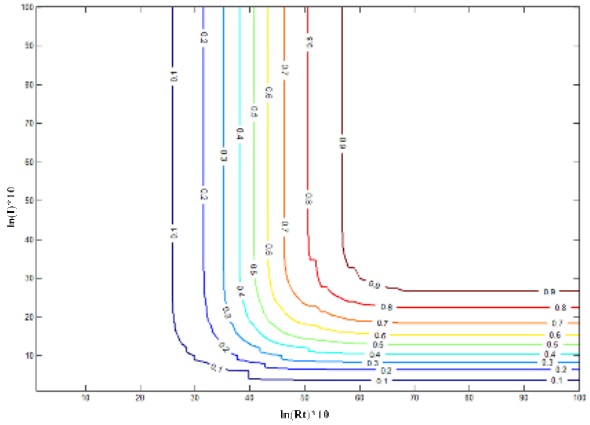

Figure 13. *The rainfall hazard probability contour lines (R vs. I) of Shenmu area*

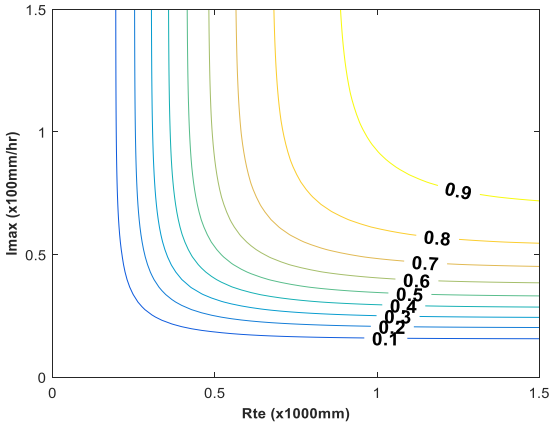

Figure 14. *The landslide fragility curves of Shenmu*

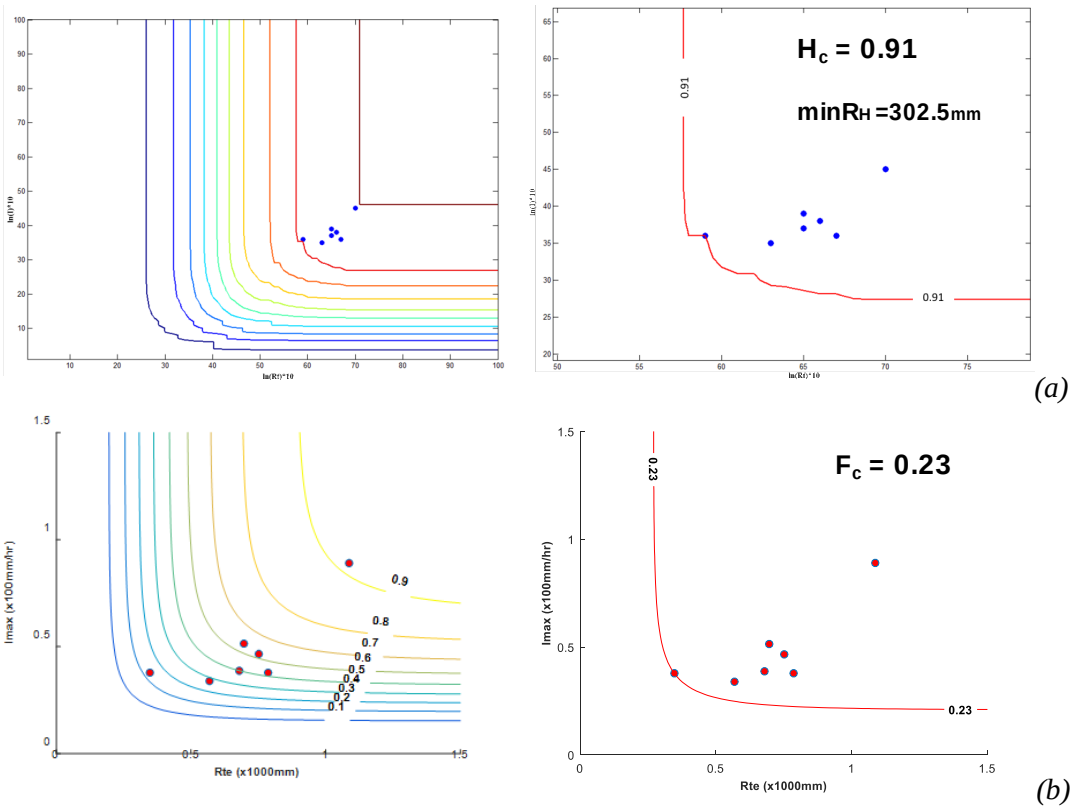

Figure 15. *The probability thresholds of rainfall hazard and landslide fragility in Shemu area. (a) rainfall warning threshold (b) landslide warning threshold*

The rainfall history of Typhoon Morakot in 2009 was used to evaluate the landslide assessment in Shemu. Fig. 16 shows the results of event and the dots in the figure represent the rainfall condition and the probability of hazard. It was noted that the dots behaved like a “snake” line going from safe stage to Red I and Red II stages. Also, the snake line stayed shortly at Red I stage, and passed to Red II in a jump. This condition implied that when the situation was beyond the Hc line, the landslide hazard was very likely to occur. The results conformed to the records of Typhoon Morakot. Severe landslides occurred at the upper stream areas in Shemu during the typhoon. Therefore, the proposed landslide potential assessment and warning stages of landslide were reasonably practical.

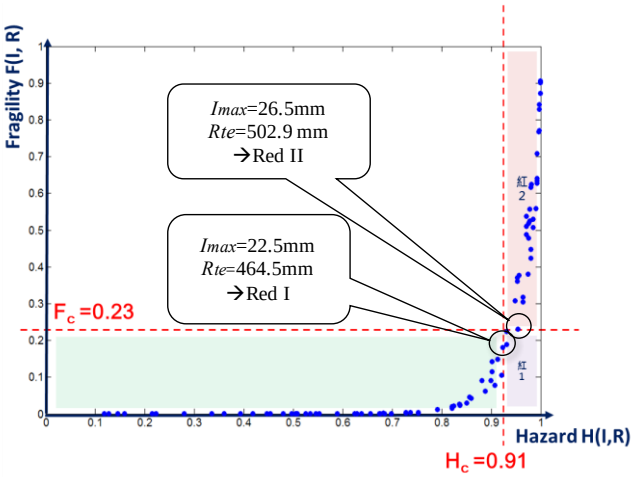

Figure 16. *The change of probability during Typhoon Morakot (2009) event in Shenmu area*

V. CONCLUSIONS

This study proposed landslide assessment using rainfall hazard potential and landslide fragility curves, and concluded findings as follows.

1. The proposed model provides considerably accurate and reliable results on landslide estimations in terms of spatial distribution.

2. Adoption of slope unit was physically proper in modeling landslide locations.

3. The proposed landslide fragility curves were derived by considering both rainfall intensity and accumulated rainfall together. The 3D-like probability model was useful for practice if converted onto a 2D contour lines.

4. The procedure of landslide assessment was useful for practical landslide disaster preparation and prediction.

5. More cases were needed in order to understand the change of "snake" line under different rainfall conditions and environment.

References

[1] *Dilley M, Chen RS, Deichmann U, Lerner-Lam AL, Arnold M*, Natural disaster hotspots. World Bank report, 2005, ISBN: 9780821359303.

[2] *Lei, T.-C., Huang, Y.-M., Lee, B.-J., Hsieh, M.-H., Lin, K.-T.* Development of an Empirical Model for Rainfall-induced Hillside Vulnerability Assessment - A Case Study on Chen-Yu-Lan Watershed, Nantou, Taiwan, Natural Hazards, 74(2), pp. 341-373, 2014.

[3] *Lee B.J. et al*. 2015 Application of Landslide Fragility Curves in Landslide Risk and Warning Criteria, Project Report, Soil and Water Conservation Bureau, 341 (in Chinese), 2016.

[4] *Lee B.J. et al*. 2016 Application of Landslide Fragility Curves in Landslide Risk and Warning Criteria, Project Report, Soil and Water Conservation Bureau, 224 (in Chinese), 2017.

[5] *Huang Y.M., Chen W.C., Fang Y.M., Lee B.J., Chou T.Y., Yin H.Y.* Debris Flow Monitoring – A Case Study of Shenmu Area in Taiwan, Disaster Advances, 6(11), 1-9, 2013.

[6] *Yi-Min Huang, Chung-Ray Chu, Yao-Min Fang, Ming-Chang Tsai, Bing-Jean Lee, Tien Yin Chou, Chen-Yang Lee, Chen-Yu Chen, and Hsiao-Yuan Yin*. Characteristics of debris flow vibration signals in Shenmu, Taiwan, In Proceedings of Interpraevent International Symposium 2016, Lucerne, Switzerland, 2016.

LANDSLIDES AND MOUNTAIN DEVELOPMENT: EXAMPLES FROM THE CHANYULAN CATCHMENT, TAIWAN

YUNG-CHUNG CHUANG
Department of Urban Planning and Spatial Information, Feng-Chia University, Taiwan
Corresponding author's email: yungcchuang@fcu.edu.tw

Abstract: *Due to the changing climate and the fragile geology, the development of mountainous regions in Taiwan is complex. Improving understanding of the relationship between human development and landslides has become an urgent issue. However, many people in Taiwan have asserted cultivation and mountain road construction as the significant cause of hillside landslides. And, the actual role of development is less well understood. This study took the Chanyulan Catchment in central Taiwan (A.D.1946~1952; A.D.1966~1968; A.D.2001) as a case study. Logistic regression was used to discuss the spatial correlation between many kinds of human development and landslides, and to find the significant factors contribute to landslides within development area. The results showed precipitation and slope were the significant independent factors affecting landslides, and the influences of human development were less conspicuous. Therefore, the selection of a safe development position on a hillside must be adapted to local natural conditions, such as precipitation, lithology, and slope, in order to prevent and mitigate the effects of disaster.*

Keywords: *Landslides; Development; Logistic regression*

I. INTRODUCTION

In many Asian countries, as the pressure on land increases continuously, human development inevitably tends to spread to mountainous regions, resulting in the continuous increase of hillside cultivation. Taiwan is not excluded. However, the topography of Taiwan's mountainous area is steep and varying, characterized by high drainage density, complex slopes, and is often affected by typhoons, heavy rainfall and earthquakes, so landslides occur frequently. The high coupling of slopes and river channels lead debris-flow occurrence in low-order catchments. These debris flows caused significant loss of life, property, and public facilities. After the serious Chi-Chi Earthquake in 1999, landslide disasters has become more frequent [1]. The Soil and Water Conservation Bureau in Taiwan also announced an increase in the number of potential debris flow torrents, from 400 to 1420 during the period of 1999 to 2006 for hazard mitigation.

Although almost all landslide events were triggered by typhoons and heavy rainfall in Taiwan, many people concluded that development and mountain road construction were also the significant factors of hillside landslides, because the locations of landslides, debris flows, and the dense development areas often overlapped. Laws on development limitation (e.g., aboriginal reserved lands, ARL) have been enacted, and the net result is that the indigenous people, who live in mountainous regions, bear the brunt of the impacts. Poor living conditions are now coupled with government restrictions. The indigenous people have become an especially vulnerable group.

For this reason, the challenge of this study is to understand the impact degree of human

development in Taiwan mountainous regions during typhoon season. this study chose the Chanyulan Catchment as representative study area. The aims of this study are: (1) to figure out whether hillside development is a significant factor related to landslides from different times and locations; (2) to discuss the significant related factors of new landslides and landslide recovery in development areas. Through the analysis of this study, we can further understand the role of development in the hillside landslide events, and provide a reference for hazard mitigation and prevention in the future.

II. PREVIOUS STUDIES

Landslides are controlled by a complex set of natural and man-made site factors. Human development is one of them. The influences of development on landslides have been addressed in many research studies from different points of view (e.g.,[2][3][4][5][6][7]). The main effect of development is to change the land cover as it relates to soil moisture, pore pressure, surface erosion rate and root strength (e.g.,[8][4]).

Taking Taiwan mountainous catchments as examples, due to high transport accessibility and human-induced land use pressure, development is one of the major factors influencing land cover and morphology change. Jan [9] pointed out that mountain road construction would change the slope shape and influence the slope stability. Chung [10] thought that human development and precipitation are the main causes of terrain morphology and land cover change in Taiwan. In more detailed discussions, logging activities, mountain road construction, and extreme typhoon and earthquake events all lower the stable-status thresholds and produce the short-term acceleration of landslides (e.g.,[11][12][13]).

However, all factors, including natural factors and man-made factors, will interact and compound together to cause various results (e.g.,[14][15][16]). In short, it is difficult to define the impact degree of development decisively from a single point of view.

III. STUDY AREA AND MATERIALS

3.1. Study Areas

The Chenyulan Catchment has an area of 449 km^2 and is located in central Taiwan (fig.1). The Chenyulan Catchment is a typical mountainous drainage catchment elongated in a northsouth direction with a mean altitude of 1,540 m and a slope of 32 degree. The gradient of the main course is 6.1% and more than 60% of its tributaries have gradients that are steeper than 20% [17]. Slates and meta-sandstones are the dominant lithologies. With several large river terraces and fan terraces, settlements and development are mainly located in flat areas.

The Chenyulan Catchment is also the traditional home of the Bunun aboriginals. In the past years, aborigines mainly lived on dry farming, supplemented by ramie, bamboo, fruit trees, and other crops, but gradually have applied larger-area farming, logging, and the plantation of highland vegetables and fruits in last 100 years, following the introduction of Chinese farming technology. The impact degree of the dramatic change of cultivation is worth of discussion.

3.2. Materials

For general researchers in Taiwan, the most common materials for landslide analysis are: (1) digital terrain models; (2) Aerial photos or ortho-images; (3) geologic maps; and (4) precipitation

data, which are all produced and released by Taiwan government agencies. In this study, we gathered the materials as the source data, and generated different kind of basic raster maps (A.D.1946~1952; A.D.1966~1968; A.D.2001) for analysis (by representing 20 m), including: (1) cultivation (e.g., settlement buildings, farms, paddy fields, dry fields, orchards, vegetable gardens, bamboo, artificial soil preparation, logging, etc.); (2)mountain roads; (3)geology distribution; (4) precipitation maps (e.g., average precipitation, maximum precipitation); (5) slope, plane curvature, slope curvature and aspect; (6) topographic index; (7)elevation.

In brief, Table 1 shows the data source, resolution/scale, and application procedures of these materials.

Table 1. *Data, resolution/scale, data source, and procedure for the independent variables*

Data	Resolution/Scale	Data source	Procedure
DEM	20m	Aerial Survey Office of Taiwan's Forestry Bureau	Elevation, Slope, Aspect, Curvature, Topographic Index, and Flow accumulation are generated from DEM
Historical aerial photo	1:6,000	GIS center, Academia Sinica	Landslides distribution and land cover distribution maps are digitized from historical aerial photo.
Corona satellite image	1:10,000	USGS	Landslides distribution and land cover distribution maps are digitized from Corona satellite image.
Ortho-image	1:1,000	Aerial Survey Office of Taiwan's Forestry Bureau	Landslides distribution and land cover distribution maps are digitized from ortho-images.
Geologic map	1:50,000	Taiwan's Central Geological Survey	Lithology and fault lines are compiled from the geologic map.
Distribution of precipitation	1:5,000	Taiwan's Central Weather Bureau	Grid format of precipitation distribution map are compiled from vector format precipitation distribution map.

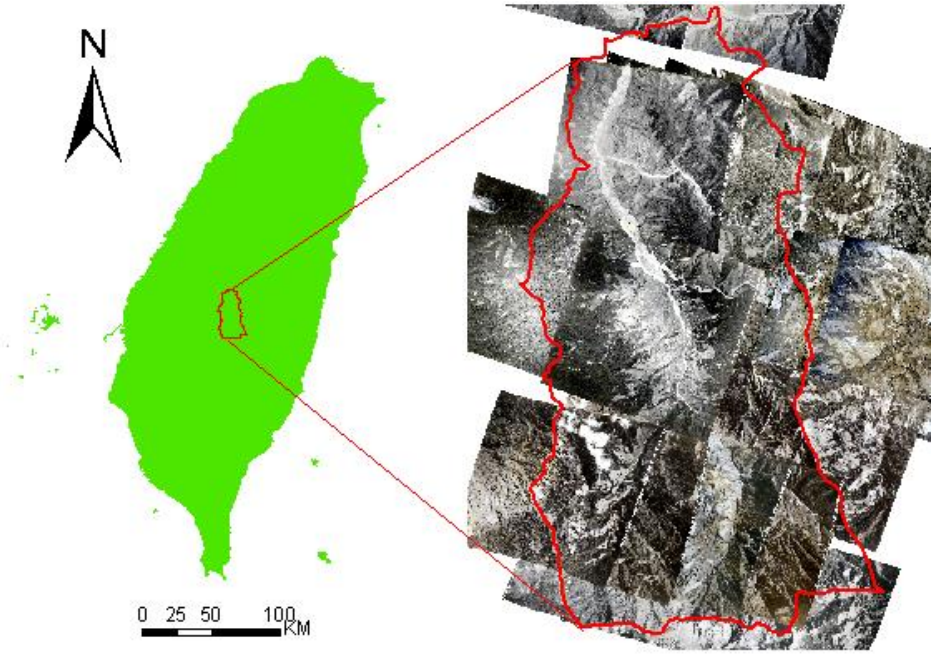

Figure 1. *Location map of Chanyulan Catchment*

IV. METHODOLOGY

4.1. Logistic regression analysis

In this study, we applied logistic regression analysis, a log-linear model suitable for quantitative analysis, to find the best fitting function to interpret the relationship between independent environmental variables and landslide conditions of different time periods. Logistic regression analysis is useful when the dependent variable is categorical (e.g., presence or absence) and the explanatory (independent) variables are categorical, numerical, or both (e.g.,[18][19][20]). Generally speaking, a logistic regression model can be expressed in the following forms [21]:

$$P(y_i = 1) = [1 + \exp(\alpha + x_i\beta)]^{-1} \quad (1)$$

In Eq. (1), $P(y_i = 1)$ means the conditional probability of landslide changes; x_i is the vector of independent variable; if $p = P(y_i = 1)$, the above equation can be revised to:

$$\ln(p/(1-p)) = \alpha + \beta_1 x_1 + \beta_2 x_2 + \cdots + \beta_n x_n \quad (2)$$

In Eq. (2), $\ln(p/(1-p))$ is the occurrence probability; α is the intercept; and β_1, β_2,... β_n are the regression coefficients. In order to interpret the occurrence probability, one has to use the coefficients as a power to the natural log (e). The result represents the corresponding coefficient of each responding independent variable is the effect on odds (landslide occurrence or restoration), and when $\beta_n = 0$ it means that the odds will not change. In this way, we can sum up the main factors related to new occurrence and restoration of landslides.

In this study, all vector format maps were first converted into raster format with 20 m resolution. Landslide maps in grid format were used to produce a dependent variable, which took a value of 1 for landslides and 0 for constant. As for independent variables, 12 environmental factors were selected: (1) slope; (2) aspect; (3) elevation; (4) plane curvature; (5) slope curvature; (6) lithology type; (7) topographic index; (8) maximum precipitation distribution; (9) average precipitation distribution; (10) cultivation; (11) road development; (12) Upstream contribution area. We derived terrain attributes such as slope, elevation, and aspect from 20×20m digital terrain model, and applied 8-direction algorithm for the calculation of UCA.

V. RESEARCH RESULTS

5.1. Results of Logistic Regression Analysis in Chanyulan Catchment

In order to learn factors related to landslides in different time and space, and the impact degrees, this study applied logistic regression analysis in the Chanyulan Catchment with landslides-related factors. In logistic regression, if variables are involved in interdependencies, multicollinearity occurs. Multicollinearity is a result of strong correlations between independent variables and may cause wrong estimation of regression coefficients, even accordingly in incorrect conclusions about relationships between independent and dependent variables. Therefore, we used multicollinearity diagnostic statistics to exam the correlations between independent variables at the very start, and an absolute value of the correlation coefficient larger than 0.5 is thought to represent a high correlation between two variables. The results showed the correlation between

every pair of variables was relatively low, so we can determine the models with all possible combinations of low correlation variables.

After that, we evaluated the contribution of variables to landslides through regression coefficients comparison. When considering a viewpoint of the Chanyulan catchment, it can be seen that the significant factors affecting landslides in 1946~1952 were almost natural factors, such as elevation, slope, and plane curvature (table 2A.), human development and road construction were insignificant factors. The meaning behind the results might be: (1) human development, such as forest logging and clear cut were mostly located in lower landslide potential area (e.g., flat river terraces and other hillside with gentle slopes); (2) most landslides occurred in inaccessible areas and were impacted by natural forces; or (3) the precipitation intensity in 1946~1952 might have been too strong or homogeneous to induce the non-significant of development effect.

Besides, the parameter estimation showed the impact degree of plane curvature was much better than elevation and slope. It also meant that higher plane curvature with higher water concentration capacity is one of the important factors causing landslides during typhoon season in the Chanyulan catchment.

In 1966~1968, elevation, aspect, and precipitation were still significant factors related to landslides, especially average precipitation. But it worth a mention that cultivation, including logging, and road development, had become significant factors during 1966~1968. The possible reason might be: (1) The road systems were dramatically increased after 1960's in Chanyulan Catchment, such as industrial roads, but many of the new roads were inevitable to pass through steeper slopes and fragile geology with relative high landslide probability (old roads were remaining on flat area, river terraces and fan terraces). The distribution of flat areas and gentle slopes in southern area of Chanyulan Catchment was very scattered, but development and mountain roads were often developed with high continuity and large areas; therefore, many extended development areas overlapped with landslide-prone areas, and they also enhanced the probability of landslide occurrence eventually. For this reason, even if the illegal or improper road development on steep slope was very small, the landslide suffering rate was greater; (2) large area of forest logging and clear cut since 1940's coupled with heavy typhoon rainfall every year had reduced the soil cohesion, influenced the slope stability and cause failure.

Table 2. *Significant factors related to landslides in Chanyulan Catchment through logistic regression analysis (A) 1946~1952*

Summary of Stepwise Procedure		
Factors	**Parameter Estimate**	**Pr > Chi-Square**
Elevation	0.308	0.00**
Slope	0.937	0.00**
Plane Curvature	2.017	0.00**

(B) 1966~1968

Summary of Stepwise Procedure		
Factors	**Parameter Estimate**	**Pr > Chi-Square**
Elevation	0.957	0.00**
Aspect	0.765	0.00**
Plane Curvature	0.523	0.00**
Geology	2.140	0.02*
Average Precipitation (1966~1968)	4.012	0.00**
Maximum Precipitation (1966~1968)	1.145	0.00**
Cultivation (1966~1968)	2.824	0.00**
Road Development (1966~1968)	4.226	0.00**

(C) 2001

Summary of Stepwise Procedure		
Factors	**Parameter Estimate**	**Pr > Chi-Square**
Slope	1.821	0.00**
Geology	5.487	0.00**
Average Precipitation (2001)	4.776	0.00**

In 2001, by analyzing the parameter, the results showed the average precipitation, slope and geology were highly related to landslides, but the human impact factors became insignificant again. The meaning behind the results might be: (1) In 2001, forest logging had been banned for 10 years in Taiwan, many deforestation area had fully recovered, human developments were only a small part of the entire Chanyulan Catchment; (2) the typhoon precipitation might have been too strong to induce the non-significant of development effect.

From the results obtained here, we can find many interesting points. As for the long-term change of development from 1946 to 2001, if we take the deforestation led by the Taiwan government into account, it can be found that the hillsides have suffered large-scale deforestation in 1900's~1990's, but the extent of deforestation during 1966~1968 reduced compared with 1946~1952, and many large-scale deforested areas had been greatly recovered by 2001~2004. This phenomenon represents that the area impacted by development was gradually decreased in the long-term perspective. The only imperfection worth mentioning was that although the overall area of development was continuing to shrink (development on river terraces and fan terraces are excluded), as the density of mountain roads increased in order to connect the scattered distributed developments, some improper land use, such as orchards, dry farmland, and trials gradually extended along both sides of those roads, and some steep slopes on both sides of roads received varying degrees of human reclamation again. Moreover, many mountain roads went through steep slopes or fractured geological areas just because people had no alternative but to choose the shortest way and to maintain the continuity of the road systems. It is a typical phenomenon in the Taiwan mountainous area. Since the mountainous area in Taiwan faces high development pressure, a comprehensive exam of the existing development and mountain roads would be a good way to evaluate the rationality and safety from the perspective of disaster prevention and mitigation in the future.

5.2. The landslide characteristics in development positions

Corresponding to the above results, there will be two questions we need to be concerned about: (1) what kind of natural environmental factors were highly related to landslides within the development positions; (2) within these development positions, were the landslide-related factors all the same? The answers to these two questions would be very helpful for testing the lack of attention to landslide prevention in the current development positions. Residents could also understand the environmental factors that need to be considered on future development in different regions.

If considering the scope of development by using logistic regression analysis, we can find the significant factor related to new landslides and the restoration of old landslides in human cultivation positions during 1946~2004 were mainly precipitation, geology and slope (Table 3.), indicating that if human cultivation was located on steep slopes, there was greater opportunity for landslides. It also means that the probability of suffering landslides would significantly be reduced if people did not cultivate on steep slopes. Besides, few repeated landslides happened on gentle slopes, so they had better chances to be restored from landslides. Therefore, when people are developing mountain roads in the future, the slope and elevation should be taken into serious consideration.

Table 3. *Significant factors related to new occurrence and restoration of landslides in Chanyulan Catchment through logistic regression analysis*

Types & Lacations	Significance factors affecting new landslide occurrence	Significant factors affecting landslide restoration
Human cultivation positions of the Chanyulan Catchment (1948~1966)	Slope; Geology	Slope; Precipitation
Mountain road positions of the Chanyulan Catchment (1948~1966)	Slope; Geology	Slope; Elevation
Human cultivation positions of the Chanyulan Catchment (1968~2001)	Slope; Precipitation	Slope; Precipitation
Mountain road positions of the Chanyulan Catchment (1968~2001)	Slope; Precipitation	Slope; Precipitation
Human cultivation positions of the Chanyulan Catchment (2001~2004)	Slope; Precipitation	Slope; Precipitation
Mountain road positions of the Chanyulan Catchment (2001~2004)	Slope; Precipitation	Slope; Elevation

VI. CONCLUSION

On the issues of the relationship between development and landslides, this study found through logistic regression analysis could the actual role of development be discovered. Although many development areas were very close to landslides, we conclude that the correlation between development and landslides was not as significant as many people have supposed them to be. Otherwise, landslides were mainly related to some natural environmental factors such as huge precipitation and steep slope. Besides, we also found that most of the residents living in mountainous regions have avoided relatively high landslide–prone areas, and have chosen safer and flatter places for cultivation, but the high terrain complexity and steep slope made for a scattered distribution of development, and they helped to form the dense network of road construction and some improper land use along the road system. The further research of this study

pointed out that precipitation and slope were the most significant factors related to landslides in development positions, so far as the steep slope was the main factor that caused landslides in road positions. Therefore, people have to keep off places with steep slopes and higher precipitation probability when arranging development areas. After all, as the phenomenon of the Chanyulan Catchment was very similar to other mountainous regions in Taiwan, the results of this research would be a good reference of future disaster prevention and mitigation in Taiwan.

References

[1]. *Lin, C. W., Liu, S. H., Lee, S. Y. and Liu, C. C.*, "Impacts of the Chi-Chi earthquake on subsequent rainfall-induced landslides in central Taiwan", Engineering Geology, 86:87–101, 2006.
[2]. *Glade, T.*, "Landslide occurrence as a response to land use change: a review of evidence from New Zealand", Catena, 51:297-314, 2003.
[3]. *Runqui, H. and Lungsang, C.*, "Human-induced landslides in China: mechanism study and its implication on slope management", Chinese Journal of Rock Mechanics and Engineering, 23:2766–2777, 2003.
[4]. *Vanacker, V., Vanderschaeghe, M., Govers, G., Willems, E., Poesen, J., Decker, J., and De Bievre, B.*, "Linking hydrological, infinite slope stability and land-use change models through GIS for assessing the impact of deforestation on slope stability in high Andean watersheds", Geomorphology, 52(3-4): 299-315, 2003.
[5]. *Remondo, J., Soto, J.S., Onzalez-Diez, A., De Teran, J. R. D. and Cendrero, A.*, "Human impact on geomorphic processes and hazards in mountain areas in northern Spain", Geomorphology, 66:69-84, 2005.
[6]. *Goudie, A.*, "The human impact on the natural environment", Blackwell Publishing, Oxford, 2006.
[7]. *Preutha, T., Glade, t., and Demoulin, A.*, "Stability analysis of a human-influenced landslide in eastern Belgium", Geomorphology, 120(1-2):38-47, 2010.
[8]. *Terzaghi, K.*, "Mechanism of landslides": In: Paige, S., Application of geology to engineering practice (Berkey Volume): New York, Geological Society of America, p. 83-123, 1950.
[9]. *Jan, B. W.*, "Landslide hazards in Taiwan", Journal of Engineering Environment, 6: 23-47, 1995.
[10]. *Chung, J. C., Shen, S. M., Liu, Y. S.*, Debris flow in four small catchments of the Chenyulan River, Geographical Research, 34:63-83, 2001.
[11]. *Huang, S. L. and Long, M. C.*, "Applied erosion control cost function", City and Planning, 20(1): 89-108, 1993.
[12]. *Chang, J. C. and Slaymaker, O.*, "Frequency and spatial distribution of landslides in a mountainous drainage basin: Western Foothills, Taiwan", Catena, 46:285-307, 2002.
[13]. *Cheng, S. H.*, "Management system assessment for illegal slope land development", Journal of Chinese Soil and Water Conservation, 35(4):361-373, 2004.
[14]. *Keefer, D. K.*, "Landslides caused by earthquakes", Geological Society of America Bulletin, 95: 406–421, 1984.
[15]. *Aleotti, P., Chowdhury, R.*, "Landslide hazard assessment: summary review and new perspectives", Bulletin of Engineering Geology and the Environment, 58:21–44, 1999.
[16]. *O'Hare, G., Rivas, S.*, "The landslide hazard and human vulnerability in La Paz City, Bolivia", Geographical Journal, 171:239–258, 2005.
[17]. *Chang, K. T., Chiang, S. H., Hsu, M. L.*, "Modeling typhoon- and earthquake-induced landslides in a mountainous watershed using logistic regression", Geomorphology, 89:335-347, 2007.
[18]. *Feinberg S.*, "The analysis of Crossclassfied categorical data" (2nd edition), Cambridge, MA: MIT Press, 1985.
[19]. *Agresti, A.*, "Categorical data analysis", 2nd edition, New York: Wiley, 2002.
[20]. *Menard, S.*, "Applied logistic regression analysis" (2nd edition). Sage, Thousand Oaks, CA, 2002.
[21]. *Ohlmacher, G. C. and Davis, J. C.*, "Using multiple logistic regression and GIS technology to predict landslide hazard in northeast Kansas, USA", Engineering Geology, 69 :331-343, 2003.

DEMAND AND SUPPLY ANALYSIS OF SMART PARKING IN FENG-CHIA UNIVERSITY

LIANG-TAY LIN[1], JAU-MING SU[2], CHAO-FU YEH[2], PEI-JU WU[2], BO-XIONG SHENG[3]
[1]College of Construction and Development, [2]Department of Transportation and Logistics
[3]Innovation center for Intelligent Transport and Logistics
Feng-Chia University, Taichung City, Taiwan
Corresponding author's email: ltlin@mail.fcu.edu.tw

Abstract: *With the rapid economy development, the dense urban population, and the serious traffic jam in the dense area. Most of the vehicles meet the difficult situation of parking, such as insufficient information, useless travel time. Following the rapid development of parking technologies such as Internet of Vehicles (IoT), telecommunications, and cloud computing services, the smart parking system is expected to become an important role for solving urban parking problems. This article chose Feng-Chia University as a demonstration field. Through the automatic vehicle identification (AVI) at the gates in the campus and the parking detection system (Infrared detection, geomagnetic detection) in the indoor parking lot and on street parking lot, the article proposed a method to analyze characteristics of parking and user attributes based on data collection, such as time of in-and-out vehicle, time interval of parking and number of parking demand and supply.*

This article aims at providing decision-maker with all-round parking management through the data collection of smart parking technology in order to make space more efficient use. Thus, this article analyzed the characteristic of parking based on data collection and data mining. Through the analysis results of research, in addition to clearly depicting the occupancy rate of each parking areas in the campus, it is also possible to observe the user attributes of the parking lots in each area, and further provide manager with diverse strategy for parking management.

Keywords: *Smart parking, Demand and supply analysis, Feng Chia University.*

I. INTRODUCTION

Motorized vehicles ownership has increased year by year, resulting in an increasingly serious imbalance between supply and demand of parking, causing parking problems and reducing the road service level. According to the statistics of the Ministry of Transportation and Communications (MOTC) in 2017, the number of cars has reached 7.9 million (about 340 cars per thousand people), especially the high car ownership in urban area. In addition to the high ownership of private motorized vehicles, the current situation of urban parking is still serious. Users need to spend a considerable fee to find a parking lot. Besides, the imbalance between supply and demand in parking spaces in the urban area is serious. Therefore, solving the parking problem is an important issue for the city government.

With the development of Internet of Things (IoT) technology and the construction of smart

cities, the topic of smart parking management has gradually become the hottest application in smart transportation systems in the past few years. Smart parking lots have sprung up in the country, and the application of various technologies has been dazzling. Following the increase of demand level, smart parking management has gradually grown into the hottest potential industry. Relevant operators have begun to try to cooperate with domestic manufacturers, and can introduce new technological elements and develop more smart parking market.

The parking guidance and information system (PGIS) is an important development project in the intelligent transportation system. Therefore, PGIS is also a model for parking management. From the user perspective, they often spent much time to find parking lots. When vehicles circumnavigate on the road, its would produce the traffic jam and illegal parking, even if the user needs to arrive at the parking lot entrance to confirm how much available parking lot it has. Thus, the accuracy of parking information is very important when the users not yet arrive the parking space.

This study focuses on smart parking management. After exploring the application of technology such as vehicle identification system and communication technology on the campus parking, the identification data collected by the detection equipment, such as e-Tag, automatic vehicle identification, is used to analyze the demand of parking users. The important topics of research aim at making a maximum benefit of parking management and analyzing the characteristics of parking users. The result of this research can provide a reference to help the campus to improve the overall parking management efficiency, and create a integration model of smart campus and parking management.

II. LITERATURE REVIEWS

This literature review can be divided into the definition of parking lot, parking behavior, parking supply and demand analysis, and parking operation management.

2.1. Definition of parking lot

The term “Parking lot” can divided into 2 types, such as outdoor parking lot and indoor parking lot. In addition, the outdoor parking lot can also divide into 2 types, like curbside parking lot and off-street parking lot. According to typology of space use, the parking lot can be defined as plane parking lot, mechanical parking lot, three-dimensional parking lot and mixed parking lot.

Chen (2010) pointed out that curbside parking can supplement an insufficient off-street parking lot, but it can also influence the road space distribution. It can be divided into 3 types according to the time interval of parking demand[10]:

(1) Short parking demand: parking time is about several minutes to one hour, such as temporary parking in the supermarket, short-distance visitors；

(2) Middle parking demand: parking time is about one hour to four hours, such as shopping malls；

(3) Long parking demand: parking time is usually more than four hours, such as long-term parking of work, leisure recreation parking, etc.

2.2. Driving behavior of parking

The driver's parking behavior is greatly affected by the parking facility and individual demand behavior. Thus, the study on relationship between parking supply and demand should be considered the availability of parking facilities and the parking supply conditions in different zones. Related research review is shown as following :

Adib Kanafani (1983) in his book "Transportation Demand Analysis" has proposed four factors related to user choice of parking facilities[1]: (1) walking distance between the destination and parking lot ; (2) parking operation time (including travel time and parking time) ; (3) Parking fee ; (4) Size of parking space. This, the walking distance is most important factor for the driver's parking choice behavior.

Tsai (1987) pointed out that the searching time of parking lot and walking time from parking lot to destination are complementary[15]. Thus, weighting these 2 time factors could be an useful evaluation index to estimate the level of service of parking.

Lu (1990) analyzed the characteristics of demand behaviors based on the impact of parking location. The research used several factors weighted such as parking fee, parking time, walking time, trip purpose, personal and vehicle attributions. The survey data (walking time, walking distance, satisfaction with parking facilities, parking fee etc.) made by different areas.

Chen (2010) mentioned that the allowable walking time was about 15 minutes, thus, the parking lot choice needs to consider this distance factor[10].

The choice behavior of parking type is greatly affected by the situation of parking supply. Therefore, Study on the relationship between the supply and demand of parking should be considered to ensure the supply of parking facilities and the impact of parking conditions in different areas. In recent years, the research on the parking demand has been oriented towards the disaggregate parking choice model.

2.3. Analysis of demand and supply

Lin (1986) made a detailed comparative analysis; including the nine modes of car growth mode, travel attraction mode, generation rate mode, multiple regression mode[9], traffic demand flow mode, land use parking demand mode, and multi-growth rate geometry mode.

Yu and Lincoln (1973) proposed a report “Parking Facility Layout: Level-of-Service Approach” to indicate the 5 design viewpoints for level of service of parking, such as convenience, economy, safety and comfort[6]. According to these 4 viewpoints, it can summarize the quantitative factors including "effective use rate, average parking time, accessibility, flow/capacity rate.

Wung and Kindra (1992) established an innovative method for estimating the trip generation rate caused by parking equipment in the study area, which is mainly divided into (1) parking

analysis and (2) traffic analysis (3) traffic impact analysis. In the aspect of parking analysis, it is first necessary to analyze the parking demand and supply in the study area. The parking demand is estimated by the trip generation manual. The parking supply is calculated by the existing parking equipment (plane parking, mechanical parking etc.).

Wang (2005) used the telephone survey and regression model to analyze the potential parking demand according to different trip purposes.

2.4. Technology application on smart parking

With the development of various technologies such as the Internet of Things (IoT), cloud computing, image recognition, and communication technology, the construction of smart parking focus only on the parking detection system (residual parking lot) and entrance vehicle detection (AVI, e-tag). The technology categories of smart parking can be divided into the following:

2.4.1. Parking lot navigation

The existing parking lot does not provide information of residual parking lot, so that car users need to spend a lot of time for searching available parking lot. Besides, car users also need to spend a time to find the car, because they forgot the exact location of vehicle. In order to solve this defect, the parking lot navigation (indoor and outdoor) can lead user to find a car by means of signal, CCTV, GIS etc., as shown in fig. 1.

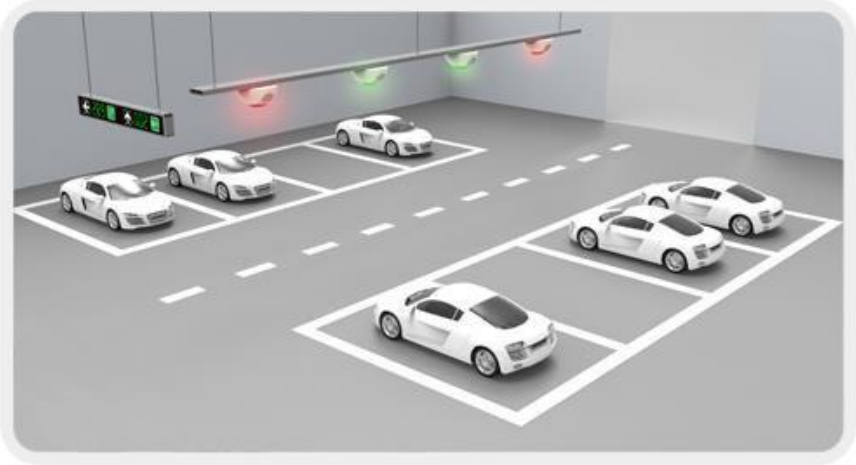

Fig. 1. *Parking detection system Source : http://www.akeparking.com/*

2.4.2. Vehicle detection system

Traditionally, parking lots are often equipped with fences or guard at the entrances and exits to manage the parking charges. However, this traditional system does not know the real-time situation of parking lot, such as the available parking lot location, total residual parking lot etc. In recent year, the vehicle detection technology progresses quite fast and vast, in which the main technologies of smart parking including image recognition, indoor positioning based on wireless communication technologies such as Bluetooth and Wi-Fi.

2.4.3. Payment system

The existing parking lot may be charged manually, and sets up a semi-automatic charging

process such as a fence, a vending machine, a ticket reader, and an electronic ticket at the in-and-out gates. Regardless of the above-mentioned, it is necessary to stop a car in front of gate and read a e-card, wait for exiting. In the future, the parking lot charge may be automatically deducted through automatic vehicle identification (AVI), RFID authentication, wireless communication technology and electronic payment system in order to simplify and speed up the process of smart parking.

2.4.4. Information distribution and reservation system

For driver in urban areas, the biggest problem of parking is how to find an available parking lot in the peak hour. Thus, most drivers always obtained the information of residual parking lot when they arrived at parking lot. To improve this problem, it can introduce into following technologies.

(1) Parking Information Sharing (PIS)；

(2) Buffered Parking Information Sharing (BPIS)；

(3) Reservation-based Smart Parking System (RSPS)。

III. CASE STUDY ON CAMPUS OF FENG-CHIA UNIVERSITY

This study chose the Feng-Chia University as a demonstration field. Because the University is closed to the Feng-Chia business district, it is first night market in Taiwan. According to the research report, the Feng-Chia business district is crowded. The number of people on weekdays is about 20,000 tourists or so, and the average number of holidays is about 70,000 tourists. The survey results show that there are 97.2% tourists of Feng-Chia business district using the smart phones. As well as, there are 80% respondents who care about the information of parking location and real-time available parking lot. In addition, Feng-Chia University has more than 20000 students and staffs who live in this area.

The distribution of parking space in Feng-Chia University is shown in Fig. 2. There are four types of campus parking lots: outdoor parking lot, indoor parking lot, plane parking lot, and mechanical parking lot. There are about 800 parking lot (for car) in Feng-Chia University. Vehicle access management must be checked by guards in the past. Although, the guards can control the vehicles in and out, they cannot clearly know the real time residual parking lots in the campus.

When car users enter the campus to find an available parking lot, they first choose the nearest destination. From the management viewpoint, it is possible to increase the useless travel time and illegal parking phenomena in the campus, if users cannot promptly get the information of available parking lot.

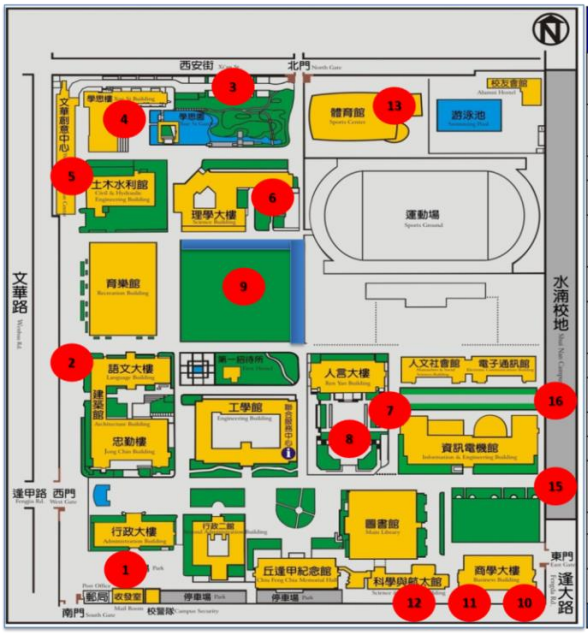

No.	Parking Areas	Normal Space	Accessible Space
1	Administration Bldg. southwest side	66	1
2	Jong-Chin Bldg. and Recreation Bldg. west side	68	1
3	Xue Si Bldg.(plane)	44	-
4	Xue Si Bldg. (underground B1)	53	-
5	Wenhwa Innovation Center (B1)	37	1
6	Science Bldg. north side	2	2
7	Information/Electrical Eng. Bldg. northwest side	3	2
8	Ren-Yan Bldg. B2	68	1
9	Lawn east and north side	28	-
10	Business Bldg.B2	42	1
11	Business Bldg.B3	81	-
12	Science and Aeronautical Eng. Bldg.B2	24	-
13	Sports Center B2	113	3
15	East Gate Parking Lot (1)	80	-
16	East Gate Parking Lot (2)	191	-
	Total	900	12

Figure 2. *Distribution of parking lot in Feng-Chia University*

The Feng-Chia University constructed smart parking devices in 2017, which is located at 3 gates in the campus. It used the automatic vehicle identification (AVI) and parking lot detection system. Using the real-time data from parking detection device can provide us to analyze the supply and demand of parking, and understand well the occupancy rate of parking, illegal parking and reserved parking lot. The analysis result of demand and supply of parking could give us a feedback for reasonable parking space planning and improvement of parking lot distribution and parking fee in order to increase the use rate of parking lot in the campus.

This study explores the characteristics of parking lots based on different times. Through technology of smart parking device, it can explore the imbalance between parking demand and supply (parking lots) based the number of staff and students in the campus and Feng-Chia business district.

After the analysis of parking data, it can improve the imbalance between demand and supply of parking in the campus according to time interval and user attribution, such as different parking fee, quota hour parking management, reserved parking zone and E-parking pass, see Fig. 3, in order to improve the efficiency of parking management in the campus.

Figure 3. *Future development direction for camp parking*

3.1. Parking data and analysis method

This study explores the occupancy rate of parking and in and out record of vehicles through the data collected by parking detection system and automatic vehicle identification. Using the AVI data at 3 gates (West, north and East) in the campus can estimate the in and out number of vehicles, entry/exit time of vehicles. The information on attribution and use time can help us to understand the difference between demand and supply for parking in the campus.

The research process needs to first determine the research scope of Feng-Chia University and the necessary information of parking. The survey object is automobile (including general car, van, trucks and special vehicles, such as disability car). During the study period, it needs to record entry time and exit time of vehicles and collects the total parking lots and real-time residual parking lots.

Analysis of the number of parking aims at using the rate of demand and supply (D/S) and level of service of parking to explore the changes of parking lots and users attribution.

1. Parking demand and supply ratio: parking demand (a) divided by parking supply (b), can reflect the proportion of parking number to total parking lots, such as eq. (1).

$$\frac{\mathrm{D}}{\mathrm{S}}\ \mathrm{rate} = \frac{\mathrm{(a)Parkingdemand}}{\mathrm{(b)\ Parking\ Supply}} \qquad (1)$$

2. Parking level of service: The parking level of service can be divided into A, B, C, D, E and F grades (see table 1).

Table 1. *Level of service based on demand and supply of parking*

Level of Service	Demand/Supply	Description
A	< 0.50	Good condition of parking
B	0.50~0.75	Normal condition of parking (a few travel time on searching parking lot)
C	0.75~1.00	Near saturated condition of parking (Tolerable travel time on searching parking lot)
D	1.00~1.25	Saturated condition of parking (Minimum tolerance travel time on searching parking lot)
E	1.25~1.5	Serious saturated condition of parking
F	> 1.5	Unbearable condition of parking

3. Occupancy rate of parking on peak hour: it is possible to understand the level of service of parking during the peak hour in the campus, see eq. (2).

$$\frac{\mathrm{D}}{\mathrm{S}}\mathrm{in\ peak\ hour} = \frac{\mathrm{Demand\ in\ peak\ hour}}{\mathrm{Supply(Parking\ lots)}} \qquad (2)$$

4. Number of parking car during the peak hour: understanding the real-time number of vehicles during the peak jour in the campus.

The model of this study focuses on the efficiency of parking use. This analysis model can immediately estimate the efficiency of parking use according to real-time data from smart parking devices. The analysis result can provide useful information for decision maker to improve the level of service of parking and increase the benefit of parking operation.

The installation of smart parking device, such as AVI, at 3 gates in the campus can collect entry and exit data of vehicles. Though these data from AVI, it can provide data quantification of

parking based on different ethnic groups, time interval and zones. To understand the correlation between demand variables and supply constraint, it can explore the characteristics of parking users according to the different time and space, as shown in fig. 4.

By means of the analysis result of research, it can know well the characteristic of users, such as teachers, students, staff and visitors. According to the level of service of parking, it can provide decision maker to make different strategies of parking for different type of activities. In addition, all parking data can store in the cloud database and offer a reference for managers to establish the operation plan, parking fee, manpower plan etc.

Relation Matrix				
	Period	Group	Area	Frequency
Period		1	2	3
Group	1		4	5
Area	2	4		6
Frequency	3	5	6	

	Correlation Analysis
1	Parking group on peak and off-peak period
2	Parking area on peak and off-peak period
3	Parking number on peak and off-peak period
4	Group distribution in each parking area
5	Parking number distribution by each group
6	Parking number in each parking area

Figure 4. *Relationship diagram of parking characteristics*

IV. ANALYSIS RESULT OF PARKING DEMAND AND SUPPLY

Through the parking lot detection system, this analysis result shows that average residual parking lot is 50 to 70 for the peak hour (from 09:00 to 18:00) in the weekday and 100 to 200 for the off-peak hour (from 19:00 to 21:00). In addition, average residual parking lot is 80 to 100 for the peak hour (from 10:00 to 18:00) in the weekend and 150 to 200 for off-peak (from 19:00 to 21:00) in the weekend. The average overnight parking on campus is about 40 cars (about 2 %).

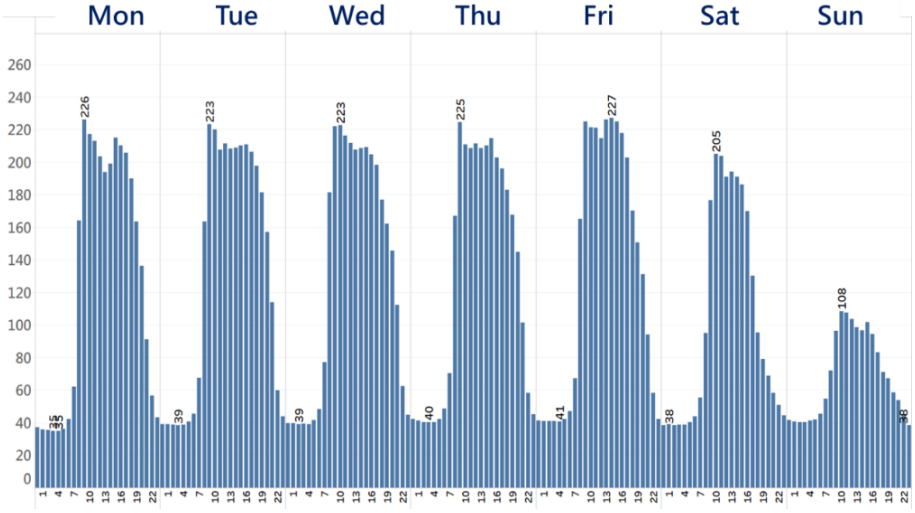

Figure 5. *Hour parking number weekly in the campus*

From the data analysis, see, it can be known that the occupancy rate of parking lots in the campus is about 47% in the weekday, and the average parking time is about 5 hours. However, the occupancy rate of parking lots in the campus is about 24% in the weekend, and the average parking time is about 4 hours. In other words, there is still considerable to improve the use rate of parking lot during many time intervals in the campus.

Table 2. *Occupancy rate of plane parking lot in the campus*

		Parking Space Usage Rate						
Area	Space	Mon	Tue	Wed	Thu	Fri	Sat	Sun
Administration Bldg.	82	37.16%	43.69%	43.10%	41.97%	39.78%	30.31%	9.87%
Jong-Chin And Recreation Bldg.	68	49.05%	49.90%	54.02%	52.89%	52.67%	43.01%	23.28%
Information/Electrical Eng. And Humanities/Social Sciences Bldg.	97	45.77%	51.63%	50.86%	52.03%	49.09%	36.50%	16.42%
Xuesi Bldg.	30	31.75%	36.97%	35.08%	34.50%	25.84%	22.58%	8.26%
All Areas	277	42.51%	47.27%	47.63%	47.36%	44.70%	34.76%	15.28%

Table 3. *Average plane parking time in the campus*

		Average Parking Delay(hour)						
Area	Space	Mon	Tue	Wed	Thu	Fri	Sat	Sun
Administration Bldg.	82	5.23	5.54	5.48	5.61	5.26	5.52	4.63
Jong-Chin And Recreation Bldg.	68	4.42	4.51	4.44	4.45	3.86	3.63	2.52
Information/Electrical Eng. And Humanities/Social Sciences Bldg.	97	4.82	4.96	4.78	5.14	4.45	5.04	3.66
Xuesi Bldg.	30	4.23	4.41	4.11	4.10	3.62	4.46	3.01
All Areas	277	4.74	4.92	4.78	4.94	4.37	4.56	3.20

In addition, the time-of-use analysis of occupancy rate for the plane parking space in the administrative building southwest side parking lot shows that the high occupancy period is mainly from 09:00 to 16:00, and the use rate of parking lot is high as 80%, see table 4.

Table 4. *Use-of-time analysis of occupancy rate for plane parking lot*

	00:00	01:00	02:00	03:00	04:00	05:00	06:00	07:00
Mon	4.09%	3.64%	2.98%	2.82%	2.62%	3.07%	4.69%	8.80%
Tue	4.01%	3.56%	2.62%	2.74%	2.63%	2.95%	4.83%	11.78%
Wed	4.62%	3.04%	2.45%	2.56%	2.45%	3.05%	4.58%	12.84%
Thu	4.07%	3.31%	2.58%	2.19%	2.29%	2.90%	5.16%	11.03%
Fri	3.51%	2.75%	2.38%	2.49%	2.54%	2.99%	4.94%	10.20%
Sat	11.59%	12.45%	12.36%	12.17%	12.18%	12.45%	13.76%	15.93%
Sun	2.99%	2.45%	1.75%	1.51%	1.85%	1.94%	3.96%	6.67%
	08:00	09:00	10:00	11:00	12:00	13:00	14:00	15:00
Mon	43.50%	69.71%	72.33%	71.83%	67.26%	70.07%	72.39%	74.63%
Tue	52.98%	82.34%	84.30%	83.36%	81.66%	84.42%	85.81%	85.77%
Wed	55.24%	80.57%	82.64%	82.72%	81.41%	83.68%	84.91%	85.35%
Thu	50.01%	80.58%	82.57%	82.31%	81.60%	83.79%	85.14%	85.72%
Fri	47.97%	79.18%	80.93%	81.89%	77.09%	81.20%	82.92%	82.55%
Sat	27.70%	54.87%	65.13%	65.51%	63.18%	63.23%	63.03%	61.68%
Sun	9.72%	16.00%	18.20%	16.67%	16.34%	16.19%	16.66%	17.31%
	16:00	17:00	18:00	19:00	20:00	21:00	22:00	23:00
Mon	73.69%	68.09%	54.81%	47.94%	38.90%	22.07%	11.33%	6.00%
Tue	85.07%	78.03%	66.19%	58.95%	49.30%	26.83%	8.87%	4.73%
Wed	84.23%	74.22%	55.07%	54.87%	47.99%	32.57%	12.62%	6.92%
Thu	82.30%	73.59%	57.14%	50.28%	40.84%	26.31%	10.30%	6.46%
Fri	79.43%	71.36%	48.77%	41.23%	34.17%	22.89%	11.35%	5.35%
Sat	52.01%	38.53%	22.34%	15.82%	12.63%	9.85%	7.37%	6.21%
Sun	16.97%	15.89%	14.03%	12.10%	9.91%	9.01%	6.52%	4.58%

4.1. Characteristics of parking users

This study collected the entry and exit data through automatic vehicle identification in west gate, north gate and east gate. By reading the data from CCTV for in and out vehicles, the number of in and out vehicles were counted every 15 minutes, and compiled statistics the in and out vehicle number based on the time interval (peak and off-peak hour).

According to the analysis of semi-annual data, the proportion of parking use for visitors is about 60 % in the weekday, and the number of staff and students is about 40% in the weekday. In addition, the proportion of parking use for visitors is about 70% in the weekend, and the number of faculty and students on campus is about 30%. According to the data, the average number of parking hours for staff is about 5 to 9 hours, and the average number of parking hours for visitors is about 1 to 6 hours.

Table 5. *Attribution analysis of parking use in the campus*

	Day	Day	Day	Day	Day	Day	Day	Day
Groups	Mon	Tue	Wed	Thu	Fri	Sat	Sun	Total
Visitor	61.47%	61.89%	62.42%	62.45%	63.66%	72.86%	73.60%	64.60%
Office Staff	16.84%	16.12%	15.59%	15.74%	16.39%	8.82%	9.28%	14.66%
Professor	15.48%	15.98%	16.11%	15.78%	14.27%	9.28%	10.80%	14.35%
Retired professor	1.68%	1.41%	1.39%	1.44%	1.27%	0.96%	1.14%	1.35%
Office Staff	0.01%	0.04%	0.00%	0.02%	0.00%	0.01%		0.01%
Student (Ph. D.)	0.89%	0.84%	0.87%	1.00%	0.95%	1.01%	0.72%	0.91%
Student(Bachelor)	1.30%	1.56%	1.48%	1.44%	1.29%	2.49%	1.69%	1.58%
Student (Master)	0.84%	0.83%	0.68%	0.82%	0.75%	3.71%	1.66%	1.23%
Firm	1.48%	1.32%	1.45%	1.29%	1.40%	0.85%	1.09%	1.29%
Gym Member	0.01%	0.02%	0.01%	0.01%	0.01%	0.00%	0.02%	0.01%
Total	100.00%	100.00%	100.00%	100.00%	100.00%	100.00%	100.00%	100.00%

V. CONCLUSION

This study explores the information of user attribution and vehicle in-and-out in order to understand the occupancy rate in the peak hour and off-peak hour in the Feng-Chia University. When the occupancy rate of parking in the campus is low at night and in the weekend, the residual parking lots can be opened to public in order to reach the sustainable financial development.

The parking lot in the campus can satisfy the demands of staff and students, but there are still residual 50 to 100 parking lots. There is still a lot of demand for payment parking lots during the daytime. Outside visitors have too many vehicles which take up more 60% parking lots in the campus. Therefore, it could be considerable to charge a parking fee in the future in order to increase the turnover rate of parking in the campus.

Parking difficulties are common traffic problems in the popular business districts. Users are concerned about the real-time information of available parking lot, if the parking fee is reasonable. Thus, this study aims at improving parking service through smart technology, which effectively control vehicles based on smart technology devices, to provide various parking users based on time and area in order to increase the use rate of parking lots.

Smart parking system can improve traffic congestion at the entrance of parking lots. The smart parking solution in the business district changes the habits of users and managers, enhances the parking information service function, and introduces the service mechanism of the smart business

district to provide users with parking discounts or store coupons. This service could provide mutually beneficial sharing services and attract consumers to increase the expenditure force in the Feng-Chia business district.

References

[1]. Adib Kanafani (1992) Transportation Demand Analysis

[2]. The authority board (2009) on-street parking management and pricing study

[3]. Washington Metropolitan Area Transit Authority (2009) feasibility study of real time parking information at metrorail parking facilities (virginia stations)

[4]. Adib Kanafani (1983) Transportation Demand Analysis, (McGraw-Hill series in transportation

[5]. Erik Verhoef, Peter Nijkamp, Piet Rietveld (1995) "The Economic of Regulatory Parking Polices: The (Im)possibles of Parking Polices In Traffic Regulation" Transportation Res.-A, Vol, 29A, No.2, pp. 141-156

[6]. Jason C. Yu and Alexander R. Lincoln (1973) Parking Facility Layout: Level-of-Service Approach, ASCE Journal of Transportation Engineer, Vol. 99.

[7]. 黃進明 (1997)，路外停車場區為之研究-以台中市市中心區為例

[8]. 交通部統計網 (2017)，自用小客車數量變動概況

[9]. 交通部運研所 (1986)，停車場規劃手冊

[10]. 陳惠國、邱裕鈞、朱致遠 (2010)，交通工程

[11]. 李天翔、包蒼龍 (2010)，以影像辨識為基礎之停車場車位管理之研究

[12]. 張家榕、蔡玫亭 (2011)，停車場預約機制的設計與模擬

[13]. 陽益 (1982)，市中心區停車延時管制最適化之研究

[14]. 葉祖宏 (1993)，陳述性偏好法在個體停車選擇行為之研究

[15]. 蔡輝昇 (1987)，台北市停車問題改善方案之研究

[16]. 林振揚 (1992)，公共路外停車場績效評估之研究

[17]. 胡宇載 (1983)，台北市停車特性與土地使用之關係

[18]. 徐慶文 (1994)，路外停車場區位之研究

[19]. 黃仲誼 (2004)，智慧型停車場管理系統

[20]. 陳俊毓、洪稱營、郭朝雲 (2001)，自動停車場管理系統設計與探討

[21]. 吳韋翰 (2004)，影像辨識在停車場監控之應用與設計

METHODS FOR DETERMINING VEHICLE TRAJECTORY BASED ON MOTION MODEL

TRAN VAN LOI[1], NGUYEN VAN BINH[2]
[1]Mechanical Engineering Section, [2]Electrical and Electronic Engineering Section,
University of Transport and Communications, Campus in Ho Chi Minh City, Ho Chi Minh City, Vietnam.
Corresponding author's email: tvloi@utc2.edu.vn

Abstract: *The autopilot system is a combination of two main programs: determining the desired trajectory and the actual trajectory of the automobile. The desired trajectory of the automobile is built by the GPS system, the laser scanner, the radar sensor, the position sensor, the camera... The actual trajectory of the automobile is obtained by the throttle by wire, brake by wire and steer by wire. The main content in this paper is about the method of determining the actual trajectory of the automobile using the automatic steering system.*

Keywords: *Steer By Wire, autopilot, self-driving cars.*

I. INTRODUCTION

The automatic steering system is the main research direction in today's automobile. According to the SAE 2014 standard, the automatic steering system is classified into two categories: the driver's driving environment, the driving environment. The highest level in autopilot allows vehicles to perform all driving functions and monitor road conditions when traveling. In order to study the driving dynamics, it is necessary to study the combination of various technologies (Figure 1): driving motion trajectory, vehicle movement trajectory, information network Intelligent traffic signals connected to cars, the ability to connect information between vehicles involved in traffic,...

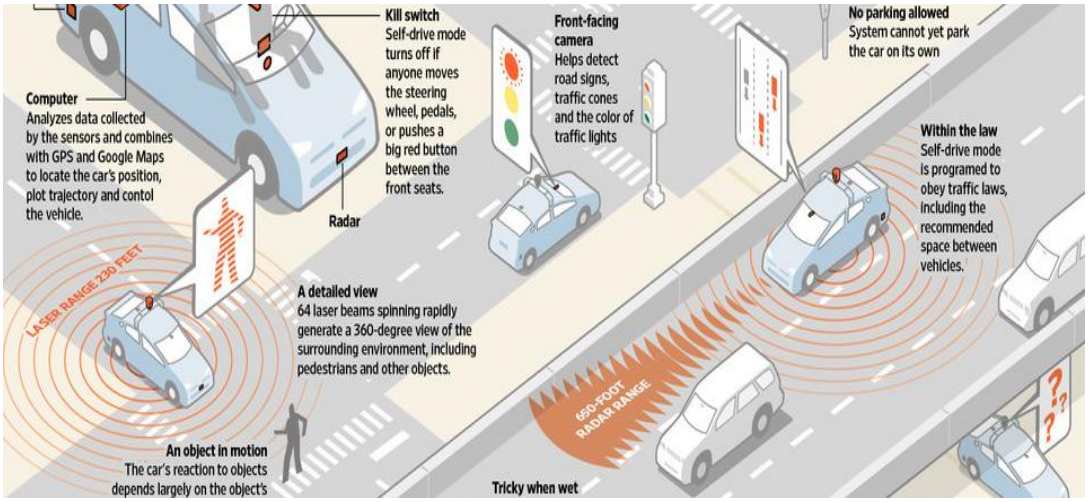

Figure 1*. Google's intelligent traffic description system*

In particular, the motion trajectory of the car can be determined by GPS, laser scanner, radar sensor, position sensor, camera... The actual trajectory of the automobile is determined by the throttle by wire, brake by wire and steer by wire.

II. MODEL AND TRAJECTORY DETERMINATION

2.1. Steer system model

The autopilot system consists of the desired trajectory systems and the actual trajectory system (including electric drive system, electric system, electric braking system). The system determines the desired orbit of the system: GPS, laser scanner, radar sensor, position sensor, camera and computer control. The electric drive system is a component system in the autopilot. The electric drive system consists of three main components: the signal generator, the control unit and the actuator (Figure 2).

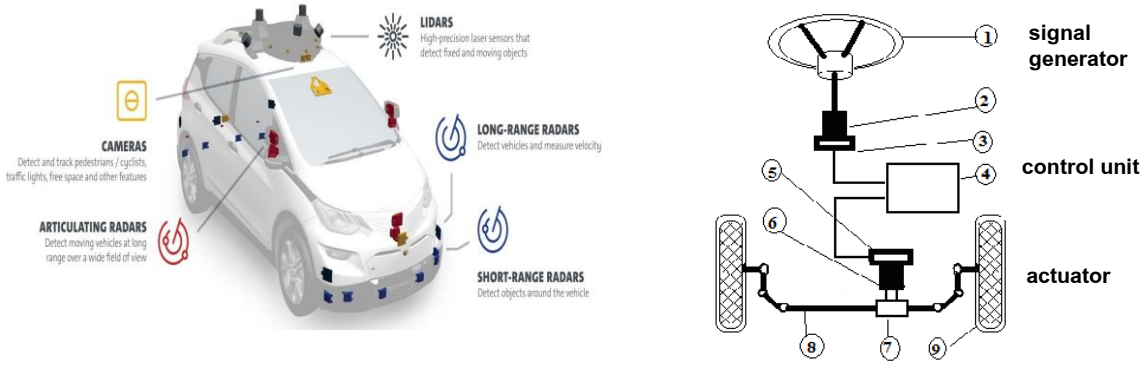

Figure 2. *Autopilot system*
1-Steering wheel; 2-Generating sensory motor; 3-Moment sensor of sensitivity and steering shaft speed; 4-Controlling unit; 5- Sensor of moment and steering shaft speed; 6-Motor controlling rotation; 7-Rack and pinion; 8-rack; 9- wheel.

The controller includes steering wheel, steering shaft and DC motor. Steering wheel has an inertial moment J_s that is affected by steering moment, shifting angle θ_d. The steering shaft has friction coefficient K_{ss}, torsional rigidity C_s, shifting angle θ_1. DC motor has an inertial moment of J_{e1}, a steering sensitivity moment τ_1 (Figure 3).

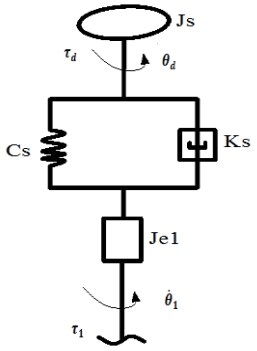

Figure 3. *Mechanical model of the steering part*

By ignoring the effects of the gaps in the components, the above steering-wheel mathematical model is represented by the equations:

$$\begin{cases} J_s.\ddot{\theta}_d = \tau_d - C_s\left(\theta_d - \theta_1\right) - K_s\left(\dot{\theta}_d - \dot{\theta}_1\right) \\ J_{e1}.\ddot{\theta}_1 = C_s\left(\theta_d - \theta_1\right) + K_s\left(\dot{\theta}_d - \dot{\theta}_1\right) - \tau_1 \end{cases} \quad (1)$$

The above equations are rewritten in equation 2.

$$\begin{bmatrix} J_s & 0 \\ 0 & J_{e1} \end{bmatrix}.\begin{bmatrix} \ddot{\theta}_d \\ \ddot{\theta}_1 \end{bmatrix}+\begin{bmatrix} K_s & -K_s \\ -K_s & K_s \end{bmatrix}.\begin{bmatrix} \dot{\theta}_d \\ \dot{\theta}_1 \end{bmatrix}+\begin{bmatrix} C_s & -C_s \\ -C_s & C_s \end{bmatrix}.\begin{bmatrix} \theta_d \\ \theta_1 \end{bmatrix}=\begin{bmatrix} \tau_d \\ -\tau_1 \end{bmatrix} \quad (2)$$

The executive unit is analyzed as Figure 4. In the above model, DC motor has the main function of providing the moment τ_M that replaces the steering torque. DC motor has inertia moment J_0, which is connected to the steering part via a shaft with torsional rigidity C_0 and displacement with the damping factor K_0. The steering part is a toothed rack structure, with r_p being the distance between the rack center and the gearing point. The rack has a mass m, hardness C_1, displacement with the damping factor K_1.

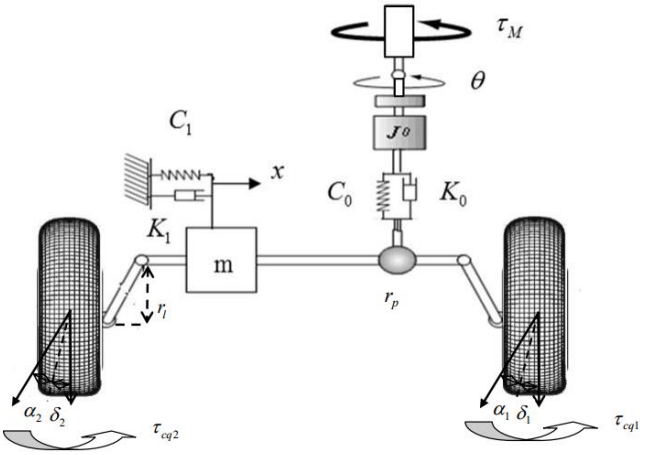

Figure 4. *Executive unit model of Steer by Wire*

The distance between the rack and the wheel shaft is r_l, where the wheels have inertia moment J_{bx}. Under the assumption that the two directional wheels that have the rigidity, the angle of rotation and the damping coefficient are replaced by a wheel with the rigidity C_2, the damping coefficient K_2, the average angle of rotation of directional wheel $\delta = (\delta_1 + \delta_2)/2$, the average deformation angle of directional wheel $\alpha = (\alpha_1 + \alpha_2)/2$.

The resistance torque on the rotation of directional wheel includes the resistance torque at the right wheel and the left wheel. When the car turns round, the tire deformation causes a partial slip that creates a resistance torque on the rotation due to the influence of the horizontal force acting on the chassis F_y.

The value of this torque is not large enough to cause the vehicle to rotate, but this is the main resistance torque in the steering process that can be considered as a resistance torque on the rotation. The resistance torque on the rotation at the directional wheel is determined by

$$\tau_{cq} = \tau_{cq1} + \tau_{cq2} \approx M_z = (l_c + l_p).F_y = C_2.(l_c + l_p).\alpha\,. \quad (3)$$

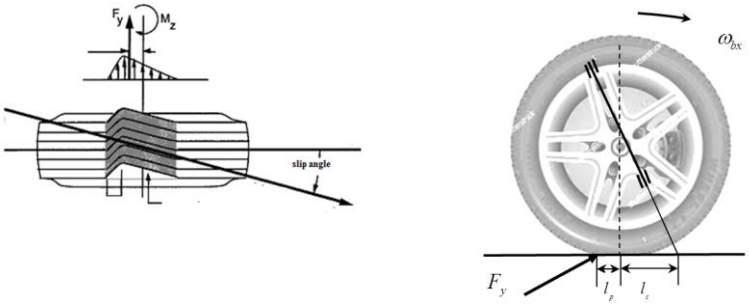

Figure 5*. Diagram of identifying resistance torque on the rotation*

In which, l_c, l_p are the distances determined by wheel angle and tire pressure. The mathematical model of the executive unit is represented by the differential equation (4).

$$\begin{cases} J_0\ddot{\theta} = \tau_M - K_o(\dot{\theta} - \frac{\dot{x}}{r_p}) - C_o(\theta - \frac{x}{r_p}) \\ m.\ddot{x} = \left[K_o(\dot{\theta} - \frac{\dot{x}}{r_p}) + C_o(\theta - \frac{x}{r_p})\right]\frac{1}{r_p} - C_1(x - \delta.r_l) - K_1(\dot{x} - \dot{\delta}.r_l) \\ J_{bx}\ddot{\delta} = \left[C_1(x - \delta.r_l) + K_1(\dot{x} - \dot{\delta}.r_l)\right]r_l - C_2.(l_c + l_p).\alpha \end{cases} \quad (4)$$

Basing on the equations of the steering system that is analyzed above, we can examine the state of system controlling, test different controllers, compare the controlling quality, simulate the working status of the system in different experimental conditions.

2.2. Establishing the model of surveying of automobile movement

The Steer by Wire is one of the integrated mechatronic systems, so the survey model should be described with the important dynamics of the automobile such as wheel dynamics, rotation dynamics, straight-movement dynamics, automobile vibration and electromechanical components. The model above is divided into five components linked together as: control signal, steering wheel dynamics, electronic parts, steering system controller, executive unit and vehicle dynamics (Figure 6).

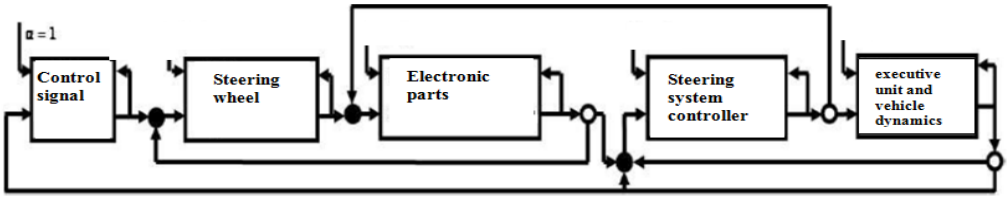

***Figure 6**. Establishing the model of surveying of automobile*

Figure 7 illustrates the two-track automobile model that studies the deviated movement of automobile in the general case of being affected by the horizontal wind force F_{wy} and the air resistance F_{wx}. It is assumption that the static load that is distributed symmetrically in the direction of the motion of the vehicle, the speed of motion is a constant, the road surface is flat, the structure parameters of the suspension affect the movement negligibly.

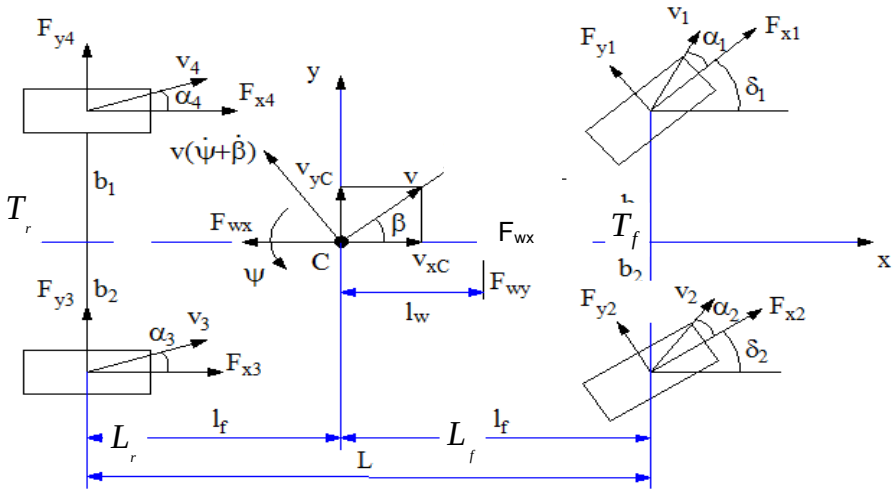

***Figure 7**. The motion model of the car on the plane of the road*

The symbols in the figure are explained as follows:

C The center of the automobile

δ_i Rotation angle of wheel $\left(\delta_1, \delta_2 \neq 0,\ \delta_3, \delta_4 = 0\right)$

αi Deviated angle of the ith wheel i (i = 1 ÷ 4)

ψ Angle of rotation of the vehicle chassis around the vertical axis through the center

β Deviated angle between vehicle chassis and movement direction

v The velocity of car.

v_{xc} , v_{yc} The components of the velocity of car in centralised coordinates

v_i The velocity of the ith wheel (i = 1÷ 4)

F_{yi} Horizontal force between the road and the ith wheel (i = 1÷ 4)

F_{xi} Vertical force affecting ith wheel (i = 1÷ 4)

F_{wx} Air force $F_{wx} = 0,5.C_w.A.\rho_w.v_x^2,$ in which C_w is the air resistance coefficient, ρ_w is the density of air, and A is the resistance area of the car

F_{wy} Horizontal wind force effecting on car

T_f , T_r The distance between the centers of the front and rear wheels

L_f, L_r The distance between the center and of the centers of front and rear wheels

Vehicle motion dynamics in orbit can be described by three parameters: the vehicle velocity v_x, the horizontal velocity v_y and the rotational angle of the vehicle body $\dot{\psi}$ that characterizes the deviated movement of the vehicle. The balanced equation of force in the road coordinates I (x_I, y_I) is:

$$m\frac{d}{dt}\begin{bmatrix} v_{Ix} \\ v_{Iy} \end{bmatrix} = \begin{bmatrix} F_{Ix} \\ F_{Iy} \end{bmatrix} = \boldsymbol{f_I} \qquad (5)$$

where

m The mass of car including mass of the wheels.

v_{Ix} , v_{Iy} The components of the velocity of car in road coordinate.

$\boldsymbol{f_I}$ External force vector affecting the car.

F_{Ix} , F_{Iy} The partial forces in road coordinate.

The relationship between the vertical and horizontal forces affecting on the wheels from the road is shown in Figure 8.

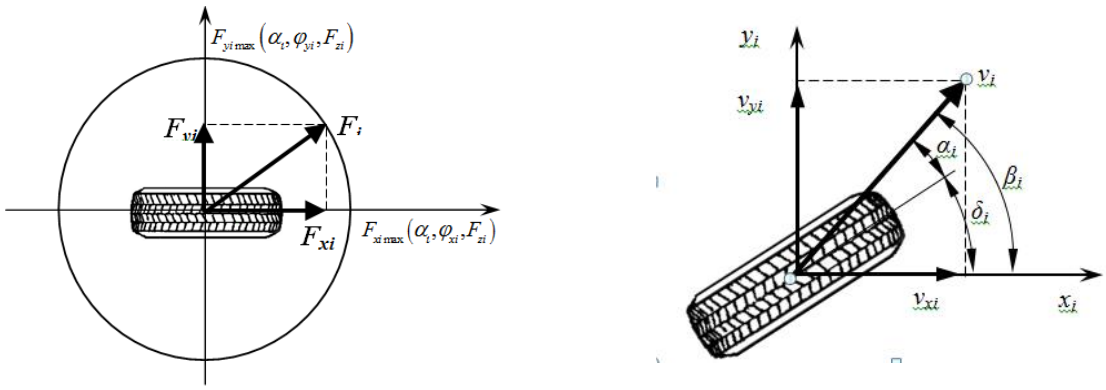

Figure 8. *Force components affecting on the wheel*

The longitudinal forces vary according to the state of motion, the maximum value that can be transmitted down the road is limited by the clinging coefficient $\boldsymbol{\varphi_{xi}}$ and the vertical load F_{zi} following the Equation (5)

$$F_{xi\max} = \varphi_{xi\max} F_{zi} \tag{6}$$

Assuming that the lateral deviation angle of the tire is small, the horizontal reacting force from the road that affects on the wheels has the linear relationship with the lateral deviation angle as follows:

$$F_{yi} = C_{\alpha i}\ \alpha_i \tag{7}$$

Then, equation (4) that describes the deviation motion is rewritten as follows:

$$\begin{cases} \dot{v}_x = \left(\dot{\psi} + \dot{\beta}\right) v_y + \dfrac{1}{m}\left[\sum_{i=1}^{4}\left(F_{xi}\cos\delta_i - F_{yi}\sin\delta_i\right) - F_{wx}\right] \\ \dot{v}_y = -\left(\dot{\psi} + \dot{\beta}\right) v_x + \dfrac{1}{m}\left[\sum_{i=1}^{4}\left(F_{xi}\sin\delta_i + F_{yi}\cos\delta_i\right) + F_{wy}\right] \end{cases} \tag{8}$$

The deviation angle of the vehicle chassis β is determined by the formula:

$$\tan\beta = \frac{v_y}{v_x} \tag{9}$$

The moment equation for gravity center of vehicle is written as follows:

$$\begin{aligned} J_z\ddot{\psi} &= \sum_{i=1}^{4}\left(\begin{bmatrix} -r_{yi} & r_{xi} \end{bmatrix}\begin{bmatrix} F_{xi} \\ F_{yi} \end{bmatrix}\right) \\ &= \sum_{i=1}^{4}\left[r_{yi}\left(F_{yi}\sin\delta_i - F_{xi}\cos\delta_i\right) + r_{xi}\left(F_{yi}\cos\delta_i + F_{xi}\sin\delta_i\right) + l_w.F_{wy} \right] \end{aligned} \tag{10}$$

In which, J_z is the inertia moment of the automobile mass in the Z axis, $\boldsymbol{r_{xi}}$ and $\boldsymbol{r_{yi}}$ are the coordinates of the wheel in the motion reference attached to the automobile center. Synthetic equations into the equations describing the motion orbit of an automobile:

$$\begin{cases} \dot{v}_x = \left(\dot{\psi}+\dot{\beta}\right)v_y + \dfrac{1}{m}\left[\sum_{i=1}^{4}\left(F_{xi}\cos\delta_i - F_{yi}\sin\delta_i\right) - F_{wx}\right] \\ \dot{v}_y = -\left(\dot{\psi}+\dot{\beta}\right)v_x + \dfrac{1}{m}\left[\sum_{i=1}^{4}\left(F_{xi}\sin\delta_i + F_{yi}\cos\delta_i\right) + F_{wy}\right] \\ \ddot{\psi} = \dfrac{1}{J_z}\left\{\sum_{i=1}^{4}\left[r_{yi}\left(F_{yi}\sin\delta_i - F_{xi}\cos\delta_i\right) + r_{xi}\left(F_{yi}\cos\delta_i + F_{xi}\sin\delta_i\right)\right] + l_w.F_{wy}\right\} \end{cases} \quad (11)$$

2.3. Surveying the vehicle using Steer by Wire through DLC changing lane experiment

The results of the study on the real model combined with driving conditions and velocity are used in the general model for the studying and evaluating the steering system standards according to international standards to the quality of Steer by Wire.

In the contents of the paper, Fuzzy-PID controller is used to find the appropriate controller for the steering system (steering wheel controller and executive unit controller). The main controller programmed in the steering system controlling program includes: steering wheel controller and executive unit controller. The controlling diagram for the Steer by Wire in the paper is shown in Figure 9.

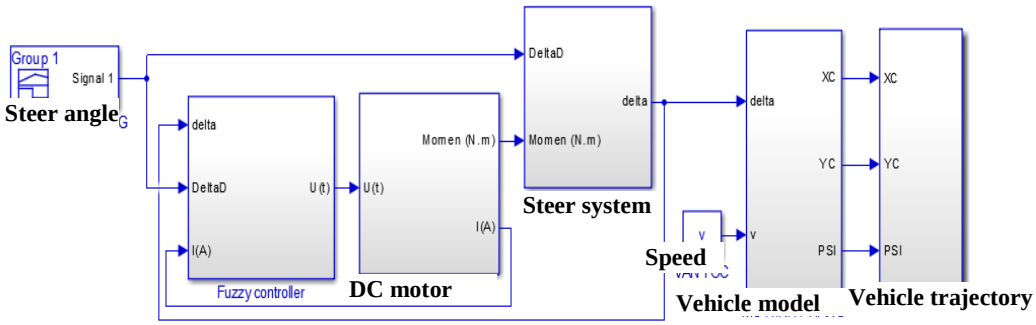

Figure 9. *The program of simulating the vehicle trajectory using Steer by Wire when conducting the experiment of DLC changing lane*

Steering angle signal is shown in Figure 10:

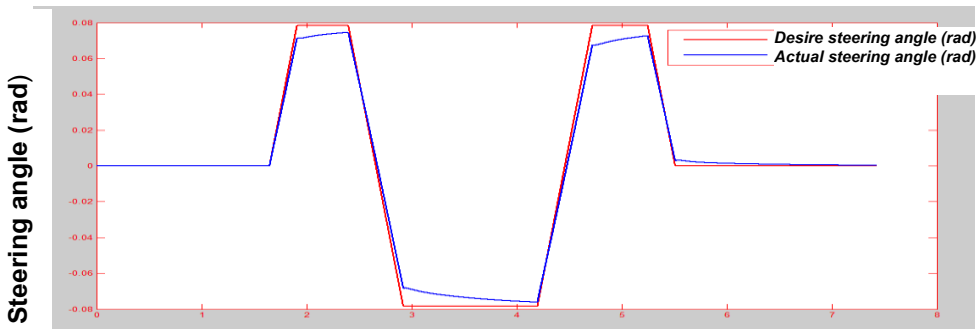

Figure 10. *Steering angle*

Result of determining the vehicle trajectory based on motion model is shown in Figure 11.

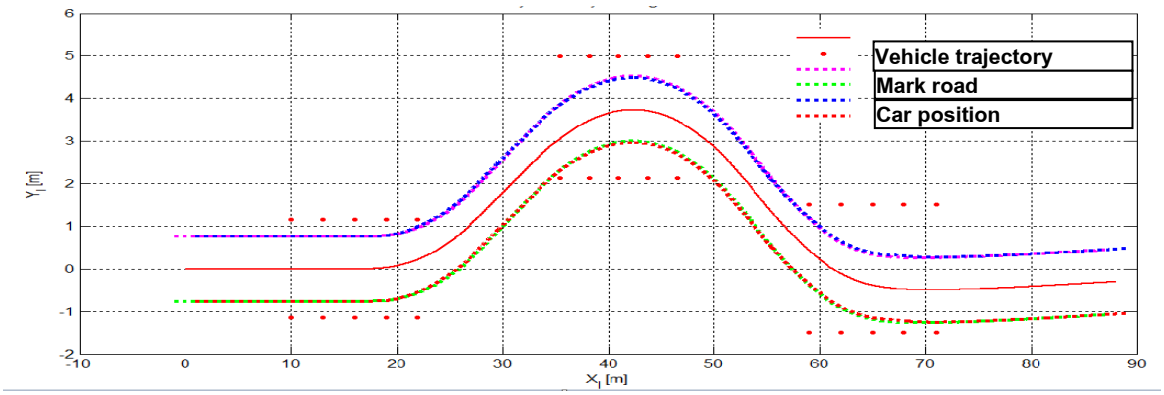

Figure 11: *The result of simulating the vehicle trajectory 60km/h*

III. CONCLUSION

The results of the automotive revolving survey using the electric drive system in the DLC test according to international standards show that the electric drive study system meets the requirements set in motion at a speed 60 km/h. This is result of the method of determining the actual trajectory of the automobile using the automatic steering system. The algorithm can be developed for smart vehicles to ensure safety for persons on the vehicle as well as for the smart community.

References

[1] *Liu, A. Chang, S,* Force feedback in a stationary driving simulator, Systems, Man and Cybernetics Intelligent Systems for the 21st Century, IEEE International Conference, Canada, vol. 2, pp. 1711-1716, 1995.

[2] *E.R. Hoffmann and P.N.* Joubert, The effect of. changes in some vehicle handling variables on driver steering performance, Human Factors, vol.8, 1996.

[3] *Ba-Hai Nguyen, Jee-Hwan Ryu,* Semi-Experimental Results on a Measured Current Based Method for Reproducing Realistic Steering Feel of Steer-By-Wire Systems, School of Mechanical Engineering, Korea University of Technology and Education, Cheonan, Korea, 2010.

[4] *Man Hyung Lee, Seung Ki Ha* "Improvement of the Steering Feel of an Electric Power Steering System by Torque Map Modification" 792 Journal of Mechanical Science and Technology, Vol19, No.3, pp792-801, 2005.

[5] *Thomas D. Gillespie* "Fundamental of Vehicle Dynamics", 1992.

[6] *Junjie He, BEng, Meng* "Integrated Vehicle Dynamics Control Using Active Steering, Driveline and Braking" The University of Leeds School of Mechanical Engineering, 2010.

RED LIGHT RUNNING OF MOTORCYCLES AT SIGNALIZED INTERSECTIONS IN VIETNAM: INFLUENTIAL FACTORS AND COUNTERMEASURES

VUONG XUAN CAN[1, 2,4], MOU RUI-FANG[1],
NGUYEN HOANG SON[1], VU TRONG THUAT[3,4]

[1]School of Transportation and Logistics, Southwest Jiaotong University, Chengdu, China
[2]Faculty of Environment and Transport Safety,[3]Faculty of Electrical-Electronic Engineering, [4]University of Transport and Communications, Hanoi, Vietnam
Corresponding author's email: 1323972686@qq.com

Abstract: *Red-light running (RLR) of road users, especially motorcyclists is a common behaviour in cities of Vietnam, and potentially high risk accidents, so it is necessary to reduce this behaviour. This paper analyses influential factors of red light running of motorcycles, and some countermeasures are put forward to reduce the occurrence of RLR behaviour in mixed traffic flow, and to decrease their exposure, as well as to improve their awareness in context of Vietnam's road transport.*

Keywords: *Countermeasures, Signalized Intersections, Influential Factors, Red-Light Running (RLR).*

I. INTRODUCTION

Motorcycles are one of the important transportation modes and represent a significant portion of the vehicle fleet in Vietnam. According to the Asian Development Bank [1], motorcycles have an 80% share of the private transportation used in urban sectors, with a projected growth rate of 9% yearly. Compared to other vehicle types, motorcycles have distinct advantages such as small size, capable of "zigzag" manoeuvers, creep up

Figure 1. *Woman is seen jumping the red light on Pham Van Dong Street while many other stop at the light (Source: Tuoitrenew.vn, 2016)*

slowly to the front of the queue, not follow the "First In First Out" rule at intersections with queues, economy in fuel consumption and price [2,3], but they have poorer safety records. According to statistic information from the National Traffic Safety Committee of Vietnam (NTSC) [4], in 2016, there were 21,094 traffic accidents, 8,417 fatalities and 19,035 injured people. Traffic accidents involved motorcyclists account over 66.7%% of road traffic accidents, and over 71,6% of the road traffic accidents were attributed to risk-taking behaviours of road users, including misuse of lanes (25.32%), speeding (9.35%), unsafe lane shifting (8.91%), drunk-driving (3.5%), etc. and about 32.65% of traffic accidents occurred on urban roads, involved intersections. According to JICA (2006) [5] reported that around 80% of the urban intersections in Hanoi are prone to increasingly serious accidents and heavy congestions. In Ho Chi Minh City (HCMC), in 2014, traffic accidents at signalized intersections about 45% of the total accident occurrence at all the intersections [6]. Red-light running (RLR) of road users involving motorcycles is one of risk-taking behaviours lead to traffic accidents at signalized intersections in major cities of Vietnam, such as Hanoi and HCMC (see Figure1). An RLR behaviour occurs when a motorist (motorcyclist) crosses a stop after a traffic signal has turned red. According to DOT of Hanoi (2016) reported, 15,654 cases of RLR at signalized intersections were captured [7]. In HCMC from 2009 to 2013 period, RLR and not accepted priority are the most significant accident cause in zone 1 (City Centre), and zone 2 (Newly developed areas) accounted for 26%, 29%, respectively. RLR and wrong lane are main causes in zone 3 (Rural areas), accounted for 35% (Vuong and Tuan, 2014 [8]).

In addition, a right turn is allowed on red when warning sign using the message "A right turn on red is allowed" and/or "Yield to pedestrians" is installed at some intersections (Figure 2). Even when traffic is sparse, motorcycles tend to disregard red lights completely when it comes to turning right. Motorcycles and/or cars turning right on red might conflict with pedestrians and other traffic directions, slowing traffic on the other street.

***Figure 2**. A right turn on red is allowed (Source: Plo.vn, 2016)*

Hence, it is very necessary to reduce RLR of road users in Vietnam, especially motorcyclists. The objective of this paper is to find out the factors that affect RLR behaviour of motorcyclists in Vietnam, suggesting some countermeasures to reduce RLR violations and to improve traffic safety at signalized intersections.

II. MAIN CONTENTS

2.1. Influential factors of RLR at signalized intersections

Auearree and Kunnawee (2018) [9] considered RLR of motorcycle riders as one of the most dangerous behaviours at intersection. RLR could be influenced by human (driver) factors or road

environment, such as human characteristics, physical condition of intersection, traffic signal operation, and traffic condition.

2.1.1. Driver Characteristics

McGee et al. (2003) [10] stated that some of the causes for RLR are associated with motorist psychology. Young and old drivers have different behavioural changes. Luot and Ha (2015) [11] surveyed with 170 youths, randomly selected from various areas in Hanoi to understand risk-taking behaviours when using motorcycles, e-bicycles and e-scooters by using questionnaires and in-depth interviews, 60.6% of participants had less than 3 red-light running behaviors in recent 30 days. Wu et al. (2012) [12] stated that young and middle-aged two-wheelers (e-bikes, bicycles) riders being more likely than the old ones to run against a red light at in China. Motorists and motorcyclists who run red lights intentionally could cross the intersection whether there is a camera or not. Sometimes, RLR violations occur because of the drivers' false stop/go judgment. In many cases, although the drivers at the top have strictly followed the stop for the red light, but have to endure the glare, even the bad words of the people behind, so RLR violations are very easy to happen.

2.1.2. Intersection Characteristics

The design of the intersection and the location of the warning signals are also important factors contributing to RLR. Bonneson and Zimmerman (2004) [13] reported that the number of RLR is associated with the traffic volume and also whether there is shorter or longer cycle length. Hawa et al. (2012) [14] found that drivers facing short cycle length (less than 120 s) were more likely to run red lights in Malaysia, and compared with vehicle-actuated control, fixed-timed control recorded 1.5 times more cases of red light running. Increase in traffic volume is known to be associated with an increase in RLR (Council et al. 2005 [15], Wang et al. 2016 [16]). The yellow time interval should be properly calculated using the speed and pertinent traffic conditions at the specific intersection (Bonneson et al., 2002 [17]). Chang et al. (1985) [18] have found that slope of approach is one of the factors that affect a driver's decision to stop at the onset of a yellow light, and they suggested that drivers on a downgrade were less likely to stop and more likely to go through a red light.

2.1.3. Vehicle Characteristics

Vehicle characteristics have influence on road users' tendency for RLR. In comparison with passenger cars if trucks are too close to the intersection it could be impossible for them to stop before the intersection, which could result in a RLR because trucks and heavy vehicles require more acceleration and stop time than passenger cars. In comparison with passenger cars, motorcycles are so flexible that more dangerous behaviours can occur. Motorcyclists were 4.32 times more likely to run the red light compared to other drivers in Malaysia [14]. Guo et al. (2014) [19] conducted to compare the RLR behaviours of the riders of e-bikes, e-scooters and bicycles at crossing signalized intersections in China, and they found that bicycles were slightly more likely to be involved in traffic conflicts than others.

2.1.4. Weather condition

Hot weather conditions have also influence on road users' tendency for RLR. Vietnam features the specific tropical monsoon climate humid, with the temperature of the summer can reach 40 degree Celsius. Therefore, stopping traffic signals under high temperatures causes road users to feel tired and have a tendency to pass red lights.

2.2. Countermeasures for red light running at signalized intersections

These countermeasures to reduce RLR violations at intersections involve combinations of engineering judgment, traffic enforcement, and driver education as following. Generally, red light runners can divide into two categories. The first is the intentional violator who could avoid an RLR event but still proceeds through the intersection. The second type is an unintentional driver, for whom an RLR is an 'unavoidable' event [17]. The former is most affected by enforcement countermeasures, such as Red-Light Cameras, and the latter is most affected by engineering countermeasures, such as physical improvement of intersections (Baratian-Ghorghi et al., 2017 [20]).

2.2.1. Physical improvement of intersections

Physical improvement of intersections is one form of engineering countermeasures, including additional traffic lanes and flattening sharp curves [20]. Chandler et al. (2013) [21] stated that installation of a left-turn lane can be expected to decrease rear-end crashes and RLR crashes. The ITE suggested that engineering countermeasures are conducted to reduce RLR in horizontal and vertical curves, such as improve sight distances, soften sharp horizontal curves, flatten sharp vertical curves, increase the conspicuity of signal, and on downhill slopes, including increase the duration of the yellow light, extend the green light, provide a pre-yellow signal, and add advance warning signs.

2.2.2. Variable message warning signs and pavement marking

With respect to the distance-warning methods, warning signs and pavement marking can be to help the drivers make correct decisions. Warning signs use the "Signal Ahead" (symbolic) message (i.e., Traffic lights ahead sign (W.209) in QCVN 41/2016/BGTVT [22]) or the "Be Prepared to Stop When Flashing" sign to be effective at reducing red-light-running and associated crashes. Radwan et al. (2005) [23] reported a 74.3% drop in RLR by placing word message "Signal Ahead" on the pavement before the intersection to warn motorists about the signal change. Similarly, Yan et al. (2009) [24] stated that a pavement marking with a word message "Signal Ahead" to help drivers decide whether to stop or go at the onset of the yellow indication (Figure 3).

Figure 3*. Pavement marking countermeasure*

2.2.3. Signal timing adjustment

Almost intersections in Vietnam use fixed-time signal control plan for time of day. It is not able to identify the traffic conditions to change, easily leading to the phenomenon of "missing" or "excess" green time, extended vehicle delay. Fixed-time control is work well in low demand traffic but not well in high demand traffic like Hanoi, HCMC. So firstly, the cycle length needs to be efficiently set for the traffic in all directions to avoid unnecessary delays, then intelligent control needs to be deployed to improve traffic quality and traffic safety (Figure 4). Increasing the yellow interval duration has a direct effect on the frequency of red-light running. A study shown suggests that yellow intervals in excess of 3.5 s are associated with minimal red-light-running [17].

2.2.4. Red Light Cameras (RLCs)

One of effective measures to reduce RLR behaviour at intersections is the presence of red light cameras (RLCs). RLCs not only lower traffic crashes due to reduced RLR in the conflicting stream but also decrease their exposure, as well as has a great influence on the traffic participants who are aware of their law enforcement. RLCs are used world-wide, such as Australia, New Zealand, Canada, the United Kingdom, Singapore, the United States and so on. In Vietnam, several cities, such as Hanoi, HCMC have installed RLCs at signalized intersections where have been a lot of violations. For example, in Hanoi, in 2015, 360 cameras had been installed at heavy-traffic intersections and other locations. RLCs have initially brought about certain effects in reducing RLR violations. However, the number of RLCs is still very limited and there are many difficulties, such as no-changing owner of vehicles, without coordinated processing. Hence, it is necessary to strengthen the installation of RLC system and vehicle management.

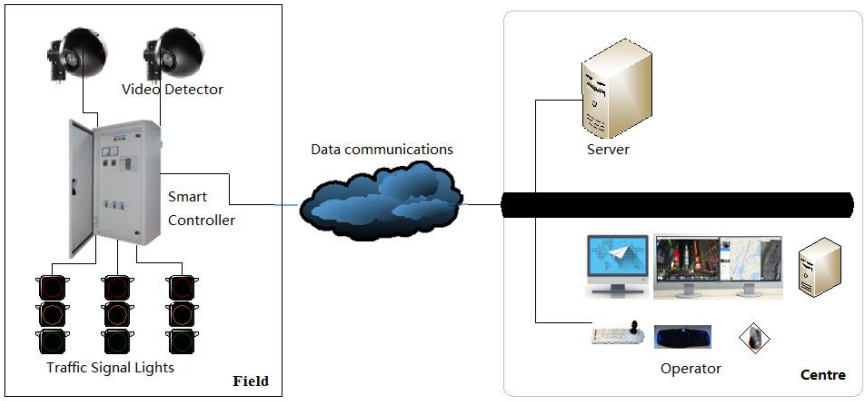

***Figure 4**. Overview of the Intelligent Traffic Signal Control System*

RLCs that detect vehicles that cross a stop line while a red traffic light is showing by automatically photographing vehicles and records the vehicle speed, date, and time (Figure 5). The photo is evidence that assists authorities in their enforcement of traffic laws. Overview of RLC system is shown in Figure 6. In Vietnam, the working principle and requirements of the system are based on the Ministry of Public Security's Decision No. 1914/2009/QD-BCA-E11.

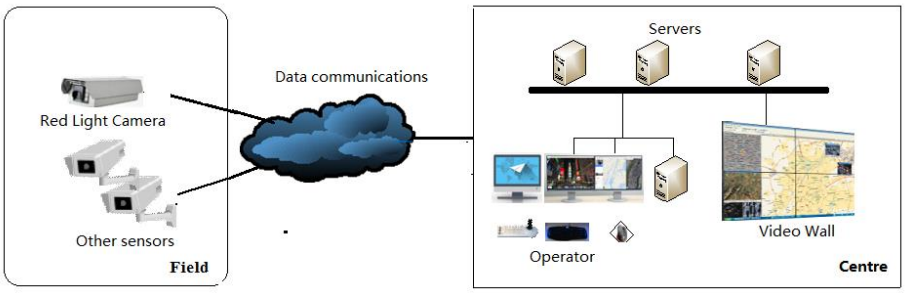

Figure 6. *Overview of RLC system*

Generally, for each violation, the RLC will capture a sequence of two or three photos. The first photo shows the vehicle just before it enters the intersection, with the light showing red. License plate of the vehicle and its position is identified. The second photo, taken a second or two later, shows the vehicle when it is in the intersection, and the third photo shows the vehicle when it is at a position at/or passes the centre of the intersection. Details that may be recorded by the camera system, including the date and time, the location, the vehicle speed, and the amount of time elapsed since the light turned red and the vehicle passed into the intersection, and are sent to the relevant law enforcement agency (Centre). The information is typically reviewed by operator, who determines if a violation occurred and, if so, approves issuing a citation to the vehicle owner, who may challenge the citation [25].

2.2.5. Educational and Public Awareness Campaigns

In Vietnam, the low level of knowledge and awareness when controlling vehicles is one of main causes lead to road accidents. The legislators, the public, and transportation agencies need to work together in reducing risk-taking behaviours, involved RLR. Educational and public awareness campaigns are low-cost countermeasures to solve those problems in general and to reduce RLR in particular. Their associated objectives are stimulate a voluntarily change in the driver's behaviour, gain public support for treatment, and minimize negative public reaction and avoid accusations of deception [13]. The methods are often used to convey the campaign message and heighten motorist awareness, including public service announcements on television and radio, newspaper and magazine articles, posters, warning signs, a banner, billboards, developing and distribution of educational material dealing with red light running, distribution of literature in businesses, and pledge boards where individuals pledged to stop red light running and so forth.

III. EXPERIMENT

To consider the RLR violation, Tran Phu- Nguyen Van Loc intersection at Ha Dong district of Hanoi was selected. The RLR violation was collected by videography and manual counting from 14 pm to 15 pm in working day in August 2018 under hot weather conditions (about 35^0C). This intersection with three-leg has the pedestrian bridge on Tran Phu Street (Eastbound). Camera was setup at the Eastbound to analyse traffic flow of Tran Phu approach (see Figure 7). The Eastbound approach has 5 lane-cross section (2-straight; 2-straight and U-turn; 1-free-right-

turn). This approach is controlled with a cycle length of 93s. Green time, yellow time and red time are 44s, 3s and 46s respectively. RLR violation as shown in Table 1.

a) Location by Google map

b) Real picture at the intersection

Figure 7. *Tran Phu- Nguyen Van Loc intersection*

Table 1. *RLR violations on the Eastbound approach*

Directions	Motorists		Non-motorists		Total		
	Volume	Violations	Volume	Violations	Volume	Violations	%
Straight	1456	12	4701	840	6432	852	13.2
Right-turn	184	0	498	0	709	0	0.0
U-turn	205	3	1108	447	1329	450	33.9
Total	1845	15	6307	1287	8470	1302	15.4

Table 1 shows that there are 1302 cases of RLRs during the observation period, of which, non-motorists (motorcycle, bicycle) account for a large proportion of RLR violations, approximately 98.8% of the total number of violations. Particularly, U-turn movements of non-motorists. Observation has shown that the main causes of the RLR violations include the low awareness of riders of non-motorists, the inadequacies of signal timing plan and hot weather. Besides, some straight vehicles occupy the free right-turn lane with low traffic volume, so there is the possibility of red light passing by those vehicles. To reduce the phenomenon of RLR to improve the current traffic situation at this intersection, adjustment of the cross section, signal timing adjustment and RLCs are proposed. The free right-turn lane might be converted into straight and right-turn lane, and right-turn movements are not allowed on red. Because there are no conflicts between vehicles and pedestrians on Tran Phu street, only the merge conflicts between the U-turn of vehicles on the Eastbound approach with other flow. Hence, it is possible to allow U-turn movements on red at inter-peak hour to reduce the RLR violations, while enhancing capacity of intersection while still ensuring traffic safety. In addition, due to the large number of violations, it is necessary to install the RLCs to handle these offenses in time, and solutions related to public awareness and education also need to be respected.

IV. CONCLUSION

The paper analyses some of the key factors affecting RLR behaviour of traffic participants, and has provided some low-cost countermeasures to reduce RLR violations and to raise the awareness of the participants, as well as contributing to improving traffic safety at intersections in urban areas of Vietnam.

References

[1] *The ADB,* "Viet Nam: Strengthening Sustainable Urban Transport for Hanoi Metro Line 3," 30 9 2014. [Online]. Available: http://www.adb.org/projects/40080-023/details. [Accessed 1 7 2018].

[2] *Minh. C.C., Sano K., Matsumoto S.* , "The speed, flow and headway analyses of motorcycle traffic," J. of the EASTS 6, 1496-1508, 2005.

[3] *Huynh D. N, Boltze M., Vu A. T.,* "Modelling Mixed Traffic Flow at Signalized Intersection Using Social Force Model," J. of the EASTS 10, 1734-1749, 2013.

[4] *NTSC,* "Traffic Safety Annual Reports" Hanoi, 2017.

[5] *JICA,* "Comprehensive Urban Development Programme in Hanoi Capital City (HAIDIEP)-Interim Report", 2006.

[6] *Vuong T.Q.,* "Traffic Conflict Technique Development for Traffic Safety Evaluation under Mixed Traffic Conditions of Developing Countries," Journal of Traffic and Transportation Engineering, vol. 5, 228-235, 2017.

[7] *Hanoi Department of Transport,* "General Report", Hanoi, 2016.

[8] *Vuong T. Q., Tuan V. A.,* "Analysis of traffic accidents at signalized intersections", ASTRAN Symposium-Transportation for A Better Life: Towards Better ASEAN Connectivity and Safety, Bangkok, 2014.

[9] *Auearree J., Kunnawee K.,* "Influences of motorcycle rider and driver characteristics and road environment on red light running behavior at signalized intersections", Accident Analysis and Prevention, vol. 113, 317-324, 2018.

[10 *McGee, H., Eccles, K., Clark, J., Prothe, L., and O'Connell, C.,* "Making Intersection Safer: A Toolbox of Engineering Countermeasures to Reduce Red-Light Running: An Information Report", Institute of Transportation Engineers, Washington D.C., 2003.

[11] *Luot N.V., Ha P.T.T.,* "Risky Behaviors among Youth in Road Traffic", VNU Journal of Science, Vol. 31, No. 5, 26-33, 2015 (in Vietnamese).

[12] *Wu C., Yao L., Zhang K.,* "The red-light running behavior of electric bike riders and cyclists at urban intersections in China: An observational study", Accident Analysis and Prevention 49, 186–192, 2012.

[13] *Bonneson, J. A. and Zimmerman, K.,* "Development of Guidelines for Identifying and Treating Locations with a Red-Light-Running Problem", Texas Department of Transportation, Austin, Texas, 2004.

[14] *Hawa, M.J., Akmalia, S.,Ho, J.S.,* "A Case Study of the Prevalence and Characteristics of Red Light Runners in Malaysia", Injury Prevention, vol.1, A201, 2012.

[15] *Council, F., Persaud, B., Lyon, C., Eccles, K., Griffith, M., Zaloshnja, E., & Miller, T.,* "Implementing red light camera programs: guidance from economic analysis of safety benefits", J. of the Trans. Res. Board, Vol. 1922, 38-43, 2005.

[16] *Wang, X., Yu, R., Zhong, C.,* "A field investigation of red-light-running in Shanghai, China", Transportation Research Part F 37, 144–153, 2016.

[17] *Bonneson, J. A., Brewer, M., and Zimmerman, K.,* "Engineering Countermeasures to Reduce Red Light Running", 2002.

[18] *Chang, M., Messer, C. J., Santiago, A. J.,* "Timing traffic signal change intervals based on driver behavior," Transportation Research Record 1027, 20-30, 1985.

[19] *Guo Y., Liu P., Bai L., Xun C., Chen J., "*Comparative Analysis of Red-light Running Behaviors of E-bikes at Signalized Intersections", TRB 2014 Annual Meeting, Washington, D.C., 2014.

[20] *Baratian-Ghorghi, F., Zhou, H., Ahmadian-Yazdi, H., "*Associations between the characteristics of intersections and the risk of red-light-running crashes", International Journal of Urban Sciences, Vol. 21, No. 2, 172–184, 2017.

[21] *Chandler, B. E., Myers, M. C., Atkinson, J. E., Bryer, T. E., Retting, R., Smithline, J., Izadpanah, P.,* "Signalized Intersections Informational Guide, Second Edition (FHWA-SA-13-027)", Federal Highway Administration, Washington D.C ., 2013.

[22*] MOT of Vietnam,* "National Technical Regulation on Traffic Signs and Signals (QCVN 41:2016/BGTVT", Hanoi, Ministry of Transport, 2016.

[23] *Radwan, E., Yan, X., Harb, R., Klee, H., and Abdel-Aty, M.,* "Red-light Running and Limited Visibility Due to LTV's Using the UCF Driving Simulator", Center for Advanced Transportation Systems Simulation, University of Central Florida, Orlando, Florida, 2005.

[24] *Yan X., Radwan E., Guo D., Richards S.,* "Impact of ''Signal Ahead" pavement marking on driver behavior at signalized intersections", Transportation Research Part F 12, 50–67, 2009.

[25] *ELSEC,* "Technical Proposal For Vinh Phuc Smart Transportation Solution (Draft)", Elbit Security Systems LTD , Vinh Phuc, Vietnam, 2017.

[26] *Y. Wu,* Artist, A Comparative Analysis of Different Dilemma Zone Countermeasures at Signalized Intersections Based on Cellular Automaton Model. University of Central Florida, Orlando, Florida, 2014.

[27] *ST Electronics,* "Integrated ITS Systems Proposal for Hai Phong (Draft)", ST Electronics Ltd, Hai Phong, Vietnam, 2016.

THE REVIEW OF SMART CITY DEVELOPMENT

NGUYEN VAN MINH[1], CHU VIET CUONG[2], DAO NGOC T.TUYEN[3]
[1]*Construction Project Department, Ho Chi Minh City University of Transport, Ho Chi Minh City, Vietnam*
[2]*Academic of Managers for Construction and Cities, Hanoi, Vietnam*
[3]*University of Leeds, Leeds, United Kingdom*
Corresponding author's email: minh.nguyen@ut.edu.vn

Abstract: *Smart City Development is a hot topic, receiving serious attention from government agencies, private sectors and academic institutions. This study classifies ten characteristics of Smart City Development (SCD) of ten cites around the world, which given by the research results of Korea Research Institute for Human Settlement (KRIHS) and Inter-American Development Bank (IDB). From systematic review, the research summaries three problems of SCD of the ten cities, which are (1) Financial-related problems, (2) Organizational-related problems, and (3) Technical-related problems, which come up with pragmatic solutions to solve each problem*

Keywords: *Smart City, Smart City Development (SCD), Sustainable, Urbanization, Public Private Partnership (PPP)*

I. INTRODUCTION

Although the governments worldwide have brought policies about the equity of metropolitan and countryside areas, it is calculated that around 50% of human population is now living in cities and predicted that the number would be 60% in 2030 and reach 70% in 2050 [11]. This is one of the main factors contributing to the development of urbanization [14], which is considered to be an unavoidable step of human development [4]. The urbanization process increases the urban infrastructure, living conditions and public services for the urban people, which results in the national economic growth. Along with the advantages, there are drawbacks needed to be studied, which are second-class citizens with low living standard, high resources consumption with low utilization efficiency, rapid increasing pollutant emission and environment deterioration and explosive and disorderly construction land expansion [13]. These urgent pressures require cities to be smarter to manage them, which then being described with the label smart city [5]. However, smart city is defined in various contexts and meanings [1, 2], which are inconsistent [5, 2] and in a fuzzy concept [2]. Dameri had proposes a comprehensive definition of smart city, which is "a smart city is a well-defined geographical area, in which high technologies such as ICT, logistic, energy production, and so on, cooperate to create benefits for citizens in terms of well-being, inclusion and participation, environmental quality, intelligent development; it is governed by a well-defined pool of subjects, able to state the rules and policy for the city government and development" [7].

This study reviews the current classifications of the characteristics of Smart City Development (SCD), based on qualitative research method. Among current classifications to smart cities, one of them is selected to provide analyses to the SCD of ten cites around the world, which given by the research results of Korea Research Institute for Human Settlement (KRIHS) and Inter-American Development Bank (IDB) [8]. The study will categorize the difficulties and development strategies that ten cities have in its SCD.

II. LITERATURE REVIEW

Smart City phenomenon has been witnessed all over the world. Cocchia studied and divided 162 case studies from 705 papers [6]. His study found that Asia hold the highest number of Smart City, with 49 % of cases, following by Europe with 36 % of cases. North America stands the third position with 9 % of cases. Oceania, Africa and Middle/South America had the lowest number, with respectively 3, 2 and 1 % of cases. Along this study, Smart Cites share the two common features as follow: (1) the widespread and development of Information and Communication Technology (ICT) infrastructures of Internet, data sharing, e-government, public services, innovation and entrepreneurship, and social cohesion; (2) green policies for a smart growth with environmental protection policies, and traffic congestion.

Several studies have been conducted to examine the characteristics of SCD. In the perspective of considering building environment as the foundation of Smart city infrastructure, Mardancany proposed seven major characteristics of Smart City [9], which are (1) Smart Polities, (2) Smart Governance, (3) Smart People, (4) Smart Science and Technology, (5) Smart Environment, (6) Smart Living, and (7) Smart Built Environment. Smart-cities.eu (2014) suggested 6 characteristics of small-scale Smart city, which are (1) Smart City, (2) Smart Mobility, (3) Smart Environment, (4) Smart People, (5) Smart Living, and (6) Smart Governance. For medium-sized cities (Smart-cities.eu,2014), these characteristics are then divided into 28 domains, following by 81 components. With regards to large cities, it is divided into 27 domains, following by 90 components [12], which then applied to be Smart City Key Performance Indexes (KPIs) in Quang Ninh [10] and Bac Ninh [11] city, Vietnam. Additionally, Angelidou had recently reviewed and concluded ten distinctive characteristics of smart cities [3]. They are (1) Technology, ICTs, and the Internet, (2) Human and Social Capital Development, (3) Entrepreneurship Promotion, (4) Global Collaboration and Networking, (5) Privacy and Security, (6) Locally Adapted Strategies, (7) Participatory Approach, (8) Top-Down Coordination, (9) Explicit and Workable Strategic Framework, and (10) Interdisciplinary Planning.

Among these classifications, there is only Angelidou's classification that covers the networking of SCD [3], its privacy conditions and its internal coordination in its main categories of SCD. However, these characteristics widely affect the application of SCD [3]. In a holistic approach of SCD, the paper decides to apply 10 characteristics of SCD proposed by Angelidou to examine and categorized major characteristics of SCD from ten cases given by the research results of Korea Research Institute for Human Settlement (KRIHS) and Inter-American Development Bank (IDB). The cities are Anyang, Namyangju, Songdo, Pangyo, Singapore, Rio de Janeiro, Santander, Medellin, Orlando, and Tel Aviv.

The first characteristic names **Technology, ICTs, and the Internet** (table 1). The ten cities

share the same common in this area with small differences of some sub-components. There are only 20% (2/10) that develop IoT devices and 50% (5/10) that invest in ICT system. In contrast, some devices such as sensor devices, CCTV network, optical fiber infrastructure, internet and mobile apps are installed in all reviewed cities. The noticed figure is Singapore with its ambitious and unique E-Government system. With city infrastructure and utilities, almost all cities are similar to transportation, energy, water, waste. The only difference can be seen with the case of Songdo, Korea since the city allow private sector to provide other services such as Home, Store, Learning, Health, Money and Car.

Table 1. *Collected data for Characteristic 1*

City	Technology, ICTs, and the Internet
Anyang	Tools and solutions for data management (sensor devices, CCTV, optical fiber infrastructure, internet and mobile apps, electronic map, communications equipment, Information collection equipment), public participation (mobile application), city infrastructure and utilities (transportation, energy, water, waste)
Namyangju	Tools and solutions for data management (ICTs, sensor devices, CCTV, optical fiber infrastructure, internet and mobile apps), public participation (social networking websites, smartphone application), city infrastructure and utilities (transportation, energy, water, waste)
Songdo	Tools and solutions for data management (sensor devices, traffic detectors, Wifi, CCTV, IOTs, optical fiber infrastructure, internet and mobile apps), citizen interaction, city infrastructure and utilities (Transportation, Home, Store, Learning, Health, Money and Car)
Pangyo	Tools and solutions for data management (sensor devices, traffic detectors, CTV, optical fiber infrastructure, internet and mobile apps), citizen interaction, city infrastructure and utilities transportation, energy, water, waste)
Singapore	Tools and solutions for data management (sensor devices, traffic detectors, CTV, internet and mobile apps), citizen interaction (social media and mobile applications), city infrastructure and utilities (transportation, energy, water, waste), E-Government
Rio de Janeiro	Tools and solutions for data management (sensor, CCTV, GPS devices, radar), information of public (social media, social networking website) and applications for city infrastructure and utilities (transport, ICTs), Citizen (safety and security, environmental alert)
Santander	Tools and solutions for data management (IoT, sensor devices, traffic detectors, internet and mobile apps), citizen interaction, city infrastructure and utilities (transportation, energy, water, waste)
Medellin	Tools and solutions for data management (ICTs, sensor devices, CCTV, optical fiber infrastructure, radar, internet and mobile apps), public participation (social networking websites, smartphone application), city infrastructure and utilities (transportation, energy, water, waste)
Orlando	Tools and solutions for data management (sensor devices, CCTV, optical fiber infrastructure, radar, internet and mobile apps), public participation (social networking websites, smartphone application), city infrastructure and utilities (transportation, energy, water, waste)
Tel Aviv	Tools and solutions for data management (sensor devices, traffic detectors, Wifi, CCTV, ICT optical fiber infrastructure, internet and mobile apps), citizen interaction, city infrastructure and utilities (Transportation, Waste, Energy, Water)

The second characteristic is **Human and Social Capital Development** (table 2). The ten cities all consider human development and environmental sustainability as the most important factors affecting the success of smart city development. Therefore, they all bring about holistic approaches to access the matter.

Table 2. *Collected data for Characteristic 2*

City	Human and Social Capital Development
Anyang	Objectives: environmental sustainability/sustainable lifestyles Means: accessibility of citizens via application and Web citizens may submit their opinions various communication channels for citizen's participation
Namyangju, Pangyo, Singapore, Rio de Janeiro	Objectives: environmental sustainability/sustainable lifestyles Means: initiatives for awareness/education/digital inclusion and civic involvement
Songdo, Santander, Medellin, Orlando	Objectives: environmental sustainability/sustainable lifestyles Means: initiatives for awareness/education/digital inclusion and civic involvement, business participation.
Tel Aviv	Objectives: focusing on its residents rather than on physical infrastructure Means: initiatives for awareness/education/digital inclusion and civic involvement

The third characteristic is **Entrepreneurship Promotion** (table 3). Two (2/10) cities don't stress the importance of this characteristic. Noticeable, four (4/10) cities apply the Public-Private Partnership (PPP) Model, which then come up with many successes of these cities. The rest introduce some minor incentives to promote its business development in SCD.

Table 3. *Collected data for Characteristic 3*

City	Entrepreneurship Promotion
Anyang	Promotion of Entrepreneurship not a priority.
Namyangju	Business model development is a major area of development
Songdo	At establishment of Incheon U-city Corporation. Incheon U-city Corporation holds private-public partnership (PPP) formation, where the city of Incheon holds 28.6% of the share and the rest are held by private firms.
Pangyo	Attracting advertisement on media boards and kiosks, and providing charged contents or education materials directly to citizens and receiving low-cost usage fee
Singapore	Business through E-Government Platform. Entrepreneurial activity dispersed through entire city.
Rio de Janeiro	Promotion of Entrepreneurship not a priority
Santander	Businesses participate through sectoral innovation meetings held at least once or twice a year, and through active participation in R&D projects as partners.
Medellin	An inter-administrative agreement with a public-private company for the modernization and optimization of the management of administrative services of the Medellin Transportation and Transit Secretariat.
Orlando	Private sector contractors to provide maintenance service.
Tel Aviv	Businesses participation are encouraged through PPP model, data -sharing, business contracts with government agencies.

The following characteristic is **Global Collaboration and Networking** (table 4). The haft number (5/10) has no connection with the other cities in terms of SCD. The most promising case can be seen in Songdo, Korea with its dynamic activities to the world. It operates numerous events to spread out its symbol and make business. Four cities (4/10) choose to participate in the international Smart City event and invite some professionals to their cities for knowledge and cooperation exchange.

Table 4. *Collected data for Characteristic 4*

City	Global Collaboration and Networking
Anyang	A model city and a benchmark smart city for other cities of Korea.
Namyangju	In a mature phase of Smart city and a benchmark smart city
Songdo	Leader of smart cities of the world by actively hosting international business events, and to attract IT, BT, R&D Handling general system construction, maintenance business, as well as international consulting business for countries that wishes to create smart cities
Singapore	Various stakeholders such as technology builders and entrepreneurs around the world have visited
Rio de Janeiro	Participating in numerous Smart City Competition, which enable Rio to connect to other city.
The rest	No known initiatives

Privacy and Security (table 5) is the characteristic received the lowest attention from the ten mentioned cities. The majority (8/10) cities are not show their effort in protecting the risk of data leaking. Singapore is the only place releasing its ICT Security Masterplan, aiming at protecting smart data. Tel Aviv, meanwhile, conducts efforts to prevent the data from illegally being shared.

Table 5. *Collected data for Characteristic 5*

City	Privacy and Security
Singapore	ICT Security Masterplan, The attention on data security transferring to providers.
Tel Aviv	The city conducts efforts to prevent the data from illegally being shared
The rest	Ambiguous/undefined

Table 6. *Collected data for Characteristic 6*

City	Locally Adapted Strategies
Anyang	Vision of happy citizen. Serving local needs and the city's strategic priorities in three specific areas (Traffic, Safety and Disaster Prevention)
Namyangju	Serving local needs and the city's strategic priorities in three specific areas (Traffic, Safety and Disaster Prevention)
Songdo	Serving local needs and the city's strategic priorities. Public service sectors are designed to provide 24 services in 6 categories. Private service sectors are to provide services relating to home, store, learning, money, health, and car.
Pangyo	Serving local needs and the city's strategic priorities. 5 services including U-portal, U-facility management, U-crime prevention and disaster prevention, U-traffic and U-environment.
Singapore	Designed as an "living lab".
Rio de Janeiro	Addresses the city's major problems (floods and landslides, traffic congestion).
Santander	Serving local needs and the city's strategic priorities. 5 services including U-portal, U-facility management, U-crime prevention and disaster prevention, U-traffic and U-environment.
Medellin	Serving local needs and the city's strategic priorities to create free Internet access zones, community centers, open government, social innovation in problem solving, and project sustainability, reduction in the number of accidents, improvement in mobility, and a reduction in incident response time.
Orlando	Serving local needs and the city's strategic priorities. 6 services including Transport and urban mobility, Citizen safety and security, Emergency and response, Environment, Energy efficiency, Citizen interaction
Tel Aviv	Serving local needs and the city's strategic priorities. It has three categories including Citizen Engagement, Smart Infrastructure, and Ecosystem

The sixth characteristic is **Locally Adapted Strategies** (table 6). Based on the geographical and social characteristics, each city builds its own strategies. In Rio, due to the natural problem with flood and low-level infrastructure, the city has chosen floods and landslides, traffic congestion are the main strategies. In Anyang and Namyangju, Disaster Prevention is one of three key strategies since the city is vulnerable with natural disaster.

The seventh characteristic is **Participatory Approach** (table 7). All cities witness the meaningful connection between the citizens and the government agencies. The information of the citizens is not only collected from the installed devices, but also from their comments from Social networking website and Mobile application such as Facebook and Twister. Under PPP model, there are four cities having strong connection with the private sectors and there are two cities allow the Academic institution participate in the SCD.

Table 7. *Collected data for Characteristic 7*

City	Participatory Approach
Anyang, Namyangju, Pangyo, Singapore, Rio de Janeiro	Involved actors: citizen and authorities. Stage of involvement: Citizens contribute their data to the smart city system
Songdo, Tel Aviv	Involved actors: citizen, Businesses and authorities. Stage of involvement: Citizens contribute their data to the smart city system. Entrepreneurs sign contract with government agencies
Santander	Involved actors: citizen, University, Businesses and authorities Stage of involvement: Citizens contribute their data to the smart city system. Entrepreneurs sign contract with government agencies. University collaborates with Council
Medellin	The Medellin Smart City programs line in: Citizen participation, Open government, Social innovation, Sustainability
Orlando	Involved actors: citizen, University, Businesses and authorities Stage of involvement: Citizens contribute their data to the smart city system. Entrepreneurs sign contract with government agencies. University collaborates with the City to train their staffs.

The next characteristic is **Top-Down Coordination** (table 8). Basically, all cities are managed by the public sector. With the success of SCD in such cities, the government agencies have proved its working efficiency in accomplishing a very new task. The Leading figure of five cities is its mayor.

Explicit and Workable Strategic Framework (table 9) is the ninth characteristic of smart city. It is noticeable that there are only two cities (2/10) conducting the pilot program. Instead of doing pilot test, the other bring out step by step project from time to time. Anyang, Korea accomplishes its nine-phases projects in more than a decade, resulting in the success of Bus Information System, Intelligent Transport System, Bus Rapid Transit, Criminal Prevention System. The special case is from Tel Aviv city, which has its initial purpose of improving resource allocation. This purpose seems to be similar to many other normal cities. However, with a decentralized, low-cost method that builds on a modular approach and an open architecture, Tel Aviv city has become a unique example for SCD.

Table 8. *Collected data for Characteristic 8*

City	Top-Down Coordination
Anyang	Initiating and driving authority: local government. Leading figure: Anyang City public officials; police officers Socially determined (long-term outlook).
Namyangju	Initiating and driving authority: local government. Leading figure: local government Socially determined (long-term outlook).
Songdo	Initiating and driving authority: local government. Leading figure: CEO Socially determined (long-term outlook).
Pangyo	Initiating and driving authority: local government. Leading figure: Director Socially determined (long-term outlook).
Singapore	Implementing agencies operate in a discrete manner. The Smart Nation Program Office that lies directly under the Prime Minister's Office of Singapore has been set up to act as a coordinating body. Initiating and driving authority: national government (Infocomm Development Authority of Singapore-IDA). Leading figures: IDA's Senior Leadership Team. Socially determined (long-term outlook)
Rio de Janeiro, Santander, Medellin, Orlando, Tel Aviv	Initiating and driving authority: local government. Leading figure: Mayor. Socially and politically determined (long-term outlook)

Table 9. *Collected data for Characteristic 9*

City	Explicit and Workable Strategic Framework
Anyang	Initiatives are assorted under development-related sectors (Traffic, Safety and Disaster Prevention) since 2003. The 9 phases were developed.
Namyangju	Three key area with Smart Traffic, Smart Safety and Smart Disaster Prevention since 2008 by three stages.
Songdo	The smart city project of Songdo is largely divided into six sectors to provide smart applications. The development involves three stages which started in 2004 with the participation of Private sectors (PPP)
Pangyo	The smart city project of Pangyo is largely divided into five sectors to provide smart applications
Singapore	Serving local needs and the city's strategic priorities. 5 sectors including Transport and urban mobility, Citizen safety and security, Environment, Energy efficiency, and Citizen interaction. Pilot projects before implementing smart
Rio de Janeiro	Initiatives assorted under strategic priorities (traffic management, weather forecasting, urban safety/weather alerts).
Santander	Initiatives assorted under strategic priorities (Transportation and Mobility, Environment, Public Safety, Emergencies and Civil Protection, Energy efficiency, and Interaction with Citizens).
Medellin	Initiatives are assorted under development-related sectors (Traffic, Safety and Environment).
Orlando	Initiatives assorted under strategic priorities (Transport and urban mobility, Citizen safety and security, Emergency and response, Environment, Energy efficiency, Citizen interaction).
Tel Aviv	Initiatives assorted under strategic priorities (Digi-Tel, I-view, Traffic Management,...).

The last characteristic of smart city is **Interdisciplinary Planning** (table 10). Five of ten cities strategies leverage multi-layer expertise of its SCD, including private sector and academic groups. Such these parties enable the city to utilize all necessary resources in a most effective manner. In Orlando, the University of Central Florida and University of Florida train the relevant people with specific and major lessons, which requires numerous hours and resources to understand without being taught.

Table 10. *Collected data for Characteristic 10*

City	Interdisciplinary Planning
Anyang	Government & city employees from District Office, police stations, fire departments and military units
Namyangju	Government & city employees from District Office, police stations, fire departments, Information departments
Songdo	Private and public sector
Pangyo	Government & city employees from Information Policy Division, Administration and Planning Bureau
Singapore	Government officials nationally
Rio de Janeiro	The operation along with municipal, state and federal agencies, in addition to utilities.
Santander	Collaboration between the City Council, the University of Cantabria, and the private sector
Medellin	Collaboration between government entities in different sectors, with the participation of academic institutions and innovation, science, and technological entities
Orlando	Collaboration between the City Council, the University of Central Florida and University of Florida, and the private sector
Tel Aviv	Collaboration between the City and the private sector

III. FINDINGS

Although the ten given cities have shown its success features in SCD, a number of difficulties resulting from its characteristics can be seen. This study classifies three problems from SCD of the ten cities, which are (1) Financial-related problems, (2) Organizational-related problems, and (3) Technical-related problems.

Financial-related problems: SCD requires a large amount of budget for its preparation, operation and maintenance. Since most cities utilize SCD from national/ regional funds, the lack of money arises. Namyangju faces difficulties in establishing systems in the long term, Pangyo has problem of covering operations cost. In Santander, the absence of a clear framework for standardization and regulation results in the increase of required budget.

Realizing this potential problem is a key factor to fulfil the need of money in every city. A Public-Private Partnership (PPP) Model may a good choice since its solve budget inefficiency for Songdo, Tel Aviv, Santander, Medellin. In other cases, the step-by-step development process is a realistic option. This method requires a small and an acceptable amount of money for investing.

Organizational-related problems: Most cities are confronted with the problems arising from its organizational structure. Anyang has trouble with the conflicts of project group. In

addition, Anyang and Singapore share the same problem with the lack of information sharing between government agencies. In Pangyo, the difference of the designer and head of project construction has brought difficulties for its U-City project. In Songdo and Namyangju, the structure problems have also led to the investment overlap, consumed more than one time for each element.

To solve conflicts, a special team who are responsible for mediating decisions if any conflicts arisen and an information survey team who can equalize the relationship between the stakeholders should be established. Moreover, an operations management system should be the information hub to classify, divide and oversee the gap of data sharing and overlapping. In case of building properties, it should be a high ability company who both take charge in the design and construction works to minimize risks and conflicts. It is essential to create partnership among government agencies for the integration of services in shared territories to get rid of investment overlap.

Technical-related problems: SCD requires the development of many sectors, leading to the installation of the variety of state-of-the-art equipment. Thus, there may be many technical problems that each city would face with. Anyang has the problem when establishing the smart system. In Songdo, the authorities realize that the current cameras only function for the single purpose of detecting illegal parking, which could be act as crime prevention cameras during the night time. Pangyo alarms the case that the new technology may become depended on the old technology. Additionally, since the Namyangju U-Integrated Traffic Information Center locate inside the City hall building, the problem arises when the Center operates 24 hours every day but the government working time is much limited.

Since not much people can be professional at more than one particular area, separate group should be trained and organized to operate the system. Pilot projects could be a wise step before entering in a mass scale project since it helps the participant with the characteristics of the equipment. If the available budget is enough, a Smart City Center may be a good option for creating a totally new and isolate working environment for not being dependent on the other agencies.

IV. CONCLUSION

Smart City Development is now a controversial topic, receiving serious attention from researchers, developers, government agencies, and private companies. SCD may be an ideal chance for creating and testing cutting-edge technologies for the developers. If applicable, this model will bring the citizens and governments with numerous benefits. Moreover, the Smart City surrounding environment is predicted to be in a better manner compared to the old version ones. Although several difficulties will be arisen, this is an undeniable trend of the human development. This studies have reviewed the development of ten cities, namely Anyang, Namyangju, Songdo, Pangyo, Singapore, Rio de Janeiro, Santander, Medellin, Orlando, and Tel Aviv. The comparison has drawn a concise and full picture of the SCD in the mentioned cities in ten categories. The difficulties of SCD in these cities have been divided in three main areas, which are Financial-related problems, Organizational-related problems, and Technical-related problems.

In Vietnam, SCD has been received great attention from Central and Local government. Smart city term has been officially mentioned in around 30 cities. Specifically, Lao Cai, Bac Ninh, Quang Ninh, Thua Thien Hue, Da Nang, Binh Duong, and Ho Chi Minh City have approved its Scheme of Smart City Development. The unique characteristics of each city has resulted in different methods for taking SCD. Some cites have reviewed and received consultant services from the international firms, who have experiences from the other projects. The other rely on the domestic consultant companies to develop its SCD. While the working methods may be different, all cities share the common goal of being smarter. Studying the lessons from above SCD cases may help Vietnam with valuable experiences and knowledge to bring out proper SCD strategies.

References

[1]. *Alawadhi, S., Aldama-Nalda, A., Chourabi, H., Gil-Garcia, J., Leung, S., Mellouli, S., Nam, T., Pardo, T., Scholl, H. and Walker, S*. (2012). Building Understanding of Smart City Initiatives. Lecture Notes in Computer Science, pp.40-53.

[2]. *Albino, V., Berardi, U. and Dangelico, R*. (2015). Smart Cities: Definitions, Dimensions, Performance, and Initiatives. Journal of Urban Technology, 22(1), pp.3-21.

[3]. *Angelidou, M*. (2017). The Role of Smart City Characteristics in the Plans of Fifteen Cities. Journal of Urban Technology, 24(4), pp.3-28.

[4]. *Bai, X., Shi, P. and Liu, Y*. (2014). Society: Realizing China's urban dream. Nature, 509(7499), pp.158-160.

[5]. *Chourabi, H., Nam, T., Walker, S., Gil-Garcia, J.R., Mellouli, S., Nahon, K., Pardo, T.A., Scholl, H.J.*: Understanding Smart City Initiatives: An Integrative Framework. In: Proceedings of the 45th Hawaii International Conference on System Sciences, pp. 2289–2297 (2012)

[6]. *Cocchia, A*. (2014). Smart and Digital City: A Systematic Literature Review. Smart City, pp.13-43.

[7]. *Dameri, R*. (2012). Searching for Smart City definition: a comprehensive proposal. INTERNATIONAL JOURNAL OF COMPUTERS & TECHNOLOGY, 11(5), pp.2544-2551.

[8]. Inter-American Development Bank. (2018). International Case Studies of Smart Cities - Inter-American Development Bank. [online] Available at: https://idblegacy.iadb.org/en/topics/emerging-and-sustainable-cities/international-case-studies-of-smart-cities,20271.html [Accessed 10 Jul. 2018].

[9]. *Mardacany, E*. (2014). Smart cities characteristics: Importance of built environment components. IET Conference on Future Intelligent Cities.

[10]. National Institute of Information and Communications Strategy - NIICS (2016), Building the Smart City Model for Quang Ninh Province Period 2017 -2020.

[11]. National Institute of Information and Communications Strategy - NIICS (2017), Building the Smart City Model for Bac Ninh Province Period 2017 -2020 Vision 2030.

[12]. Smart-cities.eu. (2018). European smart cities. [online] Available at: http://www.smart-cities.eu/ [Accessed 10 Jul. 2018].

[13]. *Guan, X., Wei, H., Lu, S., Dai, Q. and Su, H*. (2018). Assessment on the urbanization strategy in China: Achievements, challenges and reflections. Habitat International, 71, pp.97-109.

[14]. *Wang, X., Hui, E., Choguill, C. and Jia, S*. (2015). The new urbanization policy in China: Which way forward? Habitat International, 47, pp.279-284.

TOWARDS A CLOUD-BASED FRAMEWORK FOR RECONFIGURATION IN INTERNET OF THINGS

NGUYEN ANH TUAN
The University of Danang, School of Information and Communication Technology, Da Nang, Vietnam
Email: natuan@sict.udn.vn

Abstract: *The Internet of Things (IoTs) connects sensors, actuators and autonomous objects interacting with each other. Since IoTs devices can be deployed in remote or dangerous locations, it is necessary to reconfigure remotely over-the-air (OTA) to change the behaviors of IoTs applications and IoTs devices upon unpredicted events. Therefore, the reconfiguration of IoTs devices and applications over-the-air (OTA) through the IoTs network protocols is of vital importance. Furthermore, when the IoT device number is up to the large amount, IoTs reconfiguration will cost many time and the precision. The main contribution in this paper is the proposes a framework for reconfiguring IoTs applications and devices upon the dynamic changes or unpredicted events of environments. The proposed framework is also compared with ESP8266 solution for smart temperature context. Experimental evaluation shows the proposed framework reduced the time cost on reconfiguration process.*

Keywords: *Reconfiguration; IoTs middleware; Cloud; OTA; ESP8266*

I. INTRODUCTION

IoTs applications often employ in large number of small-size devices, very limited battery power and deploy in large area, e.g. the early warning system for natural environment or the forest environmental monitoring system. Normally, these systems are difficult to change behavior when we need to update new functions. Besides, each node in wireless sensor networks may have a different configuration that application can long-term work stability. To solve this problem, reprogramming and reconfiguration for those IoT devices are very necessary. There are 02 main reasons to prove the necessity for remote reconfiguration in IoTs:

(i) IoTs application places are inaccessible places, dangerous places, danger spots are not accessible: mountain donkeys, deep forests, chemical plants, nuclear plants where people are hard to intervene.

(ii) IoTs systems often encounter problems with energy saving equipment, maintenance time and operating costs. Specifically, when deploying many IoTs projects, the problem of cost, time and effort for maintenance is a big obstacle. For example, for the implementation of 100 IoTs projects, the company has to spend the cost of building maintenance teams across the provinces to implement the project. However, with a remote reconfiguration solution, the company only

needs to head out from a central technical department and maintenance team to solve the problem if it wants to change the needs of the system and the customer.

To address these challenges, we propose an IoTs reconfiguration framework. Specifically, this article makes the following contributions: (1) We propose an IoTs reconfiguration framework architecture which is built on many components and approach to construction is the combination between SOA and the cloud. (2) We deployed the solution and it proved that the reconfiguration problem for the smart temperature test context was well done. The rest of this paper is organized as follows. In Section II presents related works of IoTs reconfiguration based on many approaches. In Section III, we introduce the proposed IoTs Framework architecture and Section V illustrates the performance evaluation of the proposal based on actual experiments. Section V concludes the paper.

II. RELATED WORK

In the face of these difficulties, in IoT reconfiguration domain, there are many differences sub-class in many approaches. Many solutions have been proposed and implemented, especially in recent years. Generally, depending on the needs and the different characteristics of deploying reconfiguration for applications on IoTs devices, solutions have been developed based on different approaches as follows

2.1. Reconfiguration at IoTs Things layer

Deluge [6] know as full image replacement approaches. Replacing the entire image running on the device, this is the common solution. Easy to deploy, but it takes a lot of resources, energy and time to load the structure form. DIP, Drip [5] are protocols of parameters setting approaches. The goal of this approach is to reliably deliver a piece of data to every node in the network. It must allow reconfigure, query, and reprogram a network. Reliability is important because it makes the operation robust to temporary disconnections or high packet loss.

2.2. Reconfiguration at IoTs Middleware layer

- **Event-based approach** is mentioned and surveyed at [1] as a popular method to re-configure Wireless Sensor Network (WSN). The complete separation of time, space, and synchronization of WSN with contextual information changes makes solutions regard to event based middleware. According to [13], this is a real time WSN based event driven middleware that is highly re-configurable and is developed to support popular computing applications that use heterogeneous networks and devices. GREEN is developed to operate in diverse network types such as MANETs and WANs. It also supports inter-active styles for complex context based, content based, context rich events. The strengths of GREEN support reprogramming and operate on heterogeneous network types. However, GREEN is not a fully automated reconfiguration system and in limited support for interoperability. In addition, its synchronization support is limited at the network level. The use of complex WSN will bring serious security challenges and high cost for deployment.

- **Service-oriented architecture (SOA) approach**: OpenCOM [5] has proposed as an open source model for building component-oriented middleware (CORBA, EJB, NET). OpenCOM is a generic model developed specifically for resource-rich platforms. Therefore, it is possible to reconfigure the components for relatively flexible component domains while still solving system performance problems. We think that OpenCOM has a problem related to IoT reconfiguration: the cost of deploying the system. Research [24] has suggested RemoWare is a real time reconfigurable middleware that reduces the cost of updating software after deployment on sensor nodes through the concept of onsite reconfiguration. In addition, RemoWare offers a programming model based on component models, which facilitates the development of dynamic WSN applications. It is an open source framework based on OpenCOM that provides a variety of approaches for dynamically configuring wireless sensor networks. It has many features of OpenCOM, but only supports single configuration for wireless sensor networks, besides the framework does not support multiple configurations for complex WSN networks. Specially, in [3], we believe there is a conclusion that the SOA-approach is applied to control with special emphasis on reconfiguration in industrial automation systems.

- **Virtual machine approach**, the Virtual machine (VM) Oriented Middleware model helps solve the problem of safe and cost effective environment [12]. Specifically, this model will support programming for a particular environment, enforcing security by virtualizing the infrastructure. Applications are divided into separate small modules, which are interoperable, processed and distributed throughout the network. This approach addresses architectural requirements such as self management, while supporting in heterogeneous distribution. Virtual machines can be divided into two categories:1) intermediate level VMs (VMs placed between the operating system and applications) and 2) system level virtual machines (replacing or replacing the entire operating system). It is now primarily focused on this research task scheduling task to optimize performance or economic problems; this study does not cover intelligent context management.

- **Database approach**, Aberer [9] has proposed a popular project between developers and researchers on database driven model redirection, and has been integrated into other projects such as OpenIoT. It uses virtual sensors to control processing priority, manage resources, and store data. Since GSN recognizes the declared parameters, the virtual sensor to deploy the reconfiguration in the GSN at runtime. It creates highly dynamic reconfigurable environments and allows the system to respond quickly to changing requirements and harsh environmental conditions. This approach is not a fully automated reconfiguration, and it currently does not provide support for real time interoperability and security requirements.

- **Cloud integration approach**, we see that there is no middleware currently available to trigger the IoT reconfiguration on the cloud [2]. According to [2] IoT-LAB provides a very large scale infrastructure facility suitable for testing small wireless sensor devices and heterogeneous communicating objects. It helps reprogramming via executable file upload on IoT-LAB website. IoT-LAB allows manual reconfiguration of nodes by uploading directories, and does not support intelligent context management to manually reconfigure. According to [11] MoteLab helps

programming, developing Mica2 based on Board 6 EPRB device through web interface, executable file upload, interact with individual nodes and central server for scheduling, reprogramming and logging.

III. CR-IOT FRAMEWORK

Through the study of related work on many approaches, we see the motivations of optimizing IoTs reconfiguration. We have proposed a framework called CR-IoT (Cloud-Based Reconfiguration IoTs) to perform better IoTs reconfiguration in the context of increasingly complex IoTs applications on hardware devices, intelligent contexts. The main components of the CR-IoT framework are described at Fig 1. In case data from the wireless sensor network are collected at the gateway and disseminated by the framework, the Pub-Sub mechanism will be activated. Sensor data transmitted to the framework uses Message Queuing Telemetry Transport (MQTT) to assemble data and store raw data in the Relational Database Management System (RDBMS) or Non SQL (NoSQL). Raw data will be modelled as semantic Web in the form of particular ontologies for the components of the query framework. The Intelligent Context Management component which is the important component of the framework will be using semantic, machine learning and then make decision to request the reconfiguration. When the framework receives a request for the reconfiguration, the code distribution will transfer the corresponding firmware to the relevant nodes to be reconfigured. Dashboard allows administrators to view data parameters from the WSN, manage reconfiguration rules or manually reconfigure them. The CR-IoT framework is designed with a flexible architecture described as a set of abstract components. These components include the following ones:

3.1. Device Management Component

This component helps to manage hardware/sensor hardware for IoTs applications, it also supports for ESP8266 [Fig 2]. It establishes an extensible identity lifecycle that can be applied to your organization and can be tailored based on the lifetime of the device and the identifier and define how to perform authentication for IoTs devices that are only intermittently connected to the network.

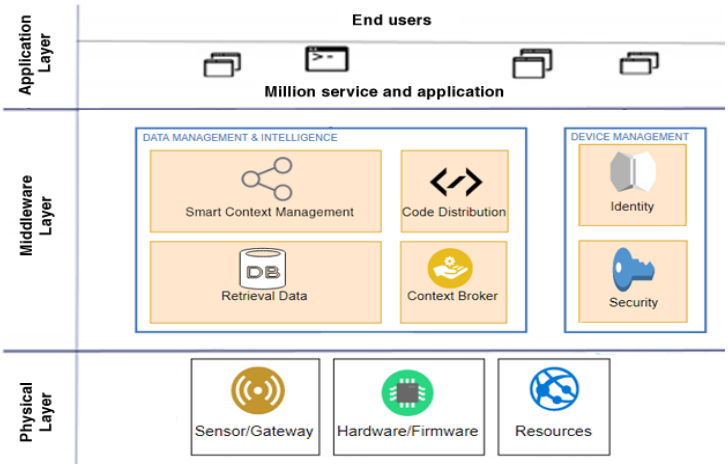

Figure 1. *Framework Architecture*

3.2. Context Broker Component

It implements various protocols for talking to sensor networks, automation systems, or cloud services. One such protocol is MQ Telemetry Transport (MQTT) [4], a Pub-Sub based light weight messaging protocol for use on top of the TCP/IP protocol, which is popular for building cloud. According to the discussion about the open source MQTT Broker, we choose using the Mosquito.

3.3. Retrieval Data Component

It helps to store raw data with large volumes of data using time series analysis and data compression techniques to reduce the size of raw sensory observations. With specific reference were evaluated in [7], we choose MySQL and MongoDB to make this retrieval data. For complex context, we use Sesame, which is an open source framework [10] for Resource Description Framework (RDF) query and analyze data. This component first finds relevant streams according to the requirements specified in the request. Then, it translates users' requests into RDF Stream Processing (RSP) queries and evaluates the queries to obtain results. RDF-based reasoning is supported through CSPARQL and CQELS [10], which are RDF query languages managing continuous data streams.

3.4. Intelligent Context Management

To semantically annotate data streams, R-IoT uses Web semantic models developed on top of well-known models, such as the SSN [14] and OWL2 ontologies. We describe streams coming from sensors deployed using the Stream Annotation Ontology and events using the Complex Event Ontology. According to the advantages of open source systems that support OWL2, we built based on Protege [14], which is open-source ontology editor and framework for building intelligent systems. Through the aforementioned ontologies, we semantically describe the sensors' real-time data streams, their metadata. When the real-time data streams are semantically annotated, we can use both SWRL (Semantic Web Rule Language) and RDF Stream Processing (RSP) techniques [6] to easily process heterogeneous data streams.

Table 1. *Some SWRL rules for Intelligent Temperature Context*

SWRL Rule for Parameter Setting	SWRL Rule for App Removing
Node(?a) ^ hasEnergyValue_percent(?a, ?b) ^ swrlb:greaterThan(?b, 0.75) -> hasThreshold_second(?a, 10)	Node(?a) ^ hasHumidityStatus(?a, false) ^ ^ basedOnApplication(?a, ?c) ^ basedOnHumiditySensor(?c, true) -> removeApplication(?a, ?c)

Besides, Intelligent Context Management can read information from raw data by using RSP, one can use SPARQL-like query languages to evaluate query patterns over static/dynamic knowledge, facilitating on-demand stream discovery to serve the code distribution for re-configuration.

3.5. Code Distribution Component

It allows real-time alarms monitoring and alarms propagation to related entities hier-archy and have been built in Linux/Apache HTTP Server/NodeJS Server. It transfers firmware from the cloud to the WSN which nodes that need to update the source code. The progress control four stages: initialization, code image building, verification and loading. Finally, API Runtime Management Component provides immediate visual access to the results of processing and analysis of data. This component adjusts the rules for auto reconfiguration triggers and it also facilitates manual reconfiguration. It been built in Linux/Apache HTTP Server/NodeJS Server.

IV. EXPERIMENTS AND EVALUATION

4.1. Evaluating environment

We validate the reconfiguration of the proposed framework on the adjustment of the air conditioner settings. This solution adjusts the room temperature of the air conditioner to suit the outdoor weather in the real time.

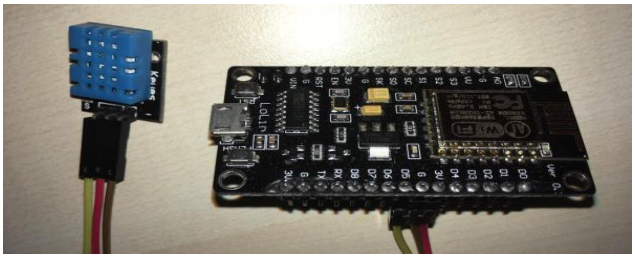

Figure 2. *ESP8266 with DHT11*

The sensor receives data for temperature, humidity outside in every 30 seconds. This information is transmitted to the CR-IoT Framework with separate processing components. The proposed framework will perform manual reconfiguration by administrator. Specifically, the administrator will monitor the temperature in the room, they think the temperature is higher than 26°C, so the temperature is adjusted to 17°C using the admin dashboard to reconfigure the room. To adjust the temperature, they can choose the available firmware or upload another firmware as shown in Figure 8.

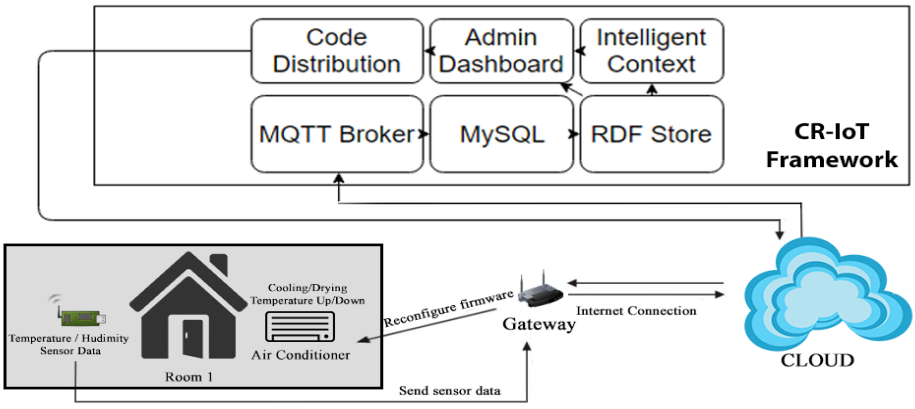

Figure 3. *Temperature Measurement flow applied CR-IoT framework*

4.2. Experiments

With code distribution component, it provides immediate and intuitive visual access to the track real time and historical sensor data as shown in Figure 4. By observing the data, we perform reconfiguration by choosing or uploading firmware image from admin dashboard to reconfigure ESP8266 devices. In this experiment, we choose the firmware which will adjust the room 2 of Floor 1 temperature to 24°C. After getting the new firmware, air conditioning is adjusted to the desired temperature. We compared the reconfiguration of the ESP8266 device using the OTA popular method via HTTP Server [8]. This section evaluates certain aspect of our approach by comparing cost to those of reconfiguration. In this paper we compare at the reconfiguration time cost. The time cost of the reconfiguration process starts from when the user loads the firmware until the device has changed the behavior. The ESP8266 OTA via HTTP Server time measurement method is shown in the "Serial Monitor" window of the Arduino IDE.

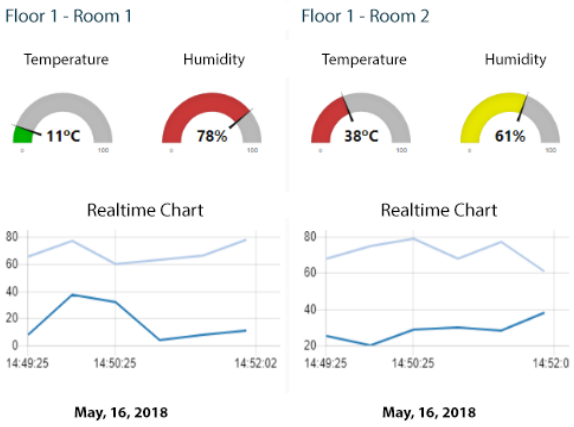

Fig. 4. *Report temperature, humidity in real time*

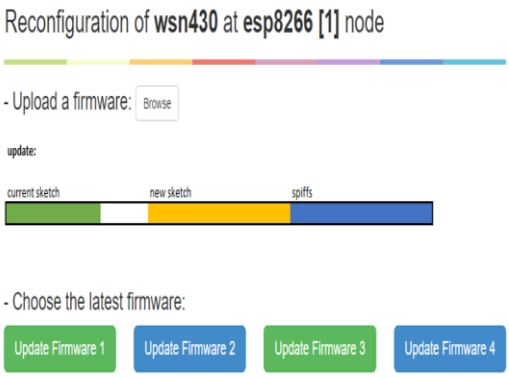

Fig. 5. *Display firmware update status*

The cost of the proposed framework time is displayed on the Dashboard Admin screen. We conducted two test cases: re-configuration for 01 and 10 temperature change devices of the air conditioner. In each experiment, we collected 10 tests and analyze the data as Figure 6, 7. In case of reconfiguration for 01 node, the average of reconfiguration time of ESP8266 via HTTP Server and ESP8266 Via CR-IOT is 591.7ms and 658.2ms. Still in case of reconfiguration for 10 nodes, the results are in order 6216.5ms and 1553.2ms. The result of the data, we can conclude that, the cost of time when applying the proposed framework is not optimal for reconfigure 01 node. But in case 10 nodes, the results show very clearly, the proposed framework saves on the cost of deploying re-configuration. The result is a cloud-based code distribution solution that enables the firmware to automatically load to the device quickly and efficiently. This approach is more efficient than the direct configuration of each node in terms of time cost.

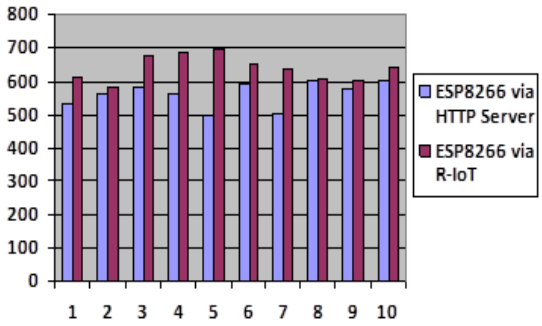

Fig. 6. *The reconfiguration process time for 01 node in 10 tests*

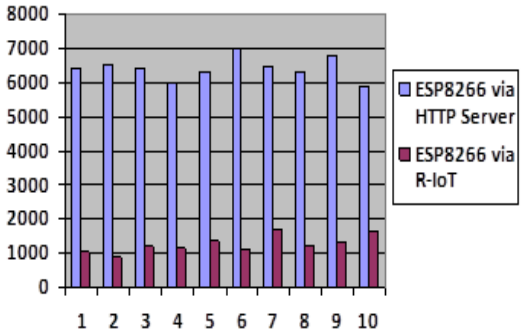

Fig. 7. *The reconfiguration process time for 10 nodes in 10 tests*

V. CONCLUSION

In this work, I have done related work in many reconfiguration approaches {Reconfiguration at IoTs Thing layer, Middleware layer (event-driven, SOA, Virtual Machine, Agent, Database, Cloud)}. I have proposed a novel approach for building the reconfiguration framework on Cloud. We have tested a smart temperature context to adjust the temperature. Experimental results have shown that the reconfiguration has been resolved according to the set criteria. In particular, the proposal has significantly reduced the time cost on reconfiguration. In the future, we will continue to improve the intelligent context management component and perform on more complex scenarios that serve large numbers of nodes.

References

[1]. *K. Lingaraj, Rajashree V. Biradar, V.C. Patil*, "A Survey on Middleware Challenges and Approaches for Wireless Sensor Networks," 2015 International Conference on Computational Intelligence & Communication Networks, 2015

[2]. *Cedric Adjih, Emmanuel Baccelli, Eric Fleury, Gaetan Harter, Nathalie Mitton*, "FIT IoT-LAB: A large scale open experimental IoT testbed," IEEE World Forum Internet Things, WF-IoT 2015 – Proc, 2015

[3]. *Andrea Azzarà, S. Bocchino, Paolo Pagano, Giovanni Pellerano, Matteo Petracca*, "Middleware solutions in WSN: The IoT oriented approach in the ICSI project", Proc. 21st Int. Conf. Softw. Telecommun. Comput. Network, 2013.

[4]. *Geoff Coulson, G., Blair, G., Grace, P., Taiani, F., Joolia*, "A generic component model for building

systems software," ACM Transactions on Computer Systems, 26(1), 2008.

[5]. *A. Dunkels, B. Gronvall, T. Voigt*, "Contiki - a lightweight and flexible operating system for tiny networked sensors", 29th Annual IEEE International Conference Computer Network, 2004.

[6]. *Jonathan W. Hui and David Culler*, "The dynamic behavior of a data dissemination protocol for network programming at scale" Proceedings of the 2nd international conference on Embedded networked sensor systems, pp. 81-94, 2004.

[7]. *Van der Veen, van der Waaij*, "Sensor data storage performance: SQL or NoSQL, physical or virtual,", Cloud Computing, 2012 IEEE 5th International Conference on. IEEE, 2012.

[8]. *AH Shajahan*, "Data acquisition and control using Arduino- Android platform", Energy Efficint Technologies for Sustainability, 2013.

[9]. *K. Aberer, M. Hauswirth, A. Salehi*, "A middleware for fast and flexible sensor network deployment", Proc. 32nd Int. Conf. Very Large DataBase, 2006.

[10]. *M. Udin Harun Al Rasyid, Achmad Sayfudin, Arif Basofi, Amang Sudarsono*, "Development of semantic sensor web for monitoring environment conditions", Intelligent Technology and Its Applications (ISITIA), 2016 International Seminar on, 2016.

[11]. *Peter Ruckebusch, Jo Van Damme*, "Dynamic reconfiguration of network protocols for constrained Internet-of-Things devices", Dynamic network stack reconfiguration, 2016.

[12]. *S. Michiels, W. Horré*, "DAViM: A dynamically adaptable virtual machine for sensor networks," Proc. Int. Workshop Middleware Sensor Network, 2006.

[13]. *T. Sivaharan, G. Blair*, "Green: A configurable and reconfigurable publish-subscribe middleware for pervasive computing", On the Move to Meaningful Internet Systems 2005: CoopIS, DOA, and ODBASE, 2005.

[14]. *Michael Compton et al*. "The SSN ontology of the W3C semantic sensornetwork incubator group", Web Semantics: Science, Services and Agentson the World Wide Web, 17(1):25–32, 2012.

THE UTILIZATION OF UAV IMAGING OF DIGITAL SURFACE MODEL AND ACCURACY ANALYSIS OF URBAN DETENTION BASIN

HOANG THANH VAN[1], TIEN YIN CHOU[1], LIANG-TAY LIN[2], CHO-YI LIN[1], YEN-HUNG CHEN[1], MEI-LING YEH[1]
[1]Geographic Information System Research Center, [2]College of Construction and Development
Feng Chia University, Taichung, Taiwan
Corresponding author's email: van@gis.tw

Abstract: *This study aimed to collect image data and three dimensional ground control points of Taichung's Maple Garden with Unmanned Aerial Vehicle (UAV), general camera and Real-Time Kinematic with positioning accuracy down to centimeter. A digital surface model (DSM) was also built with Agisoft PhotoScan, and a high resolution orthophotos has been generated.*

There were two conditions in this study, surveying with or without ground control points. Both of the digital surface models were discussed and compared for the level of accuracy. According to the check point deviation estimate, the model without ground control points had an average two-dimension error up to 40 centimeters, altitude error within one meter. In the case of the model with ground control points, the accuracy of x, y, z coordinates has gone up by 54.62%, 49.07%, and 87.74%, and the accuracy of altitude has improved the most.

Keywords: *UAV, Agisoft PhotoScan, DSM, Orthophoto, GCP*

I. INTRODUCTION

Extreme weather is a worldwide issue and appeared to be more frequent under the global warming. As locating in the sub-tropical region, Taiwan is often suffered from unexpected strong precipitation and urban area is often heavily hit. Therefore, environmental data collection and analysis, before and after flooding with the post-disaster emergency investigation are the key studies nowadays. UAV is an ideal platform to build up environmental data and collect real-time disaster information due to its features such as high mobility and efficiency, less weather restricted and low-level operating capability. Meanwhile, urban planning and development are highly relied on basic environmental information. It is the foundation for analysis and decision-making. In the past years, the update of information required on-site investigation with the aid from aerial-photography. Equipment limitation and weather restriction always prevent researchers from getting the most up-to-date information. With the unique operating features, UAV is able to capture real-time images to integrate with existing aerial photographs and satellite images for situation analysis in a short period of time. This high mobility and working efficiency greatly reduce the manpower required.

Aerial photogrammetry is the image obtainment which make use of flying vehicle or satellite as the platform [4]. General cameras or various sensors could be carried and used to obtain images and other information for geographic mapping. [5] Nevertheless, due to the information

confidential regulations in Taiwan, aerial photos are difficult to be reached by civilians. Moreover, the islandic climate often deteriorate the quality of aerial photos. [1] Therefore the utilization of UAV imaging became a key role for real-time image capturing, disaster data analyzing and discussion making. [3] The technology development of UAV and associated cameras rockets in the recent years. Drones become tiny in size, simpler in structure and highly advanced in navigation. With the accompany of high definition, stable and low cost non-surveying camera, UAV imaging is ready to replace the traditional aerial photogrammetry in small region mapping [2].

II. REGION OF STUDY

This study focused at the Maple Garden, which located at the heart of Taichung urban area. The total area is approximately 30,000 square meters with 28,000 square meters of green land around the lake. It is designed to hold 200,000 cubic meters of water, functioning as the lung of the city and the flooding buffer in the case of extreme weather.

III. STUDY PROCEDURE AND METHOD

This study made use of UAV to capture vertical aerial images in the area of interest. Digital processing such as photo combination and 3-dimensional point cloud construction were applied afterward.

Two cases were studied as the following. In case 1, 3-dimensional raw coordinates were used to construct the DSM. In case 2, Ground Control Points were added to enhance the accuracy of the coordinates before constructing DSM. Orthographic image and DSM were then generated. Comparisons of the errors in horizontal and vertical plans between these two cases would be done and the overall workflow is listed in figure 1.

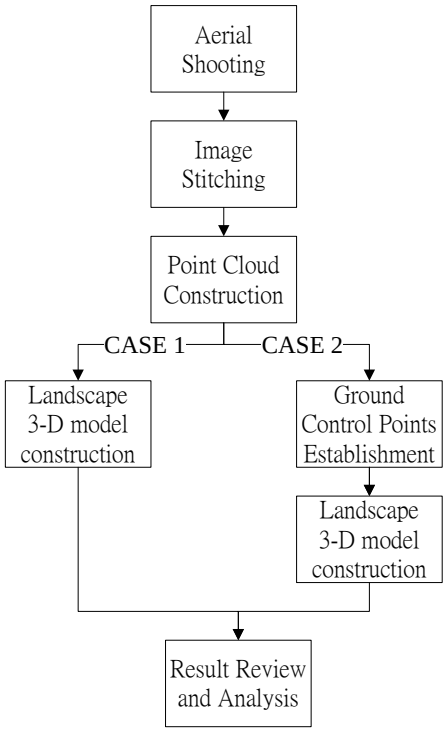

Figure 1. *Study workflow*

3.1. Specification of UAV and camera

This study used DJI Phantom 3 Professional as the flying platform, accompanying with 3-axis self-stabilizing gimbal and FC300S camera. The image resolution was 4000x3000 pix and the lens angle was 94°. The self-contained GPS + GLONASS dual satellite positioning system provided accuracy down to centimeter standard. When the image being captured, photo coordinates were stored instantly in the file for further processing.

3.2. Conducting Aerial Photography

The study showed that when the altitude of UAV maintained 300, 600 and 900 meters, the 3-dimensional accuracies were 6, 13 and 19 centimeters and the geometry accuracies were 10, 53 and 23 centimeters respectively. The accuracy did not show a direct relationship with UAV's altitude and it might due to the choice of control points.

100 meters height was chosen in this study to uphold the resolution and accuracy. Flying path and waypoints were inserted in the ground station and the drone flow according to its navigation system. The forward overlapping rate was greater than 75% while the sideway overlapping rate was greater than 50%. The image distribution is shown in Figure 2, and the overlapping area and rate are shown in figure 3. The black dots represented the center of image, darker the color means higher the overlapping rate.

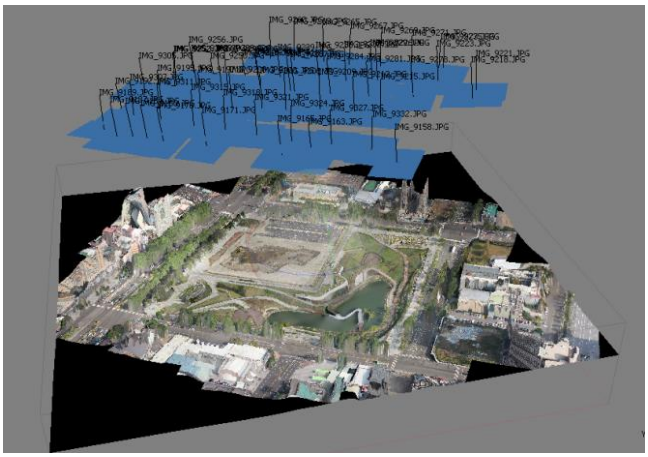

Figure 2. *Aerial images distribution*

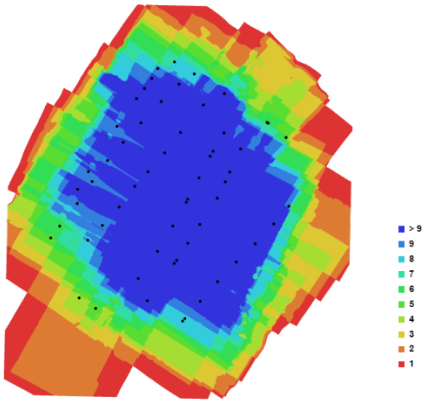

Figure 3. *Images location and overlapping rate*

3.3. Image Processing

Coordinates-embedded photos were imported into the processing software. The photos were then aligned with their correspondent location. 226,000 matching points were calculated and showing as the right angle in figure 4.

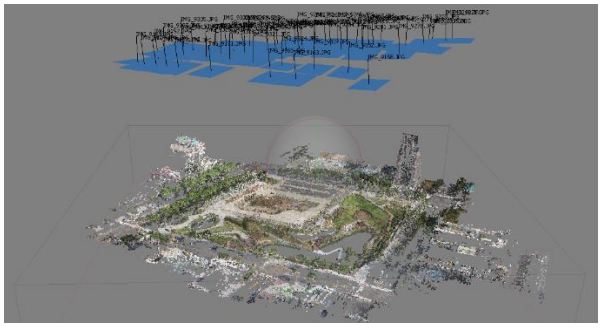

Figure 4. *Point Cloud Distribution*

3.4. Constructing the Triangular Irregular Network, TIN (Case 1)

Triangular Irregular Network was constructed with the use of point cloud. In Figure 5, each face of the model was constructed by triangular network. Color was inserted in Figure 6 according to the height above reference point. Red color represented tall trees and light blue represented detention basin. Lastly, pattern projection technique was used. Aerial photos were inserted into the 3-dimensional model in order to retain the orthographic image.

In this study, DSM was produced without the aid of control point. The highest point was 131.4 meter while the lowest point was 70.5 meter. The ground resolution was 1.3cm/pix, covering 0.155 square kilometer (figure 8).

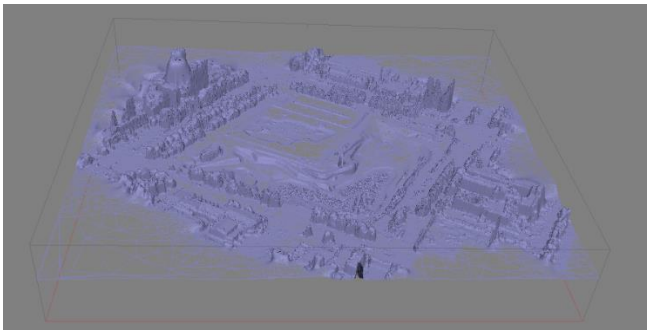

Figure 5. *Triangular Irregular Network, TIN*

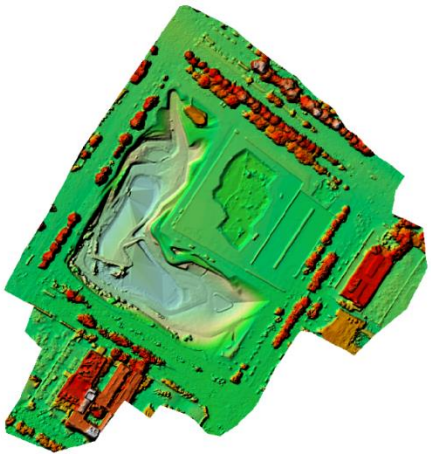

Figure 6. *Color inserted Triangular Irregular Network*

Figure 7. *Orthographic image*

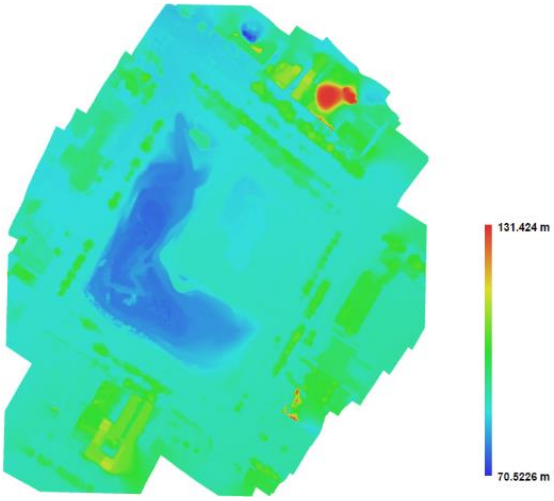

Figure 8. *DSM without GCP*

3.5. Ground control point survey

10 distinctive land features were picked in the study area as the ground control point (i.e. point 1-10) as GCP (shown in Figure 9). 3-dimensional coordinates were surveyed on site by using VBS-RTK as shown in Table 1. DSM accuracy was expected to increase with the high surveying grade measurement.

Figure 9. *Distribution of Ground Control Points*

Table 1. *Coordinates of GCP (TWD1997)*

Point	***X***	Y	Z
Point 1	213340.3546	2673499.4864	82.24
Point 2	213398.4376	2673435.3482	92.38
Point 3	213473.5673	2673363.5273	83.43
Point 4	213430.5487	2673273.1678	79.47
Point 5	213384.3546	2673194.6783	85.65
Point 6	213218.3678	2673294.7354	83.44
Point 7	213318.3453	2673407.7823	76.35
Point 8	213294.1423	2673258.7838	82.48
Point 9	213318.6542	2673268.3572	74.43
Point 10	213373.3287	2673269.4789	75.17

3.6. Reconstructing DSM with Ground Control Points

DSM was reconstructed with the aid of ground control points (figure 10). The highest point was 140.329 meters while the lowest point was 82.3191 meter. The ground resolution was 1.3cm/pix, covering 0.15 square kilometer.

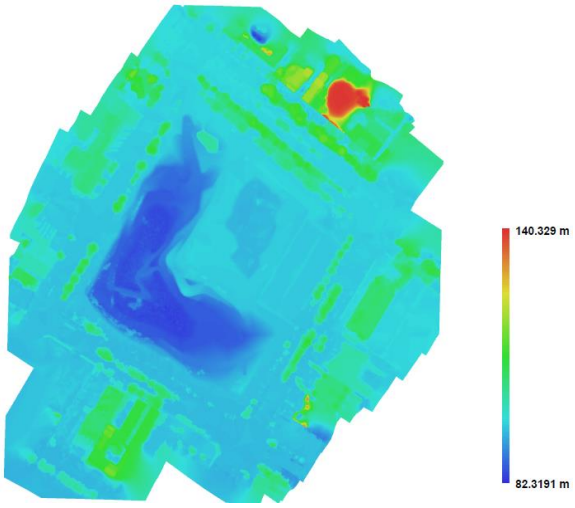

Figure 10. *Result of DSM reconstruction (with GCP)*

IV.RESULT ANALYZING AND ERROR REVIEW

4.1. Building reviewing points coordinate

Another 8 distinctive land features (i.e. point 11-18) were picked as reviewing points, evenly disturbed as shown in figure 11. The surveying method remained the same, accuracy brought below 10 centimeters and the coordinates are shown in table 2.

Figure 11. *Distribution of Reviewing Points*

Table 2. *Coordinates of Check Points (TWD1997)*

Point	x	y	z
Point 11	213370.6347	2673369.5210	82.03
Point 12	213275.2375	2673353.7578	82.51
Point 13	213323.7836	2673318.3758	81.96
Point 14	213332.7836	2673342.3785	81.70
Point 15	213398.1423	2673303.1578	80.66
Point 16	213296.587	2673304.8574	80.10
Point 17	213448.9675	2673380.942	73.05
Point 18	213337.7869	2673468.5724	80.35

4.2 Case 1 result review (without Ground Control Points)

Error values were calculated by comparing Case 1 result with reviewing coordinates. Point 16 showed the greatest error in X-axis (0.5104 meter), point 18 showed the greatest error in Y-axis (0.4451 meter) and point 11 showed the greatest error in Z-axis (1.7963 meter). The RMSE values on X, Y and Z axis were 0.3958 meter, 0.2739 meter and 0.8704 meter respectively (table 3).

Table 3. *Error of Reviewing Points in Case 1 (without GCP) (Unit: m)*

Point	X error	Y error	Z error
Point 11	0.4927	0.4338	1.7964
Point 12	0.3242	0.2713	0.4544
Point 13	0.3370	0.1307	0.0674
Point 14	0.4890	0.0450	0.7091
Point 15	0.1198	0.3363	0.3316
Point 16	0.5104	0.0701	0.2594
Point 17	0.3367	0.0565	1.2630
Point 18	0.4056	0.4451	0.5896
RMSE	**0.3958**	**0.2739**	**0.8704**

4.3. Case 2 result review (with Ground Control Points)

Error values were calculated by comparing Case 2 result with review coordination. Point 18 showed the greatest error in X-axis (0.3017 meter), point 18 showed the greatest error in Y-axis (0.2667 meter) and point 11 showed the greatest error in Z-axis (0.163563 meter). The RMSE values on X, Y and Z axis were 0.1796 meter, 0.1395 meter and 0.1067 meter respectively (table 4).

***Table 4**. Error of Reviewing Points in Case 2 (with GCP) (Unit: m)*

Point	X error	Y error	Z error
Point 11	0.0640	0.1156	0.1636
Point 12	0.1014	0.0982	0.1014
Point 13	0.0477	0.0208	0.0372
Point 14	0.2861	0.0425	0.1026
Point 15	0.0198	0.2128	0.0458
Point 16	0.2298	0.1175	0.1386
Point 17	0.1236	0.0076	0.0019
Point 18	0.3017	0.2667	0.1446
RMSE	**0.1796**	**0.1395**	**0.1067**

4.4. Summary

DSM Error was reduced by using 10 Ground Control Points. 8 reviewing points reflected the result. RMSE of X, Y and Z reduced by 0.2162meter, 0.1344meter and 0.7637meter respectively.

***Table 5.** Comparison of Case 1 and Case 2 (Unit: m)*

RMSE	**X error**	**Y error**	**Z error**
CASE 1	0.3958	0.2739	0.8704
CASE 2	0.1796	0.1395	0.1067
Error Reduction	0.2162	0.1344	0.7637
Percentage(%)	54.62	49.07	87.74

V. CONCLUSION

This study focused at the urban detention basin. UAV was used for image collection and Agisoft PhotoScan was used for digital processing. In case 1, overall accuracy remained below 40 centimeters and vertical accuracy below 1 meter without using the Ground Control Points. The whole process was completed in one working day, which demonstrated the high mobility and rapid information obtainment with UAV application. The study proved that UAV can be used in the early phase of database construction in urban disaster prevention.

DSM accuracy could be improved by applying ground control points with the use of RTK surveying equipment. The centimeter-graded positioning system provided 3-dimensional coordinates to reduce the horizontal and vertical errors. The DSM accuracy of X,Y and Z increased by 0.2162m, 0.1344m and 0.7637m respectively, the improvement in Z-axis was high in particular.

Besides the early phase of urban disaster prevention database construction, this study can also be applied to rapid and instant disaster information collection. On the other hand, such technique can eventually be applied to the landslide emergency assessment, soil volume quantification in the non-urban area.

ACKNOWLEDGEMENTS

With boundless appreciation, the researchers would like to extend their heartfelt gratitude and appreciation to Taiwan Ministry of Science and Technology for their fully support to the image processing and relevant study. Project ID: 103-2632-E-035-001-MY3.

References

[1]. *Shui-Ji Wu*, "Application of Aerail Photography in Land Surveying", National Geographic Information System Seminar, 2011.

[2]. *Yao-zong Lin, Wen-Lian Que, Yi-Ho Yen*, "Discussion on the Application of Unmanned Aerial Vehicle for 1/1000 Topographic Map Surveying", CECI Engineering Technology 107(2015.07), 128-138.

[3]. *Guo-Zhen-Zhang*, "Unmanned Aerial Vehicle", NTUTCE Newsletter, 006, 2013.

[4]. *Yi-Ho Yen, Shih-Hong Chio, Pai-Hui Hsu, Jen-Luan Liu, Gi-Sing Tsai, Gean-Whei Ci*, "The Investigation on Aerial Triangulation of UAV Imagery by Diverse Conditions of Camera Calibration", Taiwan Geographic Information Society, 2011.

[5]. Ministry of the Interior, Surveying and Mapping Law, 2007.

ESTIMATING SPATIAL DISTRIBUTION OF HEAVY METALS IN URBAN SOIL FOR URBAN ENVIRONMENTAL MANAGEMENT: A CASE STUDY IN HOC MON DISTRICT, HO CHI MINH CITY, VIETNAM

TRAN QUANG TUAN[1,2], CHOU TIEN YIN[3], HOANG THANH VAN[3], YEH MEI LING[3], CHEN MEI HSIN[3], FANG YAO MIN[3], LUU HAI TUNG[2], DANH MON[2]

[1]*Ph.D Program of Civil and Hydraulic Engineering, Feng Chia University, Taichung, Taiwan*

[2]*Department of Land Resources, Ho Chi Minh City Institute of Resources Geography, Ho Chi Minh City, Vietnam*

[3]*GIS research Center, Feng Chia University, Taiwan*

Corresponding author's email: tqtuan@hcmig.vast.vn

Abstract: *Metal concentration in urban soil is one of big environmental problem that contributes directly or indirectly to the general life quality in city areas. The study site is located in Hoc Mon district, Ho Chi Minh City, Vietnam that is the home to many industrial activities and is the populous area. Heavy metals can affect to the human health and might cause toxic effects to biological organism. There has been no investigation of urban soil pollution in Ho Chi Minh for the purpose of soil quality assessment. This study is focused on the investigation of urban soil to determine the concentration of metals in soil; to perform an interpolation method for mapping the spatial distribution of heavy metal and understanding their contamination characteristics. There are 120 soil samples were collected by surveying for chemical analysis and determining amount of heavy metals. The Ordinary Kriging technique was applied to estimate the spatial distribution of metal concentrations at unknown points using a linear weight function of adjacent data points.*

The results showed that the spatial distribution of heavy metals is well interpolated. There are 3 major heavy metals contaminated in the study site including Cu, Pb and Zn. The highest contamination is found for Cu and Zn. The impact of polluted soil was assessed by comparing the results to National Technical Regulation on the allowable limits of heavy metals in the soils, Vietnam (QCVN03-MT2015/BTNMT).

Keywords: *Heavy metals, Kriging, GIS technique, spatial interpolation.*

I. INTRODUCTION

Heavy metals are naturally present in the soil, however, their concentration has been changed and increased caused by geologic and anthropogenic activities. Especially in the urban soil, the metal contamination is being to be a serious environmental problem that is harmful to human being and plants. Plants growing on heavy metal polluted soils show a reduction in growth due to changes in their physiological and biochemical activities and it is especially true when the heavy metal involved does not play any beneficial role towards the growth and development of plants [1]. Soil polluted with high concentration of heavy metals is one problem that directly or indirectly gives a bad influence to general quality of life in the city. The contamination and extent of heavy metals

such as Cd, Cu, Pb Cr, Ni, Cr, As and Zn have identified by previous studies [2, 3]. These toxic heavy metals in soil strongly impact on natural ecosystem and are threat to human health through food chain [4, 5]. Estimating and analyzing the spatial distribution of heavy metals are particular interest for the purpose of controlling and managing soil quality in urban areas.

Geostatistics and Geographic Information System (GIS) allowing for faster and more accurate information have been widely used in numerous studies. And they are power tools for determination of spatial distribution in soil pollution study [1, 3, 7, 8]. Kriging is a geostatistical and one of the most commonly used method for spatially interpolation in environmental studies [3, 9]. This study aims to determine the concentration of heavy metals in urban soil; to produce geochemical maps of heavy metals and identify possible hot spots of elevated concentration using GIS technology

II. MATERIALS AND METHODS

2.1. Study area

Ho Chi Minh (HCM) is the largest and the most developed city in Vietnam, with an area of 2,095 km^2 and population estimated to be about 10 million in 2020. It is located in the Southern part of Vietnam. A small area was chosen as a test site in Hoc Mon district since there is a currently existing environmental problem caused by Dong Thanh landfill (DT) (Figure 1). DT landfill is one of three main landfills in HCM city. It is the official dumping site form 1992 with an area of 43 ha and its capacity of 4000 tons/day. There have been many problems on odour's and leachate in landfills for a long time that cause adverse impacts on the soil environment and public health. Moreover, most of land in Hoc Mon district is used for growing vegetables and these products are then delivered for selling in HCM city and surrounding areas. The main soil types in the study site are Acrisols, Ferralsols and Fluvisols and the average elevation of 1.5 m above sea level.

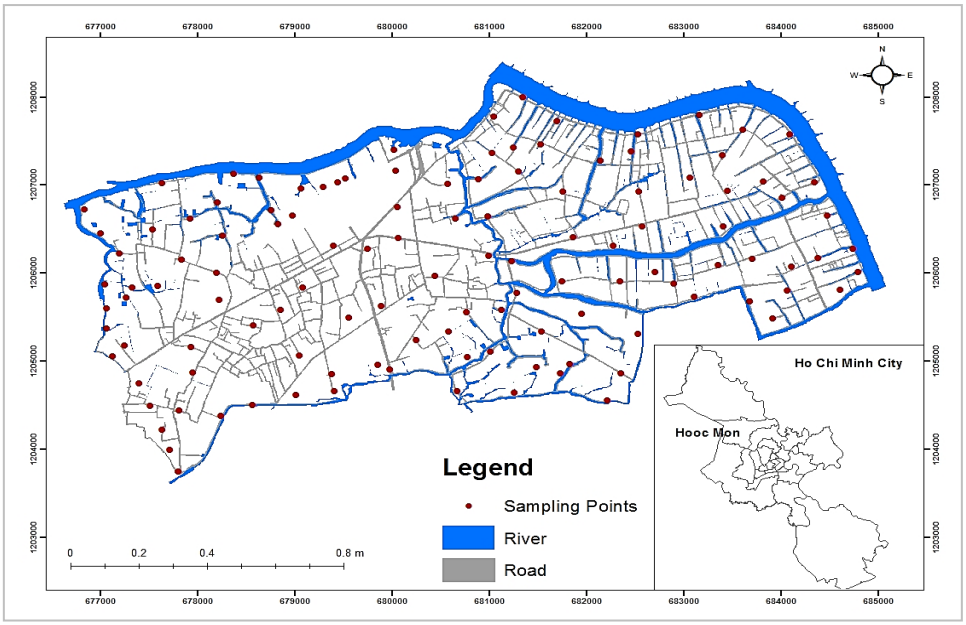

Figure 1. *Sampling points denoted in the map of the study area*

2.2. Soil sampling

The total number of soil sampled was 120. And they are randomly taken across the study area (figure 1). They were collected from the surface to 30 cm depth with a total 2-3 kg of soil per sample following the Guidance on sampling techniques of Vietnam (TCVN 7538-2:2005 (ISO 10381-2:2002). They are stored in polyethylene bag for transport and then analysed in the laboratory in accordance with the standard of Vietnam (TCVN 6647:2007; ISO 11464:2006).

2.3. Chemical analysis

Chemical properties were obtained following the standard procedures. The soil samples were air-dried at room temperature and milled to a particle size of < 2 mm after dried. They will be then classified as representative samples for later analysis.

The total concentrations of heavy metal were determined using Flame Atomic Absorption Spectrophotometry method (TCVN 8246:2009; EPA Method 7000B).. For determining the concentration of heavy metals, the soil samples were digested in a combination of acids including hydrochloric acid and nitric acid. In the following step, the concentration of metals was determined by ICP:OES in accordance with EPA method.

2.4. Geostatistical analysis based on GIS

Geostatistic method as employed in this study for estimating spatial distribution of heavy metals. Ordinary Kriging is a linear spatial interpolation that estimates spatial data at unknown location using a weight function of adjacent data points [13]. The general equation for estimating the z value as a point is:

$$Z_0 = \sum_{i=1}^{n} Z_x W_x \quad (1)$$

Where Z_0 is the estimated value, Z_x is the known value at point x, W_x is the weight associated with point x. And n is the number of sample points used in estimation.

III. RESULTS AND DISCUSSION

3.1. Heavy metal concentration

The concentration of heavy metals and statistical analysis results of the soil in the study site can be seen as Table 1. There are 3 heavy metals that can be identified from soil samples in the study site including Cu, Pb and Zn. Among these 3 metals, Cu and Zn have higher value of concentration compared to Pb. Specifically, the highest value of Cu concentration up to 1040 mg/kg that much higher than the maximum permissible concentrations as defined by government regulations (100 mg/kg for agricultural and residential lands; 200mg/kg for industrial land). The maximum concentration value of Zn is 1510 mg/kg which also much higher than permissible threshold (200 mg/kg for agricultural and residential lands; 300mg/kg for industrial land.

The variation coefficients of Cu and Zn in the soil were 2.69 and 2.59, respectively. This

indicated that Cu and Zn had larger variation than Pb throughout the study area.

Table 1. *Statistical summary of heavy metal concentration in soil (mg/kg)*

	Cu	Pb	Zn
Min	2.16	0.22	0.61
Max	1040.32	27.13	1510.02
Standard deviation	93.77	5.28	174.58
Coefficient of variation	2.69	1.18	2.59

3.2. Spatial distribution of heavy metals content in soil

Kriging interpolation method and GIS mapping technique were applied to produce the spatial distribution maps of total metal concentration for Cu, Pb and Zn in the study area. These distribution maps were illustrated in figure 2, 3, 4 for Cu, Pb and Zn, respectively.

It can be seen that the Cu content in studied soil samples ranged from 2.16 to 1040 mg/kg. This results demonstrated that the Cu concentration in the study area were above the limits of the Vietnamese standard with the allowable threshold of 100 mg/kg, especially samples located in Dong Thanh ward. This is the most heavily contaminated areas where close to DT landfill.

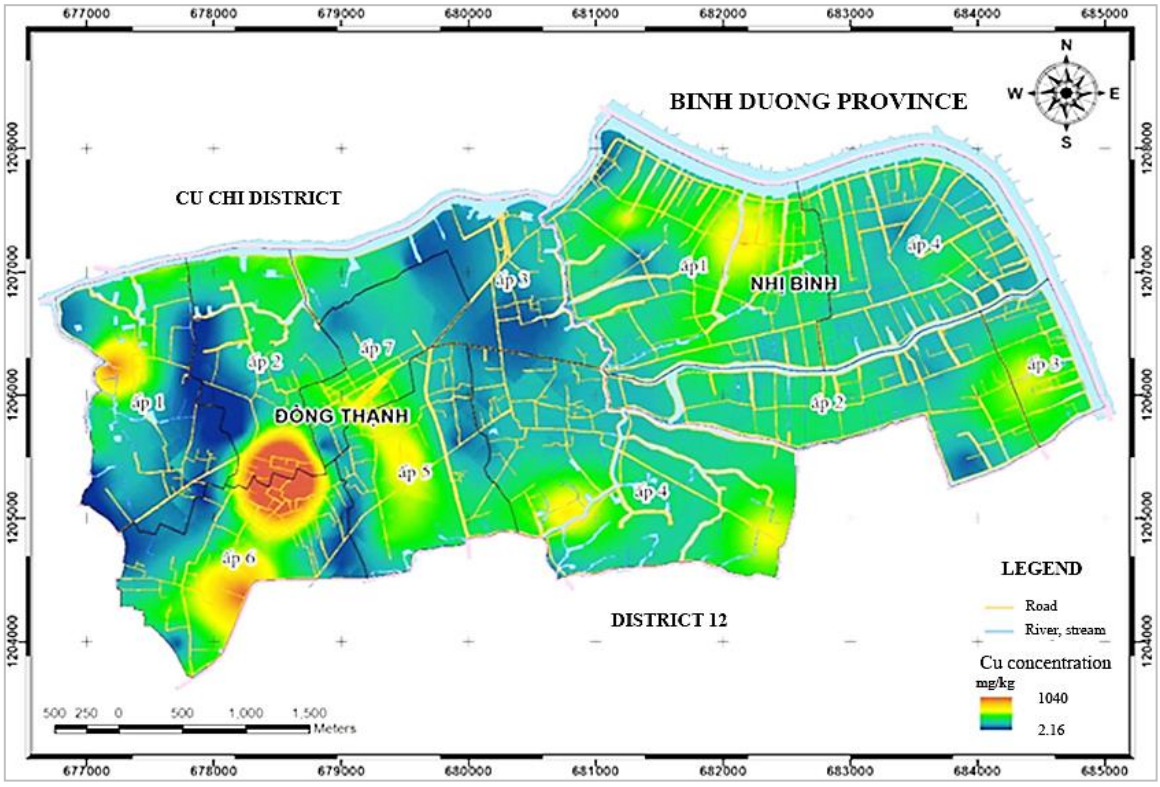

Figure 2*. The spatial distribution map of Cu concentration*

The lead (Pb) concentrations for the analyzed soil sample ranged from 0.22 – 27.13 mg/kg (figure 3). It is observed that the highest level of Pb (blue color) were recorded in central of Dong Thanh and Nhi Binh wards, and another one in the southern part of Nhi Binh ward. Pb concentration analyzed from soil samples are below the allowable threshold according to Vietnamese standard (70 mg/kg).

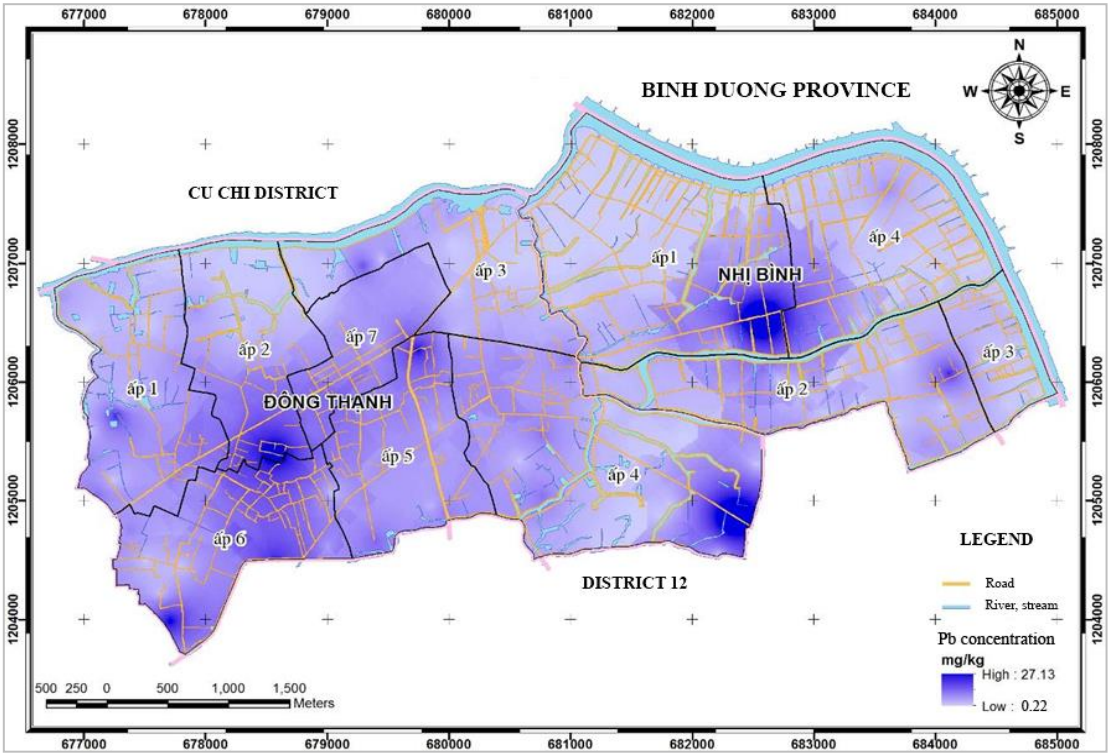

***Figure 3**. The spatial distribution map of Pb concentration*

The concentrations of Zn were found to be in the range of 0.61 to 1510 mg/kg (figure 4). Most of collected soil samples had concentration level of Zn less than the allowable threshold, however, there are 4 hotspots in Dong Thanh ward and 3 hotspots in Nhi Binh ward where are heavily contaminated by Zn element.

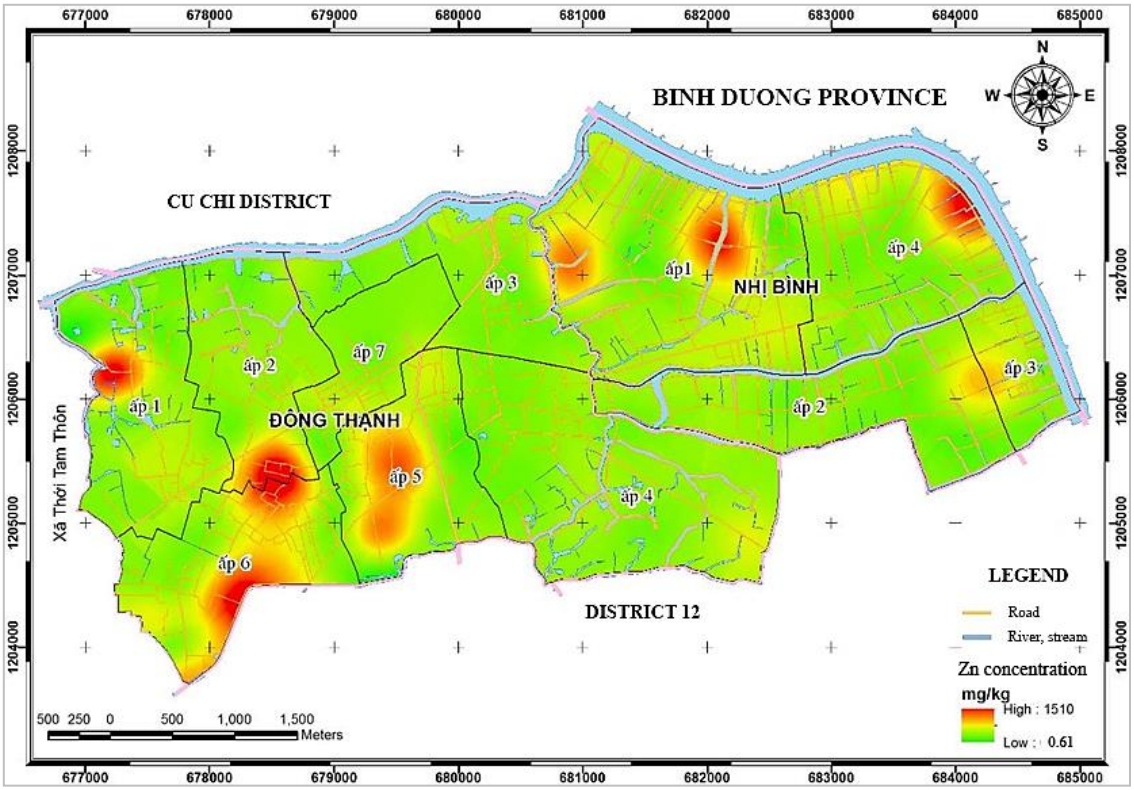

***Figure 4.** The spatial distribution map of Zn concentration*

IV. CONSLUSIONS

This study is the first attempt studying about concentration of heavy metals in the study area, Hoc Mon district, Ho Chi Minh City, Vietnam. Geostatistic and GIS-based mapping technique have applied in this study to predict spatial distribution of metals across study site.

The results showed that the concentration of Cu and Zn in some locations exceeded the allowable threshold. However, lower concentrations were found for Pb. And it can be seen from GIS-based spatial maps that a few hotspots, area of elevated concentrations, were indicated over the study area. These points were suggested an anthropogenic source for such high concentration, especially there is a big landfill located in the study area.

As a result, these metals can pose a risk to soil quality, human health and environment. This study may provide useful information on soil quality monitoring, heavy metal content in soil for better strategies protection environment and life quality in urban areas.

References

[1]. *G.U. Chibuike and S. C. Obiora*. Heavy Metal Polluted Soils: Effect on Plants and Bioremediation Methods. Applied and Environmental Soil Science, Vol. 2014. http://dx.doi.org/10.1155/2014/752708.

[2]. *F. Santos-Francés, A. Martínez-Grana, C. Asvila Zarza, A. García Sánchez, P. Alonso Rojo*. 2017. Spatial Distribution of Heavy Metals and The Environmental Quality of Soil in The Northern Plateau of Spain by Geostatistical Methods. Int. J. Environmental Research and Public Health, 14, 568. doi:10.3390/ijerph14060568.

[3]. *A. Mihailovíc, Lj. Budinski-Petkovíc, S Popov, J. Ninkov, J. Vasin, N.M. Ralevíc, M*. Vuciníc Vasíc. 2015. Spatial Distribution of Metals in Urban Soil of Novi Sad, Serbia: GIS-based Approach. Journal of Geochemical Exploration 150, 104-114. http://dx.doi.org/10.1016/j.gexplo.2015.12.017.

[4]. *Zahra, A.; Hashmi, M.Z.; Malik, R.N.; Ahmed, Z.* Enrichment and geo-accumulation of heavy metals and risk assessment of sediments of the Kurang Nallah - Feeding tributary of the Rawal Lake reservoir, Pakistan. Sci. Total Environ. 2014, 470–471, 925–933.

[5]. *Hiller, E.; Lachká, L.; Jurkovi˘c, L.; Durža, O.; Faj˘c ˇíková, K.; Vozár, J*. Occurrence and distribution of selected potentially toxic elements in soil of playing sites: A case study from Bratislava, the capital of Slovakia. Environ. Earth Sci. 2016, 75, 1390.

[6]. *M. Friedlova*, "The influence of heavy metals on soil biological and chemical properties," Soil and Water Research, vol. 5, no. 1, pp. 21–27, 2010.

[7]. *Gong, M., Wu, L., Bi, X.Y., Ren, L.M., Wang, L., Ma, Z.D., et al*. Assessing heavy-metal contamination and sources by GIS-based approach and multivariate analysis of urban–rural topsoils in Wuhan, central China. Environ. 2010. Geochem. Health 32 (1), 59–72.

[8]. *Lee, C.S., Li, X., Shi, W., Cheung, S.C., Thornton, I*. Metal contamination in urban, suburban, and country park soils of Hong Kong: a study based on GIS and multivariate statistics. 2006. Sci. Total Environ. 356, 45–61.

[9]. *Lin, Y., Cheng, B., Chu, H., Chang, T., Yu, H*. Assessing how heavy metal pollution and human activity are related by using logistic regression and kriging methods. 2011. Geoderma 163, 275–282.

[10]. *Imperato, M.; Adamo, P.; Naimo, D.; Arienzo, M.; Stanzione, D.; Violante, P*. Spatial distribution of heavy metals in urban soil of Naples city (Italy). Environ. Pollut. 2003. 124, 247–256.

[11]. *Lee, C.S.L.; Li, X.; Shi, W.; Cheung, S.C.N.; Thornton, I*. Metal contamination in urban, suburban, and country park soil of Hong Kong: A study based on GIS and multivariate statistics. Sci. Total Environ. 2006. 356, 45–61.

[12]. *Kishné, A.S.; Bringmark, E.; Bringmark, L.; Alriksson, A.* Comparison of ordinary and lognormal kriging on skewed data of total cadmium in forest soil of Sweden. Environ. Monit. Assess. 2003. 84, 243–263.

[13]. *Cressie, N.*, 1990. Statistics for Spatial Data. 1st ed. Wiley, New York.

The 2018 International Conference on Building Smart Cities in Vietnam: Vision and Solutions
Ho Chi Minh City, Vietnam, 5th September 2018

A METHOD FOR DROWSY DRIVER IDENTIFICATION BASED ON EYE BLINK DETECTION

LAI MANH DZUNG, NGUYEN QUOC TUAN
University of Transport and Communications, Hanoi, Vietnam
Corresponding author's email: dzunglm@utc.edu.vn

Abstract: *Precise eye status detection and localization is a fundamental step for evaluating emotion on driver's face like distraction, fatigue, drowsiness or drunkenness. In this article, a digital image processing method for detecting human eye blink is presented. The Haar Cascade classifiers from cascades of boosted classifiers based on Haar-like features, developed by Viola and Jones, have been trained to detect face and eyes. The accuracy rate of eyes detection method is improved by proposed adaptive Haar Cascade classifier using eyes localization and the relationship between human's eyes and facial axis. An algorithm has been proposed to calculate a value, called Classifier Threshold Value - CTV, which can be used to recognize the opening and closed states of eyelids.*

Keywords: *eye tracking, eye blink detection, eye state detection, drowsiness identification, drowsy driver identification.*

I. INTRODUCTION

Based on researches of digital image processing for face detection in 2000s, recent studies focus on detection of the facial features such as eyes, nose, mouth and their status such as eye blinking and closure, yawn expression, head swing… The implementation of these technical solutions can be applied to automatically monitor drivers and to improve driving safety not just for railway, but for other transportation in general. Eyes are the most important features of human faces. Eye sates detection has received a great deal of attention [1]. The eye states can be obtained from the eye features such as the inner corner of eye, the outer corner of eye, iris, and eyelid. There are many researches related this work. Firstly, facial axis information need to be get. For face detection, Haar Cascade Classifier [2] [3] is used for identifying sub-region image contains face base on Haar features, that are fast calculated by the integral image technique.

For eye detection, a cascade of boosted classifiers based on Haar-like features [4] is also built by two training image sets, positive samples and negative samples. These training image sets are input of the Ada-Boost learning algorithm, which is used to construct a strong classifier from the weak classifiers.

Eye state can be obtained from eye features such as eye contour, iris, corners and eyelid. For this work, geometrical approaches based on eye structure have been proposed. One of the examples is shown in [5], after obtaining the contour image of eye from binary images using chain code

tracing, Hough transform is applied to detect iris circle within an eye image. Recently, machine learning methods attract more interests of scholars. In [6], Gabor wavelets and Neural Network (NN) are used to determinate eye states. Eye corners features are extracted whereas their initial positions should be given manually in advance. In the work of [7], Support Vector Machines (SVM) and Naïve Bayes (NB) classifiers are employed for comparison by simply using intensity values of eye blocks. Local Binary Pattern (LBP) histogram features [8] and an Ada-Boost based cascaded classifier are combined to detect eye states in [9].

In this paper, we also present a method based on image processing techniques for detecting human eye blinks and generating inter-eye-blink intervals. We applied Haar Cascade Classifier algorithm for face tracking and consequently getting facial axis information. In addition, we applied an Adaptive Haar Cascade Classifier from a cascade of boosted classifiers based on Haar-like features using the relationship between the eyes and the facial axis for positioning the eyes. We proposed an algorithm to calculate a value, called Classifier Threshold Value - CTV, which can be used to detect the eye states, opened or closed.

II. MAIN CONTENTS

The proposed approach for eye states detection included 3 phases, face detection, eyes detection and eye blink detection. The overall sequence of image processing to detect eye blink has shown in following figure 1.

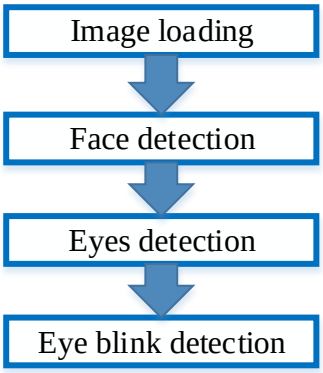

***Figure 1**. The overall sign recognition method*

2.1. Face Detection

RGB color frames, extracted from camera, are first converted to gray images. And then a Haar Cascade Classifier is applied in these gray frames to detect the location of driver face and facial axes. Haar Cascade Classifier is combined with Camshift algorithms to improve the result of face detection, not only in front view but also the different types of facial views [10]. Using the Haar Cascade Classifier, it allows to detect faces and eyes on the video stream collected from the camera. Strong classifier is constructed from weak classifiers after training process based on Adaptive Boost algorithms using samples images, which include positive samples and negative samples. The positive sample images were converted to grayscale and normalized in the same sizes. Unlike the correct samples, the negative sample images in the training image set may have

different dimensions but should be larger than the positive sample sizes. Some of the positive images in the sample set for face detection classifier training is shown in figure 2.

Figure 2. *Positive images for training Haar Cascade Classifier*

Applying Haar Cascade Classifier to detect the faces in the video stream. As the result, we can know the rectangles estimation of each face, which is later used to approximate an axis of the eyes.

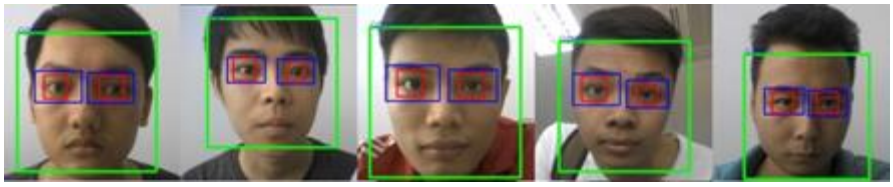

Figure 3. *Result of face detection*

2.2. Eyes Detection

The sample image set for training the strong classifier, allows to detect the eye, included human eye images in all states, opening and closed. Some of the positive sample images are shown in figure 4. Thus, the classifier trained by this set of sample images allows the detection of the eye in different states.

Figure 4. *Positive images for eye classifier training*

However, when applying this Haar Cascade Classifier to detect the eye on the frames of video stream collected from the camera, the eye detection rate is too low, especially in the case of the eye in the closed state. Otherwise, there are many cases of the wrong detections, in which, some other facial features such as nose, mouth, whiskers, and eyebrows are detected as eyes, as we can see in Figure 5. Thus, to reduce the wrong detection of eye, we proposed Haar Cascade classifiers, that adapts according to the restricted searching area of the eye and the symmetry of the eyes throw the vertical axis of face.

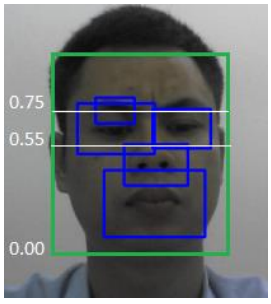

Figure 5*. Wrong detection*

Accordingly, after using the Haar Cascade classifier to identify the face area, the eye area is limited to 0.55 - 0.75 of the upper half of the face area. Limited zone for eye detection may be

customized according to the poses of identified faces. Next, based on the symmetry characteristics of the eyes, some of the constraints in size and position of the two eyes are examined to remove the misidentified objects. The author uses some of the following constraints:

- Firstly, if the search results have only one eye detected, the second eye position will be interpolated by symmetry through the face axis.

- Second, if two eyes are detected on the face, the size and location of the detected eyes are checked to eliminate the detected eyes belong to the symmetry constraint such as the formula (1) and the constraint of the similarity of size such as formula (2).

$$y_r - y_l \leq \frac{1}{3}\max(h_l, h_r) \quad (1)$$

$$\frac{\max(s_l, s_r)}{\min(s_l, s_r)} \leq 1.2 \quad (2)$$

Where y_r, y_l is the corresponding y coordinate, h_r, h_l is the corresponding height, s_r, s_l is the corresponding area of the detected region of the right eye and the left eye. As well as the limited zone for eye detection, the threshold for position and size constraints are also adjusted according to the specific face detection results.

2.3. Eye Blink Detection

For detecting eyes in the opening or closed state, the author uses the classification threshold value. This value is calculated using the algorithm of Figure 6. The goal of this algorithm is finding the smallest threshold for converting the input image to a binary image containing at least one black point after the inputted image is blurred with the medium filter. The eye region detected in the last phase of eye detection is converted to a binary image with an incremental threshold starting at 0, after Blur with the median filter and check until at least one black dot still appears. At the end of the algorithm, we obtain a classification threshold value to distinguish the states of eyes, opening or closed. The binary search algorithm may be used to improve the search speed classification threshold value.

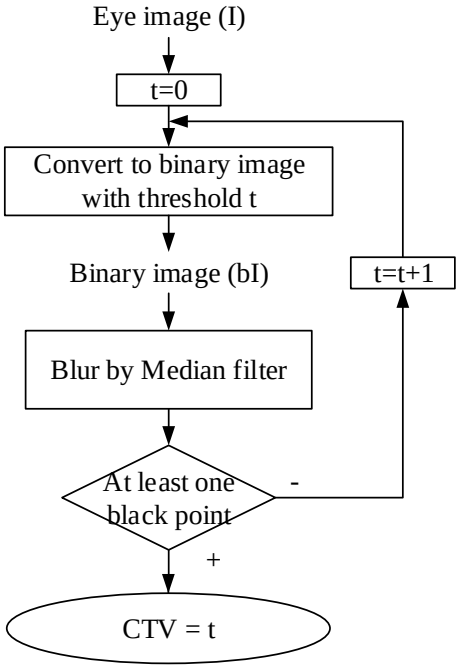

Figure 6. *CTV measurement*

Figure 7. *Opening and closed eye*

Figure 7 shows eye images in both opening and closed states. Then, the binary images and thresholds to convert to binary images corresponding these two states, opening and closed eyes are shown in figure 8 and figure 9. The upper and lower row respectively

are binary images converted by the threshold value on the third row before and after blurring using the median filter. The results show that the Classifier Threshold Value (CTV) for closed eye images are much larger than for opening eye images. Specifically, the CTV for opening eye are between 10 and 30, but for closed eye images are between 30 and 60.

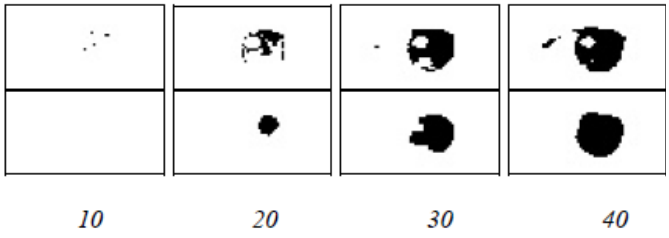

Figure 8. *Opening eye images before/after blurring*

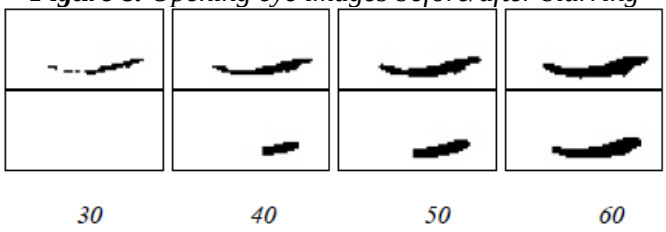

Figure 9. *Closed eye images before/after blurring*

Applying this approach for each frame from video stream, we perform a face detection, detecting the two eyes and then calculate the classifier threshold value for both left and right eye images. Drawing the graph of the multiplication of the CTV for left and right eye shown in Figure 10. Accordingly, in the graph, we can see some peak of multiplication of CTV marked by the blue circles. These peak cause of eye blinks. Therefore, we can use CTV to classify the state of eye, opening or closed, such that the high CTV indicates close state and the low value indicates open state.

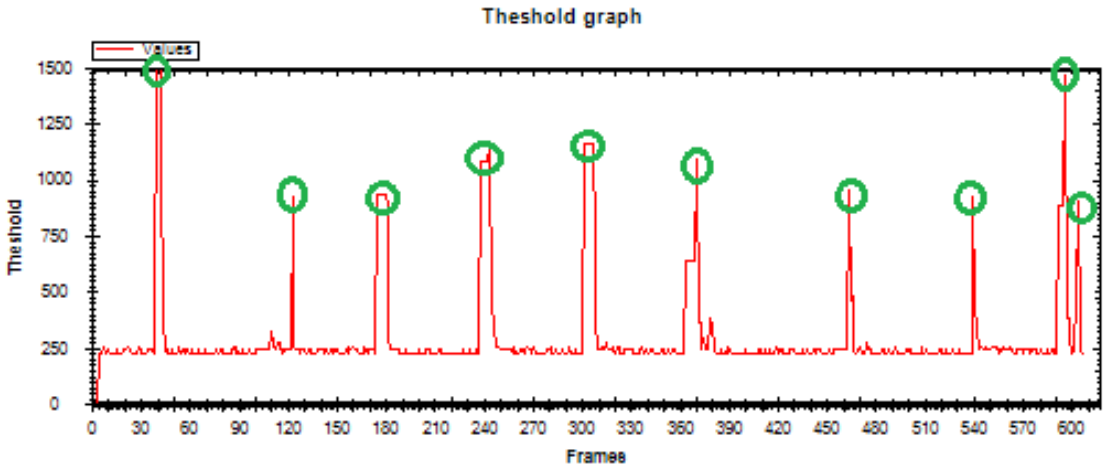

Figure 10. *Graph for eye blink identification*

2.4. Result and Discussion

Video capture and processing program has been constructed using the C#.net programming language with the assistance of the open source library EmguCV. The program was tested on a computer with the following statements: CPU - Intel® Core ™ i5-3317U, 1.70GHz; Ram - 4GB; Installed Windows 7 operating system; The image frames were continuously received from the WebCam Logitech C170 1.3 Mpi in various environments of different light conditions. The tests

show that if only the Haar Cascade classifiers are used to detect the human eye, there are many incorrect detections as shown in figure 5. So the overall accuracy is lower. The graphs of CTV belong to the frames in some cases of testing are shown in the figure 11.

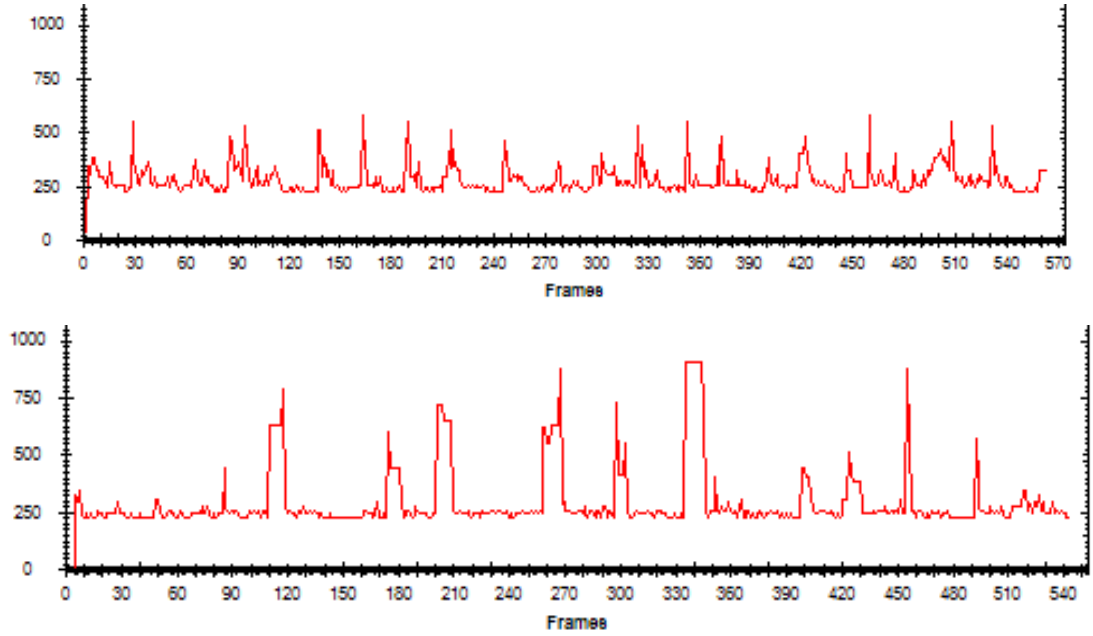

Figure 11. *Some cases of testing*

The result of testing for eye blink detection is shown in the table 1.

Table 1. *Aggregate data of test result*

Cases	Blink (True)	Not Blink (False)
Detected as blink (Positive)	546 (TP)	61 (FP)
Detected as not blink (Negative)	56 (FN)	2384 (TN)

$$\text{Overall detection accuracy} = \frac{\text{TP} + \text{TN}}{\text{TP} + \text{FN} + \text{TN} + \text{FP}} * 100\% \quad (3)$$

$$\text{Blink detetion accuracy} = \frac{\text{TP}}{\text{TP} + \text{FN}} * 100\% \quad (4)$$

We compute the overall detection accuracy and the detection accuracy of the eye blink detection by using (3) and (4), respectively. Where TP is the number of frames that are correctly detected eye blinks (true positive); FN is the number of frames that show eye blinks but the program is not detected (false negative); FP is the number of frames that are reported as eye blinks but they are not (false positive); and TN is the number of frames that are correctly reported as no blinks (true negative). Therefore, our overall detection accuracy is 96.48%, and blink detection accuracy is 90.70%.

III. CONCLUSION

With the main objective of studying is eye blink detection solution, which is able to detect distracting or drowsiness of drivers, the author inherits the object detection method based on Haar Cascade Classifier and improves the detection results by geometric constraints and the symmetry of the eyes throw facial axis, proposed a blink detection solution according to the classification threshold value, which is calculated by the difference in intensity levels of the eye images in the open and closed state. The methodology has initially led to the achievement of the given goal, but further research is needed on improving speed as well as the testing in actual environment of placing the camera in the cabin of vehicles.

References

[1]. *Wang H., Zhou L. B., Ying Y.*, "A novel approach for real time eye state detection in fatigue awareness system", IEEE Robotics Automation Mechatronics, 2010, pages 528-532.

[2]. *Viola P. and Jones M*., "Rapid Object Detection using a Boosted Cascade of Simple Features", Proc. of the Conf. on Computer Vision and Pattern Recognition (CVPR), Hawaii, USA, December 9-14, 2001, Vol. 1, pp. 511-518.

[3]. *P. Viola and M. J. Jones*, "Robust real-time face detection", International Journal of Computer Vision, 2004, p.137-154.

[4]. *Adolf, F*., "How-to build a cascade of boosted classifiers based on Haar-like features", OpenCV's Rapid Object Detection, 2003.

[5]. *Q. Wang, J. Y. Yang*, "Eye location and eye state detection in facial images with unconstrained background", Journal of Information and Computing Science, 2006, vol. 1, no. 5, pp. 284-289.

[6]. *Y. L. Tian, T. Kanade, J. F. Cohn*, "Eye-state action unit detection by gabor wavelets", Int. Conf on Multimodal Interfaces, 2000, pp. 143-150, 2000.

[7]. *R. Senaratne, D. Hardy, B. Vanderaa, S. Halgamuge, D. Liu et al*., "Driver Fatigue Detection by Fusing Multiple Cues", Lecture Notes In Computer Science, 2007, vol. 4492, pp. 801-809.

[8]. *T. Ojala, M. Pietikainen, M. Maenpaa*, "Multiresolution gray-scale and rotation invariant texture classification with local binary patterns", IEEE Trans. PAMI, 2002, vol. 24, pp. 971-987.

[9]. *C. Xu, Y. Zheng, Z. F. Wang*, "Efficient eye states detection in realtime for drowsy driving monitoring system", IEEE Conf. on ICIA, 2008, vol. 1–4, pp. 170-174.

[10]. *N. I. Ayudhya, Thitiwan Srinark*, "A Method for Real-Time Eye Blink Detection and Its Application", 2009.

DEEP-LEARNING APPLICATION FOR SOLVING THE PROBLEM OF OBSTACLE DETECTION AT THE RAILWAY LEVEL CROSSING

DANG QUANG THACH[1], NGUYEN QUANG TUAN[2], CO NHU VAN[3], NGUYEN ANH TUAN[2], TRAN NGOC TU[3]
[1]National Center for Technological Progress, Ha Noi, Vietnam,
[2]Institute of Transport Science and Technology, Ha Noi, Vietnam
[3]University of Transport and Communications, Hanoi, Vietnam
Corresponding author's email: dangquangthach@gmail.com

Abstract: *The railway level crossings are the intersection of railroads and road traffic, which are the locations dangerous for the accidents between the trains and road traffic. The detection and timely warning of obstacles the railway level crossing will contribute limiting the accidents in the railway level crossing. Currently, the number of railway level crossing in the country is quite large, which is requiring 24-hour of the monitoring to ensure the safety for people and vehicles in this area. This is a very difficult task that the transportation branch is dealing. The detection of the optimal solution for this problem is very meaningful, which not only contributes to ensure the traffic safety but also helps to reduce the pressure on the barriers at the railway level crossing. This report introduces some results from the national level project "Research and manufacture of the system of automatic monitoring and centralized control for the horizontal signal equipment" with number code ĐTĐLCN.47/16, which is implemented by the Ph.D. Nguyen Quang Tuan in the Institute of Transport Science and Technology.*

Keywords: *Railway Level Crossing Safety, Deep Learning, Convolutional Neural Network, Image processing.*

I. INTRODUCTION

Currently, there are many railway level crossings along the national railway, which are equipped with the cameras. These cameras are remotely connected to the service center of status monitoring of the railway level crossing. The simultaneous observation of multiple cameras will become impossible if the number of cameras is increased. Therefore, the gathering solution of automatic information is used by the computer image processor from the cameras, which is absolutely necessary.

In recent years, the image processing technology has Considerable developed by the integrating of artificial intelligence in the software of image processing. For some specific problems such as object detection and identification, the software of image processing has been

applied to Deep Learning, Convolutional Neural Network - CNNs, which is obtained high precision. Specially, the processing speed is higher than that of the human eye.

The application of image processing technology for the data collection of highway traffic has been quite early investigatived in Vietnam. The image processing technology for the data collection of the traffic has been studied by the University Transportation and communications in 2003[1]. This system has been applied to collect the traffic data at the Km 192+422 of Phap Van highway in 2007. Follow the applications of image processing for the highway road, in 2015, National Center for Technological Progress (NACENTECH) introduces the image processing technology with the artificial intelligence integration to collect the Urban transport data [3].

1.1. Deep learning

The deep learning is an advanced machine learning technique that allows learning directly from a sample set (image, sound, text ...) instead of implemental variety of a lot of steps as in the traditional machine learning methods. Deep learning has become popular in the last decade due to the need of large automatic process for the amount of digital data that humans have created. The rapid development of Deep Learning is partly due to the high processing of computers. At present, Deep learning is being applied to effectively solve the problems of digital image and video processing, speech and natural language processing, handwriting recognition.

1.2. Convolutional Neural Network - CNNs

CNN is one of the Deep Learning models suitable for image processing applications requiring high accuracy. The CNN structure consists of multiple layers, interconnected through the convolution mechanism (the data inputs of back layer is equal to the data inputs of preview layer multiplied a matrix called the Filter or Kernel). The Filter Matrix acts as an image filter, and the value of the Filter matrix is determined by the training process. CNN is now commonly used to solve the problem of classifying and identifying objects in images.

1.3. Model of Region-based Convolutional Network (R-CNN)

Region-based Convolutional Network [4] is an application of CNN for the problem of detecting and classifying objects on image. The R-CNN model is introduced by Ross Girshick et al in 2014 to solve the problem of detecting and classifying objects in images. In the experiment, this method has the better result than the previous methods. However the disadvantage of this method is the high computational cost. The following R-CNN models, Fast R-CNN [5] and Faster R-CNN [6] publishing in September 2015 and January-March respectively are advances of the R-CNN model to increase calculation speed. The basic principle of R-CNN is illustrated in Figure 1, which includes the steps:

- (1) Receive input image;

- (2) Identify approximately 2000 image regions that may contain object, these object are called the Region of Interest (ROI);

- (3) ROIs are standardized to 227x227 RGB images, after which is processed sequentially in a network of five convolutional layers and two fully connected layers. At the output of this network, corresponding to each ROI, we obtain a characteristic vector of 4096 elements;

Finally, the output characteristics of the network are entered in the classifiers to classify the ROI, the output of this classifier is the sets including two informations: <object class name, probability to Object in ROI of specified class.

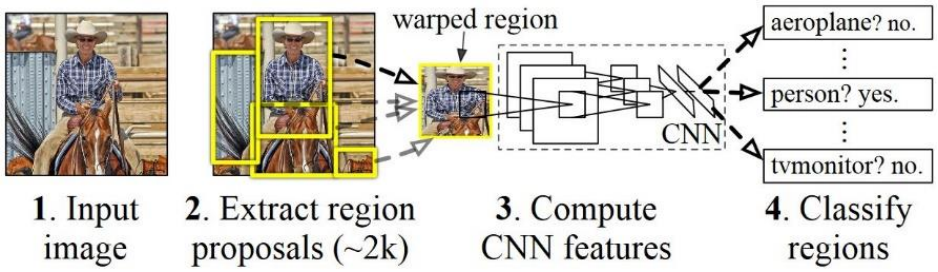

Figure 1. *The perform steps of the R-CNN model [4]*

II. MAIN CONTENTS

2.1. System model of railway level crossing monitoring by image processing

System of railway level crossing monitoring by image processing implements the main functions as follows:

- Detect the objects in the area of railway level crossing;

- Estimate the size of the object and classify the object;

- Monitor the position of the object;

- Warning when the object is the motionless standing on the safe area of the railway in the range time (> 10 seconds).

The processing system of railway level crossing image consists of the following main components:

(1) The surveillance camera is located at a position that can record the whole area of the railway level crossing, depending on the railway level crossing plane; one or more cameras can be installed to ensure the monitoring for all position of the railway level crossing. In case you need to observer images in high detail (such as license number of car), you need to select a camera with PTZ function (rotate, scan, zoom);

(2) Image processing computer has responsible for analyzing images from the camera to detect the obstacles in the railway level crossing area and warn about the center when detecting obstacles. The image processing computer also ensures image storage for post-processing;

(3) The control cabinet is located at the railway level crossing containing the signal processing equipment from the sensors detecting the ship to control the devices operating at railway level

crossing (lights, horn, Barrie). The control cabinet is also the place that the communication device is located to connect and exchange data with the control center. Obstacle detection results by the image processing will send to the same work center of the other equipment at the railway level crossing;

(4) The database at the control center, which is responsible for storing all data on the operation status of the monitoring system, warning of the railway level crossing. Images of obstructed objects and related information will be stored in this database;

(5) Centralized monitoring system includes operating status displays of horizontal guard system and remote control systems for signaling information equipment installed in the field.

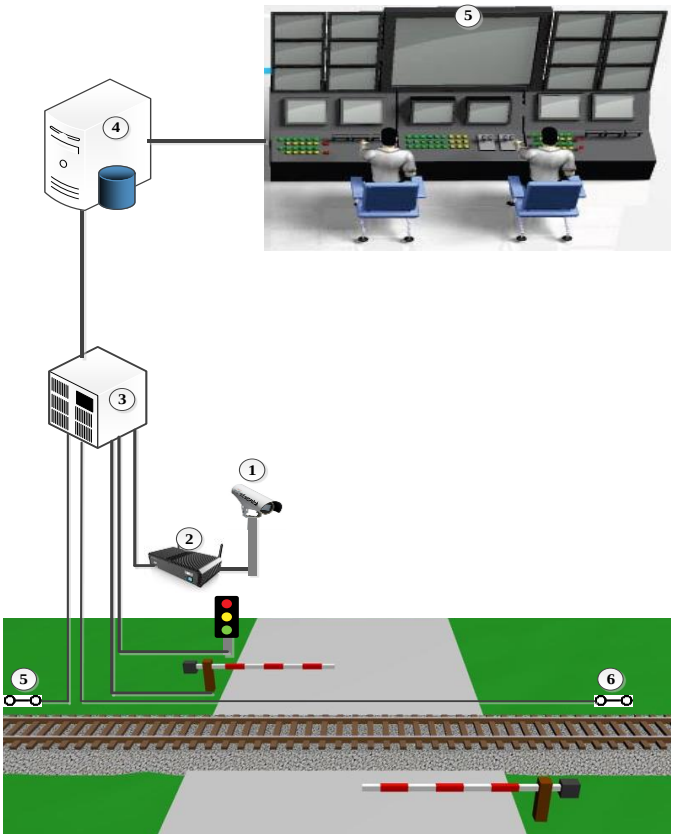

Figure 2. *The system structure of image processing monitoring the railway level crossing*

2.2. Image processing software for the obstacle detection at the railway level crossing using Faster R-CNN network

As discussed above, the Faster R-CNN is the next generation of the R-CNN model, which is improved to increase processing speed to respond the requirements of real-time systems. The Faster R-CNN network structure used in this report is illustrated in Figure 3. This model has main components the following:

- Convolutional network: including 13 layers implement to generate features map of image;

- Region Proposal Network: Use the special mapping processing to localize the image containing a certain object, ending this step we obtain a set of image that may have obstacles;

- Fully Connected FC6 and FC7: Using to classify the objects contained within image areas found by the Region Proposal network;

- The Softmax layer is responsible for calculating the suitability of an object to a particular class;

The Non-Maximum Suppression layer will remove the low-matched pairs <object-class> pairs, keeping only the pair that has the highest matching. <objects - layers> pairs are matcher greater than a preset threshold that are objects in the image.

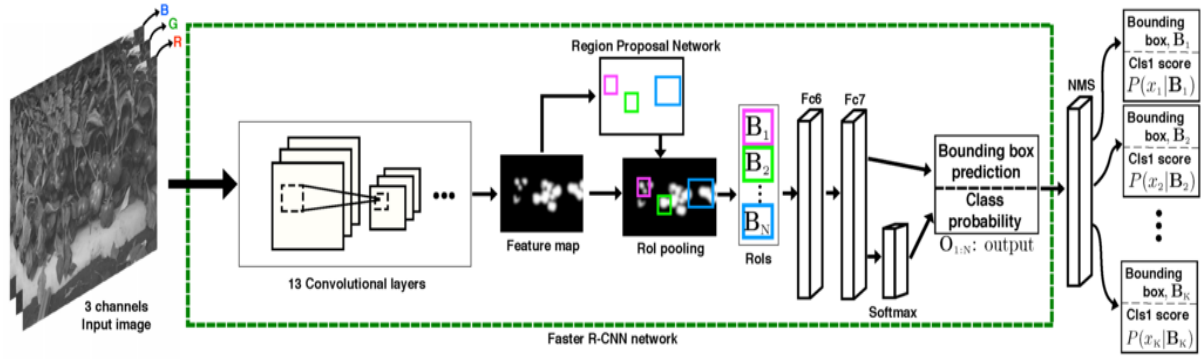

Figure 3. *Faster R-CNN model use detection and classification the obstacles [6]*

2.3. Convolutional network settings

The layers in the convolutional network are connected in the following structure: CONV1 → ReLU → Pool1 → CONV2 → ReLU → Pool2 →…

Where:

- CONVx is xth-convolution layer with parameters as follows: Filter matrix (Kernel): is a convolution matrix with the dimension 7x7 (can choose other dimensions as 5x5 or 3x3) is used to multiply the input image. The value of the elements in the Filter matrix is found at the network training stage. Multiplying is implemented on the whole image by moving the filter on the image with a stride of 1 pixel. To ensure that the result is a snapshot of the size of the input image, the outline of the image is enlarged by a few pixels (padding) depending on the size of the filter matrix (7x7 → padding: 3 pixels, filter: 5x5 → padding: 2 pixels, filter: 3x3 → padding: 1 pixel), the pixels in the extension area are equal to 0. Each color channel of a convolution layer has a number of filters corresponding to the number of object group to need to search.

- ReLU: ReLU nonlinear function adjusts the value of the multiplication results.

- Pool: The layer used to synthesize the multiply results with parameters as the following.

2.4. Setting of region proposal network

After the processing of the convolution network we obtain the feature maps, the Region Proposal network is responsible for analyzing this map to identify areas of obstructions. The ROI pooling layer is responsible for standardizing the image regions proposed by the Region Proposal Network into sized the same rectangle to transfer on the classifier to process. Regression methods are applied to train the Region Proposal Network; the goal of the training process is to improve the accuracy of function of object detection and to determine the location and size of the image area of the object. Region proposal network training needs to solve the optimal problem with the cost function which is errors minimizing of classification loss and bounding-box regression loss with variables. These variables are the parameters of Region Proposal network.

2.5. Classification layers

The classification function is implemented at two fully-connected layers (FCC) FC6, FC7. The object found on the Region Proposal Network will be placed into a specific group (motorcycles, cars or bus). These last two layers also work to determine the location and size of the object. Regression methods are also used to improve the accuracy of classification results and the size of objects.

2.6. Experiment result

The image processing software integrated the network of Faster R-CNN has described above, which are applied to analyze the video data from the camera at the railway level crossing given the results in the following:

Table 1. *Evaluation criteria*

No.	Evaluation criteria	Accuracy
1	Detect the object entering the railway level crossing	100%
2	Classify the object entering the railway level crossing including the groups: (1) the walker, (2) the motorbike, bicycle; (3) the car, (4) the bus, (5) the truck; (6) the group of other objects.	80%
3	Estimate the moving speed of the objects in the image	60%
4	Locate the objects in the image	90%
5	Estimate the size of the object	60%
6	Detect and warn the motionless objects in the area of railway level crossing	100%

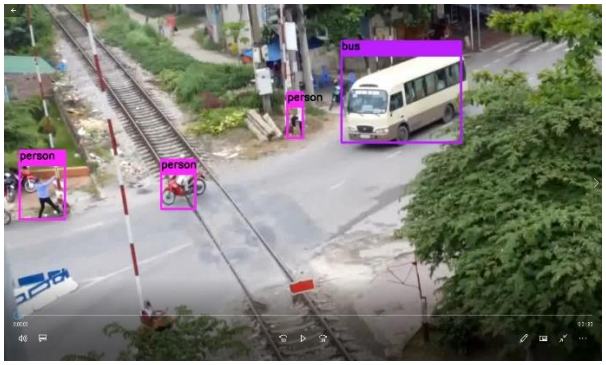

a. The detection for the motorbike and bus

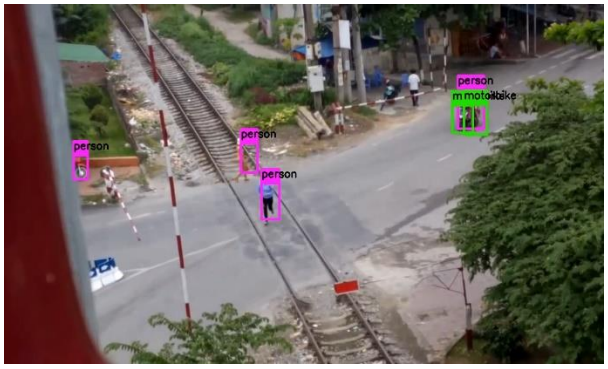

b. The detection for the walker

c. The detection for the train

d. The detection for the car

Figure 4. *The results of the image processing about the detection and classification of objects at the railway level crossing*

III. CONCLUTION

The experiment results of image processing system detect the obstacles at the railway level crossing, which are showed that this solution can effectively help for the problem of ensuring traffic safety at the railway level crossing.

The important criterion directly helps to detect the obstacles such as: detect the objects entering the surveillance area, detect the immovable object, the location of the image is the high accuracy, eligible to consider the integrated in the systems that requiring the high safety such as the surveillance system of railway level crossing.

In addition, the ability to detect the obstacles, the image processing system has also the ability to collect more the other information through the camera such as: The automatic detection of the devices has the corrupt phenomena; the identification of the vehicle license creates the traffic accidents at the surveillance area and so on.

References

[1]. *Le Hung Lan et al*, "Research on application of information technology and automation in urban traffic management", Summary report on the state-level project of research and technological development with number code: KC-03-21, Vietnam, 2005.

[2]. *Le Hung Lan et al*, "Research, design, equipment manufacture, instrument and automatic control system, monitoring and management in service of road traffic safety", Summary report on the state-level project of research and technological development with number code: KC.03.05/06-10, Vietnam, 2008.

[3]. *Le Hung Lan et al*, "Application of integrated technology monitoring traffic data for improving road efficiency and safety in Vietnam", Summary report on the cooperative- international project with Japan, Vietnam, 2015.

[4]. *Girshick, R.; Donahue, J.; Darrell, T.; and Malik, J*, "Rich feature hierarchies for accurate object detection and semantic segmentation". In Proc. IEEE Conference on Computer Vision and Pattern Recognition, pages 580--587, Columbus, OH, June 24-27 2014.

[5]. *Ross Girshick*, "Fast R-CNN", Proc. IEEE Int. Conf. Comput. Vis., pp. 1440-1448, 2015.

[6]. *Shaoqing Ren, Kaiming He, Ross Girshick, Jian Sun*, "FasterR-CNN: TowardsReal-TimeObjectDetection withRegionProposalNetworks", arXiv preprint arXiv:1506.01497, 2015.

NHÀ XUẤT BẢN GIAO THÔNG VẬN TẢI

80B Trần Hưng Đạo - Hoàn Kiếm - Hà Nội
Điện thoại: 024. 39423345 * Fax: 024. 38224784
Website: www.nxbgtvt.vn * Email: nxbgtvt@fpt.vn

Chịu trách nhiệm xuất bản: Lê Tử Giang
Chịu trách nhiệm nội dung: Nguyễn Hồng Kỳ
Biên tập: Nguyễn Ngọc Sâm
Thiết kế bìa: Phân hiệu Trường Đại học GTVT tại TP.HCM
Trình bày: Phân hiệu Trường Đại học GTVT tại TP.HCM

Đối tác liên kết xuất bản: Trường Đại học Giao thông Vận tải
Địa chỉ: Số 3 phố Cầu Giấy, Láng Thượng, Đống Đa, Hà Nội

In 200 cuốn khổ 20,5 x 29,5 cm tại Xưởng in Trường Đại học Giao thông Vận tải
Địa chỉ: Số 3 phố Cầu Giấy, P. Láng Thượng, Q. Đống Đa, TP. Hà Nội
Số xác nhận đăng ký xuất bản: 1975-2018/CXBIPH/1-89/GTVT.
Mã số sách tiêu chuẩn quốc tế - ISBN: 978-604-76-1628-2.
Quyết định xuất bản số: 73LK/QĐ-XBGT ngày 14/6/2018.
In xong và nộp lưu chiểu năm 2018.

SMART CITIES

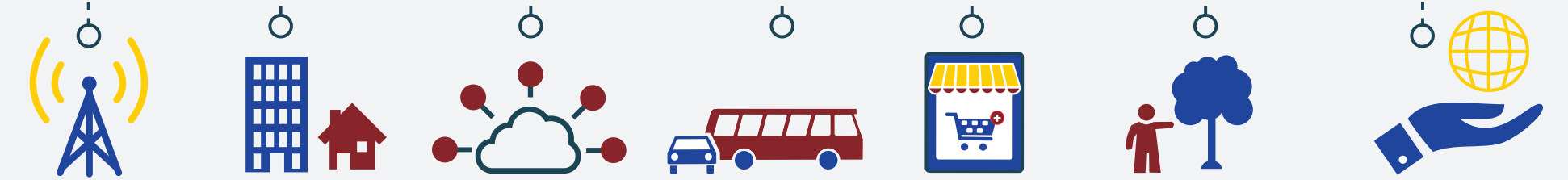

9 786047 616282